Mechanisms Underlying Cell-to-Cell Diversity in Clonal Populations of Yeast

By

Stacie L. Bumgarner

B.S., B.F.A., University of Michigan, Ann Arbor, MI
1997

M.A., The Johns Hopkins University, Baltimore, MD
2001

SUBMITTED TO THE DEPARTMENT OF BIOLOGY
IN PARTIAL FULFILLMENT OF THE REQUIREMENTS
FOR THE DEGREE OF

DOCTOR OF PHILOSOPHY
at the
MASSACHUSETTS INSTITUTE OF TECHNOLOGY

June 2008

Signature of Author_____
Department of Biology

Certified by _____
Gerald R. Fink, PhD.
Professor of Biology
Thesis Advisor

Accepted by_____
Stephen P. Bell, PhD.
Professor of Biology
Chairperson of the Graduate Committee

Mechanisms Underlying Cell-to-Cell Diversity in Clonal Populations of Yeast

By

Stacie L. Bumgarner

Submitted to the Department of Biology
in partial fulfillment of the requirements for the degree of

Doctor of Philosophy in Biology

Abstract | The *FLO* promoters are among the largest promoters in yeast and receive a complex combination of signals from upstream signaling pathways through their association with downstream DNA binding factors and chromatin remodelers. The genes regulated by these promoters encode cell-surface glycoproteins that mediate a range of cell-to-cell and cell-to-surface adhesions. Phenotypic diversity in clonal populations of yeast cells is mediated in part by epigenetic silencing of the *FLO10* and *FLO11* promoters. Silencing of the *FLO* promoters is heterogeneous, or variegated, within a clonal population of cells. The variegated transcription of *FLO10* and *FLO11* results in a population of yeast cells that exhibits cell-to-cell variability in flocculation, adhesion to and invasion of inert surfaces, and filamentous growth. In this thesis, I discuss chromatin modifying proteins that localize to the *FLO10* and *FLO11* promoters and act in *trans* to affect transcription and silencing at these promoters. I describe the results of genome-wide screens to identify additional *trans*-acting chromatin modifying factors that play roles in the transcriptional regulation and silencing of the *FLO10* and *FLO11* promoters. Some of the candidates identified in these screens had effects on *FLO* transcription that initially seemed paradoxical in light of contemporary theories regarding the role of chromatin structure in regulating transcription. Given that histone deacetylases generally repress transcriptional activity, we were particularly surprised to find that mutations in components of the Rpd3L histone deacetylase complex reduce *FLO* promoter activity, indicating that Rpd3L plays a role in transcriptional activation of *FLO* genes. Careful analysis of these mutants, their phenotypes, the transcription of *FLO11*, and most importantly, the noncoding transcripts that we have detected in the promoter region of *FLO11*, have revealed the basis for this apparent paradox.

Thesis Advisor: Gerald R. Fink, PhD.
Title: American Cancer Society Professor of Genetics, M.I.T.

Dedicated to my father
and to my grandfather,
Roger L. and Paul H. Bumgarner,
both naturally curious creatures
from whom I inherited
my own very curious nature.

Acknowledgements

I thank my thesis advisor, Gerry Fink. Gerry has an eye for the unusual and the unexpected, and his vision and creativity have inspired this project. He has cultivated a laboratory environment that fosters intellectual freedom and that is filled with supportive, motivated scientists. I am grateful for the opportunity to be a part of it. Ironically, Gerry has also instilled in me a healthy respect for the capriciousness of the gods. Behind the yellow moon, the gods watch, and laugh.

Each and every member of the Fink laboratory has contributed to this thesis project in some way: by sharing advice, a protocol, a reagent, or morale support in those trying laboratory moments. The Finklets are a group of smart, collaborative, spirited, and incredibly unique individuals. It has been an honor to work with them and to know them. Many helpful conversations with Chia Wu, Cintia Hongay, An Jansen, Sudeep Agarwala, Valmik Vyas, Brian Chin, and Josh Wolf have been much appreciated. Two Finklets deserve special acknowledgement: Adrian Halme and Paula Grisafi. Adrian Halme, who began this story when he was a graduate student in the lab, had the investigations described in Chapter Two of this thesis underway when I joined the Fink laboratory. I had the good fortune to join in and work with him on the project. I benefited a great deal from Adrian's knowledge and years of experience working with yeast. And I thank Paula Grisafi, who has worked alongside me on this project during these last several months. Paula's contributions have been indispensable to what has been accomplished here.

I also thank Professor David Gifford of MIT and the members of his group, especially Robin Dowell, Alex Rolfe, and Tim Danford, who brought new insight and computational expertise to this project. Their contributions, especially to the whole-genome portions of this work, have been invaluable. Robin, in particular, has made thoughtful contributions to this work.

I have been very fortunate to have the guidance of the members of my thesis committee, Professors Frank Solomon, Stephen Bell, Fred Winston, David Gifford, and Hazel Sive. They have provided helpful advice and support along the way. I also offer my appreciation to Professor Alan Grossman, who was a valued member of the committee during my early years at MIT.

A special thank you to Professor Frank Solomon, who has been a trusted mentor since my very first days on the MIT campus. He is a wise person who shares his wisdom with a rare combination of honesty and kindness.

Tremendous thanks to good friends for their support from nearby and from afar. Especially to Lourdes Aleman and Tyler Berzin, Bryan Davies, Annie Kays and Kimi Tsuji, and Paula Grisafi, all of whom are like family to me. Much love and appreciation to my parents, Roger and Levenia Bumgarner, and to my little sister, Natalie, for their encouragement, love, and endless patience. And immeasurable love, gratitude, and admiration for my amazing partner in all things, Benjamin Voight. He has been a pillar of support. And, among other things, has taught me that it's okay to make a mess sometimes.

S. L. B.

Table of Contents

Chapter 1

INTRODUCTION

Transcriptional variegation describes the phenomenon in which the cells that make up a genetically identical clonal population exhibit heterogeneous expression from a given promoter. Although these cells are experiencing equivalent environmental conditions, the variegating promoter exists in an active state in some cells and in an inactive state in the remaining cells of the population. Cells that carry the inactive promoter can produce progeny with either active or inactive promoters and, conversely, cells that carry the active promoter can also produce progeny with promoters in either activation state. Thus, the transcriptional state of a variegating promoter is reversible. Another component of transcriptional variegation is heritability. An active or repressed transcriptional state may be inherited over several cellular generations, producing a clone of cells that share the same phenotype by a mechanism termed epigenetic because it is not a simple Mendelian inheritance of segregated DNA sequence. The result of transcriptional variegation is phenotypic diversity within a cellular population caused by heterogeneous expression of the gene driven by the variegating promoter.

The phenomenon of variegated expression raises a number of questions. First, how common is this phenomenon within the biological world? Second, what are the biological mechanisms that give rise to variegated transcription? And third, is variegated transcription merely noise, resulting perhaps from random stochastic fluctuations in cellular levels of activators and repressors that regulate a variegating promoter? Or, alternatively, has variegated expression evolved at certain promoters because it provides some selective advantage for the cellular population carrying them?

In the introduction to this thesis, I begin by considering examples of transcriptional variegation that occur across a range of species and the biological mechanisms known to underlie these cases. These examples demonstrate that transcriptional variegation occurs naturally or can be easily engineered in many genomes. In some instances, variegated expression provides an unquestionable selective advantage to clonal populations of cells. Because chromatin structure has been shown to play an important role in the variegated transcription observed in nature, I discuss in this chapter the impact of chromatin structure on transcription, a subject of intense study in recent years. Noncoding RNAs have also been implicated as having important roles in regulating transcription and chromatin structure in many organisms, with the exception, it was believed until recently, of the budding yeast *Saccharomyces cerevisiae*. I include in this introduction a discussion of recent findings regarding transcriptional regulation by noncoding RNAs in yeast, as these findings are relevant to work presented in later chapters of this thesis. I then consider competing viewpoints regarding how observations of transcriptional variegation should be explained and interpreted. Finally, I conclude this chapter by introducing the *FLO* (*FLO*culin) gene family of *S. cerevisiae* that is the subject of the work presented in later chapters.

In Chapter Two, I present our characterization of the variegated transcription that is observed from the promoters of the *FLO* gene family in *S. cerevisiae* and our finding that, as is the case in other examples of variegated expression, chromatin remodeling at *FLO* promoters is a critical component in the mechanism underlying the observed variegation (Halme et al., 2004).

In Chapter Three, I present the results of two screens that I conducted in order to identify additional effectors of the variegated transcription at *FLO* promoters. The screens identified chromatin remodelers and other transcriptional regulators not previously known to affect *FLO* gene transcription.

In Chapter Four, I present findings that point to a new model for the mechanism underlying transcriptional variegation of *FLO* genes. This model involves competitive binding to DNA by proteins that may determine whether histone deacetylases are present or absent at local regions within the *FLO* promoters. Such competitive binding could be the root of a simple toggle between two exclusive transcriptional states. The model also involves bistable changes in local chromatin structure resulting from recruitment of histone deacetylases and regulatory noncoding RNAs transcribed from within *FLO* promoter regions.

Finally, in Chapter Five, I summarize these findings, discuss some implications of the results reported here, and propose future avenues of research,

Variegated Expression Observed Across Species

Instances of variegated transcription have been described across biological kingdoms from Protista to Animalia. Some key examples include Position Effect Variegation in fruit flies (Henikoff, 1979, 1990; Spradling and Karpen, 1990), Telomere Position Effect in yeasts (Gottschling et al., 1990; Grewal and Klar, 1996), Antigenic Variation in pathogenic protists and fungi (Borst, 2002; De Las Penas et al., 2003; Kutty et al., 2001; Rubio et al., 1996; Underwood et al., 1996), and X-inactivation in female mammals (Migeon, 1994; Panning and Jaenisch, 1998). In each of these cases, all

genetic information remains present and intact, but only a subset of cells within the clonal population expresses the variegating gene or genes in question.

Position Effect Variegation (PEV) in *Drosophila melanogaster* was first described in 1930 by H. J. Müller (Spradling and Karpen, 1990). Among progeny of X-ray treated flies, Müller recovered five mutants with "white-mottled" eyes. Each of these mutants exhibited variable expression of the *white* gene in the cells making up the hundreds of ommatidia in the fly compound eye. Linkage analysis revealed that chromosomal rearrangements had occurred in each of these mutants. Other genes that are linked to *white*, such as *Notch*, also exhibited variable expression proportional to that of the *white* gene in these mutants. Puzzled by these findings, Müller remarked that no contemporary theories were adequate to explain these "peculiar manoevers of some portion of chromatin larger than a gene which has been displaced from its original position." The variegated expression observed by Müller was later shown to be an effect of placing genes near heterochromatic regions such as centromeres. The ectopic placement of genes near these transcriptionally silent chromosomal regions results in metastable gene silencing due to the spreading of heterochromatic structure into a gene that normally resides in a euchromatic region, thus resulting in variegated gene expression in clonal populations of cells (Messmer et al., 1992).

Such position-dependent silencing effects have also been observed in the yeasts *S. cerevisiae* and *Schizosaccharomyces pombe*. When reporter genes, such as *ADE2* or *URA3*, are placed near yeast telomeres or the silent mating type (MAT) loci, these heterochromatic regions exert a metastable silencing effect on the expression of the reporter genes (Gottschling et al., 1990; Grewal and Klar, 1996). In the case of the *URA3*

gene relocation to a position near heterochromatin results in a mixed population of cells, some of which express *URA3* and are therefore able to grow on media lacking uracil because they are capable of synthesizing it on their own and some of which fail to express *URA3* and are therefore resistant to the drug 5-FOA, which is toxic to *URA3*-expressing cells. When the *ADE2* gene is placed near heterochromatin, the resulting colonies contain white sectors, consisting of cells expressing the *ADE2* gene, and red sectors, consisting of cells in which loss of the *ADE2* product due to gene silencing results in the accumulation of a red pigment in these cells. Mutations in genes that encode factors necessary to establish or maintain telomeric and MAT loci heterochromatic structure in yeast, such as the histone deacetylase *SIR2*, disrupt position-dependent silencing in yeast (Wyrick et al., 1999).

Antigenic variation is a form of variegated transcription that has evolved in many types of unicellular pathogens. The phenomenon results in clonal variation of cell surface proteins and serves these organisms well as a means of host immune evasion. The pathogenic yeast *Candida glabrata*, the yeast-like fungus *Pneumocystis carinii* that causes pneumonia, and the protist responsible for malaria, *Plasmodium falciparum*, all contain within their genomes subtelomeric gene families that encode the self-surface glycoproteins that enable these organisms to adhere to and infect the cells of their hosts (De Las Penas et al., 2003; Rubio et al., 1996; Underwood et al., 1996). The individual members of these gene families are heterogeneously expressed such that only a single glycoprotein is present on the organism's cell surface at any given time. Meanwhile, the other genes in the families are transcriptionally silenced. As in the position effects previously described, the chromosomal context of these gene families is important to this

silencing. Furthermore, factors necessary for the formation of heterochromatic structure in these chromosomal regions have been shown to be necessary for antigenic variation. In *P. falciparum,* a homolog of the yeast Sir2 protein is required for the dynamic chromatin remodeling that leads to antigenic variation in this organism (Freitas-Junior et al., 2005). In *C. glabrata,* this silencing has been shown to be dependent on Sir3, a silencing protein that interacts with Sir2 to establish and maintain heterochromatin. The protist *Trypanosoma brucei*, responsible for African sleeping sickness, presents perhaps the most elaborate version of antigenic variation that has yet been observed (Borst, 2002). Within its genome are more than 1100 different genes that encode variant cell surface glycoproteins (VSGs). Trypanosomes escape immune clearance by regularly switching the glycoprotein that is being transcribed. The cell-surface protein expressed at any given time in a given cell is transcribed from a telomeric expression site. The remaining approximately 1099 genes that encode VSGs are transcriptionally silenced. The genetic sequence of the transcribed gene is transferred into a telomeric expression site by a gene conversion event that displaces the VSG-encoding DNA sequence that previously occupied the site. Thus, in this case, antigenic variation involves not only silencing but also a gene conversion event similar to that which occurs in mating type switching in *S. cerevisiae*. These examples of variegated transcription within clonal populations of cells are biologically relevant, since they contribute to the virulence of these pathogens by effectively enabling them to play hide-and-seek with their host's adaptive immune system.

In mammals, the diploid somatic cells of males each carry one X chromosome whereas the diploid somatic cells of females each carry two X chromosomes. Dosage

compensation, or equalization of expression levels of genes located on the X chromosome, is accomplished by random inactivation of one of the X chromosomes in the somatic cells of females (Migeon, 1994; Panning and Jaenisch, 1998). This inactivation results in one silenced X chromosome that persists in a tight heterochromatic state and one X chromosome that contains euchromatic regions that are transcriptionally active. The phenotypic outcome of these silencing events is a clonal population of somatic cells that are variegated, or mosaic, in the chromosomal copy of their X-linked genes that is being expressed.

Chromatin Structure and its Effects on Transcription

In the nuclei of eukaryotic cells, genomic DNA is folded by its association with histone and other proteins into dynamic higher-order structure called chromatin (Jenuwein and Allis, 2001; Kornberg and Thomas, 1974). Chromatin in a structurally open and active state is called euchromatin. Highly compacted and constrained inactive chromatin is referred to as heterochromatin. These two forms of chromatin can be distinguished microscopically because they stain differently at the cytological level. It is generally believed that these two chromatic states, euchromatin and heterochromatin, correlate with active or inactive transcriptional states, respectively (Berger, 2007; Grunstein, 1997a; Jenuwein and Allis, 2001; Li et al., 2007a), although there are exceptions (for examples, see Devlin et al., 1990 and Carrel and Willard, 1999). In all of the examples of variegated transcription discussed above, chromatin structure plays a critical role in the mechanisms underlying the observed phenomena.

Chromatin structure is mediated (i) by occupancy and positioning of nucleosomal proteins associated with DNA, (ii) by post-translational modifications, such as acetylation

and methylation, to the histone proteins in the nucleosomes, and, in some organisms, (iii) by DNA methylation (Berger, 2007). In yeast, where DNA methylation does not occur, chromatin structure is believed to be largely determined by nucleosome localization and post-translational modifications to the histone proteins.

The nucleosome particle has been described as "the fundamental component of chromatin" (Durrin et al., 1992). The canonical nucleosome consists of a histone octamer made up of two molecules each of the histone proteins H2A, H2B, H3, and H4. Around this histone octamer, 146 base pairs of DNA are wrapped approximately 1.8 times.

Nucleosome positioning at TATA promoter elements has been shown to prevent transcription by preventing the binding of transcription initiation factors to these sequence elements (Knezetic et al., 1988; Knezetic and Luse, 1986; Lorch et al., 1987). It has also been reported that well positioned nucleosomes are actively evicted from the promoters of some genes upon promoter activation, thereby allowing the transcriptional machinery access to the promoter DNA (Korber et al., 2006; Korber et al., 2004). In experiments in which expression of the essential genes that encode histone proteins is conditionally downregulated, transcription levels have been shown to increase as nucleosomes are lost from DNA (Durrin et al., 1992; Han and Grunstein, 1988; Han et al., 1988; Kim et al., 1988; Wyrick et al., 1999). These findings suggest the existence of chromatin remodeling factors with the ability to displace nucleosomes in order to facilitate transcription. Such factors have indeed been identified in eukaryotic organisms and include complexes such as SWI-SNF and RSC, which catalyze nucleosome displacement in an ATP-dependent manner (Burns and Peterson, 1997; Cairns et al., 1996; Hirschhorn et al., 1992; Winston and Carlson, 1992).

The amino terminal tails of histone proteins contain lysine residues that are sites for reversible post-translational modifications, including acetylation, SUMOylation, methylation, and ubiquitylation, (Berger, 2007; Grunstein, 1997a; Strahl and Allis, 2000). Other residues in the histone tails, such as serines, threonines, and arginines, also undergo post-translational modifications. The histone tails are flexible and are largely external to the core nucleosome particle, so they are accessible to histone modifying enzymes that add or remove these modifications (Davey et al., 2002; Luger et al., 1997).

Certain histone modifications have been associated with transcriptionally active chromatin and others with transcriptionally repressed chromatin. Histone acetylation, for example, is strongly correlated with transcriptional activation (Grunstein, 1997a). Current thinking is that the addition of the acetyl group neutralizes the positive charge of the lysine residue, thereby decreasing the affinity of the histone for its associated DNA. This modification results in a more relaxed chromatin structure that renders DNA more accessible to transcription factors involved in transcription initiation. On the other hand, deacetylated chromosomal regions, such as telomeres, rDNA repeats, and the mating type cassettes in yeast, are heterochromatic and are associated with transcriptional silencing (Armstrong et al., 2002; Braunstein et al., 1993; Braunstein et al., 1996; Fritze et al., 1997). The observation that deacetylation of histones occurs within transcribed open reading frames (ORFs) to prevent the occurrence of spurious transcription initiation from cryptic start sites located within these ORF sequences (Carrozza et al., 2005b), an activity that appears to be particularly important at long and/or infrequently transcribed ORFs (Li et al., 2007b), is an indicator of the ability of chromatin structure to regulate transcription initiation in very localized regions at a given locus. SUMOylation, which adds large

moieties that are two-thirds the size of the histones themselves, seems to be repressive on transcription and may lead to profound chromatin structure changes owing to their bulk (Shiio and Eisenman, 2003). It has been proposed that SUMOylation might serve to block the addition of other modifications, such as acetyl groups, to histone tails, thereby inhibiting transcriptional activation (Iniguez-Lluhi, 2006). Histone methylation appears to have variable effects on transcription, perhaps depending on the precise lysine residues that are affected, the number of methyl groups added to the residue, and the positional context of nucleosomes (Briggs et al., 2001; Bryk et al., 2002; Dehe and Geli, 2006; Fingerman et al., 2005; Li et al., 2007b; Mueller et al., 2006; Ng et al., 2003; Nislow et al., 1997; Santos-Rosa et al., 2004; Tompa and Madhani, 2007). Ubiquitylation of histones also appears to have variable effects on transcription (Henry et al., 2003; Mutiu et al., 2007; Weake and Workman, 2008; Zhou et al., 2008).

Histone modifications also create binding sites for proteins by creating new surfaces for protein attachment (Verdone et al., 2005). Acetylation of lysines creates binding sites for proteins that contain bromodomains (Yang, 2004), which include proteins such as the SAGA histone acetyltransferase complex and the ATP-dependent Swi/Snf chromatin remodeling complex (Hassan et al., 2001; Hassan et al., 2002; Marmorstein and Berger, 2001; Winston and Allis, 1999). Histone methylation creates binding sites for proteins that contain chromodomains, which include examples such as the *Drosophila* HP1 and Polycomb proteins that participate in chromatin packaging and gene silencing (Nielson et al., 2002; Fischle et al., 2003).

The various enzymes that are responsible for adding and removing covalent modifications to the amino terminal tails of histones are conserved from yeast to humans

(Doyon et al., 2004; Michan and Sinclair, 2007; Schneider et al., 2005; Wang et al., 1997; Yang and Seto, 2008). These chromatin regulators do not, themselves, have sequence-specific DNA-recognition properties of their own. Instead, they appear to be recruited to specific locations in the genome by interacting with other proteins that do have target-specificity (Cosma, 2002). Histone acetyltransferases (HATs) catalyze acetylation of specific lysine residues on histone tails. Complexes with HAT activity include SAGA, ADA, NuA3, and NuA4. Histone deacetylases (HDACs) catalyze the deacetylation of lysine residues in histone tails and are found in large multiprotein complexes with transcriptional co-repressors. HDACs are grouped into three classes based on their similarity to known yeast factors: class I HDACs are similar to yeast Rpd3, class II HDACs are similar to yeast Hda1, and class III HDACs are similar to yeast Sir2 (Verdin et al., 2003; Yang and Seto, 2008). Site-specific lysine methylation of histones is catalyzed by a family of methyltransferase proteins that contain the evolutionarily conserved SET domain (Qian and Zhou, 2006).

Some chromatin remodeling enzymes work globally to alter chromatin structure, whereas others appear to have more specific roles. For example, the histone acetyltransferase component of the SAGA complex, Gcn5, is recruited to most transcriptionally active protein-coding genes, suggesting a genome-wide role for this HAT in regulating transcription (Robert et al., 2004). The HDAC Sir2 is important for heterochromatin formation at all yeast telomeres, as well as at specific locations within yeast genome, namely the silent mating cassettes and the rDNA region (Grunstein, 1997b; Kadosh and Struhl, 1997; Shore et al., 1984). The HDACs Rpd3 and Hst1 have been shown to be recruited to specific gene families in yeast. Rpd3, for example, is

recruited to the promoters of some genes involved in sporulation by the gene-specific transcription factor Ume6 (Kadosh and Struhl, 1997, 1998). Hst1, a homolog of Sir2, has also been shown to be recruited to a subset of genes involved in sporulation, in this case by the gene-specific transcription factor Sum1 (Xie et al., 1999).

Nearly twenty distinct histone acetylation and methylation states have been identified in genome-wide studies of budding yeast (Berger, 2007; Rando, 2007). Taken together, the combinatorial complexity that can be generated with this variety of chromatin marks has lead some investigators to the notion of the existence of a histone code that could "considerably extend the information potential of the genetic [DNA] code" (Strahl and Allis, 2000; Jenuwein and Allis, 2001, quoted above; Taverna et al., 2007).

Many cases have now been reported, however, that show an apparent disparity between the effect that a particular histone modification is thought to have on transcription and the level of expression observed from the target gene (Berger, 2007). The histone deacetylase Rpd3, for example, at many target genes behaves as a transcriptional repressor (Carrozza et al., 2005; Kadosh and Struhl, 1997, 1998; Rundlett et al., 1998). Recently, however, Rpd3 has been reported to act directly as a transcriptional activator at some genes. This raises an apparent paradox regarding how this histone deacetylase can behave as both an activator and a repressor of transcription.

Roles for Noncoding RNAs in Transcriptional Variegation

Noncoding RNAs have been shown to play important roles in the regulation of gene expression in many organisms. Mechanisms include targeted degradation of messenger RNAs by small interfering RNAs (siRNAs), developmentally regulated

sequence-specific translational repression of messenger RNAs by micro-RNAs (miRNAs), and targeted transcriptional gene silencing (Carrington and Ambros, 2003; Hammond et al., 2001; Hutvagner and Zamore, 2002; Mette et al., 1999; Pal-Bhadra et al., 2002). Collectively, these mechanisms in which a noncoding RNA acts in trans to regulate gene expression fall into a category of gene regulation termed RNA interference (RNAi). Interestingly, several of the instances of transcriptional variegation described above involve a noncoding RNA regulatory component that is required for the relevant heterochromatin formation.

The formation of the heterochromatin structure that is responsible for the position effects in *Drosophila* and in the fission yeast *S. pombe* described earlier both rely on a mechanism involving noncoding RNAs (Hall et al., 2002; Lippman and Martienssen, 2004; Pal-Bhadra et al., 2002; Pal-Bhadra et al., 2004; Volpe et al., 2002). At the sequence level, most DNA found near centromeres and telomeres consists of tandem repeats (Lippman and Martienssen, 2004). The repeats at centromeres range from a few kilobases in the fission yeast *S. pombe* to 100-to-400 base-pair repeats arranged in megabase-pair arrays in *Drosophila*, plants, and mammals (Lippman and Martienssen, 2004). Although the exact sequences of these repeated regions are not conserved across species, the appearance of repeated sequence elements in heterochromatic regions is conserved (Lippman and Martienssen, 2004). The basic machinery required for RNA interference mechanisms, such as Dicer and Argonaute, are also conserved across species (Fagard et al., 2000). Mutation of the RNAi machinery in *S. pombe* results in the aberrant accumulation of complementary transcripts from centromeric heterochromatin repeats (Volpe et al., 2002). This accumulation is accompanied by transcriptional

derepression of reporter genes integrated at the centromere (Volpe et al., 2002). Furthermore, a centromere-homologous repeat at the silent mating-type region in *S. pombe* is sufficient to induce heterochromatin formation at an ectopic site, suggesting that a similar RNAi mechanism may be involved in silencing both centromeric regions and the mating-type cassettes (Hall et al., 2002). Heterochromatic silencing and PEV in *Drosophila* have been shown to be affected analogously by disruptions in the conserved RNAi machinery (Pal-Bhadra et al., 2002; Pal-Bhadra et al., 2004).

In X-inactivation, the silencing of the X chromosome is nucleated at the X-inactivation center (Xic) and is then propagated bidirectionally along the length of chromosome (Panning and Jaenisch, 1996). The mechanism underlying this silencing involves the large, polyadenylated noncoding RNA *Xist* that is encoded by a gene that resides within the Xic (Panning and Jaenisch, 1996). *Xist* RNA in embryonic cells is unstable and can be detected only at the site of transcription. It can be detected at the *Xist* locus on both X chromosomes in female cells, as well as on the single X chromosome in male cells. Upon the initiation of X inactivation, *Xist* transcripts produced from the X chromosome soon to be inactivated become stabilized and spread along the arms of that copy of the X chromosome, thereby coating the chromosome and leading to the formation of dense heterochromatic structure (Panning et al., 1997; Sheardon et al., 1997). Transcription of *Xist* from the X chromosome that remains active is silenced by a mechanism involving the covalent addition of methyl groups to the transcribed region of the *Xist* DNA itself, which results in the local formation of heterochromatic structure there (Panning and Jaenisch, 1996).

Noncoding RNAs Regulate Transcription in Yeast

S. cerevisiae, which lacks key components of the conserved machinery required for RNAi-mediated regulation of gene expression, was long thought to lack mechanisms of transcriptional regulation involving noncoding RNAs. Over the past few years, however, a flurry of publications has reported various examples of noncoding RNAs that regulate transcription in yeast (Berretta et al., 2008; Camblong et al., 2007; Hongay et al., 2006; Martens et al., 2004; Martens et al., 2005). The reported mechanisms do not require the RNAi machinery. Rather, noncoding RNAs are shown to regulate transcription in cis by mechanisms that include (i) remodeling chromatin structure, (ii) competing for template sequence by running antisense into the transcript that they regulate, and (iii) occluding transcription factor binding sites within promoters by the act of transcription itself.

At the *PHO5* locus in *S. cerevisiae*, noncoding transcription appears to play a role in activation of *PHO5* transcription (Uhler et al., 2007). A long noncoding exosome-degraded transcript synthesized by RNA polymerase II initiates in the region near the 5' end of the *PHO5* ORF and is transcribed in the antisense direction up to and across the *PHO5* promoter. This transcription appears to promote the eviction of nucleosomes from the *PHO5* promoter. This chromatin remodeling then allows for transcription of the *PHO5* gene itself. Abrogation of the long noncoding transcript delays chromatin remodeling and subsequent recruitment of RNA polymerase II to the *PHO5* promoter. It has thus been proposed that noncoding transcription through positioned nucleosomes has the ability to enhance chromatin plasticity so that chromatin remodeling and activation of antisense-traversed genes occurs efficiently.

At the yeast *IME4* locus, on the other hand, antisense transcription is repressive on *IME4* expression, presumably because the sense and the antisense transcripts compete for the same template sequence when antisense transcription is active at this locus. *IME4* transcription, and the entry into the meiotic pathway that its expression induces, is repressed in haploid yeast cells (Hongay et al., 2006). This repression is due to a haploid-specific transcript that initiates in the intergenic region downstream of the *IME4* ORF. This transcript runs antisense through the *IME4* ORF and the *IME4* promoter region. In diploid cells, this antisense transcript is repressed by the binding of the diploid-specific a1/alpha2 heterodimer to a motif in the region where the antisense transcript is promoted. Thus, regulation by a long noncoding RNA serves to regulate a key cell fate decision, namely meiotic entry, in *S. cerevisiae.*

Antisense transcription has also been reported to play a repressive role on *PHO84* transcription in *S. cerevisiae* (Camblong et al., 2007). Stabilization of *PHO84* antisense transcripts is observed in mutant cells that lack the Rrp6 component of the exosome and also in aging cells in which Rrp6 levels seem to naturally decrease. Upon stabilization of these antisense transcripts, synthesis of *PHO84* sense transcripts is repressed. It is believed that Rrp6 functions to degrade the antisense transcripts at the site of transcription. Interestingly, Hda1 histone deacetylase recruitment to the region of the DNA where *PHO84* resides coincides with the absence of Rrp6 in both *rrp6* mutants and in aged cells. Although Hda1 can be detected both at *PHO84* and its neighboring genes, the histone deacetylation catalyzed by Hda1 can only be detected in regions that are transcribed in antisense.

The tight repression of the yeast *SER3* gene during growth in rich media is also under noncoding RNA regulation (Martens et al., 2004; Martens et al., 2005). During growth in rich media, a noncoding RNA is transcribed across the promoter sequence of *SER3*. This noncoding RNA, called *SRG1*, is required for repression of *SER3*. The *SRG1* transcript is transcribed by RNA polymerase II promoted by a canonical TATA box sequence located far upstream in the *SER3* promoter. It terminates just upstream of the *SER3* ORF. When *SRG1* is transcribed, the binding of transcriptional activators is reduced at the *SER3* promoter. Thus, this example of noncoding RNA-mediated repression occurs by a regulated transcription-interference mechanism in which transcription across the *SER3* promoter interferes with the binding of transcriptional activators to promoter elements.

Beyond these confirmed instances of transcriptional regulation by noncoding RNAs, genome-wide analysis has lead to the discovery of 667 transcripts occurring in intergenic regions, as well as antisense transcripts detected at 367 confirmed genes in yeast (Miura et al., 2006). Furthermore, the very recent deep sequencing of the yeast transcriptional landscape has revealed (i) the presence of potential regulatory secondary transcripts within 6% of yeast promoter regions and (ii) that 11.8% of yeast transcripts have overlapping 3' ends that could allow genes to influence the transcription of their neighbors (Nagalakshmi et al., 2008). Thus, we might have just glimpsed the tip of an iceberg of regulation by noncoding RNAs in yeast.

Regulation of *FLO* Gene Transcription and its Phenotypic Consequences in Yeast

The *FLO* (*FLO*culin) genes in *S. cerevisiae* encode a family of cell-surface glycosyl-phosphatidylinositol (GPI)-linked glycoproteins called adhesins. In the standard laboratory strain S288C, the *FLO* gene family consists of the mostly subtelomerically located *FLO1*, *FLO5*, *FLO9*, *FLO10*, *FLO11*, and a number of pseudogenes. There are additional family members present in the Sigma 1278b strain (work in preparation by Dowell, Ryan, Jansen, Boone, Gifford and Fink).

All proteins encoded by the *FLO* genes share similarities in amino acid sequence and overall protein structure. These proteins mediate a range of cell-to-cell and cell-to-surface adhesions (Guo et al., 2000). Together, the set of proteins encoded by *FLO* genes enable yeast cells to adhere to one another in a process known as flocculation, to stick to and invade inert surfaces and, in diploids, to form long filaments called pseudohyphae under environmental conditions such as nitrogen starvation. Individual *FLO* gene products promote a distinct set of overlapping phenotypes. For instance, expression of *FLO11*, the most extensively studied member of the *FLO* gene family, promotes surface adhesion and pseudohyphal growth. Expression of *FLO10* promotes surface adhesion, pseudohyphal growth, and flocculation. Expression of *FLO1* strongly promotes flocculation but has no significant effect on surface adhesion or filamentation.

The transcriptional regulation of the *FLO* genes is complex. All of the *FLO* genes have unusually large promoter regions of greater than three kilobases (kb). Careful dissection of the *FLO11* promoter has revealed the existence of at least four upstream activation sequences (UASs) and nine repression elements which, together, span at least 2.8 kb of the region upstream of the *FLO11* ORF (Rupp et al., 1999).

The MAPK and PKA signaling pathways function in parallel to activate distinct transcription factors that are known to interact with specific regions of the long promoter of *FLO11* (Halme et al., 2004; Pan and Heitman, 2002; Rupp et al., 1999). These pathways respond to environmental stimuli and, thus, regulate *FLO* gene expression in response to changes in the levels of nitrogen, carbohydrate, salt, and pH in the yeast's surrounding environment (Cullen et al., 2004; Gancedo, 2001; Palecek et al., 2002). The filamentation MAPK pathway stimulates *FLO11* transcription through the binding of the Ste12-Tec1 heterodimeric transcriptional activator to specific binding motifs (Filamentation Response Elements, or FREs) within the *FLO11* promoter. Activation of *FLO11* transcription via the PKA pathway is primarily through the activity of Tpk2, one of three different PKA proteins in yeast. Tpk2 promotes *FLO11* transcription by (i) phosphorylating and thereby inactivating the negative regulator Sfl1 and by (ii) phosphorylating and thereby activating the transcriptional activator Flo8. Sfl1 binds to the *FLO11* promoter and may recruit the Ssn6-Tup1 general repressor (Conlan and Tzamarias, 2001; Pan and Heitman, 2002). Sfl1 has also been demonstrated to recruit the Hda1 histone deacetylase to promoters, suggesting the participation of Sfl1 in chromatin-mediated repression of the *FLO11* promoter (Conlan and Tzamarias, 2001; Wu et al., 2001). DNA mobility shift assays indicate that Sfl1 or phosphorylated Flo8 bind to the *FLO11* promoter somewhere in the region -1150 to -1400 relative to the beginning of the *FLO11* ORF (Pan and Heitman, 2002). Binding of Flo8 is thought to compete with binding of Sfl1 to this region (Pan and Heitman, 2002).

Studies of the *STA1* promoter in the yeast *Saccharomyces diastaticus* have also shed light on how the *FLO11* promoter is regulated. The 5' upstream regions of the

glucoamylase-encoding *STA1* gene and the *FLO11* gene are almost identical (96%) and the genes are coregulated to a large extent (Gagiano et al., 1999). Two UAS regions have been identified in the *STA1* promoter (Kim et al., 2004a; Kim et al., 2004b). UAS1 is defined as the region spanning -1642 to -2105 relative to the beginning of the *STA1* ORF. UAS2 is defined as the region spanning -882 to -1380. Analogous sequences are located in the *FLO11* promoter at -1760 to -2175 (UAS1) and at -1000 to -1498 (UAS2).

At the *STA1* promoter, Sfl1 competes with the Ste12-Tec1 activator complex for binding of the UAS2 region (Kim et al., 2004b). The Ste12-Tec1 complex recruits the Swi/Snf chromatin remodeling complex. The Swi/Snf complex, in turn, facilitates the binding of the activator protein Flo8 to UAS1 and the formation of a looped DNA structure in the *STA1* promoter (Kim et al., 2004a). Flo8 helps recruit RNA polymerase II to the *STA1* promoter. The Srb8-11 complex (Srb/Mediator), also represses the *STA1* promoter (Kim et al., 2004b; Song and Carlson, 1998).

The differences between the *STA1* and the *FLO11* promoters consist of two inserts of 20 base pairs and 64 base pairs, small substitutions, and small deletions (Kim et al., 2004a). Some of these differences may have a profound impact on promoter activity, however. LacZ expression driven by the entire *FLO11* promoter has been reported to be approximately 20-fold lower than expression from the *STA1* promoter (Kim et al., 2004a). It has been suggested that this difference in expression may be due to two of the changes that exist between the *FLO11* and *STA1* promoters. First, an inverted repeat sequence that is the probable binding site for Flo8 and Mss11 in UAS1 has a single base change in the *FLO11* promoter. Second, the *FLO11* promoter has an incomplete FRE motif at -1269 to -1261, resulting from the insertion of two bases. These sequence

differences suggest that Flo8, Mss11, and Ste12-Tec1 may bind less efficiently to the *FLO11* promoter than to the *STA1* promoter (Kim et al., 2004a).

The *FLO10* promoter is also activated by the MAPK and PKA pathways, but at a much lower level in wild type cells (Halme et al., 2004). The *FLO10* promoter is poorly expressed in wild type yeast cells under conditions tested thus far. However *FLO10* expression can be enhanced by mutating either *IRA1* or *IRA2*, which encode GTPase-Activating proteins (GAPs) that normally function to downregulate the activity of Ras2 (Halme et al., 2004). In *ira* mutants, increased Ras2 activity presumably hyperactivates the MAPK and PKA pathways, thereby increasing activity of the *FLO10* promoter above wild type levels.

Despite all that is known and can be inferred about the transcriptional regulation of the *FLO* genes, the collected information has still been inadequate to explain the curious observation that *FLO* gene expression is heterogeneous within clonal populations of cells. The biological consequences of this heterogeneity are particularly clear when diploid *S. cerevisiae* cells of the Sigma 1278b genetic background are grown under conditions of nitrogen starvation. Under these conditions, diploid yeast cells undergo a *FLO11*-dependent developmental transition from yeast form growth to pseudohyphal growth (Gimeno et al., 1992; Rupp et al., 1999). Pseudohyphal growth involves a change to elongated cell morphology, adhesion and invasion into surfaces, and a unipolar budding pattern in which mother and daughter cells remain attached. The result is the formation of extended chains of elongated cells called pseudohyphae. When clonal populations of diploid Sigma 1278b are grown under nitrogen starvation conditions, pseudohyphal filaments form at the edge of colonies. A peculiar feature of pseudohyphal

growth is the clonal variability in the pseudohyphal growth response. The switch to pseudohyphal growth is heterogeneous within the cellular population. Some of the cells in the colony initiate pseudohyphal filament formation and divide in a pseudohyphal growth pattern for several generations, occasionally producing yeast form cells. In contrast, cells immediately neighboring the filamentous cells fail to initiate pseudohyphal growth and continue to divide as yeast form cells. This clonal heterogeneity in the pseudohyphal growth response results from variegated expression of *FLO* genes.

Because previous studies of the regulation of *FLO* genes performed by other groups have provided results that represent an average of the regulatory and transcriptional activities occurring in large populations of cells, the question of the mechanisms that underlie cell-to-cell variation in *FLO* gene expression has gone largely unaddressed. Our studies are the first to address the phenotypic variation that occurs due to cell-to-cell variability in *FLO* gene expression and the mechanisms that underlie this cell-to-cell variation.

In the chapters that follow, I present our findings regarding the mechanistic underpinnings of the variegated expression of *FLO* genes in clonal populations of yeast cells. We have identified mechanisms of *FLO* transcriptional regulation that exist in addition to those discussed above. We have demonstrated that histone deacetylases localize to the *FLO* promoters and are required for their variegated silencing. We have also identified two noncoding RNA transcripts that originate within the promoter of *FLO11* and appear to compete with one another in *cis* to regulate *FLO11* expression. One of these noncoding transcripts promotes *FLO11* expression whereas the other prevents *FLO11* expression. We have discovered an apparently analogous pair of

noncoding transcripts at the *FLO10* promoter, as well, suggesting that noncoding RNAs may be a common regulatory component at the large *FLO* promoters of yeast. At both the *FLO11* and *FLO10* promoters, transcription of these noncoding regulatory RNAs is affected by the presence of Sfl1, thus expanding the model for how this well established repressor of *FLO* transcription performs its function.

In Chapter Four of this thesis, I will present a model in which chromatin structure and transcription of competing noncoding RNAs across regions of the *FLO* promoters regulates variegated transcription of these genes. The model proposes that dynamic competition for interactions with *FLO* promoter sequences by *trans*-acting protein factors determines a switch between chromatin states either permissive or repressive of transcription. The alternate chromatin states regulate transcription of noncoding RNAs, which themselves ultimately affect *FLO11* expression. Thus, competitive binding by transcription factors forms the basis of a toggle switch between exclusive transcription states that underlie the observed cell-to-cell variation in *FLO* gene expression.

Contemporary shifts in the way that we understand alternate promoter states help to inform this matter. The large protein complexes that regulate transcription have long been thought to form stable, multi-factor complexes that remain in residence on a DNA template for extended periods of time. These complexes are thought then to recruit other transcription factors in stepwise development towards an active or repressed promoter state. New technologies have allowed direct measurement of the residence times of protein factors on promoters (Hager et al., 2006). In contrast to the long accepted paradigm, the reality appears to be one of regulatory proteins moving rapidly on and off the promoters they regulate (Hager et al., 2006). This “return to template” model, as it is

called, suggests that interactions between promoters and transcription factors are dynamic and even stochastic (Hager et al., 2006). Dynamic sampling of and competition for *FLO* promoter interaction by *trans*-acting regulators thus forms the toggle between alternate chromatin states that determine which regulatory noncoding RNA is transcribed at any given time, which in turn determines whether or not *FLO11* is expressed.

Just Noise, or Something More?

There has been debate in the literature over how to think about this phenomenon that we call transcriptional variegation. Others have referred to variegated expression as "noise" in gene expression (Raser and O'Shea, 2005). They claim that such biological variation is inevitable because of the random stochastic nature of chemical reactions within the cell. They argue that, when large numbers of molecules are present, chemical reactions may proceed in a predictable manner, but when a specific type of molecule exists in very low numbers, stochastic effects due to limitation of this molecule may become prominent. Since only one or a few copies of DNA, RNA, and proteins of a certain type might be present and active in each cell at any given time, the abundance of a given gene product is theoretically sensitive to stochastic fluctuations. In a different line of argument, they point out that, despite the fact that we might believe that clonal populations of cells are growing in identical conditions, microenvironments might exist that are undetectable to the experimenter but that are influencing the cellular population differentially. Apparently disregarding the observation that the transcriptional activation state is reversible in instances of transcriptional variegation, they also suggest that the random mutation that occurs within a population of cells compromises the notion that the clonal population is genetically identical and may explain, or at least contribute to, the

observed variation. These arguments, therefore, attempt to explain away phenotypic variation in clonal populations of cells resulting from transcriptional variegation as a problem of small numbers or limitations in experimental detection.

Even if mechanisms that underlie transcriptional variegation involve some measure of stochastic activity, it is important to keep in mind that "stochastic" does not imply "unimportant" or "unselected". Cell-to-cell variation in gene expression has been measured on a global scale, but its importance to the fitness of an organism is not yet entirely clear. Recent findings do suggest that evolution actually selects against "noise" in gene expression (Lehner, 2008). Global analyses of gene expression in yeast have revealed that essential genes tend to show lower cell-to-cell fluctuation in their expression than nonessential genes do (Batada and Hurst, 2007; Newman et al., 2006). Addressing the "small numbers" argument, this finding could be explained by all essential genes being highly expressed, but it turns out that this is not the case. The set of yeast genes shown to have high levels of cell-to-cell variation is depleted of genes that reduce fitness when their expression is increased, as well as of those that reduce fitness when their expression is reduced (Lehner, 2008). From these observations that cell-to-cell fluctuations in gene expression appear to be subject to biological selection, the conclusion has been drawn that such variation represents an important biological trait (Lehner, 2008).

Minimally, it follows from the above observations that genes which show high levels of cell-to-cell variation in expression do not reduce organismal fitness. These findings also raise the possibility that the high levels of variation in gene expression observed at some loci might actually increase fitness. Under the "return to template"

model for regulation of promoter activity discussed above (Hager et al., 2006), one might predict that genes subject to very complex regulation with the involvement of many competing activator and repressor signals, such as those converging on the unusually large *FLO* promoters (Pan and Heitman, 2002; Kim et al., 2004a; Kim et al., 2004b), would be more likely to exhibit high levels of transcriptional variegation because of the wide range of possible dynamic interactions occurring between the promoter and *trans*-acting factors at any given time. Most interactions occurring at any given time are non-productive because the promoter itself must be in the appropriate state for interaction with a given regulator to be effective (Hager et al., 2006). As productive interactions occur, the promoter chromatin could evolve through a series of modified states, each state serving as a new substrate for subsequent dynamic interactions with *trans*-acting regulators (Hager et al., 2006).

Complex regulatory mechanisms that introduce fluctuation in gene expression have apparently been selected against in nature (Lehner, 2008). Perhaps where such regulatory mechanisms do exist, they have been selected in evolution because they provide a net benefit for the organism. If this prediction is reflective of reality, then the variegated transcription observed from the large promoters of the *FLO* genes in *S. cerevisiae* may have been selected in evolution because it provides a net benefit to the yeast population. As in the examples of microbial antigenic variation discussed above, the variegated expression of members of the *FLO* gene family may have evolved because it provides a selective advantage to clonal populations of yeast cells. In *S. cerevisiae*, variegated transcription is observed from the promoters of at least three members of the *FLO* gene family, namely the promoters of *FLO1*, *FLO10*, and *FLO11* (Halme et al.,

2004). This pattern of gene expression translates into the potential for variegated promotion of flocculation (i.e., cell-to-cell adhesion), haploid adhesion to surfaces and invasive growth, and diploid pseudohyphal growth within a clonal population of yeast cells (Palecek et al., 2002; Verstrepen et al., 2004). What could this mean for a population of yeast out in the wild? Within a clonal population growing under the same environmental conditions, some of the cells in the population may have an active *FLO* promoter and will be expressing the *FLO* gene under its control while other cells in the population will be silent at this *FLO* promoter and will not be expressing the given *FLO* gene. This variegated expression from *FLO* gene promoters may well promote survival of clonal populations of yeast when these populations are exposed to various environmental stresses. Imagine the likely case in which a nutrient in the yeast population's immediate environment becomes depleted. It would be advantageous for some cells within the clonal population to be poised, as a result of variegated transcription from the *FLO11* promoter, to produce pseudohyphal filaments able to grow directionally toward neighboring environments that may be more hospitable. Meanwhile, other cells in the population would, as a result of heterogeneous *FLO* gene expression, be poised to maintain the initial colony (perhaps a good thing in the case that the current environment is actually the best available), or to wash off to far away places that may prove more hospitable to the yeast.

In summary, the *FLO11* promoter is one of the largest promoters in yeast and receives a complex combination of signals, some of them competitive, from upstream signaling pathways. The net effect of all regulatory stimulus on the *FLO11* promoter is variegated transcriptional silencing that results in phenotypic variation within a clonal

population of yeast cells. In this thesis, I examine the chromatin modifying proteins that localize to *FLO* promoters and act in *trans* to affect *FLO* gene transcription. I describe the results of genome-wide screens that identified additional *trans*-acting chromatin modifying factors that play a role in regulating the *FLO* promoters. Some of the candidates identified in these screens, in particular the components of the Rpd3L histone deacetylase complex, have effects on *FLO* gene transcription that initially seemed paradoxical because their net effect is the opposite of that predicted by contemporary theories regarding the role of chromatin structure in regulating transcription. Careful analysis of these mutants, their phenotypes, the transcription of *FLO11*, and most importantly, the noncoding transcripts that we have detected in the promoter region of *FLO11*, have revealed the basis for this apparent paradox.

References

Armstrong, C.M., Kaeberlein, M., Imai, S.I., and Guarente, L. (2002). Mutations in Saccharomyces cerevisiae gene SIR2 can have differential effects on in vivo silencing phenotypes and in vitro histone deacetylation activity. Molecular Biology of the Cell *13*, 1427-1438.

Batada, N.N., and Hurst, L.D. (2007). Evolution of chromosome organization driven by selection for reduced gene expression noise. Nature Genetics *39*, 945-949.

Berger, S.L. (2007). The complex language of chromatin regulation during transcription. Nature *447*, 407-412.

Berretta, J., Pinskaya, M., and Morillon, A. (2008). A cryptic unstable transcript mediates transcriptional trans-silencing of the Ty1 retrotransposon in S. cerevisiae. Genes & Development *22*, 615-626.

Borst, P. (2002). Antigenic variation and allelic exclusion. Cell *109*, 5-8.

Braunstein, M., Rose, A.B., Holmes, S.G., Allis, C.D., and Broach, J.R. (1993). Transcriptional silencing in yeast is associated with reduced nucleosome acetylation. Genes & Development *7*, 592-604.

Braunstein, M., Sobel, R.E., Allis, C.D., Turner, B.M., and Broach, J.R. (1996). Efficient transcriptional silencing in Saccharomyces cerevisiae requires a heterochromatin histone acetylation pattern. Molecular and Cellular Biology *16*, 4349-4356.

Briggs, S.D., Bryk, M., Strahl, B.D., Cheung, W.L., Davie, J.K., Dent, S.Y., Winston, F., and Allis, C.D. (2001). Histone H3 lysine 4 methylation is mediated by Set1 and required for cell growth and rDNA silencing in Saccharomyces cerevisiae. Genes & Development *15*, 3286-3295.

Bryk, M., Briggs, S.D., Strahl, B.D., Curcio, M.J., Allis, C.D., and Winston, F. (2002). Evidence that Set1, a factor required for methylation of histone H3, regulates rDNA silencing in S. cerevisiae by a Sir2-independent mechanism. Curr Biol *12*, 165-170.

Burns, L.G., and Peterson, C.L. (1997). Protein complexes for remodeling chromatin. Biochimica et Biophysica Acta *1350*, 159-168.

Cairns, B.R., Lorch, Y., Li, Y., Zhang, M., Lacomis, L., Erdjument-Bromage, H., Tempst, P., Du, J., Laurent, B., and Kornberg, R.D. (1996). RSC, an essential, abundant chromatin-remodeling complex. Cell *87*, 1249-1260.

Camblong, J., Iglesias, N., Fickentscher, C., Dieppois, G., and Stutz, F. (2007). Antisense RNA stabilization induces transcriptional gene silencing via histone deacetylation in S. cerevisiae. Cell *131*, 706-717.

Carrel, L., and Willard, H.F. (1999). Heterogeneous gene expression from the inactive X chromosome: an X-linked gene that escapes X inactivation in some human cell lines but is inactivated in others. Proc Natl Acad Sci *96*, 7364-7369.

Carrington, J.C., and Ambros, V. (2003). Role of microRNAs in plant and animal development. Science *301*, 336-338.

Carrozza, M.J., Florens, L., Swanson, S.K., Shia, W.J., Anderson, S., Yates, J., Washburn, M.P., and Workman, J.L. (2005). Stable incorporation of sequence specific repressors Ash1 and Ume6 into the Rpd3L complex. Biochimica et Biophysica Acta *1731*, 77-87; discussion 75-76.

Conlan, R.S., and Tzamarias, D. (2001). Sfl1 functions via the co-repressor Ssn6-Tup1 and the cAMP-dependent protein kinase Tpk2. Journal of Molecular Biology *309*, 1007-1015.

Cosma, M.P. (2002). Ordered recruitment: gene-specific mechanism of transcription activation. Molecular Cell *10*, 227-236.

Cullen, P.J., Sabbagh, W., Jr., Graham, E., Irick, M.M., van Olden, E.K., Neal, C., Delrow, J., Bardwell, L., and Sprague, G.F., Jr. (2004). A signaling mucin at the head of the Cdc42- and MAPK-dependent filamentous growth pathway in yeast. Genes & Development *18*, 1695-1708.

Davey, C.A., Sargent, D.F., Luger, K., Maeder, A.W., and Richmond, T.J. (2002). Solvent mediated interactions in the structure of the nucleosome core particle at 1.9 a resolution. Journal of Molecular Biology *319*, 1097-1113.

De Las Penas, A., Pan, S.J., Castano, I., Alder, J., Cregg, R., and Cormack, B.P. (2003). Virulence-related surface glycoproteins in the yeast pathogen Candida glabrata are encoded in subtelomeric clusters and subject to RAP1- and SIR-dependent transcriptional silencing. Genes & Development *17*, 2245-2258.

Dehe, P.M., and Geli, V. (2006). The multiple faces of Set1. Biochemistry and Cell Biology *84*, 536-548.

Devlin, R.H., Bingham, B., and Wakimoto, B.T. (1990). The organization and expression of the light gene, a heterochromatic gene of Drosophila melanogaster. Genetics *125*, 129-140.

Doyon, Y., Selleck, W., Lane, W.S., Tan, S., and Cote, J. (2004). Structural and functional conservation of the NuA4 histone acetyltransferase complex from yeast to humans. Molecular and Cellular Biology *24*, 1884-1896.

Durrin, L.K., Mann, R.K., and Grunstein, M. (1992). Nucleosome loss activates CUP1 and HIS3 promoters to fully induced levels in the yeast Saccharomyces cerevisiae. Molecular and Cellular Biology *12*, 1621-1629.

Edwards, J.R., and Bestor, T.H. (2007). Gene regulation: stochastic and deterministic effects in gene regulation. Heredity *99*, 243-244.

Fagard, M., Boutet, S., Morel, J.B., Bellini, C., and Vaucheret, H. (2000). AGO1, QDE-2, and RDE-1 are related proteins required for post-transcriptional gene silencing in plants, quelling in fungi, and RNA interference in animals. Proc Natl Acad Sci *97*, 11650-11654.

Fingerman, I.M., Wu, C.L., Wilson, B.D., and Briggs, S.D. (2005). Global loss of Set1-mediated H3 Lys4 trimethylation is associated with silencing defects in Saccharomyces cerevisiae. The Journal of Biological Chemistry *280*, 28761-28765.

Fischle, W., Wang, Y., Jacobs, S.A., Kim, Y., Allis, C.D., Khorasanizadeh, S. (2003). Molecular basis for the discrimination of repressive methyl-lysine marks in histone H3 by Polycomb and HP1 chromodomains. Genes & Development *17*, 1870-1881.

Freitas-Junior, L.H., Hernandez-Rivas, R., Ralph, S.A., Montiel-Condado, D., Ruvalcaba-Salazar, O.K., Rojas-Meza, A.P., Mancio-Silva, L., Leal-Silvestre, R.J., Gontijo, A.M., Shorte, S., *et al.* (2005). Telomeric heterochromatin propagation and histone acetylation control mutually exclusive expression of antigenic variation genes in malaria parasites. Cell *121*, 25-36.

Fritze, C.E., Verschueren, K., Strich, R., and Easton Esposito, R. (1997). Direct evidence for SIR2 modulation of chromatin structure in yeast rDNA. The EMBO Journal *16*, 6495-6509.

Gagiano, M., Van Dyk, D., Bauer, F.F., Lambrechts, M.G., and Pretorius, I.S. (1999). Divergent regulation of the evolutionarily closely related promoters of the Saccharomyces cerevisiae STA2 and MUC1 genes. Journal of Bacteriology *181*, 6497-6508.

Gancedo, J.M. (2001). Control of pseudohyphae formation in Saccharomyces cerevisiae. FEMS Microbiology Reviews *25*, 107-123.

Gimeno, C.J., Ljungdahl, P.O., Styles, C.A., and Fink, G.R. (1992). Unipolar cell divisions in the yeast S. cerevisiae lead to filamentous growth: regulation by starvation and RAS. Cell *68*, 1077-1090.

Gottschling, D.E., Aparicio, O.M., Billington, B.L., and Zakian, V.A. (1990). Position effect at S. cerevisiae telomeres: reversible repression of Pol II transcription. Cell *63*, 751-762.

Grewal, S.I., and Klar, A.J. (1996). Chromosomal inheritance of epigenetic states in fission yeast during mitosis and meiosis. Cell *86*, 95-101.

Grunstein, M. (1997a). Histone acetylation in chromatin structure and transcription. Nature *389*, 349-352.

Grunstein, M. (1997b). Molecular model for telomeric heterochromatin in yeast. Current Opinion in Cell Biology *9*, 383-387.

Guo, B., Styles, C.A., Feng, Q., and Fink, G.R. (2000). A Saccharomyces gene family involved in invasive growth, cell-cell adhesion, and mating. Proceedings of the National Academy of Sciences of the United States of America *97*, 12158-12163.

Hager, G.L., Elbi, C., Johnson, T.A., Voss, T., Nagaich, A.K., Schiltz, R.L., Qiu, Y., and John, S. (2006). Chromatin dynamics and the evolution of alternate promoter states. Chromosome Res *14*, 107-116.

Hall, I.M., Shankaranarayana, G.D., Noma, K., Ayoub, N., Cohen, A., and Grewal, S.I. (2002). Establishment and maintenance of a heterochromatin domain. Science *297*, 2232-2237.

Halme, A., Bumgarner, S., Styles, C., and Fink, G.R. (2004). Genetic and epigenetic regulation of the FLO gene family generates cell-surface variation in yeast. Cell *116*, 405-415.

Hammond, S.M., Caudy, A.A., and Hannon, G.J. (2001). Post-transcriptional gene silencing by double-stranded RNA. Nat Rev Genet *2*, 110-119.

Han, M., and Grunstein, M. (1988). Nucleosome loss activates yeast downstream promoters in vivo. Cell *55*, 1137-1145.

Han, M., Kim, U.J., Kayne, P., and Grunstein, M. (1988). Depletion of histone H4 and nucleosomes activates the PHO5 gene in Saccharomyces cerevisiae. The EMBO Journal *7*, 2221-2228.

Hassan, A.H., Neely, K.E., and Workman, J.L. (2001). Histone acetyltransferase complexes stabilize swi/snf binding to promoter nucleosomes. Cell *104*, 817-827.

Hassan, A.H., Prochasson, P., Neely, K.E., Galasinski, S.C., Chandy, M., Carrozza, M.J., and Workman, J.L. (2002). Function and selectivity of bromodomains in anchoring chromatin-modifying complexes to promoter nucleosomes. Cell *111*, 369-379.

Henikoff, S. (1979). Position Effects and Variegation Enhancers in an Autosomal Region of DROSOPHILA MELANOGASTER. Genetics *93*, 105-115.

Henikoff, S. (1990). Position-effect variegation after 60 years. Trends Genet *6*, 422-426.

Henry, K.W., Wyce, A., Lo, W.S., Duggan, L.J., Emre, N.C., Kao, C.F., Pillus, L., Shilatifard, A., Osley, M.A., and Berger, S.L. (2003). Transcriptional activation via sequential histone H2B ubiquitylation and deubiquitylation, mediated by SAGA-associated Ubp8. Genes & Development *17*, 2648-2663.

Hirschhorn, J.N., Brown, S.A., Clark, C.D., and Winston, F. (1992). Evidence that SNF2/SWI2 and SNF5 activate transcription in yeast by altering chromatin structure. Genes & Development *6*, 2288-2298.

Hongay, C.F., Grisafi, P.L., Galitski, T., and Fink, G.R. (2006). Antisense transcription controls cell fate in Saccharomyces cerevisiae. Cell *127*, 735-745.

Hutvagner, G., and Zamore, P.D. (2002). RNAi: nature abhors a double-strand. Current Opinion in Genetics & Development *12*, 225-232.

Iniguez-Lluhi, J.A. (2006). For a healthy histone code, a little SUMO in the tail keeps the acetyl away. ACS Chemical Biology *1*, 204-206.

Jenuwein, T., and Allis, C.D. (2001). Translating the histone code. Science *293*, 1074-1080.

Kadosh, D., and Struhl, K. (1997). Repression by Ume6 involves recruitment of a complex containing Sin3 corepressor and Rpd3 histone deacetylase to target promoters. Cell *89*, 365-371.

Kadosh, D., and Struhl, K. (1998). Targeted recruitment of the Sin3-Rpd3 histone deacetylase complex generates a highly localized domain of repressed chromatin in vivo. Molecular and Cellular Biology *18*, 5121-5127.

Kim, T.S., Kim, H.Y., Yoon, J.H., and Kang, H.S. (2004a). Recruitment of the Swi/Snf complex by Ste12-Tec1 promotes Flo8-Mss11-mediated activation of STA1 expression. Molecular and Cellular Biology *24*, 9542-9556.

Kim, T.S., Lee, S.B., and Kang, H.S. (2004b). Glucose repression of STA1 expression is mediated by the Nrg1 and Sfl1 repressors and the Srb8-11 complex. Molecular and Cellular Biology *24*, 7695-7706.

Kim, U.J., Han, M., Kayne, P., and Grunstein, M. (1988). Effects of histone H4 depletion on the cell cycle and transcription of Saccharomyces cerevisiae. The EMBO Journal *7*, 2211-2219.

Knezetic, J.A., Jacob, G.A., and Luse, D.S. (1988). Assembly of RNA polymerase II preinitiation complexes before assembly of nucleosomes allows efficient initiation of transcription on nucleosomal templates. Molecular and Cellular Biology *8*, 3114-3121.

Knezetic, J.A., and Luse, D.S. (1986). The presence of nucleosomes on a DNA template prevents initiation by RNA polymerase II in vitro. Cell *45*, 95-104.

Korber, P., Barbaric, S., Luckenbach, T., Schmid, A., Schermer, U.J., Blaschke, D., and Horz, W. (2006). The histone chaperone Asf1 increases the rate of histone eviction at the yeast PHO5 and PHO8 promoters. The Journal of Biological Chemistry *281*, 5539-5545.

Korber, P., Luckenbach, T., Blaschke, D., and Horz, W. (2004). Evidence for histone eviction in trans upon induction of the yeast PHO5 promoter. Molecular and Cellular Biology *24*, 10965-10974.

Kornberg, R.D., and Thomas, J.O. (1974). Chromatin structure; oligomers of the histones. Science *184*, 865-868.

Kutty, G., Ma, L., and Kovacs, J.A. (2001). Characterization of the expression site of the major surface glycoprotein of human-derived Pneumocystis carinii. Molecular Microbiology *42*, 183-193.

Lehner, B. (2008). Selection to minimise noise in living systems and its implications for the evolution of gene expression. Molecular Systems Biology *4*, 170.

Li, B., Carey, M., and Workman, J.L. (2007a). The role of chromatin during transcription. Cell *128*, 707-719.

Li, B., Gogol, M., Carey, M., Pattenden, S.G., Seidel, C., and Workman, J.L. (2007b). Infrequently transcribed long genes depend on the Set2/Rpd3S pathway for accurate transcription. Genes & Development *21*, 1422-1430.

Lippman, Z., and Martienssen, R. (2004). The role of RNA interference in heterochromatic silencing. Nature *431*, 364-370.

Lorch, Y., LaPointe, J.W., and Kornberg, R.D. (1987). Nucleosomes inhibit the initiation of transcription but allow chain elongation with the displacement of histones. Cell *49*, 203-210.

Luger, K., Mader, A.W., Richmond, R.K., Sargent, D.F., and Richmond, T.J. (1997). Crystal structure of the nucleosome core particle at 2.8 A resolution. Nature *389*, 251-260.

Marmorstein, R., and Berger, S.L. (2001). Structure and function of bromodomains in chromatin-regulating complexes. Gene *272*, 1-9.

Martens, J.A., Laprade, L., and Winston, F. (2004). Intergenic transcription is required to repress the Saccharomyces cerevisiae SER3 gene. Nature *429*, 571-574.

Martens, J.A., Wu, P.Y., and Winston, F. (2005). Regulation of an intergenic transcript controls adjacent gene transcription in Saccharomyces cerevisiae. Genes & Development *19*, 2695-2704.

Messmer, S., Franke, A., and Paro, R. (1992). Analysis of the functional role of the Polycomb chromo domain in Drosophila melanogaster. Genes & Development *6*, 1241-1254.

Mette, M.F., van der Winden, J., Matzke, M.A., and Matzke, A.J. (1999). Production of aberrant promoter transcripts contributes to methylation and silencing of unlinked homologous promoters in trans. The EMBO Journal *18*, 241-248.

Michan, S., and Sinclair, D. (2007). Sirtuins in mammals: insights into their biological function. The Biochemical Journal *404*, 1-13.

Migeon, B.R. (1994). X-chromosome inactivation: molecular mechanisms and genetic consequences. Trends Genet *10*, 230-235.

Miura, F., Kawaguchi, N., Sese, J., Toyoda, A., Hattori, M., Morishita, S., and Ito, T. (2006). A large-scale full-length cDNA analysis to explore the budding yeast transcriptome. Proceedings of the National Academy of Sciences of the United States of America *103*, 17846-17851.

Mueller, J.E., Canze, M., and Bryk, M. (2006). The requirements for COMPASS and Paf1 in transcriptional silencing and methylation of histone H3 in Saccharomyces cerevisiae. Genetics *173*, 557-567.

Mutiu, A.I., Hoke, S.M., Genereaux, J., Liang, G., and Brandl, C.J. (2007). The role of histone ubiquitylation and deubiquitylation in gene expression as determined by the analysis of an HTB1(K123R) Saccharomyces cerevisiae strain. Mol Genet Genomics *277*, 491-506.

Nagalakshmi, U., Wang, Z., Waern, K., Shou, C., Raha, D., Gerstein, M., and Snyder, M. (2008). The Transcriptional Landscape of the Yeast Genome Defined by RNA Sequencing. Science *320*, 1344-1349.

Newman, J.R., Ghaemmaghami, S., Ihmels, J., Breslow, D.K., Noble, M., DeRisi, J.L., and Weissman, J.S. (2006). Single-cell proteomic analysis of S. cerevisiae reveals the architecture of biological noise. Nature *441*, 840-846.

Ng, H.H., Robert, F., Young, R.A., and Struhl, K. (2003). Targeted recruitment of Set1 histone methylase by elongating Pol II provides a localized mark and memory of recent transcriptional activity. Molecular Cell *11*, 709-719.

Nielsen, P.R., Nietlispach, D., Mott, H.R., Callaghan, J., Bannister, A., Kouzarides, T., Murzin, A.G., Murzina, N.V., Laue, E.D. (2002). Structure of the HP1 chromodomain bound to histone H3 methylated at lysine 9. Nature *416*, 103-107.

Nislow, C., Ray, E., and Pillus, L. (1997). SET1, a yeast member of the trithorax family, functions in transcriptional silencing and diverse cellular processes. Molecular Biology of the Cell *8*, 2421-2436.

Pal-Bhadra, M., Bhadra, U., and Birchler, J.A. (2002). RNAi related mechanisms affect both transcriptional and posttranscriptional transgene silencing in Drosophila. Molecular Cell *9*, 315-327.

Pal-Bhadra, M., Leibovitch, B.A., Gandhi, S.G., Rao, M., Bhadra, U., Birchler, J.A., and Elgin, S.C. (2004). Heterochromatic silencing and HP1 localization in Drosophila are dependent on the RNAi machinery. Science *303*, 669-672.

Palecek, S.P., Parikh, A.S., and Kron, S.J. (2002). Sensing, signalling and integrating physical processes during Saccharomyces cerevisiae invasive and filamentous growth. Microbiology (Reading, England) *148*, 893-907.

Pan, X., and Heitman, J. (2002). Protein kinase A operates a molecular switch that governs yeast pseudohyphal differentiation. Molecular and Cellular Biology *22*, 3981-3993.

Panning, B., and Jaenisch, R. (1996). DNA hypomethylation can activate Xist expression and silence X-linked genes. Genes & Development *10*, 1991-2002.

Panning, B., Dausman, J., and Jaenisch, R. (1997). X chromosome inactivation is mediated by Xist RNA stabilization. Cell *90*, 907-916.

Panning, B., and Jaenisch, R. (1998). RNA and the epigenetic regulation of X chromosome inactivation. Cell *93*, 305-308.

Qian, C., and Zhou, M.M. (2006). SET domain protein lysine methyltransferases: Structure, specificity and catalysis. Cell Mol Life Sci *63*, 2755-2763.

Rando, O.J. (2007). Chromatin structure in the genomics era. Trends Genet *23*, 67-73.

Raser, J.M., and O'Shea, E.K. (2005). Noise in gene expression: origins, consequences, and control. Science *309*, 2010-2013.

Robert, F., Pokholok, D.K., Hannett, N.M., Rinaldi, N.J., Chandy, M., Rolfe, A., Workman, J.L., Gifford, D.K., and Young, R.A. (2004). Global position and recruitment of HATs and HDACs in the yeast genome. Molecular Cell *16*, 199-209.

Rubio, J.P., Thompson, J.K., and Cowman, A.F. (1996). The var genes of Plasmodium falciparum are located in the subtelomeric region of most chromosomes. The EMBO Journal *15*, 4069-4077.

Rundlett, S.E., Carmen, A.A., Suka, N., Turner, B.M., and Grunstein, M. (1998). Transcriptional repression by UME6 involves deacetylation of lysine 5 of histone H4 by RPD3. Nature *392*, 831-835.

Rupp, S., Summers, E., Lo, H.J., Madhani, H., and Fink, G. (1999). MAP kinase and cAMP filamentation signaling pathways converge on the unusually large promoter of the yeast FLO11 gene. The EMBO Journal *18*, 1257-1269.

Santos-Rosa, H., Bannister, A.J., Dehe, P.M., Geli, V., and Kouzarides, T. (2004). Methylation of H3 lysine 4 at euchromatin promotes Sir3p association with heterochromatin. The Journal of Biological Chemistry *279*, 47506-47512.

Schneider, J., Wood, A., Lee, J.S., Schuster, R., Dueker, J., Maguire, C., Swanson, S.K., Florens, L., Washburn, M.P., and Shilatifard, A. (2005). Molecular regulation of histone H3 trimethylation by COMPASS and the regulation of gene expression. Molecular Cell *19*, 849-856.

Sheardon, S.A., Duthie, S.M., Johnston, C.M., Newall, A.E., Formstone, E.J., Arkell, R.M., Nesterova, T.B., Alghisi, G.C., Rastan, S., and Brockdorff, N. (1997). Stabilization of Xist RNA mediates initiation of X chromosome inactivation. Cell *91*, 99-107.

Shiio, Y., and Eisenman, R.N. (2003). Histone sumoylation is associated with transcriptional repression. Proceedings of the National Academy of Sciences of the United States of America *100*, 13225-13230.

Shore, D., Squire, M., and Nasmyth, K.A. (1984). Characterization of two genes required for the position-effect control of yeast mating-type genes. The EMBO Journal *3*, 2817-2823.

Song, W., and Carlson, M. (1998). Srb/mediator proteins interact functionally and physically with transcriptional repressor Sfl1. The EMBO Journal *17*, 5757-5765.

Spradling, A.C., and Karpen, G.H. (1990). Sixty years of mystery. Genetics *126*, 779-784.

Strahl, B.D., and Allis, C.D. (2000). The language of covalent histone modifications. Nature *403*, 41-45.

Jenuwein, T., and Allis, C.D. (2001). Translating the histone code. Science *293*, 1074-1080.

Taverna, S.D., Li, H., Ruthenburg, A.J., Allis, C.D., and Patel, D.J. (2007). How chromatin-binding modules interpret histone modifications: lessons from professional pocket pickers. Nature Structural & Molecular Biology *14*, 1025-1040.

Tompa, R., and Madhani, H.D. (2007). Histone H3 lysine 36 methylation antagonizes silencing in Saccharomyces cerevisiae independently of the Rpd3S histone deacetylase complex. Genetics *175*, 585-593.

Uhler, J.P., Hertel, C., and Svejstrup, J.Q. (2007). A role for noncoding transcription in activation of the yeast PHO5 gene. Proceedings of the National Academy of Sciences of the United States of America *104*, 8011-8016.

Underwood, A.P., Louis, E.J., Borts, R.H., Stringer, J.R., and Wakefield, A.E. (1996). Pneumocystis carinii telomere repeats are composed of TTAGGG and the subtelomeric sequence contains a gene encoding the major surface glycoprotein. Molecular Microbiology *19*, 273-281.

Verdin, E., Dequiedt, F., and Kasler, H.G. (2003). Class II histone deacetylases: versatile regulators. Trends Genet *19*, 286-293.

Verdone, L., Caserta, M., and Di Mauro, E. (2005). Role of histone acetylation in the control of gene expression. Biochem Cell Biol *83*, 344-353.

Verstrepen, K.J., Reynolds, T.B., and Fink, G.R. (2004). Origins of variation in the fungal cell surface. Nat Rev Microbiol *2*, 533-540.

Volpe, T.A., Kidner, C., Hall, I.M., Teng, G., Grewal, S.I., and Martienssen, R.A. (2002). Regulation of heterochromatic silencing and histone H3 lysine-9 methylation by RNAi. Science *297*, 1833-1837.

Wang, L., Mizzen, C., Ying, C., Candau, R., Barlev, N., Brownell, J., Allis, C.D., and Berger, S.L. (1997). Histone acetyltransferase activity is conserved between yeast and human GCN5 and is required for complementation of growth and transcriptional activation. Molecular and Cellular Biology *17*, 519-527.

Weake, V.M., and Workman, J.L. (2008). Histone ubiquitination: triggering gene activity. Molecular Cell *29*, 653-663.

Winston, F., and Allis, C.D. (1999). The bromodomain: a chromatin-targeting module? Nature Structural Biology *6*, 601-604.

Winston, F., and Carlson, M. (1992). Yeast SNF/SWI transcriptional activators and the SPT/SIN chromatin connection. Trends Genet *8*, 387-391.

Wu, J., Suka, N., Carlson, M., and Grunstein, M. (2001). TUP1 utilizes histone H3/H2B-specific HDA1 deacetylase to repress gene activity in yeast. Molecular cell *7*, 117-126.

Wyrick, J.J., Holstege, F.C., Jennings, E.G., Causton, H.C., Shore, D., Grunstein, M., Lander, E.S., and Young, R.A. (1999). Chromosomal landscape of nucleosome-dependent gene expression and silencing in yeast. Nature *402*, 418-421.

Xie, J., Pierce, M., Gailus-Durner, V., Wagner, M., Winter, E., and Vershon, A.K. (1999). Sum1 and Hst1 repress middle sporulation-specific gene expression during mitosis in Saccharomyces cerevisiae. The EMBO Journal *18*, 6448-6454.

Yang, X.J. (2004). Lysine acetylation and the bromodomain: a new partnership for signaling. Bioessays *26*, 1076-1087.

Yang, X.J., and Seto, E. (2008). The Rpd3/Hda1 family of lysine deacetylases: from bacteria and yeast to mice and men. Nature Reviews *9*, 206-218.

Zhou, W., Zhu, P., Wang, J., Pascual, G., Ohgi, K.A., Lozach, J., Glass, C.K., and Rosenfeld, M.G. (2008). Histone H2A monoubiquitination represses transcription by inhibiting RNA polymerase II transcriptional elongation. Molecular Cell *29*, 69-80.

Chapter 2

Genetic and Epigenetic Regulation of the *FLO* Gene Family Generates Cell-Surface Variation in Yeast

Author's Note | The material presented in this chapter was originally published as: Adrian Halme, Stacie Bumgarner, Cora Style, and Gerald R. Fink (2004). "Genetic and Epigenetic Regulation of the *FLO* Gene Family Generates Cell-Surface Variation in Yeast." Cell *116*, 405-415.

I contributed to this work by generating and characterizing the phenotypes of a number of the mutant yeast strains that were used in the portions of this study relating to the role of chromatin structure in mediating the epigenetic silencing observed at the *FLO10* and *FLO11* promoters.

A subset of the work presented in this chapter deals with phenotypic switching resulting from spontaneous mutations in the genes *IRA1* and *IRA2* that encode GTP-ase activating proteins. These proteins regulate Ras2 activity and the downstream PKA and MAPK pathways that converge upon the *FLO* promoters. The *IRA* phenomenon is not itself involved in the chromatin-mediated regulation of *FLO10* and *FLO11*. It does however enhance the expression of the *FLO10* gene, thereby revealing the epigenetic silencing that occurs at this promoter. In later chapters of this thesis, the *ira1* mutation is used as a tool for revealing the variegated silencing at *FLO10*, but is otherwise unimportant to this subsequent work.

Abstract | The *FLO* gene family of *Saccharomyces cerevisiae* includes an expressed gene, *FLO11*, and a set of silent, telomere-adjacent *FLO* genes. This gene family encodes cell-wall glycoproteins that regulate cell-cell and cell-surface adhesion. Epigenetic silencing of *FLO11* regulates a key developmental switch: when *FLO11* is expressed, diploid cells form pseudohyphal filaments; when *FLO11* is silent, the cells grow in yeast form. The epigenetic state of *FLO11* is heritable for many generations and regulated by the histone deacetylase (HDAC) Hda1p. The silent *FLO10* gene is activated by high frequency loss-of-function mutations at either *IRA1* or *IRA2*. *FLO10* is regulated by the same transcription factors that control *FLO11*, Sfl1p and Flo8p, but is silenced by a distinct set of HDACs: Hst1p and Hst2p. These sources of epigenetic and genetic variation explain the observed heterogeneity of cell-surface protein expression within a population of cells derived from a single clone.

INTRODUCTION

Pathogenic microorganisms have evolved diverse mechanisms that generate phenotypic variation at the cell surface in response to the host environment. The repertoire for this phenotypic variation is often a family of genes encoding cell-surface proteins, each of which has diverged in sequence and function. A common motif among different microorganisms is that one gene family member is expressed and the other family members serve as a silent reservoir of variation. By switching surface expression from one family member to another, a pathogen can evade detection by the immune system or alter interactions with host tissues (a classic example are the *VSG* genes in *Trypanosome bruceii*, see (Pays et al., 1994) for review).

Fungi express several gene families encoding cell-surface glycoproteins that confer different adherence and immunogenic properties to the fungal cell wall. In pathogens such as *Candida albicans* (*ALS* genes) and *Candida glabrata* (*EPA* genes) the proteins encoded by these gene families are responsible for adherence to mammalian tissues (Cormack et al., 1999; De Las Penas et al., 2003; Hoyer, 2001). In *Pneumocystis carinii* (*MSG* genes) these genes encode the primary cell-surface antigen recognized by the host immune system (Stringer and Keely, 2001). In *Saccharomyces cerevisiae* (*FLO* genes), proteins encoded by these genes confer adherence to agar, solid surfaces and other yeast cells (Guo et al., 2000; Reynolds and Fink, 2001). In these examples, the protein encoded by each family member is capable of producing distinct cell surface properties and serves as a resource for cell surface variation. In addition, many of these fungal gene families are found near telomeres, a location that may play an important role in their regulation and evolution.

S. cerevisiae has five known members of the *FLO* gene family: *FLO1*, *5*, *9*, *10*, and *11*. *FLO1*, *5*, *9*, and *10* are adjacent to their respective telomeres (~ 10 to 40 kb from the telomeres), whereas *FLO11* is neither adjacent to a telomere nor a centromere. In the Σ1278b genetic background, *FLO11* is the only expressed member of this family (Guo et al., 2000); the telomere-proximal *FLO* genes are silent. *FLO11* expression is required for several important developmental transitions in yeast, including adhesion to agar and plastic surfaces (Reynolds and Fink, 2001), sliding motility (Reynolds and Fink, 2001) and pseudohyphal filament formation (Gagiano et al., 1999; Lo and Dranginis, 1998). When the silent *FLO* genes are expressed by a heterologous promoter, they confer adhesive phenotypes distinct from those produced by *FLO11*: Flo1p does not promote adherence to agar or plastic, but enhances cell-to-cell adherence that causes flocculation. Flo10p generates phenotypes that overlap those of both Flo1p and Flo11p; Flo10p promotes adhesion and pseudohyphal filamentation, but also enhances cell-to-cell adherence (Guo et al., 2000). Although these silent *FLO* genes provide a reservoir of cell surface variation, the regulatory mechanisms that permit access to this silent information have been unexplored.

This study demonstrates that expression of the *FLO* genes, which regulate the cell surface properties of yeast, is under both genetic and epigenetic control. Diploid yeast strains filament in response to nitrogen starvation, but this response is heterogeneous: some cells initiate the filamentation program, whereas other adjacent cells remain in the yeast form. This variation is the consequence of the metastable silencing of the *FLO11* gene; *FLO11* is expressed to produce filamentous cells, but silent in yeast form cells. Haploid strains do not filament, but mutate at a high frequency to express another

telomere-linked *FLO* gene, *FLO10*, resulting in hyperinvasion and flocculence. Like *FLO11*, the expression of *FLO10* is metastably silenced. This epigenetic silencing of *FLO10* and *FLO11* integrates both promoter and genomic positional information to produce variegated expression.

Materials and Methods

Strains, media, microbiological techniques and growth conditions | Yeast strains used in this study are listed in Table 1. All strains are derived from Σ1278b (also known as MB1000; (Brandriss and Magasanik, 1979; Grenson et al., 1966)) and MB758-5B (Siddiqui and Brandriss, 1988). Standard yeast media, yeast transformations and genetic manipulations were performed as described in Guthrie and Fink (2001). To induce pseudohyphal differentiation, strains were grown on nitrogen-poor SLAHD media, which was prepared as described in (Gimeno et al., 1992).

Yeast strain construction | Yeast strains carrying gene deletions were constructed by PCR amplification of a P_{TEF} promoter driven bacterial kanamycin-resistance gene (Longtine et al., 1998), with flanking sequences that would direct the *kan*^{r} gene to the appropriate locus via homologous recombination. All deletions remove the full ORF (ATG-Stop). Deletion of *HMLα* silent mating locus and replacement with the *LEU2* gene was performed using plasmid pJR826, kindly provided by the Rine lab. This plasmid contains a SalI-XhoI flanked *LEU2* gene replacing an XhoI-flanked genomic fragment containing *HMLα*. Digestion of this construction with BamHI generates a fragment containing the *LEU2* gene flanked by sequences homologous to the 5' and 3' flanking sequences of *HMLα*. Transformation and integration of this fragment replaces

the *HMLα* sequences with those of *LEU2*. a *sir2*$^{-}$ Leu^{+} transformants were assayed for mating with *lys1*$^{-}$ mating tester strains to confirm deletion of *HMLα*.

To generate *TRP1*-tagged P_{FLO10}-*GFP* and P_{URA3}-*GFP* strains, a *TRP1*-tagged *GFP* module (Longtine et al., 1998) was PCR amplified with primers that included flanking 50-mers homologous to the 5' and 3' sequences of the targeted ORF. The ATG of the tagged ORF was preserved and used as the *GFP* start codon. These amplified fragments were then transformed into our strains, selecting for Trp^{+} transformants. Proper integrations were then verified by PCR. P_{FLO10}-*URA3* and P_{FLO11}-*URA3* strains were constructed by PCR of the *URA3* ORF with primers containing 50-mer flanking sequences that are homologous to the 5' and 3' sequences flanking the target ORF. The *URA3* amplified constructs completely replaced the target ORF with the full ORF of *URA3* (ATG-Stop), so that *URA3* expression would be controlled by the target ORF promoter. Correct integration of the *URA3* construct after transformation was verified by PCR. *FLO11*::*HA* alleles were generated as described (Guo et al., 2000).

To generate the *ura3*::P_{FLO10}-*GFP* allele, the *TRP1* tagged P_{FLO10}-*GFP* allele was PCR amplified from genomic DNA of a strain containing this allele. Primers for this PCR amplified from 5000 bp upstream of the *FLO10* promoter, to the 3' end of the *TRP1* gene (the same sequence used to amplify the original *GFP*::*TRP1* construct). These oligonucleotides also contain flanking sequences that are homologous to the 5' and 3' *URA3* flanking sequences. *URA3*$^{+}$ *trp1*$^{-}$ strains were transformed with the amplification product, and Trp^{+} *ura3*$^{-}$ transformants were selected. Correct integration was verified by PCR. The *ura3*::P_{FLO10}-*URA3* allele was generated by transformation of *ira1*$^{-}$ strains containing the *ura3*::P_{FLO10}-*GFP* allele with a PCR product targeted to replace the

GFP::*TRP1* sequences with the *URA3* ORF. Transformants were selected for *URA3*$^{+}$ and *trp1*$^{-}$ then verified for correct integration by PCR.

9Myc-epitope tagged Hst1p and Hst2p were generated by PCR amplification of a *9MYC* cassette (Knop et al., 1999) with flanking sequences which targeted the construct in frame to the 5' ends of the *HST1* and *HST2* genes. Correct insertion was verified by PCR. The presence of carboxy-terminus 9Myc-tagged Hst1p and Hst2p was verified by Western blotting analysis with an antibody specific to the Myc-epitope (9E11; Accurate antibodies). The oligonucleotides used for deletion constructs are listed in Table 2.

Isolation and analysis of spontaneous *ira*$^{-}$ mutants | Colonies were grown on YPD plates for 14 days. Cells were harvested from colonies, diluted in sterile water and plated onto YPD plates at a density of between 300-500 colonies/plate. Wrinkled colony morphology variants (Figure 2A) could be observed at a frequency of roughly 1/1000. A cross of these wrinkled variants to a smooth strain demonstrated that the wrinkled phenotype (as well as the other phenotypes described in Figure 3) were linked to a single locus, segregating in a 2:2 pattern among tetrad ascospores. Complementation analysis among wrinkled mutants demonstrated that these spontaneous mutations segregated into two complementation groups. In a transposon library screen (Kumar et al., 2002), a transposon insertion in the *IRA2* gene was isolated which recapitulated the phenotypes observed in the wrinkled variants. The isolated wrinkled variants fail to complement loss-of-function *ira1*$^{-}$ or *ira2*$^{-}$ mutations, suggesting that each wrinkled variant resulted from a mutation in either *ira1*$^{-}$ or *ira2*$^{-}$. Ira^{-} mutants can also be easily identified by an iodine vapor staining assay. For iodine staining, about 30 grams of iodine crystals (Sigma) were placed evenly over the bottom of a glass dish. Plates with colonies to be

tested were inverted over the iodine crystals for 2-5 minutes. Ira^+ strains stain bright red from exposure to iodine vapors, whereas *ira1*$^-$ and *ira2*$^-$ mutants stain yellow.

Iodine staining was used to identify Ira^- mutants for frequency analysis. Eight independent colonies derived from single cells were grown on YPD plates for 14 days and harvested as described earlier for identifying wrinkled variants. 10,000-20,000 viable cells were plated from each colony at a density of 300-500 colonies/ plate, grown for three days, and assayed with iodine vapors to identify *ira*$^-$ mutants. The median frequency of mutations producing an Ira^- phenotype was 1.08×10^{-3}, with a 95% confidence interval between 7.3×10^{-4} and 1.4×10^{-3}. The same colonies were assayed for mutations in the *CAN1* gene, which could be identified as canavanine resistant colonies. $1.0\text{-}2.0 \times 10^7$ cells were assayed for canavanine resistance from each colony. The median frequency of *can1*$^-$ mutation was 1.54×10^{-6}, with a 95% confidence interval between 3.1×10^{-7} and 3.2×10^{-6}. Therefore the frequency of mutations at the *IRA* loci roughly 1000-fold higher than the frequency seen at the *CAN1* locus.

Complementation analysis | To determine of putative *ira*$^-$ mutants carried mutations in the *IRA1* or *IRA2* gene, complementation tests were performed using strains carrying *kan*^{r}-tagged deletion alleles of *IRA1* and *IRA2*. Loss-of-function mutations in these genes are recessive for all the phenotypes we have identified. Unknown *ira*$^-$ mutants were crossed to *ira1*$^-$ and *ira2*$^-$ strains and assayed for complementation of the *ira*$^-$ iodine staining phenotype. Complementation analysis of 96 putative *ira*$^-$ mutants demonstrated that all 96 were indeed *ira*$^-$ mutants, with mutations occurring in roughly similar frequencies at the two loci (31 *ira1*$^-$, 65 *ira2*$^-$).

Cloning and sequencing of *ira*$^-$ alleles | One *ira1*$^-$ allele was sequenced by PCR amplification of 10 overlapping 1 kb segments from the genomic *ira1*$^-$ allele. Both strands of these PCR products were sequenced using four sequencing reactions. Polymorphisms were verified on both Watson and Crick strands and shown to not be present in an amplified wild-type allele.

The *IRA2* gene was cloned into the MCS of plasmid pRS316 by recombinational gap-repair from the genomic *IRA2* gene in L6828. Gap-repair constructs for isolation of *ira2*$^-$ mutant alleles were generated from either 1) digestion of the pRS316 *IRA2* clone with BglII (*IRA2*-BglII) or HpaI (*IRA2*-HpaI) enzymes, which produce deletions within the *IRA2* gene, or 2) deletion of a fragment of the *IRA2* gene on pRS316 via homologous insertion of a SnaBI site-flanked *kan*^{r} gene generated by PCR amplification as described (Longtine et al., 1998). Digestion with the SnaBI restriction enzyme releases the *kan*^{r} gene and produces the four *IRA2*-SnaBI constructs used for gap-repair isolation of *ira2*$^-$ alleles. Oligonucleotide primers used to construct these plasmids are listed in Table 2.

Several *ira2*$^-$ strains were transformed with pRS316 plasmids containing 1) the full length *IRA2* complementing clone or 2-7) the *ira2*$^-$ gap repair constructs. For each *ira2*$^-$ allele, we identified a gap-repair construct that failed to complement the Ira$^-$ iodine staining phenotype. The deleted region of this gapped construct was then PCR amplified as overlapping 1 kb fragments from the genomic *ira2*$^-$ allele, and sequenced as described above.

Phenotypic analyses of *ira*$^-$ mutants | Agar adhesion assays were performed with either patches or streaked single colonies that were grown on YPD plates for 6 days, then evenly washed under a gentle stream of non-sterile R/O water. Scrubbed colonies were

rubbed with a finger after washing. For flocculation assays, cells were grown overnight in liquid YPD media until saturation (~24 hours). Cells were vortexed briefly (pulse) at time zero, and allowed to settle.

Northern analysis | Total RNA was prepared from harvested cells by using a hot acid phenol protocol. 15μg total RNA/sample was separated on a denaturing formaldehyde gel. Northern blotting was performed as described (Sambrook et al., 1989). Immobilized total RNA for each sample was probed with the following probes: A 500 bp *FLO10* probe homologous to the 5' ORF sequence of the *FLO10* gene, A 500 bp *FLO11* probe homologous to the 5' ORF sequence of the *FLO11* gene, a 300 bp *ACT1* probe homologous to the *ACT1* coding region. Oligonucleotides for generating probes by PCR are listed in Table 2.

Chromatin immunoprecipitation assays | Chromatin immunoprecipitations of 9Myc-tagged Hst1p and Hst2p were performed as described in (Knop et al., 1999). Briefly, cells were grown to between $O.D._{600}$ 0.8-1.2 units, harvested and fixed with formaldehyde. Cells were lysed in the presence of protease inhibitors, sonicated to shear the chromatin and the lysates were immunoprecipitated with a-myc antibodies (9E11) bound to Dynabeads M-450, pre-coated with pan-anti-mouse IgG (Dynal). The beads with bound protein/DNA complexes were washed and the protein/DNA complexes were eluted from the beads. Reversal of the cross links with TE/SDS was followed by ethanol precipitation of the DNA in the IP fraction. This DNA was analyzed by PCR for the presence of specific sequences in the *FLO10* promoter.

RESULTS

Epigenetic silencing of *FLO11* regulates pseudohyphal development | Flo11 protein expression was visualized by immunofluorescence using strains containing a fully functional Flo11p tagged with triple HA epitopes ((Guo et al., 2000); Table 3). A clonal population of cells arising from a single haploid cell is not homogeneous: some cells express Flo11p, staining brightly with the HA-specific antibodies, whereas other cells from the same culture do not express Flo11p and fail to stain (Figure 1A).

To demonstrate whether heterogeneous Flo11p expression is due to transcriptional regulation of the *FLO11* gene, the chromosomal *FLO11* ORF was replaced with the *URA3* ORF, to generate a P_{FLO11}-*URA3* allele (Table 3). With this allele, cells that have active transcription from the *FLO11* promoter will express the *URA3* gene and will be Ura^+ and 5-FOA sensitive, whereas cells that are either inactive at the *FLO11* promoter or have a silenced *FLO11* promoter will be Ura^- and $5\text{-}FOA^R$. A clonal population of cells bearing the chromosomal P_{FLO11}-*URA3* allele, when grown initially under non-selective conditions, contains some cells that are Ura^+ and others that are $5\text{-}FOA^R$ (Figure 1C). This heterogeneity agrees with the immunofluorescence analysis: a population derived from a single *FLO11* cell contains some cells that express the *FLO11* gene and others that do not.

To determine whether the state of *FLO11* expression is reversible, cells were isolated from colonies grown on 5-FOA, grown on YPD media overnight, and re-plated onto SC, SC-Ura and SC+5-FOA media. If the Ura^- colonies that grew up were silenced irreversibly (e.g. by mutation), then there should be very few Ura^+ colonies emerging from this population under non-selective growth. In contrast, Ura^- cells selected on 5-

FOA again generate both Ura^+ and Ura^- cells at the same frequencies as cells not grown on 5-FOA (Figure 1C). The ability of Ura^- cells selected on 5-FOA to generate both Ura^- and Ura^+ cells shows that the transition between *FLO11* silenced (Ura^-) and *FLO11* desilenced (Ura^+) is reversible and switches back and forth frequently.

The metastable silencing of *FLO11* is similar to position-effect silencing described for subtelomeric transgenes (Gottschling et al., 1990). To determine whether *FLO11* silencing is dependent upon its genomic location, the P_{FLO11}-*URA3* allele was moved to the *URA3* locus, which is located ~12 kb from the centromere on the left arm of chromosome V (see Table 3). The *ura3*::P_{FLO11}-*URA3* strains fail to grow on media containing 5-FOA (Figure 1C), suggesting that the *FLO11* promoter is not silenced when positioned at the *URA3* locus. Therefore, silencing of *FLO11* is position-dependent.

However, in contrast to telomere silencing, silencing of *FLO11* is promoter-specific. When the *URA3* gene with its own promoter is placed at the *FLO11* locus, it is not silenced (*flo11*::*URA3*, Figure 1C), suggesting that factors that specifically recognize the *FLO11* promoter regulate silencing at this locus. A candidate for this promoter-specific factor is Sfl1p, which inhibits expression of *FLO11* (Pan and Heitman, 2002). Indeed, Sfl1p is required for silencing at the *FLO11* promoter (Figure 1B, 1C), suggesting that Sfl1p recognition may be a necessary step in the silencing of the *FLO11* gene.

Genome-wide studies have demonstrated that Hda1p participates in the deacetylation of large continuous sub-telomeric regions of the yeast genome (Robyr et al., 2002). These regions extend much further away from the telomeres than Sir2p mediated silencing effects and encompass a region that includes the *FLO11* gene. The

hda1^{-} P_{FLO11}-*URA3* strain fails to grow on media containing 5-FOA (Figure 1C), demonstrating that Hda1p is necessary for silencing *FLO11*. Since Hda1p deacetylation appears to be restricted to specific regions of the genome, the requirement for Hda1p, might explain the position-dependence of *FLO11* silencing; although the factors that localize Hda1p activity are still unknown. In addition, Hda1p is recruited to specific promoters by Tup1p (Wu et al., 2001), which in turn has been shown to be recruited to the *FLO11* promoter by Sfl1p (Conlan and Tzamarias, 2001). This suggests a pathway by which Sfl1p recruits Hda1p to silence *FLO11*.

Mutations that disrupt the function of the yeast Ku proteins, the Sir complex or the Sir2p homologues, Hst1-4p, show no effect on *FLO11* silencing as measured by the activity of the P_{FLO11}-*URA3* allele (data not shown). The failure of these genes involved in telomere silencing to affect *FLO11* expression is not surprising because *FLO11* is quite far from its telomere (>40 kb).

The phenotypic consequences of *FLO11* switching are striking in diploid cells, where *FLO11* expression is required for the transition from yeast form cells to pseudohyphae. To visualize Flo11p expression in diploids during pseudohyphal development, diploid strains homozygous for the *FLO11*::*HA* allele were grown on media that induces pseudohyphal growth (see Methods). The expression of Flo11p on the surface of nitrogen-starved diploid cells is variegated, some cells express Flo11p and some do not, confirming that *FLO11* is also metastably silenced under the conditions that stimulate pseudohyphal development (Figure 1A). The elongated, pseudohyphal cell types generally express Flo11p on their surface: 90.2% of filamentous cells (n = 174)

versus 2.1% of yeast form cells (n = 188) express Flo11p, demonstrating that filamentation and Flo11p surface expression are tightly associated ($p = 6.1x10^{-64}$).

The expression of Flo11p can be visualized in a phalanx of pseudohyphal cells if the colonies are treated gently prior to staining. As shown in Figure 1B , the cells that make up the intact filament express Flo11p, whereas the yeast-form cells that surround the filament do not. Moreover, Flo11p expressing cells can be seen to be dividing to produce yeast form cells that do not express Flo11p on their surface (Figure 1B arrows). The proximity of these two forms, filamentous (*FLO11* on) and yeast (*FLO11* off), suggests that their differentiation is not the result of differing environmental inputs. Rather, it demonstrates that epigenetic controls determine the differentiation of yeast and filamentous forms.

The strong correlation between the expression of Flo11p and pseudohyphal filamentation suggests that changes in silencing at *FLO11* should affect the pattern of pseudohyphal development. During diploid pseudohyphal filamentation, the developmental transition from yeast to pseudohyphal form does not occur in concert among all the cells at the periphery of the colony. Some cells initiate pseudohyphal filaments, while adjacent cells continue to divide in a yeast form pattern (Figure 1D). In contrast, desilenced homozygous *sfl1*$^{-}$ or *hda1*$^{-}$ diploid colonies both produce an increased level of pseudohyphal filamentation (Figure 1D). This analysis of cell-by-cell distribution of Flo11p expression helps clarify previous reports of the enhancement of pseudohyphal filamentation in *sfl1*$^{-}$ mutants (Robertson and Fink, 1998). Loss of silencing produces an altered distribution of *FLO11* expression: from a heterogeneous expression in wild-type colonies, to a constitutive expression in homozygous *sfl1*$^{-}$ or

hda1^{-} colonies. Desilenced cells can then participate in pseudohyphal filamentation leading to the hyperfilamentous phenotype observed in *sfl1*$^{-}$ or *hda1*$^{-}$ homozygotes. Therefore, metastable silencing at the *FLO11* locus regulates the transition to pseudohyphal development in response to nitrogen starvation.

Phenotypic switching in *S. cerevisiae* results from mutations in *IRA1* or *IRA2* | In addition to the epigenetic variegation of *FLO11* gene expression, *S. cerevisiae* is capable of altering its cell surface properties via mutations that activate the expression of other *FLO* gene family members. These mutants appear as wrinkled colony morphology variants that have increased adhesion to the agar. Variants that have stably switched to a wrinkled colony morphology (Figure 2A) appear at a frequency of 1.1×10^{-3} (see Methods for details). The wrinkled colony morphology phenotype results from a single mutation in one of two complementation groups.

Complementation analysis of independently arising wrinkled isolates (n = 96) demonstrated that these wrinkled variants result from loss-of-function mutations in either *IRA1* or *IRA2*, the yeast Ras GTPase-activating proteins. The wrinkled *ira1*$^{-}$ and *ira2*$^{-}$ mutants are phenotypically indistinguishable and occur at similar frequencies. One *ira1*$^{-}$ and five *ira2*$^{-}$ alleles from wrinkled variants were cloned (see Methods) and sequenced (Figure 2B). Each of the cloned mutations results from a different nucleotide change within the *IRA1* or *IRA2* ORFs. The *ira1-5* allele contains an insertion of a T-A base pair at position 5705 bp of the *IRA1* ORF, among a stretch of ten A-T and T-A base pairs. Several frameshift mutations were also found among the *ira2*$^{-}$ alleles. The *ira2-19*, *ira2-24* and *ira2-26* alleles are all frameshift mutations resulting from a deletion or insertion of an A-T or T-A base pair within stretches of 8-14 successive A-T and T-A base pairs.

The other two *ira2*$^-$ mutations we sequenced, *ira2-6* and *ira2-11*, are transversions (C to G and C to A respectively). Therefore, the colony morphology variation observed in *S. cerevisiae* is a high-frequency genetic event, which can be traced to sequence polymorphisms in either the *IRA1* or *IRA2* genes.

Altered cell surface properties result from *FLO10* activation | Ira$^-$ mutants display phenotypes consistent with the activation of additional *FLO* gene family members. Ira$^+$ strains require *FLO11* for haploid invasive growth, whereas Ira$^-$ strains do not. As shown in Figure 3A, a *FLO11*$^+$ strain remains attached to the surface of the agar, whereas a *flo11*$^-$ strain washes off easily. However, the isolated Ira$^-$ mutants no longer require *FLO11* for adhesion. An *ira2*$^-$ *flo11*$^-$ strain is significantly more adherent than an *IRA2*$^+$ *flo11*$^-$ strain (similar results are observed with *ira1*$^-$ mutants). This Flo11p-independent haploid adhesion of Ira$^-$ strains depends upon the normally inactive *FLO10* gene, as *ira2*$^-$ *flo11*$^-$ *flo10*$^-$ mutants do not adhere to agar (Figure 3A). In a higher stringency assay for adhesion (Figure 3A, scrubbed), the *ira2*$^-$ *flo11*$^-$ strains are even more adherent than the *FLO11*$^+$ strain.

The wrinkled Ira$^-$ mutants also have a significant flocculation phenotype (cells adhere and aggregate into large clumps that sediment much more quickly than dispersed cells; Figure 3B). This flocculation in liquid media is also dependent upon *FLO10* gene activity as loss of *FLO10* function leads to a loss of flocculation in the Ira$^-$ mutants (Figure 3B).

Additionally, the strikingly wrinkled surface of these Ira$^-$ colonies is dependent upon the expression of the Flo11p cell-surface adhesin (Figure 3C). This wrinkled surface morphology is likely due to increased *FLO11* gene expression as mutations that

upregulate *FLO11* (*sfl1*$^{-}$ mutants show a similar wrinkled morphology), or *GAL1* promoter-driven expression of the *FLO11* gene (data not shown), also manifest the wrinkled colony morphology phenotype.

These results suggest that altered expression of *FLO10* and *FLO11* plays a role in several of the phenotypes produced in wrinkled Ira^{-} mutants. To determine whether the expression of either of these genes is altered in variant strains, total RNA was isolated from a smooth Ira^{+} strain and two rough Ira^{-} variants (*ira1-12* and *ira2-6*). Northern analysis of these RNA samples (Figure 4), demonstrates that Ira^{-} mutants have higher levels of *FLO11* (2-fold) and *FLO10* (12-fold) message. Activation of *FLO10* and *FLO11* expression in Ira^{-} strains is dependent upon Ras2p and the filamentous MAP kinase and PKA pathways ((Rupp et al., 1999) for *FLO11* and Supplemental Figure 1 for *FLO10*). Messages for the other known adhesins, *FLO1*, *5* and *9*, could not be detected by Northern analysis in either Ira^{+} or Ira^{-} strains. Therefore, mutations at the *IRA* loci result in a phenotypic switch in colony morphology, and altered cell-surface adhesion. Several of these new traits are dependent on transcriptional activation of *FLO10.*

Epigenetic regulation of *FLO10* | To determine whether the epigenetic silencing effects observed at *FLO11* extend to other *FLO* gene family members, a *TRP1*-tagged *Aequorea victoria GFP* gene (Heim et al., 1994) was inserted into the *FLO10* locus, such that *GFP* gene expression would be regulated by the *FLO10* promoter (see Table 3). As a control, the fluorescence generated by GFP expression was analyzed when transcription of the *GFP* gene is controlled by the endogenous *URA3* promoter on chromosome V (P_{URA3}-*GFP*). The expression of GFP in the *URA3* promoter-regulated construct is homogeneous (Figure 5A).

In contrast, *GFP* regulated by the endogenous *FLO10* promoter (P_{FLO10}-*GFP)* has a very different pattern of expression. In Ira^+ strains, the *FLO10* promoter is inactive and no *GFP* expression is observed. In *ira1*$^-$ strains (or *ira2*$^-$ strains; data not shown), *GFP* expression driven by the *FLO10* promoter is variegated. Some cells have a high level of *GFP* expression, whereas other cells have no evident GFP fluorescence (Figure 5A).

To dissect the *FLO10* silenced and desilenced states, we replaced the endogenous *FLO10* ORF with the *URA3* ORF (Table 3). The phenotype of *ira1*$^-$ P_{FLO10}-*URA3* strains is both Ura^+ and $5\text{-}FOA^R$ (Figure 5B). This result is consistent with the previous observation that *GFP* expression is variegated when driven by the *FLO10* promoter.

To determine whether the silenced state of *FLO10* is reversible, cells bearing the P_{FLO10}-*URA3* allele were isolated from 5-FOA grown colonies, grown on YPD media overnight, and re-plated onto SC, SC-Ura and SC+5-FOA media. The frequency of Ura^+ colonies is roughly equivalent to that observed in strains that have not been grown on 5-FOA (Figure 5B), suggesting that silencing at *FLO10*, like at *FLO11*, is metastable and switches back and forth frequently.

To establish whether the silencing at *FLO10* requires sequences specific to the *FLO10* promoter, a *flo10*::*URA3* allele was constructed. This allele is similar to the P_{FLO10}-*URA3* allele used earlier, except that in this second strain *URA3* is regulated by its own promoter (Table 3) and located at the *FLO10* locus on chromosome XI. An *ira1*$^-$ *flo10*::*URA3* strain does not silence the *URA3* gene. It grows on SC-Ura media but fails to grow on 5-FOA media (Figure 5B). Therefore, the silencing observed at the *FLO10* locus is likely to require factors that specifically recognize and associate with the *FLO10* promoter.

Sfl1p is a likely candidate for directing silencing to the *FLO10* promoter as Sfl1p represses transcription at both *FLO11* (Pan and Heitman, 2002; Robertson and Fink, 1998) and *FLO10* (Supplemental Figure 2) and is also required for silencing at *FLO11* (Figure 1C). An *sfl1*$^{-}$ mutant fails to silence the P_{FLO10}-*URA3* allele (Figure 5B) suggesting that Sfl1p recognition of the *FLO10* promoter may be important for the promoter-specificity of silencing at *FLO10*.

To determine whether the epigenetic silencing of the *FLO10* gene is position-dependent, we constructed strains in which either the P_{FLO10}-*GFP* or the P_{FLO10}-*URA3* allele was moved to the *URA3* locus (Table 3). Neither of these alleles is silenced at the *URA3* locus (Figure 5A,B). Therefore, silencing of the *FLO10* promoter is dependent on its genomic positioning. Since *FLO10* silencing is dependent on its sub-telomeric location (*FLO10* is only ~17 kb from a telomere, much closer than *FLO11*), strains containing deletions of several genes required for telomere silencing were constructed and tested for silencing of the *FLO10* promoter. Sir3p and Sir4p associate with Sir2p at the telomeres and silent mating loci, and is required for silencing at these sites (Shore et al., 1984). Deletion of the *SIR3* gene also disrupts this complex, and also disrupts silencing at the *FLO10* locus (Figure 5B). A similar result is observed with deletions of the genes *YKU70* and *YKU80* (data not shown; similar to *sir3*$^{-}$ mutants). These genes encode homologues of the mammalian Ku proteins and are required for telomere silencing, but not silencing at *HML* or *HMR* (Mishra and Shore, 1999). Since the Ku and Sir proteins are involved in regulating regional silencing effects, the position dependence of the silencing at the *FLO10* promoter is likely to be mediated by these proteins.

Silencing of *FLO10* requires Hst1p and Hst2p, which associate with the *FLO10* promoter | The pattern of variegated expression observed for *FLO10* is similar to the patterns of expression for ectopic genes regulated by telomere silencing (Gottschling et al., 1990). Data from localization experiments (Kennedy et al., 1997; Martin et al., 1999), expression of ectopic promoters (Gottschling et al., 1990), and genome-wide expression analysis (Wyrick et al., 1999) suggest that telomere silencing requires the activity of the NAD^+-dependent histone deacetylase protein, Sir2p. The P_{FLO10}-*URA3* allele is still effectively silenced *ira*$^-$ *sir2*$^-$ strains (Figure 5B), demonstrating that Sir2p does not play a role in silencing *FLO10*.

To determine whether any of the other Sir2p homologues, Hst1p-Hst4p (Brachmann et al., 1995), play a role in *FLO10* silencing, mutants lacking each of the *HST* genes were assayed for silencing of the P_{FLO10}-*URA3* allele. Both *HST1* and *HST2* are necessary for silencing at the *FLO10* promoter (Figure 5A,B), whereas deletions of either *HST3* or *HST4* have no effect on silencing at *FLO10*.

Chromatin immunoprecipitations of *MYC* epitope-tagged alleles of *HST1* and *HST2* were analyzed by PCR probes to determine whether Hst1/2p silencing of *FLO10* is through interaction of these HDAC proteins with the *FLO10* promoter. A region of the *FLO10* promoter (-900 to -1175) is enriched in the immunoprecipitate fraction of Myc-tagged Hst1p and Hst2p strains over untagged strains (Figure 5C). Different regions of the *FLO10* promoter (-2050 to -1800 and -550 to -300) as well as a probe to the *URA3* promoter, show little enrichment in the immunoprecipitate of tagged fractions over untagged fractions (Figure 5C).

To test whether Sfl1p is necessary for recruitment of the Hst1/2p HDACs to the *FLO10* promoter, *sfl1*$^{-}$ strains were analyzed for association of both Hst1p and Hst2p with the *FLO10* promoter. Loss of Sfl1p function leads to a disassociation of both Hst1p and Hst2p with the Hst1/2p-associated region described above. Immunoprecipitates of 9Myc-tagged Hst2p show no enrichment for the Hst1/2-associated region over untagged immunoprecipitates in *sfl1*$^{-}$ strains (Figure 5C). This suggests that Sfl1p regulates two distinct pathways that converge upon the *FLO10* promoter: 1) Sfl1p represses *FLO10* gene expression through inhibition of the Flo8p transcriptional activator ((Pan and Heitman, 2002) and Supplemental Figure 1) and 2) Sfl1p recruits the HDAC proteins Hst1p and Hst2p to the *FLO10* promoter to silence *FLO10* gene expression in a sub-population of Ira^{-} cells.

DISCUSSION

The experiments described here demonstrate that rapid variation in *S. cerevisiae* cell-wall glycoproteins results from both epigenetic and genetic regulation of the *FLO* gene family. Although there are five members of this family in *S. cerevisiae*, *FLO11* is the only member that is expressed in the Σ1278b background (Guo et al., 2000). *FLO11* gene expression is required for key developmental transitions in yeast, including adhesion to agar and plastic surfaces, sliding motility and pseudohyphal filament formation (Gagiano et al., 1999; Lo and Dranginis, 1998; Reynolds and Fink, 2001).

Genetic and immunofluorescent analyses (Figure 1) demonstrate that epigenetic silencing determines whether cells express the cell-surface protein Flo11p and transition to a filamentous developmental form in the presence of the appropriate environmental

signal. There are several remarkable features of silencing at *FLO11*. First, silencing of *FLO11* is a binary switch, where *FLO11* expression (silenced = OFF, desilenced = ON) determines the developmental outcome for individual cells. The state of this switch is inherited for several generations; the phalanges of filamentous cells seen in Figure 1B record lineages of more than ten generations in which *FLO11* remains in the expressed state. Second, silencing at *FLO11* is both promoter-specific and position-dependent. These considerations suggest that both global (gene non-specific) and promoter-specific factors contribute to the establishment of *FLO11* silencing (Figure 6). The dual nature of silencing at *FLO11* contrasts with most previously described positional silencing effects, which are defined by their promoter-independent ability to silence transcriptional activity. Finally, silencing at the *FLO11* gene (~ 46kb from the end of chromosome IX) reveals the presence of telomere-independent positional silencing effects within the yeast genome. Telomere-independent silencing has also been described for the rDNA locus (Smith and Boeke, 1997) and for the *HIS4* locus (Jiang and Stillman, 1996), suggesting that metastable silencing of genes may be more widespread than had been previously imagined.

The epigenetic silencing of *FLO11* explains the variation in filamentation within a genetically homogeneous colony of yeast. When *S. cerevisiae* colonies are starved for nitrogen (Figure 1B and 1D), they produce pseudohyphal filaments (Gimeno et al., 1992). However, only a subset of cells participate in forming filaments. *FLO11* is expressed in the filamentous cells and silent in the non-filamentous cells. This switch is controlled by Hda1p and Sfl1p; diploid strains lacking either Sfl1p or Hda1p show constitutive filamentation along the edge of the colonies (Figure 1D). Therefore, silencing regulates

the differentiation of cell types: Cells expressing Flo11p at their surface develop as pseudohyphae, whereas Hda1p-silenced cells do not express Flo11p and remain in the yeast form.

The ability of genetically identical cells to switch between these two morphologically distinct forms could be important for survival. In the human fungal pathogen *C. albicans* any mutation that locks the cells in either a yeast form or a hyphal form severely reduces the pathogenicity of this fungus (Braun and Johnson, 1997; Lo et al., 1997). The requirement for both yeast and hyphal forms suggests that there is a division of labor; the filamentous forms may represent the foraging form of the fungus, allowing it to find more favorable environments, whereas the yeast form is the colonizing form, growing more effectively under conditions where nutrients are available. Metastable regulation of yeast-pseudohyphal differentiation by silencing allows a clonal population of *S. cerevisiae* to test both of these different phenotypes without committing all the cells in a colony to one developmental form or another.

Saccharomyces can produce additional cell surface variation when other members of the *FLO* gene family are expressed. The other Flo proteins (Flo1p, Flo5p, Flo9p and Flo10p) are capable of producing adhesive phenotypes distinct from those of Flo11p, yet only Flo11p is normally expressed. This situation in yeast is analogous to what has been observed in several other microorganisms (De Las Penas et al., 2003; Howell-Adams and Seifert, 2000; Mehr and Seifert, 1998; Stringer and Keely, 2001; Weiden et al., 1991), where each member of a gene family produces distinct cell surface properties, yet only a limited number are expressed.

Numerous mechanisms, including gene conversion (Bernards et al., 1981; Pays et al., 1983a; Pays et al., 1983b), recombination (Howell-Adams and Seifert, 2000; Mehr and Seifert, 1998), trans-splicing (Stringer and Keely, 2001), and epigenetic regulation (De Las Penas et al., 2003; Michels et al., 1984; Rudenko et al., 1995) are utilized by these microorganisms to produce a switch in surface protein expression. In *S. cerevisiae*, a mutational mechanism governs access to the reservoir of cell-surface variation provided by the *FLO* genes (Figure 2). Surface expression of additional *FLO* genes is accomplished through mutation of the *IRA1* or *IRA2* genes (Figure 4). These loci are genetically unstable, producing loss of function *ira*$^-$ mutations at a high (~10^{-3}) frequency. The source of this high mutation frequency is unclear, although it is evident that this genetic instability is not shared across the rest of the genome. Mutations in the *CAN1* gene appear at a much lower frequency (~10^{-6}; see Methods). The *ira1*$^-$ and *ira2*$^-$ mutants have novel adhesive phenotypes, many of which result from the transcriptional activation of the *FLO10* gene (Figures 3 and 4). This transcriptional activation is dependent upon both the MAP kinase and cAMP-regulated PKA pathways (Supplemental Figure 1) and is likely due to increased Ras activity in these strains (Russell et al., 1993).

In Ira$^-$ cells, the expression of *FLO10* is variegated suggesting that *FLO10*, like *FLO11*, is regulated by metastable epigenetic silencing (Figure 6B). Although it is unclear if the telomere-associated Sir3p and Ku proteins act through Hst1p and/or Hst2p, or through some independent mechanism at the *FLO10* locus, the genetic analysis demonstrates that both promoter-specific (Sfl1p) and position-dependent (Sir3p and Ku proteins) information is integrated in the silencing of *FLO10*.

As each *FLO* gene is capable of producing distinct adhesive phenotypes, access to the silent *FLO* genes permits yeast to display different cell surface properties. This situation is analogous to VSG expression in trypanosomes (Pays et al., 1994) or the MSG switching in *P. carinii* (Stringer and Keely, 2001), where the transcriptional regulation of gene family members is a mechanism to generate diversity. In these examples, silent genes located near the telomeres provide a repository of information that, when accessed, can produce phenotypic variation. Interestingly, many of the genes found near the telomeres in yeast are members of multigene families (e.g. the *SUC*, *MAL*, *MEL*, *PAU*, and *HXT* gene families). It has been proposed (Otto and Yong, 2002) that novel gene functions can arise through the process of gene duplication and divergence. With this in mind, it is interesting that many of the genes found at metastably silenced loci, such as the yeast telomeres, are members of larger gene families. Perhaps these regions are favored for the evolution of new gene activities.

FIGURES AND TABLES

FIGURE 1 | Epigenetic control of *FLO11* expression regulates pseudohyphal differentiation. (A) Immunofluorescence analysis reveals variegated expression of Flo11p at the cell surface. All strains carry the *FLO11*::*HA* allele to visualize Flo11p expression on a cell-by-cell basis. Images show an overlay of HA-targeted immunofluorescence over a Nomarski image of the same field. Variegated expression is observed in a wild-type haploid strain, but is lost in strains that lack Sfl1p or Hda1p. Diploids (**a**/α) were grown on solid nitrogen starvation (SLAHD) media to induce pseudohyphal differentiation. Flo11p-HA expression in diploids is strongly correlated with the filamentous growth form ($p = 6.1 \times 10^{-64}$). (B) Cells isolated from filamentous diploid colonies allow the *in situ* visualization of filamentous and yeast form cells. The budding of yeast form cells off of a phalanx of filamentous cells (arrows) can be seen. (C) The P_{FLO11}-*URA3* expression construct reveals the silenced (5-FOA^R) and desilenced (Ura$^+$) states of the *FLO11* promoter. Two equivalent 10-fold dilution spots are shown for each plate. P_{FLO11}-*URA3* (*) indicates that these cells were isolated from 5-FOA media, grown on YPD, then replated onto SC, -Uracil and 5-FOA plates. See Table 3 for more detailed descriptions of the *URA3* expression constructs. (D) Silencing of *FLO11* regulates the transition from yeast to filamentous growth. In Σ1278b strains, the initiation of filamentation at the colony periphery is heterogeneous, whereas in *FLO11*-desilenced *sfl1*$^-$ or *hda1*$^-$ mutants, the cells at the periphery of the colony are uniformly filamentous.

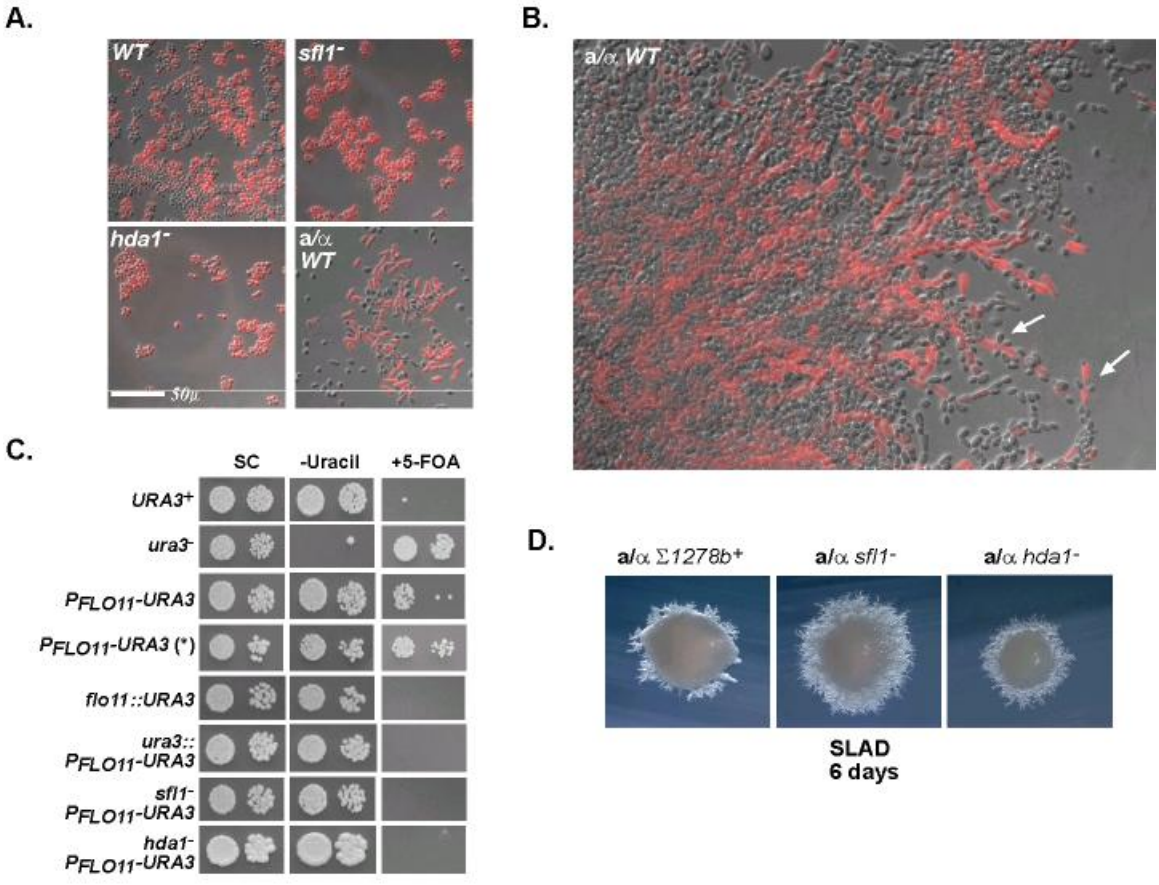

FIGURE 2 | **Spontaneous, high frequency mutations at *IRA1* and *IRA2* produce wrinkled colony morphology variants.** (A) A switch in colony morphology is the result of high-frequency mutations at *IRA1* or *IRA2*. Wrinkled colonies were isolated from haploid strains at a frequency of about $1x10^{-3}$ (see Methods for details of frequency analysis). Genetic analysis of these wrinkled colonies revealed that the phenotypic switch from smooth to wrinkled colony morphology is due to mutations in the *IRA1* and *IRA2* gene. (B) Several *IRA1* and *IRA2* mutations were cloned and sequenced to identify the loss of function mutations in these alleles. The location of each of the polymorphisms in both the *IRA1* and *IRA2* genes are shown. The consensus GTPase activating domain (Tanaka et al., 1990b) is shown for each gene. 4/6 (*ira1-5*, *ira2-19*, *ira2-24*, *ira2-26*) of the mutations sequenced are frameshift mutations, whereas *ira2-6* and *ira2-11* are transversions.

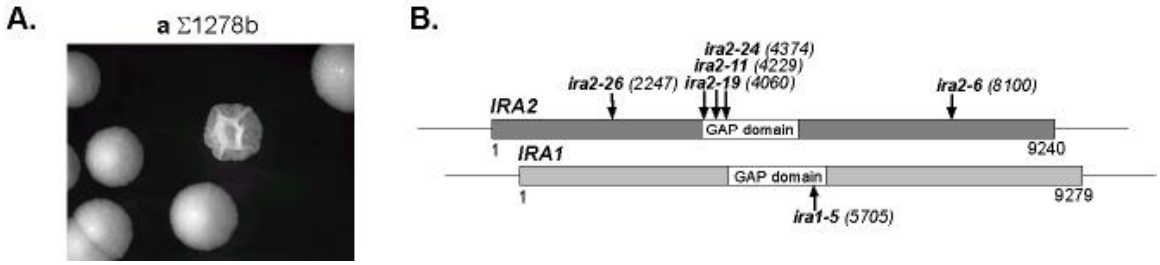

FIGURE 3 | **Ira$^-$ phenotypes require *FLO* gene activity.** (A) Flo11p-independent agar adhesion in Ira$^-$ strains requires the activity of the *FLO10* gene. (B) Flocculation of Ira$^-$ mutants requires *FLO10* gene activity. The top panel shows liquid cultures at immediately after resuspension by vortexing. The bottom panel shows the same cultures after 15 minutes. (C) The wrinkled colony morphology phenotype of Ira$^-$ mutants is dependent upon an intact *FLO11* gene.

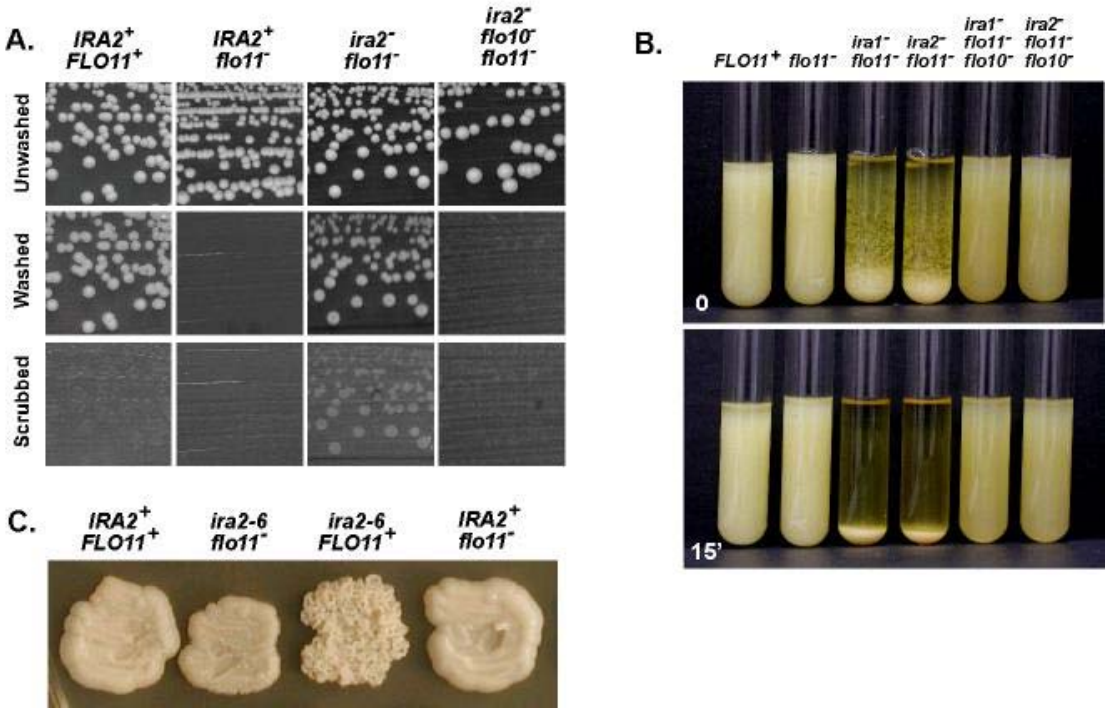

FIGURE 4 | **Northern analysis of Ira⁻ mutants reveals increased levels of *FLO11* and *FLO10* transcripts.** Ira⁻ mutants display a 2-5 fold increase in *FLO11* transcript and a 10-20 fold increase in *FLO10* transcript.

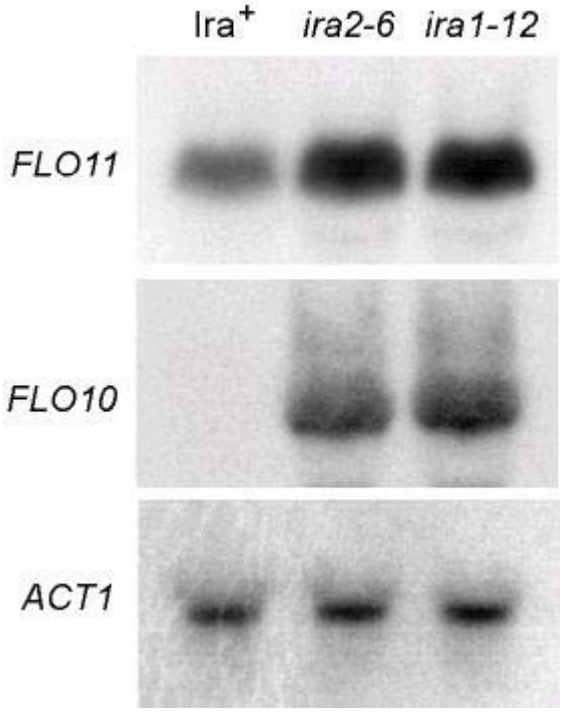

FIGURE 5 | **Telomere position effects at *FLO10* are mediated by Hst1p and Hst2p association.** (A) *FLO10* gene expression shows position-effect variegation. The *FLO10* ORF was replaced with a *TRP1*-tagged *GFP* gene such that *GFP* expression was regulated by the genomic *FLO10* promoter (P_{FLO10}-*GFP*, see Table 3 for expression constructs). As a control, a similar construct was generated at the *URA3* locus, such that the *URA3* promoter was responsible for *GFP* expression (P_{URA3}-*GFP*). (B) The P_{FLO10}-*URA3* expression construct reveals the silenced (5-FOA^R) and desilenced (Ura$^+$) states of the *FLO10* promoter. Two equivalent 10-fold dilution spots are shown for each plate. The *ira1*$^-$ P_{FLO10}-*URA3* (*) cells were initially selected on 5-FOA and grown on YPD before plating on SC, -Uracil and 5-FOA media. As is observed at *FLO11*, silencing of the *FLO10* promoter produces both Ura$^+$ and 5-FOA^R populations of cells. (D) Chromatin immunoprecipitation demonstrates Sfl1p-dependent association of Myc-tagged Hst1p and Hst2p with the *FLO10* promoter. *SFL1*$^+$ or *sfl1*$^-$ strains carrying either MYC tagged *HST1* or *HST2* alleles (*HST1* and *HST2*; + lanes) or untagged alleles (- lanes), were analyzed by chromatin immunoprecipitation. Quantitative PCR reactions from immunoprecipitate (IP) fractions were compared to those from whole cell extract (W) to determine the levels of enrichment. Precipitation of fixed whole cell extract samples with anti-Myc antibodies produced an enrichment of a fragment of the *FLO10* promoter (bases -900 to -1175) in both Myc-tagged Hst1p (43.19 fold) and Hst2p (6.93 fold) strains. In *sfl1*$^-$ strains, IP enrichment of this fragment is substantially decreased for both Myc-tagged Hst1p (15.2 fold less enrichment in an *sfl1*$^-$ strain) and Hst2p (5.2 fold less enrichment in an *sfl1*$^-$ strain), demonstrating that Sfl1p is required for the association of these HDAC proteins with the *FLO10* promoter.

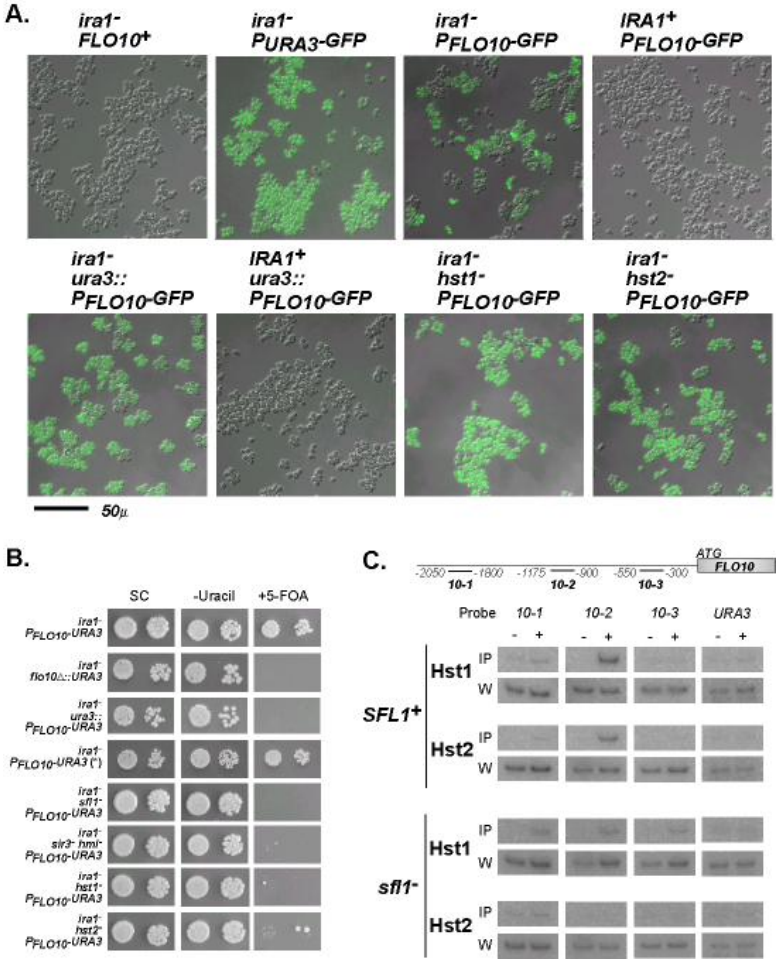

FIGURE 6 | **Silencing at *FLO10* and *FLO11* integrates both promoter-specific and genomic positional information.** (A) Hda1p regulates telomere-independent positional silencing of *FLO11*. Sfl1p, which binds the *FLO11* promoter, is required for epigenetic silencing of the *FLO11* gene (Figure 1) and likely provides the promoter-specificity to *FLO11* silencing. Although it is clear that genomic position regulates FLO11 silencing (Figure 1C), the nature of the positional determinants remains unclear. Silencing of *FLO11* also requires the Hda1p histone deacetylase (Figure 1), which is likely to integrate both positional and promoter-specific (Sfl1p) information (B) Silencing of *FLO10* is dependent upon the Hst1p and Hst2p HDACs. These HDAC proteins integrate promoter and positional information through interactions with Sfl1p and the telomere-associated Ku and Sir proteins.

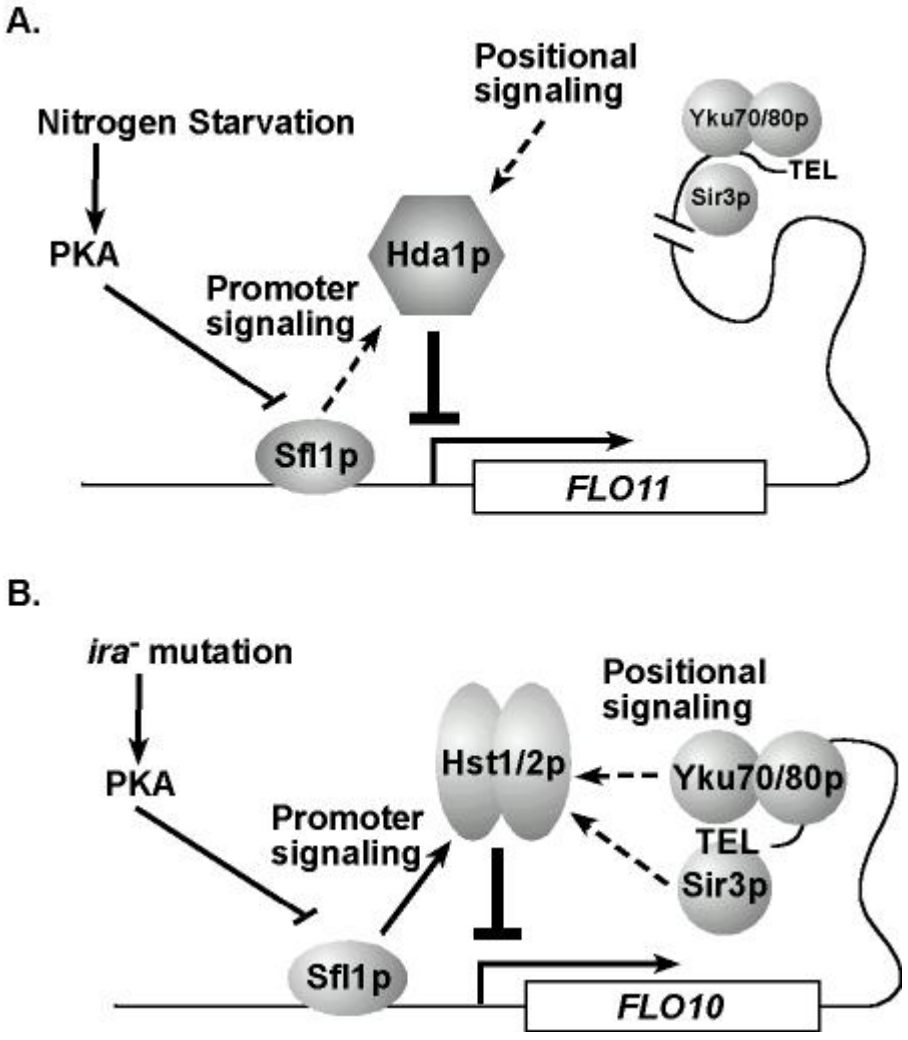

TABLE 1 | ***Saccharomyces cerevisiae*** **strains used in this study.**

Strain	***Genotype***	***Reference/Source***
L6828	*MAT***a** *ura3-52 leu2::hisG his3::hisG flo11::HIS3*	Fink laboratory Collection
10560-2B	*MAT***a** *ura3-52 leu2::hisG his3::hisG*	Fink laboratory Collection
L6906	*MAT***a** *ura3-52 his3::hisG FLO11::HA*	Fink laboratory collection
AHY957	*MAT***a** *ura3Δ0* P_{FLO11}*-URA3*	This Study
AHY958	*MAT***a** *ura3Δ0 ura3::*P_{FLO11}*-URA3*	This Study
AHY967	*MAT***a** *ura3Δ0* P_{FLO11}*-URA3 sir2::kan*^{r} *hmlα::LEU2*	This Study
AHY960	*MAT***a** *ura3Δ0 sfl1::kan*^{r} P_{FLO11}*-URA3*	This Study
L6944	*MAT***a** *ura3-52 his3::hisG leu2::hisG sfl1::HIS3 FLO11::HA*	Fink laboratory collection
AHY959	*MAT***a** *ura3Δ0 hda1::kan*^{r} P_{FLO11}*-URA3*	This Study
AHY964	*MAT***a** *ura3-52 his3::hisG leu2::hisG hda1::kan*^{r} *FLO11::HA*	Fink laboratory collection
AHY961	*MAT***a/α** *ura3Δ0/ ura3Δ0* P_{FLO11}*-URA/*P_{FLO11}*-URA3*	This Study
AHY962	*MAT***a/α** *ura3Δ0/ ura3Δ0 sfl1::kan*^{r}*/sfl1::kan*^{r} P_{FLO11}*-URA3/*P_{FLO11}*-URA3*	This Study
AHY965	*MAT***a/α** *ura3Δ0/ ura3Δ0 hda1::kan*^{r}*/hda1::kan*^{r} P_{FLO11}*-URA3/*P_{FLO11}*-URA3*	This Study
L6901	*MAT***a/α** *his3::hisG/ his3::hisG FLO11::HA/FLO11::HA*	Fink laboratory collection
L6946	*MAT***a/α** *ura3-52/+ his3::hisG/ his3::hisG leu2::hisG/+ sfl1::HIS3/ sfl1::HIS3 FLO11::HA/FLO11::HA*	Fink laboratory collection
AHY966	*MAT***a/α** *ura3-52/+ his3::hisG/ his3::hisG leu2::hisG/+ hda1::kan*^{r}*/ hda1::kan*^{r} *FLO11::HA/FLO11::HA*	Fink laboratory collection
CSY748	*MAT***a** *ura3-52 leu2::hisG his3::hisG flo11::HIS3 ira1-5*	This study
CSY749	*MAT***a** *ura3-52 leu2::hisG his3::hisG flo11::HIS3 ira2-6*	This study
CSY787	*MAT***a** *ura3-52 leu2::hisG his3::hisG flo11::HIS3 ira2-11*	This study
CSY795	*MAT***a** *ura3-52 leu2::hisG his3::hisG flo11::HIS3 ira2-19*	This study
CSY800	*MAT***a** *ura3-52 leu2::hisG his3::hisG flo11::HIS3 ira2-24*	This study
CSY802	*MAT***a** *ura3-52 leu2::hisG his3::hisG flo11::HIS3 ira2-26*	This study
AHY721	*MAT***a** *ura3-52 leu2::hisG his3::hisG flo11::HIS3 ira2::kan*^{r}	This study
AHY877	*MAT***a** *ura3-52 leu2::hisG his3::hisG flo11::HIS3 ira2::kan*^{r} *flo10::kan*^{r}	This Study
CSY770	*MAT***a** *ura3-52 leu2::hisG his3::hisG ira2-6*	This study
AHY716	*MAT***a** *ura3-52 leu2::hisG his3::hisG flo11::HIS3 ira1::kan*^{r}	This study
AHY877	*MAT***a** *ura3-52 leu2::hisG his3::hisG flo11::HIS3 ira1::kan*^{r} *flo10::kan*^{r}	This Study
AHY387	*MAT***a** *leu2::hisG his3::hisG ira1-12*	This study
AHY858	*MAT***a** *ura3-52 leu2::hisG his3::hisG flo11::HIS3 ira2::kan*^{r} *ras2::LEU2*	This Study
AHY877	*MAT***a** *ura3-52 leu2::hisG his3::hisG flo11::HIS3 ira2::kan*^{r} *flo10::kan*^{r}	This Study
AHY863	*MAT***a** *ura3-52 leu2::hisG his3::hisG flo11::HIS3 ira2::kan*^{r} *tec1::kan*^{r}	This Study

AHY869	*MAT***a** *ura3-52 his3::hisG flo11::HIS3 ira2::kan^r tpk2::kan^r*	This Study
AHY868	*MAT***a** *ura3-52 his3::hisG flo11::HIS3 ira2::kan^r flo8::kan^r*	This Study
L6874	*MAT***a** *ura3-52 leu2::hisG his3::hisG flo11::HIS3 sfl1::HIS3*	Fink laboratory collection
L6889	*MAT***a** *ura3-52 leu2::hisG his3::hisG flo11::HIS3 sfl1::HIS3 flo10::URA3*	Fink laboratory collection
AHY819	*MAT***a** *ura3-52 leu2::hisG his3::hisG trp1::hisG flo11::HIS3 ira1::kan^r*	This Study
AHY816	*MAT***a** *ura3-52 leu2::hisG his3::hisG trp1::hisG flo11::HIS3 ira1::kan^r P_{FLO10}-GFP::TRP1*	This Study
SBY009	*MAT***a** *ura3-52 leu2::hisG his3::hisG trp1::hisG flo11::HIS3 ira1::kan^r P_{URA3}-GFP::TRP1*	This Study
SBY068	*MAT***a** *ura3-52 leu2::hisG his3::hisG trp1::hisG flo11::HIS3 P_{FLO10}-GFP::TRP1*	This Study
SBY066	*MAT***a** *ura3-52 leu2::hisG his3::hisG trp1::hisG flo11::HIS3 ira1::kan^r ura3::P_{FLO10}-GFP::TRP1*	This Study
SBY123	*MAT***a** *ura3-52 leu2::hisG his3::hisG trp1::hisG flo11::HIS3 ura3::P_{FLO10}-GFP::TRP1*	This Study
SBY180	*MAT***a** *ura3-52 leu2::hisG his3::hisG trp1::hisG flo11::HIS3 ira1::kan^r P_{FLO10}-GFP::TRP1 hst1::kan^r*	This Study
SBY183	*MAT***a** *ura3-52 leu2::hisG his3::hisG trp1::hisG flo11::HIS3 ira1::kan^r P_{FLO10}-GFP::TRP1 hst2::kan^r*	This Study
SBY196	*MAT***a** *ura3-52 leu2::hisG his3::hisG trp1::hisG flo11::HIS3 P_{FLO10}-GFP::TRP1 sfl1::kan^r*	This Study
SBY022	*MAT***a** *ura3-52 leu2::hisG his3::hisG trp1::hisG flo11::HIS3 ira1::kan^r P_{FLO10}-URA3*	This Study
SBY050	*MAT***a** *ura3-52 leu2::hisG his3::hisG trp1::hisG flo11::HIS3 P_{FLO10}-URA3*	This Study
AHY963	*MAT***a** *ura3-52 leu2::hisG his3::hisG trp1::hisG flo11::HIS3 flo10::URA3*	This Study
AHY854	*MAT***a** *ura3-52 leu2::hisG his3::hisG trp1::hisG flo11::HIS3 ira1::kan^r ura3::P_{FLO10}-URA3*	This Study
AHY955	*MAT***a** *ura3-52 leu2::hisG his3::hisG trp1::hisG flo11::HIS3 ura3::P_{FLO10}::URA3*	This Study
SBY148	*MAT***a** *ura3-52 leu2::hisG his3::hisG trp1::hisG flo11::HIS3 ira1::kan^r P_{FLO10}-URA3 hst1::kan^r*	This Study
SYB163	*MAT***a** *ura3-52 leu2::hisG his3::hisG trp1::hisG flo11::HIS3 ira1::kan^r P_{FLO10}-URA3 hst2::kan^r*	This Study
SBY175	*MAT***a** *ura3-52 leu2::hisG his3::hisG trp1::hisG flo11::HIS3 P_{FLO10}-URA3 sfl1::kan^r*	This Study
SBY109	*MAT***a** *ura3-52 leu2::hisG his3::hisG trp1::hisG flo11::HIS3 ira1::kan^r P_{FLO10}-URA3 sir2::kan^r hml::LEU2*	This Study
SBY111	*MAT***a** *ura3-52 leu2::hisG his3::hisG trp1::hisG flo11::HIS3 ira1::kan^r P_{FLO10}-URA3 sir3::kan^r hml::LEU2*	This Study
SBY190	*MAT*α *ura3-52 leu2::hisG his3::hisG trp1::hisG flo11::HIS3 ira1::kan^r P_{FLO10}-URA3 yku70::kan^r*	This Study
SBY193	*MAT*α *ura3-52 leu2::hisG his3::hisG trp1::hisG flo11::HIS3 ira1::kan^r P_{FLO10}-URA3 yku80::kan^r*	This Study
AHY956	*MAT***a** *ura3-52 leu2::hisG his3::hisG trp1::hisG flo11::HIS3*	This Study
AHY881	*MAT***a** *ura3-52 leu2::hisG his3::hisG HST1::9MYC*	This Study
AHY883	*MAT***a** *ura3-52 leu2::hisG his3::hisG HST2::9MYC*	This Study
AHY896	*MAT***a** *ura3-52 leu2::hisG his3::hisG sfl1::kan^r HST2::9MYC*	This Study

AHY968	*MAT***a** *ura3-52 leu2::hisG his3::hisG sfl1::kan^r HST1::9MYC*	This Study
AHY950	*MAT***a** *ura3-52 leu2::hisG his3::hisG flo11::HIS3 ira2*::*Ty1-LacZ::LEU2*	This study

TABLE 2 | **Oligonucleotides used in this study.**

Oligo	***Sequence***	***Description***
AH179	*5′*-ACATTCTTCTTCAGCATATAACATACAACAAGATTAA GGCTCTTTCTAAACGGATCCCCGGGTTAATTAA-*3′*	To generate *ira1Δ::kan*^{r} allele 5'
AH180	*5′*-ATAATTATAAGGAAAAACGTATATAATCACTGCAATA CTCTAATTTAAAAGAATTCGAGCTCGTTTAAAC-*3′*	To generate *ira1Δ::kan*^{r} allele 3'
AH170	*5′*-TTTTTTGATATCAACTAAACTGTATACATTATCTTTCT TCAGGGAGAAGCGCAGATTGTACTGAGAGTGC-*3′*	To generate *ira2Δ::kan*^{r} allele 5'
AH171	*5′*-ATGCTTACAGATAGATATTGATATTTCTTTCATTAGTT TATGTAACACCTTCTGTGCGGTATTTCACACC-*3′*	To generate *ira2Δ::kan*^{r} allele 3'
BG152	*5′*-ATGCCTGTGGCTGCTCGATATA-*3′*	*FLO10* northern probe 5'
BG153	*5′*-AAGTAACCTGTCATTTCCACGG-*3′*	*FLO10* northern probe 3'
BG154	*5′*-ATGCAAAGACCATTTCTACTCGCTTA-*3′*	*FLO11* northern probe 5'
BG155	*5′*-TGCCAGGAGCTTGCATATTGAG-*3′*	*FLO11* northern probe 3'
ACT1L	*5′*-ATGGATTCTGAGGTTGCTGC-*3′*	*ACT1* northern probe 5'
ACT1R	*5′*-GGCAACTCTCAATTCGTTGT-*3′*	*ACT1* northern probe 3'
AH166	*5′*-TCGGTAGACACATTCAAACCATTTTTCCCTCATCGGCA CATTAAAGCTGGCGGATCCCCGGGTTAATTAA-*3′*	To generate *sir2Δ::kan*^{r} allele 5'
AH167	*5′*-TGTAAATTGATATTAATTTGGCACTTTTAAATTATTAA ATTGCCTTCTACGAATTCGAGCTCGTTTAAAC-*3′*	To generate *sir2Δ::kan*^{r} allele 3'
AH391	*5′*-AAGGAAAAAAGCGGCCGCCGAAACTCTTTACTTCCTAAG-*3′*	5' *IRA2* gap-repair cloning fragment 5'
AH392	*5′*-CGGGATCCTACGTAACGTTGGGGGAAAAGTAACAC-*3′*	5' *IRA2* gap-repair cloning fragment 3'
AH393	*5′*-CGGGATCCTACGTAAGCATGAATGTACATATCTCATG-*3′*	3' *IRA2* gap-repair cloning fragment 5'
AH394	*5′*-TCCCCCCGGGCCTCGATGAATTTGTTAAGCC-*3′*	3' *IRA2* gap-repair cloning fragment 3'
AH404	*5′*-TCGTTTGGATAATGTTTTGGAGTTATACACGCACTTTGATG ATACTGAGGTACGTACGGATCCCCGGGTTAATTAA-*3′*	5' primer *IRA2*-SnaBI::*kan*^{r} 2
AH405	*5′*-AATACCCGCGAAATTTCTGAAGTCGTTCCGTTCTTGTTTTT CTAAACTTTTACGTAGAATTCGAGCTCGTTTAAAC-*3′*	3' primer *IRA2*-SnaBI::*kan*^{r} 2
AH406	*5′*-GGTTCAATTGCTTTCCAAAGGAGGACAAGAAATAATATTTT ACGATTTGCTACGTACGGATCCCCGGGTTAATTAA-*3′*	5' primer *IRA2*-SnaBI::*kan*^{r} 3
AH407	*5′*-AATTGGCGTTGGGTCTGTTCTCACTTGGATGTCTATCGTGC GATCTGTTCTACGTAGAATTCGAGCTCGTTTAAAC-*3′*	3' primer *IRA2*-SnaBI::*kan*^{r} 3
AH408	*5′*-AGCCCTGATTCTGAAAATATCATAGATATTTCTCACTTGA GCGAAAAGCGTACGTACGGATCCCCGGGTTAATTAA-*3′*	5' primer *IRA2*-SnaBI::*kan*^{r} 4
AH409	*5′*-CAGATTCCAAGACATATTTCTTGTATCTTGTCTTCCACAC GTTTGCTTCGTACGTAGAATTCGAGCTCGTTTAAAC-*3′*	3' primer *IRA2*-SnaBI::*kan*^{r} 4
AH410	*5′*-TCAAAAGGTGAAGTTTATGTTTGGGTTCAGCGAGGACAA AGGACGAATTTTACGTACGGATCCCCGGGTTAATTAA-*3′*	5' primer *IRA2*-SnaBI::*kan*^{r} 5
AH411	*5′*-GAAAAATTAGCGATAAGAAAACCCTAACATGAGATATGT ACATTCATGCTTACGTAGAATTCGAGCTCGTTTAAAC-*3′*	3' primer *IRA2*-SnaBI::*kan*^{r} 5

AH238	*5′*-ACGTTGAAGATTTGTTTTAGGGTGCTTAATCAAAGAACA ACAAATAAAAACGGATCCCCGGGTTAATTAA-*3′*	To amplify *flo10Δ::kan*^{r} allele 5'
AH239	*5′*-GACGAATCGTAGACGCAGAAGTATCAATCCAAAGGATAT TTCTGCACCTAGAATTCGAGCTCGTTTAAAC-*3′*	To amplify *flo10Δ::kan*^{r} allele 3'
AH133	*5′*-GAGTTAGCAGCGTCGGAAAC-*3′*	To amplify *ras2Δ::kan*^{r} allele 5'
AH134	*5′*-CCCATTAATACCCGTTGTGC-*3′*	To amplify *ras2Δ::kan*^{r} allele 3'
TRO57	*5′*-CAAGAAGAATAATCCACCTATTTCAACAATTCTGATACC TGTTTACGGATCCCCGGGTTAATTAA-*3′*	To amplify *tec1Δ::kan*^{r} allele 5'
TRO58	*5′*-AGATGTATGTATGTATGTAGACATTTAATAAAAGTTCCC ATGCGAGAATTCGAGCTCGTTTAAAC-*3′*	To amplify *tec1Δ::kan*^{r} allele 3'
AH444	*5′*-GACCGCAAGCGCAGAGATAAG-*3′*	To amplify *hst1Δ::kan*^{r} allele 5'
AH445	*5′*-GAAGAGTTATCCGAGGGAATC-*3′*	To amplify *hst1Δ::kan*^{r} allele 3'
AH447	*5′*-GAAGGGAATTACAGGTTGAAG-*3′*	To amplify *hst2Δ::kan*^{r} allele 5'
AH448	*5′*-CAATTCATACACACCACACATAC-*3′*	To amplify *hst2Δ::kan*^{r} allele 3'
AH482	*5′*-CCAATATGTGTGCCTTTTTCATCAC-*3′*	To amplify *hda1Δ::kan*^{r} allele 5'
AH483	*5′*-CGATAAACTCAACTCTTCTGAG-*3′*	To amplify *hda1Δ::kan*^{r} allele 3'
AH357	*5′*-CTATCCTCGAGGAGAACTTC-*3′*	To amplify *yku70Δ::kan*^{r} allele 5'
AH358	*5′*-CCCCGTTCCTGAAAAATTTC-*3′*	To amplify *yku70Δ::kan*^{r} allele 3'
AH351	*5′*-CTTGGCGAAGAAAGGGGTCC-*3′*	To amplify *sir3Δ::kan*^{r} allele 5'
AH352	*5′*-CTTGGCGAAGAAAGGGGTCC-*3′*	To amplify *sir3Δ::kan*^{r} allele 3'
AH256	*5′*-ACGTTGAAGATTTGTTTTAGGGTGCTTAATCAAAGAACA ACAAATAAAAAATGCGGATCCCCGGGTTAATTAA-*3′*	To amplify P_{FLO10}-*GFP* 5'
AH239	*5′*-GACGAATCGTAGACGCAGAAGTATCAATCCAAAGGATAT TTCTGCACCTAGAATTCGAGCTCGTTTAAAC-*3′*	To amplify P_{FLO10}-*GFP* 3'
AH236	*5′*-ACGTTGAAGATTTGTTTTAGGGTGCTTAATCAAAGAACA ACAAATAAAAAATGTCGAAAGCTACATATAAGG-*3′*	To amplify P_{FLO10}-*URA3* 5'
AH237	*5′*-GACGAATCGTAGACGCAGAAGTATCAATCCAAAGGATA TTTCTGCACCTATTAGTTTTGCTGGCCGCATC-*3′*	To amplify P_{FLO10}-*URA3* 3'
AH464	*5′*-TCTAATTAAAATATACTTTTGTAGGCCTCAAAAATCCAT ATACGCACACTATGTCGAAAGCTACATATAA-*3′*	To amplify P_{FLO11}-*URA3* 5'
AH465	*5′*-TAAGAATGAAAACATCGTAATGAAGAAACGAACATGTT GGAATTGTATCATTAGTTTTGCTGGCCGCATC-*3′*	To amplify P_{FLO11}-*URA3* 3'
AH400	*5′*-TAACCCAACTGCACAGAACAAAAACCTGCAGGAAACGA AGATAAATCATGCGGATCCCCGGGTTAATTAA-*3′*	To amplify P_{URA3}-*GFP* allele 5'
AH401	*5′*-GCTCTAATTTGTGAGTTTAGTATACATGCATTTACTTATA ATACAGTTTTGAATTCGAGCTCGTTTAAAC-*3′*	To amplify P_{URA3}-*GFP* allele 3'
AH384	*5′*-TCTTAACCCAACTGCACAGAACAAAAACCTGCAGGAAA CGAAGATAAATCCAACAGCCCCAGATTCATTC-*3′*	To amplify *ura3::*P_{FLO10}*-GFP* 5'
AH385	*5′*-GCTCTAATTTGTGAGTTTAGTATACATGCATTTACTTATA ATACAGTTTTGAATTCGAGCTCGTTTAAAC-*3′*	To amplify *ura3::*P_{FLO10}*-GFP* 3'

TABLE 3 | **Expression constructs used in this study.** This table illustrates the expression constructs used to study epigenetic silencing at *FLO10*, *FLO11* and *URA3* and summarizes the silencing effect observed for each construct.

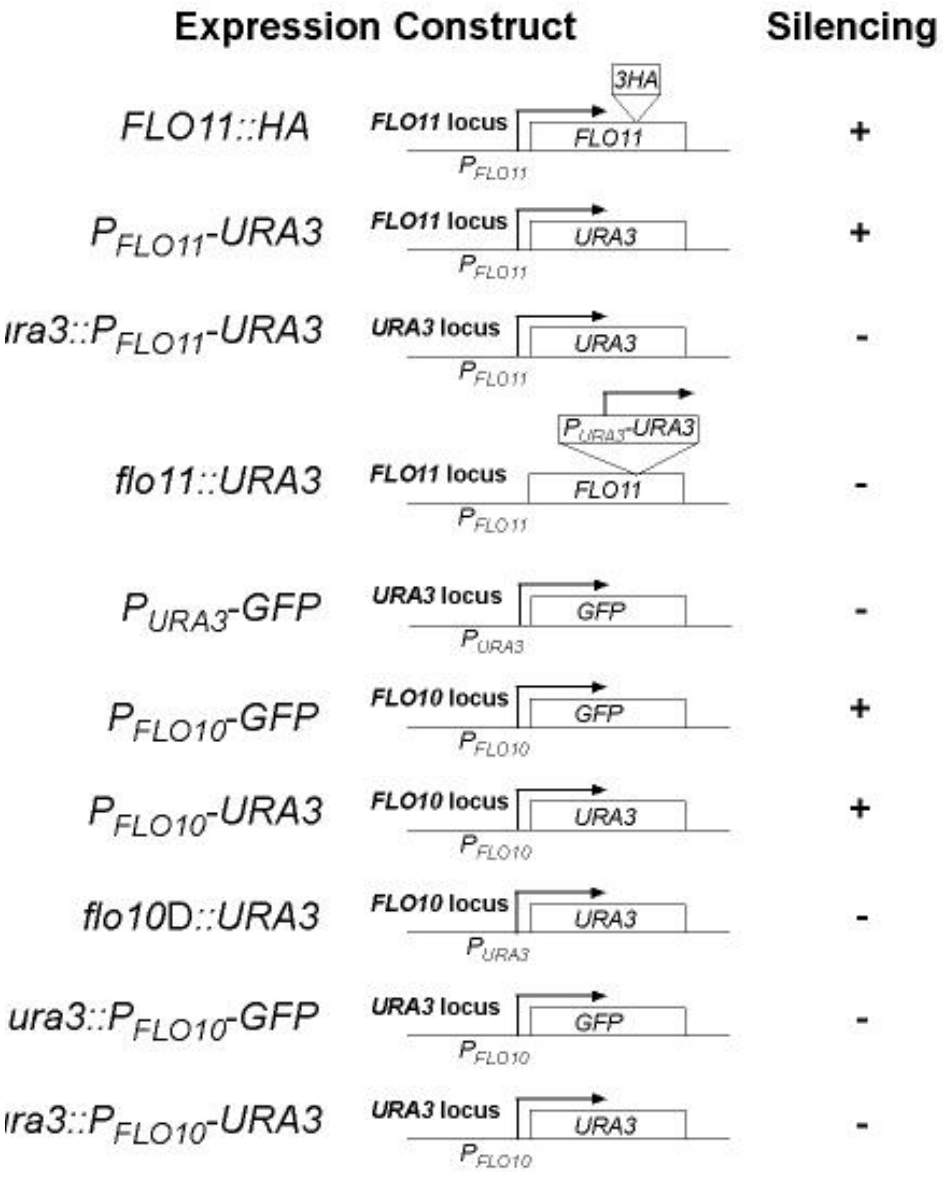

SUPPLEMENTAL FIGURE 1 | **The PKA and filamentation MAP kinase signaling pathways are required for transcriptional activation of *FLO10* in *ira1*$^-$ and *ira2*$^-$ mutants.** (A) Northern analysis of *FLO10* gene expression demonstrates that *FLO10* transcription is dependent upon the PKA and filamentation MAP kinase pathway activity. Both *IRA1* and *IRA2* encode Ras-GAP proteins and regulate Ras activity *in vitro* and *in vivo* (Tanaka et al., 1990a) and Ras2p is required for *ira2*$^-$-mediated *FLO10* gene activation. Ras2p has been demonstrated to activate both the filamentation MAP kinase and PKA signaling pathways; both pathways are important for the regulation of the *FLO11* gene (Rupp et al., 1999). Signaling via the filamentation MAP kinase pathway is required for *FLO10* expression and haploid adhesion as *tec1*$^-$ mutations are epistatic to *ira2*$^-$ mutations for *FLO10* expression. Members of the PKA pathway, Tpk2p and Flo8p, also activate expression of *FLO10* in response to *ira2*$^-$ mutations. Sfl1p, a negative regulator of *FLO11* transcription, is inhibited by PKA activity (Pan and Heitman, 2002; Robertson and Fink, 1998). Sfl1p serves a similar role at *FLO10*, as mutations in Sfl1p are sufficient to activate *FLO10* expression. Similar epistatic interactions were observed between *ira1*$^-$ mutations and mutations affecting the PKA or filamentation MAP kinase pathway. (B) Flo11p-independent agar adhesion of *ira2*$^-$ mutants requires the functional PKA and filamentous MAP kinase pathways. All strains tested for adhesion are *flo11*$^-$. This phenotypic assay for *FLO10* function recapitulates the results of *FLO10* expression analysis in (A) and demonstrates that *FLO10*-dependent adhesion requires the both PKA and filmentation MAP kinase pathway activ ity.

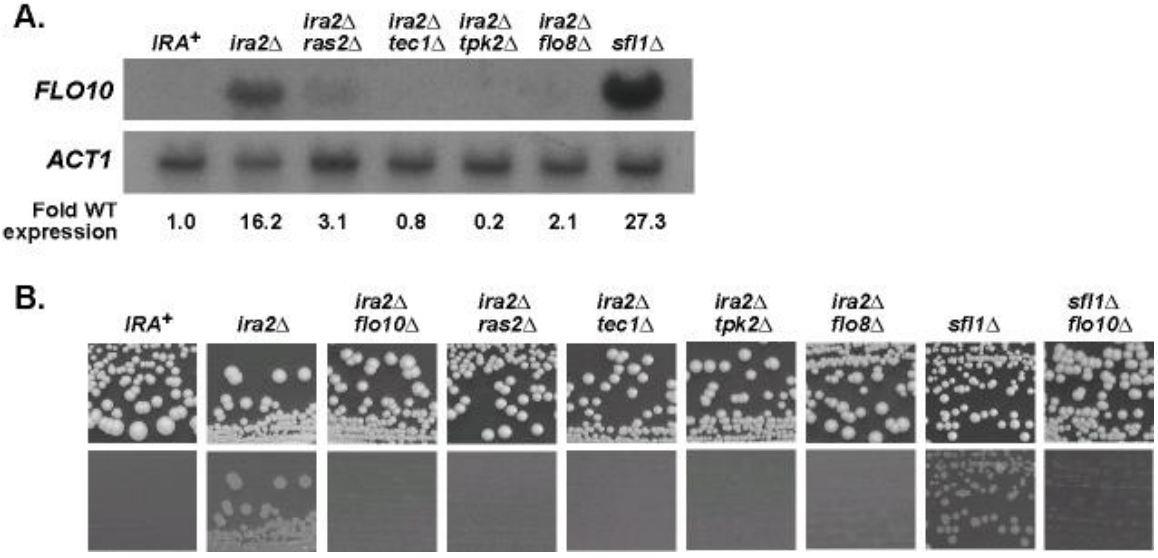

References

Boeke, J.D., Trueheart, J., Natsoulis, G., and Fink, G.R. (1987). 5-Fluoroorotic acid as a selective agent in yeast molecular genetics. Methods in Enzymology *154*, 164-175.

Borst, P. (2002). Antigenic variation and allelic exclusion. Cell *109*, 5-8.

Brachmann, C.B., Sherman, J.M., Devine, S.E., Cameron, E.E., Pillus, L., and Boeke, J.D. (1995). The SIR2 gene family, conserved from bacteria to humans, functions in silencing, cell cycle progression, and chromosome stability. Genes & Development *9*, 2888-2902.

Braun, B.R., and Johnson, A.D. (1997). Control of filament formation in Candida albicans by the transcriptional repressor TUP1. Science *277*, 105-109.

Conlan, R.S., and Tzamarias, D. (2001). Sfl1 functions via the co-repressor Ssn6-Tup1 and the cAMP-dependent protein kinase Tpk2. Journal of Molecular Biology *309*, 1007-1015.

De Las Penas, A., Pan, S.J., Castano, I., Alder, J., Cregg, R., and Cormack, B.P. (2003). Virulence-related surface glycoproteins in the yeast pathogen Candida glabrata are encoded in subtelomeric clusters and subject to RAP1- and SIR-dependent transcriptional silencing. Genes & Development *17*, 2245-2258.

Gagiano, M., Van Dyk, D., Bauer, F.F., Lambrechts, M.G., and Pretorius, I.S. (1999). Divergent regulation of the evolutionarily closely related promoters of the Saccharomyces cerevisiae STA2 and MUC1 genes. Journal of Bacteriology *181*, 6497-6508.

Gimeno, C.J., Ljungdahl, P.O., Styles, C.A., and Fink, G.R. (1992). Unipolar cell divisions in the yeast S. cerevisiae lead to filamentous growth: regulation by starvation and RAS. Cell *68*, 1077-1090.

Gottschling, D.E., Aparicio, O.M., Billington, B.L., and Zakian, V.A. (1990). Position effect at S. cerevisiae telomeres: reversible repression of Pol II transcription. Cell *63*, 751-762.

Guo, B., Styles, C.A., Feng, Q., and Fink, G.R. (2000). A Saccharomyces gene family involved in invasive growth, cell-cell adhesion, and mating. Proceedings of the National Academy of Sciences of the United States of America *97*, 12158-12163.

Haber, J.E., and George, J.P. (1979). A mutation that permits the expression of normally silent copies of mating-type information in Saccharomyces cerevisiae. Genetics *93*, 13-35.

Halme, A., Bumgarner, S., Styles, C., and Fink, G.R. (2004). Genetic and epigenetic regulation of the FLO gene family generates cell-surface variation in yeast. Cell *116*, 405-415.

Heim, R., Prasher, D.C., and Tsien, R.Y. (1994). Wavelength mutations and posttranslational autoxidation of green fluorescent protein. Proceedings of the National Academy of Sciences of the United States of America *91*, 12501-12504.

Hostetter, M.K. (1994). Adhesins and ligands involved in the interaction of Candida spp. with epithelial and endothelial surfaces. Clinical Microbiology Reviews *7*, 29-42.

Howell-Adams, B., and Seifert, H.S. (2000). Molecular models accounting for the gene conversion reactions mediating gonococcal pilin antigenic variation. Molecular Microbiology *37*, 1146-1158.

Hoyer, L.L. (2001). The ALS gene family of Candida albicans. Trends in microbiology *9*, 176-180.

Jiang, Y.W., and Stillman, D.J. (1996). Epigenetic effects on yeast transcription caused by mutations in an actin-related protein present in the nucleus. Genes & Development *10*, 604-619.

Kennedy, B.K., Gotta, M., Sinclair, D.A., Mills, K., McNabb, D.S., Murthy, M., Pak, S.M., Laroche, T., Gasser, S.M., and Guarente, L. (1997). Redistribution of silencing proteins from telomeres to the nucleolus is associated with extension of life span in S. cerevisiae. Cell *89*, 381-391.

Lo, H.J., Kohler, J.R., DiDomenico, B., Loebenberg, D., Cacciapuoti, A., and Fink, G.R. (1997). Nonfilamentous C. albicans mutants are avirulent. Cell *90*, 939-949.

Lo, W.S., and Dranginis, A.M. (1998). The cell surface flocculin Flo11 is required for pseudohyphae formation and invasion by Saccharomyces cerevisiae. Molecular Biology of the Cell *9*, 161-171.

Martin, S.G., Laroche, T., Suka, N., Grunstein, M., and Gasser, S.M. (1999). Relocalization of telomeric Ku and SIR proteins in response to DNA strand breaks in yeast. Cell *97*, 621-633.

Mehr, I.J., and Seifert, H.S. (1998). Differential roles of homologous recombination pathways in Neisseria gonorrhoeae pilin antigenic variation, DNA transformation and DNA repair. Molecular Microbiology *30*, 697-710.

Mishra, K., and Shore, D. (1999). Yeast Ku protein plays a direct role in telomeric silencing and counteracts inhibition by rif proteins. Curr Biol *9*, 1123-1126.

Moazed, D., Kistler, A., Axelrod, A., Rine, J., and Johnson, A.D. (1997). Silent information regulator protein complexes in Saccharomyces cerevisiae: a SIR2/SIR4 complex and evidence for a regulatory domain in SIR4 that inhibits its interaction with SIR3. Proceedings of the National Academy of Sciences of the United States of America *94*, 2186-2191.

Pan, X., and Heitman, J. (2002). Protein kinase A operates a molecular switch that governs yeast pseudohyphal differentiation. Molecular and Cellular Biology *22*, 3981-3993.

Rine, J., and Herskowitz, I. (1987). Four genes responsible for a position effect on expression from HML and HMR in Saccharomyces cerevisiae. Genetics *116*, 9-22.

Rine, J., Strathern, J.N., Hicks, J.B., and Herskowitz, I. (1979). A suppressor of mating-type locus mutations in Saccharomyces cerevisiae: evidence for and identification of cryptic mating-type loci. Genetics *93*, 877-901.

Robertson, L.S., and Fink, G.R. (1998). The three yeast A kinases have specific signaling functions in pseudohyphal growth. Proceedings of the National Academy of Sciences of the United States of America *95*, 13783-13787.

Robyr, D., Suka, Y., Xenarios, I., Kurdistani, S.K., Wang, A., Suka, N., and Grunstein, M. (2002). Microarray deacetylation maps determine genome-wide functions for yeast histone deacetylases. Cell *109*, 437-446.

Rubio, J.P., Thompson, J.K., and Cowman, A.F. (1996). The var genes of Plasmodium falciparum are located in the subtelomeric region of most chromosomes. The EMBO Journal *15*, 4069-4077.

Saville, S.P., Lazzell, A.L., Monteagudo, C., and Lopez-Ribot, J.L. (2003). Engineered control of cell morphology in vivo reveals distinct roles for yeast and filamentous forms of Candida albicans during infection. Eukaryotic Cell *2*, 1053-1060.

Smith, J.S., and Boeke, J.D. (1997). An unusual form of transcriptional silencing in yeast ribosomal DNA. Genes & Development *11*, 241-254.

Stringer, J.R., and Keely, S.P. (2001). Genetics of surface antigen expression in Pneumocystis carinii. Infection and Immunity *69*, 627-639.

Sundstrom, P. (1999). Adhesins in Candida albicans. Current Opinion in Microbiology *2*, 353-357.

Underwood, A.P., Louis, E.J., Borts, R.H., Stringer, J.R., and Wakefield, A.E. (1996). Pneumocystis carinii telomere repeats are composed of TTAGGG and the subtelomeric sequence contains a gene encoding the major surface glycoprotein. Molecular Microbiology *19*, 273-281.

Weiden, M., Osheim, Y.N., Beyer, A.L., and Van der Ploeg, L.H. (1991). Chromosome structure: DNA nucleotide sequence elements of a subset of the minichromosomes of the protozoan Trypanosoma brucei. Molecular and Cellular Biology *11*, 3823-3834.

Wu, J., Suka, N., Carlson, M., and Grunstein, M. (2001). TUP1 utilizes histone H3/H2B-specific HDA1 deacetylase to repress gene activity in yeast. Molecular Cell *7*, 117-126.

Wyrick, J.J., Holstege, F.C., Jennings, E.G., Causton, H.C., Shore, D., Grunstein, M., Lander, E.S., and Young, R.A. (1999). Chromosomal landscape of nucleosome-dependent gene expression and silencing in yeast. Nature *402*, 418-421.

Chapter 3

Genome-wide Screens Identify Additional Regulators of Transcription and Silencing at the *FLO10* and *FLO11* promoters in yeast

Abstract | *FLO10* and *FLO11* are members of a large gene family in the yeast *Saccharomyces cerevisiae* that encode cell-surface glycoproteins that mediate a range of cell-to-cell and cell-to-surface adhesions. We have previously shown that phenotypic diversity in clonal populations of yeast cells is mediated in part by the epigenetic silencing of the *FLO10* and *FLO11* promoters. The mechanisms that underlie this silencing rely on several identified chromatin modifying enzymes and transcription factors. Hda1 and Sfl1 play roles in silencing at both of these *FLO* promoters, whereas Hst1 and Hst2, the homologs-of-Sir2, are specific to the silencing of the *FLO10* promoter. Genome-wide Tn3-insertion screens were conducted to identify additional *trans*-acting factors involved in the transcriptional silencing of these promoters and to investigate further the similarities and differences in the regulation of the *FLO10* and *FLO11* promoters. The initial screens identified 91 Tn3 insertion mutants, representing 74 unique genes, that exhibited altered *FLO10* promoter activity, and 165 Tn3 insertion mutants, representing 102 unique genes, that exhibited altered *FLO11* promoter activity. Because of our interest in chromatin structure at the *FLO* promoters, we focused our follow-up studies on candidates likely to play a role in chromatin modification or remodeling. Among such candidates identified in the screens were components of the Rpd3L histone deacetylase complex, the Srb/Mediator complex, the COMPASS histone methyltransferase complex, and other chromatin remodeling factors such as Rsc2, Ada2, and Swi1. Most of these mutants behave as would be expected, according to contemporary knowledge of the effects of chromatin modification and remodeling on transcription. Mutants of the Rpd3L histone deacetylase complex, however, present phenotypes that were unanticipated given the canonical role of histone deacetylases in the repression of transcription.

INTRODUCTION

In *Saccharomyces cerevisiae*, *FLO10* and *FLO11* are members of a large family of genes that encode cell-surface glycoproteins that mediate a range of cell-to-cell and cell-to-surface adhesions (Guo et al., 2000). We have previously shown that the *FLO10* and *FLO11* promoters are epigenetically silenced in a position-dependent and promoter sequence-dependent manner that contributes to phenotypic diversity in clonal populations of yeast cells (Halme et al., 2004). The silencing of the *FLO* promoters is heterogeneous, or variegated, within the population of cells. Variegated transcription of *FLO10* and *FLO11* results in yeast cells that, at the population level, exhibit variability in their behavior regarding flocculation (cell-to-cell adhesion), adhesion to and invasion of inert surfaces and, in diploids, the formation of long filaments called pseudohyphae (Halme et al., 2004).

In previous studies, we identified several *trans*-acting regulators of the silencing observed at the *FLO10* and *FLO11* promoters (Halme et al., 2004). Among these, the histone deacetylase Hda1 and the DNA-binding repressor Sfl1 mediate silencing of *FLO11* transcription. Hdal also plays a role in silencing at *FLO10*, but the histone deacetylase homologs-of-Sir2 Hst1 and Hst2 have a more critical role in the silencing at this locus and are recruited to the *FLO10* promoter by a Sfl1-dependent mechanism (Halme et al., 2004).

Despite differences in histone deacetylase specificity at *FLO10* and *FLO11*, there is substantial similarity in the transcriptional regulation of these two *FLO* genes. The PKA pathway and the filamentation MAPK pathway function in parallel to regulate the expression of both *FLO10* and *FLO11* in response to environmental cues (Palecek et al.,

2002; Pan and Heitman, 2002; Rupp et al., 1999), although an additional level of negative regulation exists at the *FLO10* promoter (Halme et al., 2004). Sfl1, the downstream effector of transcriptional repression through the PKA signaling pathway, is required for silencing at both *FLO10* and *FLO11*.

Another similarity between *FLO10* and *FLO11* is their unusually large promoter regions. Careful dissection of the *FLO11* promoter has revealed the existence of at least four upstream activation sequences (UASs) and nine repression elements which, together, span at least 2.8 kb of the region upstream of the *FLO11* ORF (Rupp et al., 1999). Thus the *FLO10* and *FLO11* promoters are seemingly very busy locations where the binding of many *trans*-acting regulators occurs to determine whether the given *FLO* gene will be expressed or not.

To identify additional *trans*-acting factors involved in transcriptional silencing of the *FLO10* and *FLO11* promoters, I conducted genome-wide Tn3-insertion screens for mutants that displayed either increased (loss of silencing phenotypes) or decreased (gain of silencing phenotypes) promoter activity. These screens served as successful tools for identifying candidates not previously known to play a role in *FLO* gene transcriptional regulation. The initial screens identified 91 Tn3 insertion mutants, representing 74 unique genes, that exhibited altered *FLO10* promoter activity, and 165 Tn3 insertion mutants, representing 102 unique genes, that exhibited altered *FLO11* promoter activity.

Because of our interest in epigenetic silencing and chromatin structure at the *FLO* promoters, we focused our attention on candidates likely to play a role in chromatin modification or remodeling. Among such candidates identified in these screens were members of the Rpd3L histone deacetylase complex, the COMPASS histone

methyltransferase complex, the Srb/Mediator complex, and other chromatin remodeling factors such as Rsc2, Ada2, and Swi1. The candidate complexes of interest and their identified effects on transcription at the *FLO10* and *FLO11* promoters are summarized in Figure 1 of this chapter. Some of the candidate complexes exhibit the same effect at both *FLO* promoters, whereas others are specific to either *FLO10* or *FLO11* regulation.

Many of the mutants of the chromatin regulating complexes identified in these screens behaved as would be expected according to contemporary functional knowledge of the complexes in which they participate and the predicted effects of chromatin modification and remodeling on transcription. Rsc2 and Swi1, which are components of the RSC and Swi/Snf chromatin remodeling complexes, respectively, act as activators of *FLO* gene expression, a role in line with their known functions in remodeling DNA-nucleosomal histone interactions (Martens and Winston, 2003). Components of the SAGA histone acetyltransferase complex, including Ada2, Ada5, and Spt8, also function as activators of *FLO* transcription, again a role that is unsurprising given that acetylation of histones is known to promote transcription (Grunstein, 1997).

The Srb/Mediator complex has been previously shown by others to be involved in the transcriptional repression of the *FLO11* promoter and the *FLO11*-like *STA1* promoter (Holstege et al., 1998; Kim et al., 2004; Nelson et al., 2003; Song and Carlson, 1998). It is also included in this report because results presented here shed light on unresolved issues regarding the mechanisms through which the Srb/Mediator complex performs its repressive functions. This will be discussed later in this chapter.

Some candidate complexes identified in these screens presented phenotypes in conflict with contemporary theories regarding the role of chromatin structure in

regulating transcription. For instance, I found that members of the COMPASS complex, including the Set1 methyltransferase and Bre2, behave as repressors of *FLO11* transcription. Mutations in the COMPASS complex result in loss of silencing at the *FLO11* promoter. Disruption of silencing at telomeres, at the ribosomal DNA locus (rDNA), and at the silent *HML* and *HMR* yeast mating cassette loci have been observed by others studying COMPASS mutants (Briggs et al., 2001; Fingerman et al., 2005; Mueller et al., 2006; Nislow et al., 1997; Schneider et al., 2005), but these and my findings are in conflict with reports that the Set1 methyltransferase is involved in active transcription (Ng et al., 2003; Pokholok et al., 2005; Santos-Rosa et al., 2002). And most importantly for studies presented in Chapter 5 of this thesis, I found that components of the histone deacetylase complex Rpd3L, including Cti6, Rxt2, Pho23, and Sin3, behave as net transcriptional activators of the *FLO* promoters. Given that histone deacetylases, including Rpd3, generally repress transcriptional activity, this was a surprising finding (Grunstein, 1997; Carrozza et al., 2005; Kadosh and Struhl, 1997, 1998; Rundlett et al., 1998). Other recent studies have also demonstrated that the Rpd3L complex can act as an activator of transcription at certain target promoter regions (Sertil et al., 2007; Sharma et al., 2007; Xin et al., 2007; De Nadal et al., 2004). Taken together, these collective data raise an apparent paradox regarding the role in regulating transcription played by the Rpd3L histone deacetylase complex at different target promoters in yeast. This apparent paradox will be discussed in this chapter and in Chapter 5 of this thesis.

Materials and Methods

Strains, media, microbiological techniques and growth conditions | Yeast strains used in this study are listed in Table 1. All strains are derived from Σ1278b (also known as MB1000; (Brandriss and Magasanik, 1979; Grenson et al., 1966)) and MB758-5B (Siddiqui and Brandriss, 1988). Standard yeast media, yeast transformations and genetic manipulations were performed as described in Guthrie and Fink (2001). For analysis of P_{FLO10}-*URA3* or P_{FLO11}-*URA3,* strains were grown overnight in YPD liquid media, then diluted 1:50 in YPD liquid media and grown to OD_{600} 0.8-1.2. Cell densities were adjusted to OD_{600} 1, then cultures were serially diluted (10-fold dilutions for P_{FLO10}-*URA3* stains and 2-fold or 5-fold dilutions for P_{FLO11}-*URA3* strains) and plated synthetic complete (SC), SC-Ura, and SC+5-FOA (0.1%) agar plates. For visualization of P_{FLO10}-*GFP* or P_{FLO11}-*GFP* by fluorescent microscopy or FACS, cells were streaked onto YPD plates and harvested after one day of growth at 30 degrees C. Haploid adhesion assays were performed as described (Guo et al., 2000). To induce pseudohyphal differentiation, strains were grown on nitrogen-poor SLAD media, which was prepared as described in (Gimeno et al., 1992).

Yeast strain construction | The Tn3 insertion mutants were generated according to Kumar et al., 2002. 15 pools of yeast genomic library containing *LEU2*-marked Tn3 insertions were isolated from bacterial strains by Qiagen MaxiPrep. The resulting plasmid DNA was NotI-digested to liberate the genomic DNA inserts, which were transformed into P_{FLO10}-*URA3 ira1- leu2-* (SBY022) or P_{FLO11}-*URA3 leu2-* (SBY251) parental strains. The *ira1* mutation was used as a genetic tool to reveal variegated

epigenetic silencing at the *FLO10* promoter so that it could be studied because, in wild type genetic background, the *FLO10* promoter is not active under conditions thus far tested (Halme et al., 2004). Tn3-*LEU2* transformed cells were selected on SC-Leu plates. Leu^+ transformants were streaked onto fresh –Leu plates and then replica plated onto SC, SC-Ura, and SC+5-FOA to identify candidates of interest. 32,955 Tn3-carrying transformants were screened in the P_{FLO10}-*URA3* reporter background and 41,532 Tn3-carrying transformants were screened in the P_{FLO11}-*URA3* reporter background. Tn3 insertion sites were identified by PCR amplification using random primers in conjunction with insert-specific primers, followed by DNA sequencing of purified amplified fragments. The identified Tn3 insertion sites and flanking sequence (to direct homologous recombination) were then PCR amplified using gene-specific primers and resulting DNAs were transformed into P_{FLO10}-*GFP* and P_{FLO11}-*GFP* strains, and into *MAT* a and *MAT* alpha strains with intact *FLO* genes. Resulting haploids were mated to produce homozygous diploid mutants. Yeast strains carrying gene deletions were constructed by PCR amplification of a P_{TEF} promoter driven yeast *LEU2* or bacterial kanamycin-resistance gene (Longtine et al., 1998), with flanking sequences that would direct the deletion cassette to the appropriate locus via homologous recombination. All deletions remove the full ORF (ATG-Stop). Transformation of plasmids was performed according to standard yeast transformation protocols and maintained under appropriate selection. Plasmids used in this study are listed in Table 2. Primers used in this study are listed in Table 3.

RESULTS

Genome-wide screens identify additional regulators of *FLO10* and *FLO11* transcription and epigenetic silencing | Yeast strains carrying transcriptional reporter constructs, either P_{FLO10}-*URA3 ira1-* or P_{FLO11}-*URA3* in the Sigma 1278b genetic background (Halme et al., 2004), were mutagenized by transformation with a yeast genomic DNA library carrying Tn3 transposon insertions (Kumar et al., 2002; Seringhaus et al., 2006). I chose this approach over one utilizing the yeast gene deletion library because the gene deletion library was constructed in the S288C genetic background (Winzeler et al., 1999) and I preferred to perform my studies in the Sigma 1278b genetic background in which *FLO* gene regulatory pathways are intact (Liu et al., 1996). By utilizing *FLO* promoter fusions to *URA3*, the screens were designed to identify only transcriptional regulators of the *FLO10* and *FLO11* genes. Promoter activity was determined by assaying expression of the *URA3* reporter, thus these screens did not detect post-transcriptional regulation of *FLO* gene products. In the screen for transcriptional regulators of the *FLO10* promoter, I took advantage of the *ira1* genotype as a tool for revealing variegated silencing at the *FLO10* promoter so that it could be studied (Halme et al., 2004).

Resulting Tn3 mutants were screened for phenotypic changes in silencing of the *FLO10* and *FLO11* promoters compared to the levels of silencing observed in the parental strains (Figure 2). This was accomplished by taking advantage of the ability to select positively for and negatively against Ura3 enzymatic activity by growing yeast on media lacking uracil or containing the chemical 5-Fluoroorotic acid (5-FOA). Cells exhibiting active transcription from the given *FLO* promoter express the *URA3* gene and

are phenotypically Ura^{+}, enabling them to grow on media lacking uracil (-Ura) but not on media containing the chemical 5-FOA. Failure of Ura^{+} cells to grow on 5-FOA-containing media presumably results from the Ura3 enzyme converting 5-FOA into a compound that is toxic to the yeast cells (Boeke et al., 1987). Cells that are inactive or silent at the *FLO* promoter are phenotypically Ura3^{-} and are thus unable to grow on –Ura media but able to grow on 5-FOA-containing media because they are resistant to the 5-FOA toxicity (5-FOA^{R}). Populations of the unmutagenized parental strains, which exhibit variegated silencing at the *FLO10* and *FLO11* promoters, consist of some cells able to grow on –Ura media and some cells able to grow on 5-FOA-containing media (Figure 3). Tn3 mutants were screened to identify those that displayed a change in their ability to grow on both types of media.

The screens identified mutants exhibiting a range of transcriptional/silencing phenotypes (Figure 3). Some of the mutants have completely lost transcriptional activity at the *FLO* promoter being tested. Others have completely lost silencing at the promoter, resulting in all cells in the mutant population having an active *FLO* promoter. Still other mutants continue to exhibit variegated expression, but the numbers of cells in the on-versus-off transcriptional states have been shifted in one direction or the other.

Tables 4 through 7 provide complete lists of the candidate genes identified in these screens and the annotated biological processes with which they are associated according to the *Saccharomyces Genome Database* (www.yeastgenome.org). In the screen for regulators of P_{FLO11}-*URA3*, 102 genes were identified, 25 of which encode products that activate *FLO11* transcription and 77 of which encode products that repress *FLO11* transcription. In the screen for regulators of P_{FLO10}-*URA3*, 74 genes were

identified, 50 of which encode products that activate *FLO10* transcription and 24 of which encode products that repress *FLO10* transcription.

Given the level of coregulation known to exist between the *FLO10* and *FLO11* promoters (Halme et al., 2004), it is surprising that there is not more overlap between the lists of candidate genes identified in the two screens. If fact, the screens identified only 12 candidate genes in common (Figure 4A). This result is more a reflection of incomplete saturation in these screens than a true reflection of the level of coregulation that exists between these two *FLO* promoters.

In effort to achieve genome-wide saturation, I screened 32,955 Tn3-carrying transformants in the P_{FLO10}-*URA3* screen and 41,532 Tn3-carrying transformants in the P_{FLO11}-*URA3* screen. Given the size of the haploid yeast genome (~13 Mb) and the size of the yeast genomic DNA inserts (2-to-3 kb) in the Tn3 insertion library used in this study (Kumar et al., 2002), the numbers of transformants screened should have been sufficient for 99% probability that every 2 kilobase fragment in the yeast genome be represented at least once in each of the two screens. This calculation was made using the formula:

$$N = \ln(1 - P) / \ln[1 - (\text{insert size} / \text{genome size})]$$

which gives the number N of independently generated clones that must be screened to obtain any given genomic fragment of the insert size with a given probability P (Clarke and Carbon, 1992). For several genes identified in each screen, I verified multiple unique Tn3 insertion sites within the population of mutants (E.g., multiple unique Tn3 insertion mutations were found in *BRE2*, *HDA1*, *HDA2*, *HDA3*, *SET1*, *SIN3*, *SRB10*, *SRB11* and

other genes in the P_{FLO11}-*URA3* screen, and in *IRA2*, *RSC2*, *STE7* and other genes in the P_{FLO10}-*URA3 ira1-* screen.). Observing multiple hits in the same gene can often be taken as a sign of screen saturation, but there are other telling indicators that genome-wide saturation was not reached. Although the screens did cumulatively identify 19 genes that are established effectors of *FLO* gene transcription, these genes constitute less than 30 percent of the more than 65 published regulators of *FLO* transcription (Figure 4B) (Cullen et al., 2004; Gancedo, 2001; Halme et al., 2004; Nelson et al., 2003; Palecek et al., 2000, 2002; Rupp et al., 1999). Incomplete saturation may, to some extent, have been due to bias in integration site preference of the Tn3 transposon (Seringhaus et al., 2006).

The screens served as useful tools for identifying a number of candidates not previously known to be involved in *FLO* gene regulation. Because of our interest in epigenetic silencing of the *FLO* promoters, I focus in this report on only those candidates likely to play a role in chromatin modification or remodeling (Summarized in Figure 1). Components of the following chromatin-regulating complexes were identified in these screens:

1. The Rpd3L Histone Deacetylase Complex

The screens identified four members of the Rpd3L histone deacetylase complex (HDAC), namely *CTI6/RXT1*, *RXT2*, *PHO23*, and *SIN3*, as transcriptional activators of the *FLO11* promoter (Figure 5A). The screens also identified a fifth member of this complex, *ASH1*, as a transcriptional activator of the *FLO10* promoter, although the phenotype in this case was very mild (Figure 5B).

The catalytic member of the Rpd3L complex is the conserved Class I histone deacetylase, Rpd3 (Verdin et al., 2003; Yang and Seto, 2008). Rpd3 associates with two

distinct complexes: the larger Rpd3L complex and the functionally distinct smaller complex Rpd3S that consists of a different set of components (Carrozza et al., 2005a; Carrozza et al., 2005b). Both complexes include Rpd3, Sin3, and Ume1. The distinct members of the Rpd3L complex include Ash1, Cti6/Rxt1, Dep1, Pho23, Rxt2, Rxt3, Sap30, Sds3, and Ume6 (Carrozza et al., 2005a; Carrozza et al., 2005b). The distinct members of the Rpd3S complex are Eaf3 and Rco1 (Carrozza et al., 2005b). The Rpd3L complex specifically mediates the transcriptional repression of specific promoters, such as *INO1* and *HO* (Carrozza et al., 2005a; Carrozza et al., 2005b). Rpd3S, on the other hand, functions in a signaling pathway from the elongating form of RNA polymerase II through the Set2 histone methyltransferase (Carrozza et al., 2005b); Rpd3S recognizes methyl marks left by Set2 at sites of transcriptional elongation and deacetylates histones within these transcribed sequences to prevent the occurrence of spurious transcription initiation from cryptic start sites within open reading frames (Carrozza et al., 2005b), an activity that appears to be particularly important at long and/or infrequently transcribed open reading frames (Li et al., 2007b).

In general, histone deacetylation is strongly correlated with transcriptional repression (Grunstein, 1997). Rpd3 was indeed originally identified as a transcriptional repressor of genes involved in a diverse set of processes including meiosis, cell-type specificity, potassium transport, phosphate metabolism, methionine biosynthesis, and phospholipids metabolism (Hepworth et al., 1998; Jackson and Lopes, 1996; Kadosh and Struhl, 1997; McKenzie et al., 1993; Stillman et al., 1994; Vidal and Gaber, 1991; Vidal et al., 1991). This transcriptional repression was demonstrated to be a consequence of the histone deacetylase activity of Rpd3 (Kadosh and Struhl, 1998a; Rundlett et al., 1998),

which mediates deacetylation of lysines 5 and 12 of histone H4 *in vivo* (Rundlett et al., 1996). Rpd3 is known to be recruited to many of its target locations by promoter-specific binding factors (Carrozza et al., 2005a; Kadosh and Struhl, 1997, 1998b; Rundlett et al., 1998). Ume6, for example, is important for targeted transcriptional repression by Rpd3 at the *INO1* and *IME2* promoters, whereas Ash1 is important for targeting of Rpd3 to the *HO* locus (Carrozza et al., 2005a; Kadosh and Struhl, 1997, 1998b).

The roles for Rpd3 in transcriptional regulation discussed thus far have been in accordance with the canon that histone deacetylation is strongly correlated with transcriptional repression (Grunstein, 1997). With this in mind, my finding that members of the Rpd3L complex activate *FLO* gene transcription was initially surprising and raised the possibility of some indirect role for Rpd3L in the regulation of *FLO* transcription. Recently, however, Rpd3L has been found to play apparently direct roles in transcriptional activation at several locations within the yeast genome. The *DAN/TIR* genes induced during anaerobic growth (Sertil et al., 2007), the DNA damage-inducible gene *RNR3* (Sharma et al., 2007), the *HAP1* gene which encodes a transcription factor involved in oxygen and heme regulation (Xin et al., 2007), and osmoresponsive genes such as *HSP12* (De Nadal et al., 2004) all appear to be activated by Rpd3 localizing to their promoters. Association of epitope-tagged Rpd3 or epitope-tagged Sin3 has been detected by chromatin immunoprecipitation at *RNR3* and *HSP12*, suggesting that the activating role of Rpd3 is not indirect at these genes (De Nadal et al., 2004; Sharma et al., 2007). Furthermore, Rpd3-mediated histone deacetylation accompanies transcriptional activation at *DAN4* (Sertil et al., 2007), *RNR3* (Sharma et al., 2007), and *HSP12* (De

Nadal et al., 2004), suggesting a mechanism of transcriptional activation by Rpd3 that is in apparent conflict with current theories regarding the impact of chromatin structure on transcription (Grunstein, 1997).

2. The RSC and Swi/Snf Chromatin Remodeling Complexes

The screens identified the genes *RSC2* and *SWI1* as transcriptional activators of the *FLO10* promoter (Figure 7B). Rsc2 is a component of the RSC (remodels the structure of chromatin) remodeling complex and Swi1 is a component of the Swi/Snf chromatin remodeling complex, both of which mediate ATP-dependent alterations in DNA-nucleosome interactions (Martens and Winston, 2003).

Both the RSC and the Swi/Snf complexes change chromatin structure by altering DNA-histone contacts within a nucleosome in an ATP-dependent manner (Martens and Winston, 2003). Chromatin remodeling by Swi/Snf and by RSC involves unwrapping of nucleosomal DNA (Martens and Winston, 2003). RSC-mediated chromatin remodeling results in the transfer of the entire histone octamer from the nucleosome, leaving behind naked DNA (Lorch et al., 1999).

The Swi/Snf complex consists of at least nine protein subunits, including both conserved core and nonconserved components (Martens and Winston, 2003). This complex has been well characterized as a transcriptional activator, although there is some evidence that it can act directly to repress transcription at some loci, as well (Battaglioli et al., 2002; Martens and Winston, 2002; Zhang et al., 2002). Swi/Snf complexes are recruited to promoters by DNA-binding activators and repressors, and the Swi1 component identified in this screen has been shown to be directly involved in such interactions (Belandia et al., 2002). All Swi/Snf ATPases also contain a bromodomain

motif that is capable of binding acetylated lysine residues in histone tails *in vitro* and is required for Swi/Snf binding to at least some promoters *in vivo* (Hassan et al., 2001; Hassan et al., 2002; Marmorstein and Berger, 2001; Winston and Allis, 1999).

The fifteen-subunit RSC chromatin remodeling complex was identified in yeast based on homology to components of Swi/Snf (Cairns et al., 1996). RSC has been shown to have both activating and repressing effects on transcription (Damelin et al., 2002; Ng et al., 2002). Although the RSC and Swi/Snf complexes share very similar biological activities, they play distinct functional roles in transcriptional regulation (Cao et al., 1997; Du et al., 1998). Expression array experiments have identified several classes of genes that are regulated in a RSC-dependent manner. These include genes that encode proteins involved in ribosome biogenesis, stress response, and cell wall integrity (E.g., *CWP1*, *SCW11*, *UGP1*, and *OPI3*).

3. The SAGA Histone Acetyltransferase Complex

The screens identified the genes *ADA2* and *SPT8* as transcriptional activators of the *FLO10* promoter (Figure 7B). They also identified ADA5/SPT20 as a candidate transcriptional activator of the *FLO11* promoter (Figure 7A). All three of these genes encode components of the SAGA (SPT-ADA-Gcn5-acetyltransferase) histone acetyltransferase (HAT) complex.

SAGA is a large complex that consists of at least fifteen subunits, including Gcn5, Ada1, Ada2, Ada3, Spt3, Spt7, Spt8, and Spt20/Ada5 (Candau et al., 1997; Grant et al., 1997; Horiuchi et al., 1997; Roberts and Winston, 1997; Saleh et al., 1997). The catalytic HAT component of the SAGA complex is Gcn5, a protein that is conserved from yeasts to humans (Sterner and Berger, 2000). The functional domains of Gcn5 include a C-

terminal bromodomain, an Ada2 interaction domain, and the HAT domain (Candau and Berger, 1996; Candau et al., 1997), which preferentially acetylates lysine 14 of histone H3 and lysines 8 and 16 of histone H4 (Kuo et al., 1996).

Histone acetylation is considered a hallmark of transcriptionally active chromatin (Brownell and Allis, 1996; Grunstein, 1997). The SAGA complex has been shown to function in the activation of transcription both *in vivo* and *in vitro* (Belotserkovskaya et al., 2000; Dudley et al., 1999; Ikeda et al., 1999; Utley et al., 1998; Wallberg et al., 1999). SAGA plays an important role in transcriptional activation at a subset of genes, including *GAL1*, *TRP3*, and *HIS5* (Belotserkovskaya et al., 2000; Dudley et al., 1999). SAGA also shows genetic interactions and partial redundancy with the chromatin remodeling complex Swi/Snf in its roles in activating transcription of some genes (Sudarsanam et al., 1999).

4. The Srb/Mediator Complex

The screens identified *MED1*, *MED4*, *NUT1/MED5*, *SRB8*, *SRB9*, *SRB10*, and *SRB11* as transcriptional repressors of the *FLO11* promoter (Figure 9A). Silencing of the *FLO11* promoter is lost in these mutants. *SRB11* was also identified as a transcriptional repressor of the *FLO10* promoter (Figure 9B). All of these proteins are members of the very large, multi-subunit yeast Srb/Mediator complex.

The large multi-subunit Mediator complex in yeast was identified nearly twenty years ago as an activity that could promote transcription in an *in vitro* system by relieving transcriptional "squelching", i.e., interference caused by addition of an excess of transcriptional activators (Bjorklund et al., 2001; Kelleher et al., 1990; Myers and Kornberg, 2000). Mediator has long been known as a general transcriptional activator

that interacts with RNA polymerase II to promote transcription at almost all promoters in yeast (Bjorklund et al., 2001; Myers and Kornberg, 2000).

There have also been reports that Mediator plays an important role as a transcriptional repressor at some loci, including genes involved in cell type specificity, meiosis, and sugar utilization (Hengartner et al., 1998). This repression seems to be dependent on the association of Mediator with the Srb8-11 complex, which includes as a component the cyclin-dependent kinase (CDK) Srb10. Members of the Mediator complex itself, including the subunits Med1 and Nut1 that we identify as repressors of *FLO* gene expression, have been shown to bring about both transcriptional activation and repression depending on the locus examined (Balciunas et al., 1999; Beve et al., 2005). Since mutations in Med1 and Nut1 lead to phenotypes resembling those of *srb8-11* mutants, it has been proposed that they must interact with the Srb8-11 complex (Bjorklund et al., 2001; Myers and Kornberg, 2000). Interestingly, the Srb/Mediator proteins have also been shown to interact functionally and physically with the transcriptional repressor Sfl1 at the *SUC2* promoter in *S. cerevisiae* (Song and Carlson, 1998) and the *FLO11*-like *STA1* promoter in the yeast *S. diastaticus* (Kim et al., 2004), suggesting that this interaction is likely occurring at the Sfl1-regulated *FLO* promoters, as well.

In contrast with other candidates discussed here, the observation that the Srb proteins regulate *FLO11* is not a new one. Involvement of the Srb proteins in transcriptional repression of the *FLO11* promoter and the closely related *STA1* promoter has been shown in other studies (Holstege et al., 1998; Kim et al., 2004; Nelson et al., 2003; Song and Carlson, 1998). However unresolved issues regarding the mechanisms

through which the Srb/Mediator complex performs its repressive functions and the relative strength of the Srb/Mediator mutant phenotypes at the *FLO* promoters are reasons to take notice of the enrichment of the Srb/Mediator mutants among the candidates identified in these screens.

5. The COMPASS Histone Methyltransferase Complex

The screens identified two members of the COMPASS histone methyltransferase complex, namely *SET1* and *BRE2*, as transcriptional repressors of the *FLO11* promoter (Figure 11A). Silencing of the *FLO11* promoter is lost in these mutants.

The conserved histone methyltransferase Set1 is the catalytic subunit of the COMPASS (complex associated with Set1) complex and is solely responsible for mono-, di-, and trimethylating the lysine 4 residue of histone H3 (H3K4) (Briggs et al., 2001; Krogan et al., 2002; Nagy et al., 2002; Roguev et al., 2001; Santos-Rosa et al., 2002). Other members of the complex include Bre2, Sdc1, Sgh1, Spp1, Swd1, Swd2, and Swd3 (Dehe and Geli, 2006).

The biological significance of H3K4 methylation by Set1 has been a matter of some debate. Early gene-specific and whole-genome studies in yeast found that Set1 occupancy is enriched at the 5′ ends of actively transcribed genes (Ng et al., 2003; Pokholok et al., 2005; Santos-Rosa et al., 2002). The recruitment of Set1 to locations of active transcription is mediated by its interactions with the Paf1 complex, which is associated with the elongating form of RNA polymerase II (Krogan et al., 2003). These findings culminated in the hypothesis that trimethylated H3K4 serves as a mark of recent transcriptional activity (Ng et al., 2003). More recent whole-genome studies on human embryonic stem cells and differentiated human cells have found trimethylated H3K4 at

the promoters of virtually every protein-coding gene, including those that are not being actively transcribed (Guenther et al., 2007). In light of earlier findings, this observation has been interpreted as an indication of nonproductive transcription initiation occurring at most protein-coding genes in these cells (Guenther et al., 2007). Despite correlations between active transcription, Set1 occupancy, and H3K4 methylation state, the global importance of Set1 in active transcription remains in question, since *set1* mutants are viable and do not exhibit a significant change in transcription over the majority of the genome (Li et al., 2007a).

Deletion of *SET1* or other members of the COMPASS complex, including *BRE2*, does disrupt transcriptional silencing at telomeres, at the ribosomal DNA locus (rDNA), and at the silent *HML* and *HMR* mating cassette loci in yeast (Briggs et al., 2001; Fingerman et al., 2005; Mueller et al., 2006; Nislow et al., 1997; Schneider et al., 2005). These findings suggest the possibility of a direct role for Set1 and H3K4 methylation in gene silencing.

Confirming and further characterizing the phenotypes of the candidate genes silencing | Gene specific primers were used to PCR amplify individual insertion sites with sufficient flanking sequence to allow homologous recombination when these amplified DNAs were used to transform yeast. To confirm that the identified Tn3-insertion sites were indeed the cause of the observed phenotypes and to investigate the effects of these mutations on both *FLO10* and *FLO11* promoter activity, I transformed the parental strains carrying P_{FLO11}-*URA3* or P_{FLO10}-*URA3* (in both wild type and *ira1*- backgrounds) with the amplified Tn3-insertion site DNAs. To verify that the observed phenotypes were not artifacts of the –Ura/5-FOA selection test, I transformed strains

carrying alternative transcriptional reporter constructs, the P_{FLO11}-*GFP* or P_{FLO10}-*GFP* (in both wild type and *ira1*- backgrounds) constructs (Halme et al., 2004), with the amplified Tn3-insertion site DNAs. These strains were examined using fluorescent-activated cell sorting (FACS) and fluorescent microscopy. To examine the effects of the Tn3 insertion mutations on *FLO*-dependent phenotypes such as haploid adhesion and diploid pseudohyphal growth, I also transformed Sigma 1278b wild type haploid MAT a and MAT alpha strains with these DNAs, and then mated the resulting strains to generate homozygous Tn3 mutant diploids. The results of these tests are described below.

The disruption of a gene by the insertion of the large Tn3 transposon sequence generally causes a loss of function of the gene product. In cases where Tn3 mutations in several members of the same complex result in the same mutant phenotype, these mutations are almost certainly loss of function mutations. Rare cases have been reported, however, in which Tn3-mutants are not nulls (for an example, see Natarajan et al., 1998). Therefore the phenotypes of clean deletion strains, in which the entire ORF of the candidate gene was replaced with either a KanMx-expression cassette or a *LEU2*-expression cassette, were also checked for representative members of the candidate complexes.

The Rpd3L Histone Deacetylase Complex is a transcriptional activator of the *FLO10* and *FLO11* promoters | Tn3 insertion mutations in components of the Rpd3L complex result in fewer cells with an active *FLO11* promoter, visualized by serial dilutions of P_{FLO11}-*URA3* expressing strains grown on –Ura and 5-FOA selection media (Figure 5A). These mutations shift more of the cellular population to a silenced *FLO11* promoter state, as demonstrated by the dramatic increase in the number of cells able to

grow on media containing 5-FOA. This observation is confirmed by FACS analysis of P_{FLO11}-*GFP* strains (Figure 5A). The deletion mutant *cti6Δ* phenocopies the Tn3 insertion mutant, confirming a null phenotype in these Tn3 mutants.

Rpd3 associates with two complexes: the larger Rpd3L complex and the functionally distinct Rpd3S complex, which consists of a different set of components (Carrozza et al., 2005a; Carrozza et al., 2005b). To confirm that the phenotypes observed are specific to the Rpd3L complex, a strain was constructed in which the *EAF3* gene, which encodes a distinct member of the Rpd3S complex (Carrozza et al., 2005b), was deleted. The *eaf3Δ* mutation does not affect *FLO11* promoter activity, demonstrating that the Rpd3L, but not the Rpd3S, complex regulates *FLO11* transcription (Figure 5A).

FLO10 promoter activity is also reduced in some Rpd3L mutants (Figure 5B). P_{FLO10}-*URA3* and P_{FLO10}-*GFP* expressing strains demonstrate that Tn3-insertion mutations in *CTI6* and *ASH1* result in reduced expression from the *FLO10* promoter.

***FLO11*-dependent haploid adhesion and diploid pseudohyphal growth is abolished in Rpd3L mutants |** Loss of Rpd3L function results in the inability of haploid yeast cells to adhere to YPD-agar in plate washing assays (Figure 6A). This phenotype is also observed in an *rpd3Δ* deletion mutant, demonstrating that the catalytic component of the Rpd3L histone deacetylase complex also plays a role in activating *FLO11* promoter activity. *FLO11* is sufficient to rescue this defect, as seen when the mutant strains are transformed with a 2 micron plasmid carrying a P_{TEF}-*FLO11* construct. Mutation of Rpd3L subunits also completely abolishes *FLO11*-dependent diploid pseudohyphal growth under low nitrogen conditions (Figure 6B). When these mutant strains are

transformed with a 2 micron plasmid carrying a P_{TEF}-*FLO11* construct, however, filamentation is recovered (Figure 6C).

RSC, Swi/Snf, and SAGA activate the *FLO10* promoters, but to varying degrees and specificity | Tn3-insertion mutations in components of the RSC and Swi/Snf ATP-dependent chromatin remodeling complexes affect the activation of the *FLO11* promoter to different degrees, visualized by serial dilutions of P_{FLO11}-*URA3* expressing strains grown on selection media (-Ura and 5-FOA) and by FACS analysis of P_{FLO11}-*GFP* strains (Figure 7A). The Swi/Snf subunit Swi1 is indispensable for *FLO11* expression. Promoter activity is still detectable in the *rsc2* mutant, but is below wild type levels, suggesting some role for RSC in activation of the *FLO11* promoter, as well. The SAGA histone acetyltransferase complex mutant *ada2* exhibits only a small decrease in *FLO11* promoter activity.

In contrast, activity of the *FLO10* promoter is heavily dependent on components of RSC, Swi/Snf, and the SAGA complex, visualized by serial dilutions of P_{FLO10}-*URA3* expressing strains grown on selection media (-Ura and 5-FOA) and by FACS analysis of P_{FLO10}-*GFP* strains (Figure 7B). This observed difference between the two *FLO* promoters may be reflective of *FLO10*'s location in a subtelomeric region of chromosome XI. Its position near a telomere may result in an increased requirement for chromatin remodeling and HAT activity for its transcriptional activation.

Mutations in components of the RSC, Swi/Snf, and SAGA complexes affect haploid adhesion and diploid pseudohyphal growth | Haploid adhesion to YPD-agar in the *rsc2*, *swi1*, and *ada2* mutants correlates well with the levels of *FLO11* promoter activity

detected using the transcriptional reporter strains (Figure 7A, Figure 8A). The haploid *rsc2* strain has a moderate defect in adhesion, whereas adhesion is completely abolished in the haploid *swi1* strain. The haploid *ada2* strain, which shows very little change in *FLO11* promoter activity in the transcriptional reporter assays (Figure 7A), adheres to YPD-agar indistinguishably from the wild type haploid strain (Figure 8A). Diploid pseudohyphal growth under nitrogen starvation conditions is however severely impaired in homozygous mutants of *rsc2*, *swi1*, and *ada2* (Figure 8B). This observation suggests a possible diploid-specific or condition-specific role for the Ada2 component of SAGA in activating the *FLO11* promoter, or that there is a *FLO11*-independent cause for the filamentation defect in the homozygous *ada2* mutant diploid. The Spt3 component of SAGA has been shown by others to be required for diploid pseudohyphal growth by a *FLO11*-dependent mechanism, an observation that suggests that the filamentation defect in the homozygous *ada2* mutant is also likely due to a reduction of *FLO11* expression in diploids (Laprade et al., 2002).

Mutations in the yeast Srb/Mediator complex abolish silencing at the *FLO11* promoter and desilence the *FLO10* promoter in an *IRA+* background | Serial dilutions of P_{FLO11}-*URA3* expressing strains on –Ura and 5-FOA selection media demonstrate that Tn3 mutations in components of the yeast Mediator middle module (*med1*, *med4*), tail module (*nut1*), and Srb corepressor complex (*srb8-11*) abolish silencing at the *FLO11* promoter (Figure 9A). The *med1Δ* deletion mutant also exhibits this phenotype (Figure 9A). Fluorescence microscopy comparisons of populations of P_{FLO11}-*GFP* expressing cells in wild type and *med1* backgrounds also reveals loss of silencing at the *FLO11* promoter (Figure 9C).

The *med1* and *srb11* mutants show a loss of the repression normally seen at the *FLO10* promoter in a wild type (*IRA+*) background (Halme et al., 2004) (Figure 9B). *FLO10* promoter activity is detected in these strains without the need for the *ira1*-mediated enhancement of Ra2-cAMP signaling. This finding suggests a role for Srb/Mediator in silencing the *FLO10* promoter in wild type strains. The increased cell-to-cell adherence (compared to wild type) apparent in the *med1* population of P_{FLO11}-*GFP* expressing cells shown in Figure 9C may be due to derepression of the intact *FLO10* gene in this strain. In the *ira1* background, however, *FLO10* promoter activity is not changed in the Srb/Mediator mutants, suggesting a genetic interaction between the Ras2-cAMP pathway and the Srb/Mediator complex that suppresses the Srb/Mediator mutant phenotypes (Figure 9B).

Srb/Mediator complex mutants display striking *FLO11*-dependent phenotypes | Mutations in *med1*, *nut1*, and *srb11* in haploid strains reveal crinkly *ira*-like (Halme et al., 2004) *FLO11*-dependent colony morphologies after 3 days growth on YPD plates (Figure 10A). The *med1* phenotype is not as pronounced as the *sfl1* mutant phenotype, in which the colonies take the form of compact volcano-like structures (Figure 10A), suggesting that *med1*-mediated loss of silencing at *FLO11* may not be as complete as *sfl1*-mediated loss of silencing. Deletion of *FLO11* abolishes these phenotypes, demonstrating that they are due to upregulation of *FLO11* expression. This crinkly colony phenotype extends to *med1/med1* homozygous diploids after 6 days growth on YPD plates (Figure 10B).

MED1 was previously identified in a screen for repressors of haploid invasive growth, but the investigators found no upregulation of *FLO11* from its endogenous

promoter in their *med1* mutant (Palecek et al., 2000), a finding that is in conflict with the results reported here. The conclusion drawn by Palecek et al. was that the enhanced invasive growth in their *med1* mutant was the result of a *FLO11*-independent mechanism. When *FLO10* is expressed, it is sufficient to promote invasive growth in a *flo11*- strain (Guo et al., 2000). I performed YPD-agar adhesion tests to determine whether the "*FLO11*-independent mechanism" proposed by Palecek et al. might turn out to be the desilencing of the *FLO10* gene in an otherwise wild type background. The result was negative. Haploid adhesion to YPD-agar depends on *FLO11* even in the *med1* mutant (Figure 10C). The derepression of the *FLO10* promoter (demonstrated by serial dilutions of P_{FLO10}-*URA3* expressing strains in Figure 9B) is not sufficient to promote adhesion to YPD-agar in the *med1 flo11* strain.

Whereas wild type diploid strains do not adhere to YPD-agar due to ploidy repression of the *FLO11* promoter, adhesion to YPD-agar is enhanced in the homozygous *med1/med1* diploid (Figure 10C). This diploid adheres to YPD-agar as well as does a wild type haploid strain, suggesting that ploidy repression is interfered with in these strains.

The COMPASS Histone Methyltransferase Complex is required for silencing at the *FLO11* promoter, but has no effect on *FLO10* promoter activity | Tn3 insertion mutations in components of the COMPASS histone methyltransferase complex result in loss of silencing at the *FLO11* promoter, visualized by serial dilutions of P_{FLO11}-*URA3* strains grown on -Ura and 5-FOA selection media (Figure 11A). Clean replacement of the entire *SET1* coding region (*set1Δ*) with a *LEU2* expression cassette results in the same phenotype as that observed in the Tn3 insertion mutant, confirming a null phenotype in

the Tn3 mutants (Figure 11A). Deletion of *SET2* (*set2Δ*), another yeast methyltransferase, has no effect on *FLO11* promoter activity, demonstrating a specific role for the COMPASS complex in silencing the *FLO11* promoter (Figure 11A).

Mutations in the COMPASS complex have no effect on the *FLO10* promoter, visualized using P_{FLO10}-*URA3* expressing strains (Figure 11B). The *set2Δ* mutant exhibits no change in *FLO10* promoter activity either.

COMPASS mutants display no striking *FLO11*-dependent phenotypes | Despite the loss of silencing observed using the P_{FLO11}-*URA3* reporter strains, *set1* and *bre2* mutants in strains that have an intact *FLO11* gene display none of the phenotypes usually associated with upregulation of *FLO11* expression (Guo et al., 2000; Halme et al., 2004). The morphologies of haploid *set1* and *bre2* colonies closely resemble wild-type colony morphology rather than having the crinkled appearance often associated with increased *FLO11* expression (data not shown). Haploid adhesion and diploid pseudohyphal growth also resemble that observed in wild type (Figure12).

Silencing is restored to the *FLO11* promoter by rescue with plasmids carrying *SET1* gene sequence | The absence of any apparent *FLO11*-dependent phenotype in the COMPASS mutants raised doubts about the reporter strain data. To test further the legitimacy of the reporter strain phenotypes (Figure 13A), I performed a rescue experiment in which I restored Set1 activity by transforming a *set1Δ* strain with an expression plasmid carrying either the full-length *SET1* gene (nucleotides 1-1080) or a fragment of the *SET1* gene (nucleotides 829-1080). The 829-1080 fragment of the *SET1* gene maintains its mono- and di-, but not its trimethylation function (Fingerman et al.,

2005). Either of these two plasmids was able to rescue the loss of silencing at the *FLO11* promoter seen in the *set1* strains (Figure 13A). These findings demonstrate that loss of silencing in the *set1* strains is, indeed, due to specific loss of Set1 activity. These findings further suggest that Set1-dependent silencing at the *FLO11* promoter does not require Set1's ability to trimethylate lysine 4 of histone H3. Neither of these *SET1* plasmids had an effect on *FLO10* promoter activity in a *set1Δ* background, further demonstrating a specific role for the COMPASS complex at the *FLO11* locus (data not shown). Thus, the COMPASS complex has an apparently specific role in silencing *FLO11* that is similar to that reported at the telomeres and rDNA , but the biological ramifications of this role remain unclear (Briggs et al., 2001; Fingerman et al., 2005; Mueller et al., 2006; Nislow et al., 1997; Schneider et al., 2005).

Double mutant analyses reveal epistasis of *sfl1* and *med1* phenotypes over *cti6, ste12,* and *flo8* phenotypes | To examine the genetic interactions of known activators and repressors with the identified candidates, I constructed double mutants carrying mutations in a candidate and a deletion of one of the following established transcriptional regulators: Sfl1, Flo8, or Ste12. Sfl1 is a repressor of *FLO* transcription and acts downstream of the Ras2-cAMP PKA pathway (Gancedo, 2001). Flo8 is an important activator of *FLO* gene transcription that also acts downstream of the Ras2-cAMP PKA pathway (Gancedo, 2001). Ste12 is another activator of *FLO* gene transcription that acts downstream of the Ras2-cAMP MAP kinase pathway (Gancedo, 2001).

Serial dilutions of P_{FLO11}-*URA3* expressing cells reveal that the *med1* and *sfl1* phenotypes are epistatic to the *cti6* and *ste12* phenotypes. The *med1* mutation also activates the *FLO11* promoter in a larger proportion of a population of *flo8* cells (Figure

14A). To determine whether these results held with respect to *FLO11*-dependent morphological and developmental phenotypes, I also made double mutants in strains with an intact *FLO11* gene. The epistasis results were the same, as demonstrated by the haploid colony morphologies and YPD-agar adhesion capacities of the *med1 cti6* double mutant (Figure 14B and C).

Judging by the differences in the relative numbers of cells that are 5-FOA resistant (due to inactivity of the *FLO11* promoter) in the *flo8*, *cti6*, and *ste12* mutants, it appears that Flo8 is the strongest of these activators, followed by Cti6 and then Ste12 (Figure 14A); although data shown previously (Figure 7A) demonstrates that, of all activators tested in this study, Swi1 remains the most critical for *FLO11* transcriptional activation. Because *cti6* has a stronger mutant phenotype than *ste12* but a weaker mutant phenotype than *flo8*, I propose that the Rpd3L complex is likely to be involved somehow in counteracting repression mediated by the PKA pathway and that its most likely antagonist is Sfl1.

These results suggest very strong repression of *FLO11* promoter activity by Sfl1 and the Srb/Mediator complex. Abrogation of this repression by *sfl1* or *med1* mutation is sufficient to allow transcription from the *FLO11* promoter even when key activators, such as Flo8, Ste12, and Cti6, are absent (Figure 14A).

These epistasis tests also prove useful in discriminating between proposed explanations for Srb/Mediator repression of transcription. One proposed model, specific to the Ras-cAMP-dependent filamentation response, is that negative regulation by Srb8-10 is mediated through the Ste12 component of the MAP kinase cascade (Nelson et al., 2003). This model proposes that phosphorylation of Ste12 by the cyclin-dependent

kinase (CDK) Srb10 inhibits transcription by rendering Ste12 unresponsive to the upstream MAP kinase pathway (Nelson et al., 2003). The epistasis analysis presented here rules out this model because, contrary to its predictions, the *med1* phenotype is epistatic to the *ste12* phenotype as regards *FLO11* transcription. Another proposed model for Srb-mediated transcriptional repression is a temporal one: whereas other CDKs activate RNA polymerase II elongation by phosphorylating its C-terminal domain (CTD) after the transcription initiation complex has been formed (Lee and Young, 2000), it is proposed that Srb8-11, associated with the yeast Mediator, prematurely phosphorylates the CTD of RNA polymerase II prior to its entering the initiation complex, thereby preventing transcription initiation (Hengartner et al., 1998). This model of Srb8-10-mediated repression cannot be ruled out by our epistasis analyses.

DISCUSSION

The genome-wide screens described in this chapter have identified previously unknown regulators of *FLO* transcription and its epigenetic silencing, including the Rpd3L histone deacetylase complex, the RSC and Swi/Snf chromatin remodeling complexes, the SAGA histone acetyltransferase complex, and the COMPASS histone methyltransferase complex (Summarized in Figure 1). They have also launched experiments that have shed light on the mechanisms by which previously reported regulators of *FLO* transcription, such as the Srb/Mediator, perform their functions.

Several of the complexes identified, including RSC, Swi/Snf, and SAGA, play roles in *FLO* promoter regulation that are reasonably predictable based on their activities at other sites in the yeast genome. These three complexes have well established

capabilities in promoting transcriptional activation with well understood mechanisms. The phenotype of the COMPASS complex mutants resembles those observed at telomeres and at the rDNA, although significant controversy remains regarding this complex's biological role and its significance. The effect of Srb/Mediator function on the regulation of *FLO* gene expression is also in line with previous observations, and this study has shed additional light on its mechanism of action.

One complex identified in these screens stands out as particularly curious: the Rpd3L histone deacetylase complex. We might reasonably expect this complex to repress transcription of *FLO* genes owing to its ability to catalyze the condensation of chromatin structure, but it instead activates their transcription. It is, of course, possible that this surprising observation is the indirect shadow of direct repression by Rpd3L of direct activators of *FLO* gene expression. However other studies have demonstrated apparent activation of transcription as a result of direct binding to and deacetylation of target promoter regions by the Rpd3L complex (Sertil et al., 2007; Sharma et al., 2007; Xin et al., 2007; De Nadal et al., 2004). How does this complex activate transcription by deacetylating histones in target promoter regions? This is a question that will be addressed in the next chapter of this thesis.

FIGURES AND TABLES

FIGURE 1 | **A Summary of the chromatin modifying and remodeling complexes identified as transcriptional regulators of the *FLO10* and *FLO11* promoters in these genome-wide Tn3-insertion screens.** Components of the Srb/Mediator complex, including *MED1*, *MED4*, *NUT1/MED5*, *SRB8*, *SRB9*, *SRB10*, and *SRB11,* were found to function as transcriptional repressors of both the *FLO10* and the *FLO11* promoters. The COMPASS methyltrransferase components *SET1* and *BRE2* were found to play a specific role in repressing *FLO11* promoter activity, but no role for this complex was identified at the *FLO10* promoter. Components of the SAGA histone acetyltransferae complex, indluding *ADA2* and *SPT8*, were found to be critical to activation of the *FLO10* promoter acitivity, but less important to *FLO11* promoter function. The *RSC2* component of the RSC chromatin remodeling complex is required for transcription from the *FLO10* promoter, and has some role in activating transcription from the *FLO11* promoter, as well. The *SWI1* component of the Swi/Snf chromatin remodeling complex is necessary for transcription from either the *FLO10* or the *FLO11* promoters. Components of the Rpd3L histone deacetylase complex, including *CTI6*, *RXT2*, *PHO23*, *SIN3*, and *RPD3*, are required for transcription from the *FLO11* promoter and may have some role in activating transcription from the *FLO10* promoter, as well.

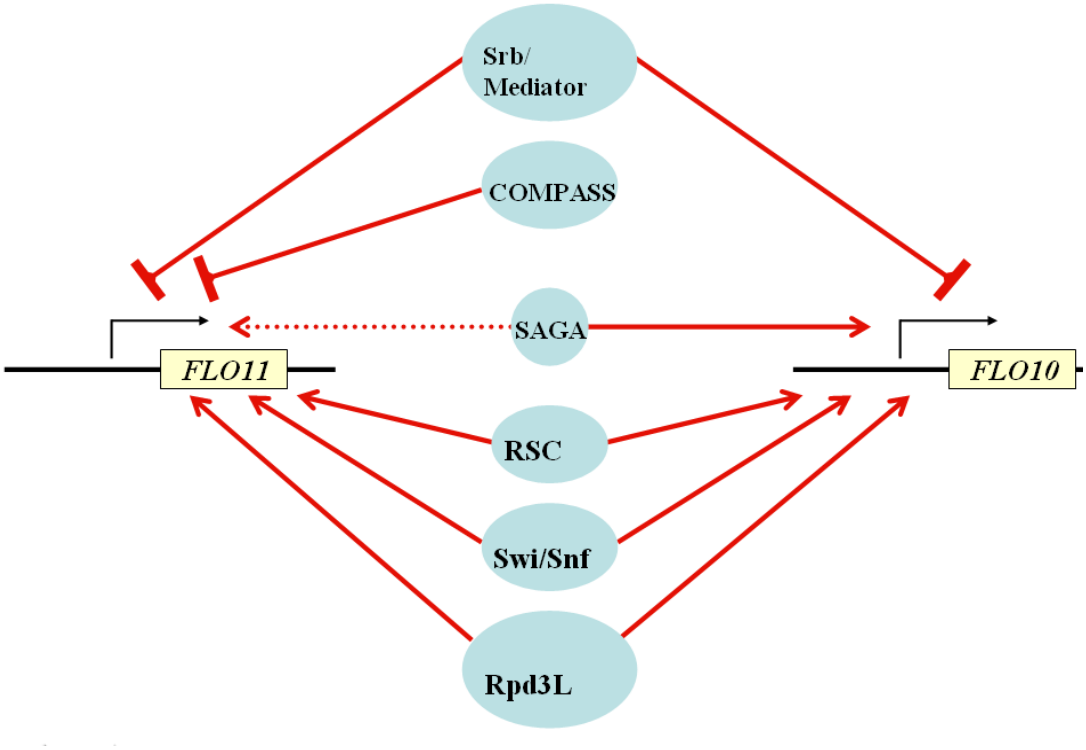

FIGURE 2 | **Experimental design of genome-wide Tn3-insertion screens to identify novel regulators of *FLO10* and *FLO11* transcription.** *(A)* Plasmids containing Tn3-mutagenized 2-to-3 kb yeast genomic DNA (*y*gDNA) inserts were *Not1*-digested to liberate these inserts, which were then used to transform Sigma 1278b yeast strains carrying P_{FLO11}-*URA3* or P_{FLO10}-*URA3 ira1-*. *(B)* Tn3-carrying transformants were patched onto YPD plates, then replica-plated onto SC-Ura and SC+5-FOA media to identify mutants with increased or decreased ability to grow on these media relative to parental strains, indicating changes in *FLO* promoter activity. *(C)* Strains identified as having phenotypes in *(B)* were then subjected to serial dilution assays on the selective media to confirm these phenotypes. *(D)* The Tn3-insertion sites were PCR amplified from genomic DNA template isolated from mutants with confirmed phenotypes using primers specific to the Tn3 insertion cassette and nested arbitrary priming. Products were confirmed by agarose gel electrophoresis, purified, and sequenced to identify candidate genes.

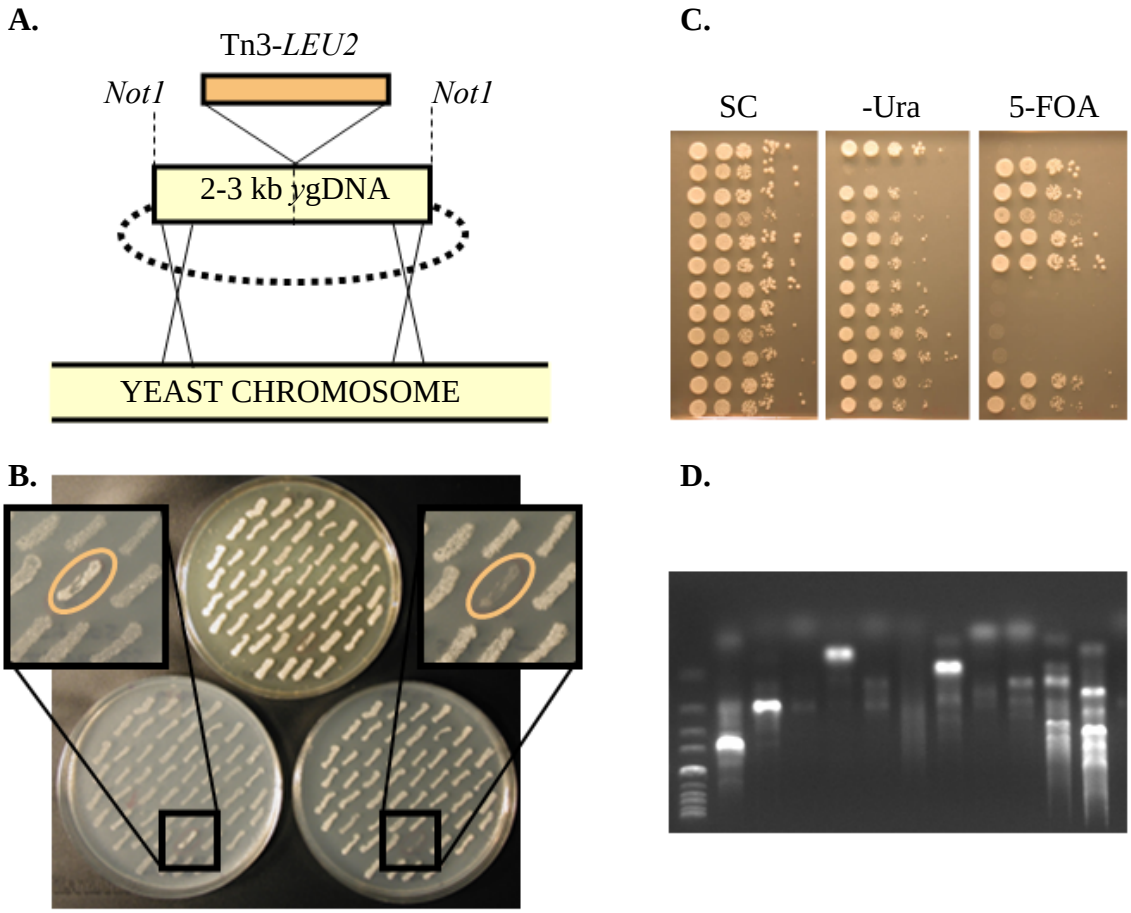

FIGURE 3 | **The range of phenotypes observed in mutants derived from the screens.** The screens identified mutants exhibiting a range of transcriptional/silencing phenotypes. Some of the mutants *(A)* have completely lost transcriptional activity at the *FLO* promoter being tested. Others have completely lost metastable silencing, resulting in all cells in the mutant population having an active *FLO* promoter *(F)*. We also identified mutants that still exhibit variegated expression, but the numbers of cells in the on-versus-off state have been shifted in one direction or the other *(B-E)*. The table to the right indicates the number of unique insertion mutants that were identified representing each phenotypic class in each of the two screens (out of 32,955 transformants in P_{FLO10}-*URA3* screen and 41,532 transformants in P_{FLO11}-*URA3* screen) and the number of candidate genes represented by each group. More than one unique Tn3 insertion site was recovered for some some genes identified in the screens.

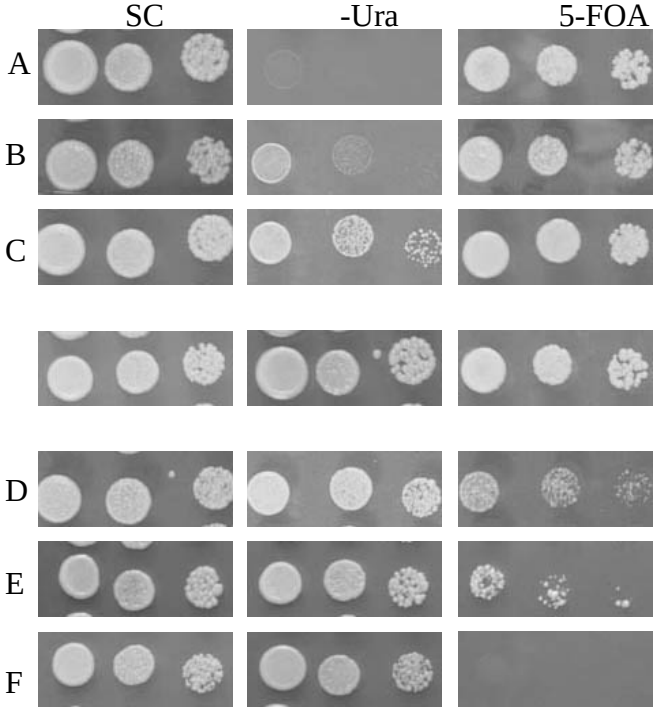

	ira1-P_{FLO10}-*URA3*	P_{FLO11}-*URA3*
A	32 insertions 27 genes	0 insertions 0 genes
B	9 insertions 8 genes	19 insertions 18 genes
C	21 insertions 15 genes	8 insertions 7 genes
PARENTAL		
D	4 insertions 4 genes	7 insertions 6 genes
E	6 insertions 4 genes	10 insertions 9 genes
F	19 insertions 16 genes	121 insertions 62 genes
Total number of candidates identified:	91 insertions 74 genes	165 insertions 102 genes

FIGURE 4 | *(A)* The P_{FLO10}-*URA3* and P_{FLO11}-*URA3* screens identified 12 candidate genes in common. Mutations in these genes affected transcription from the two *FLO* promoters in the same direction, as indicated by arrows (↑ = increased activity; ↓ = decreased activity), except in the cases of *RDN25-1*, *SRY1*, and *YDJ1*, indicated by *. *(B)* The screens identified 19 previously published regulators of *FLO* transcription.

A.

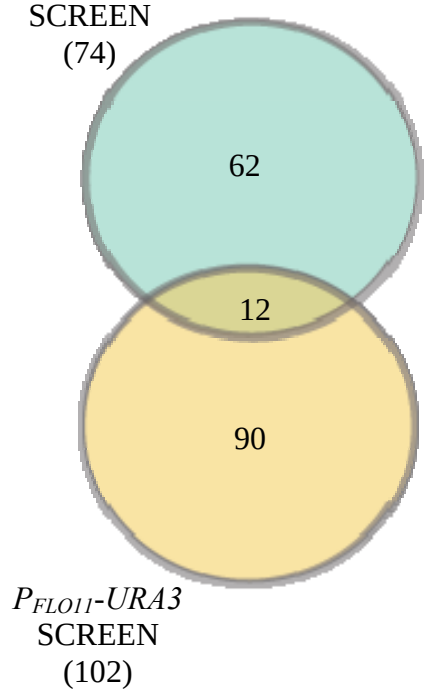

GENE	PROCESS	MUTANT PHENOTYPE P_{FLO10}	MUTANT PHENOTYPE P_{FLO11}
AKR1	Protein sorting/transport	↑	↑
CSR2	Cell Wall Organization	↑	↑
GRR1	Protein Ubiquitination	↑	↑
IRA2	Ras-cAMP Signaling	↑	↑
MAM33	Mitochondrial Function	↑	↑
∗*RDN25-1*	Translation	↓	↑
REG1	Regulator of Transcription	↑	↑
SCH9	Regulator of Transcription	↑	↑
SRB11	Regulator of Transcription	↑	↑
∗*SRY1*	Amino Acid Catabolism	↑	↓
TEP1	Cell Wall Organization	↓	↓
∗*YDJ1*	Protein Folding	↑	↓

B.

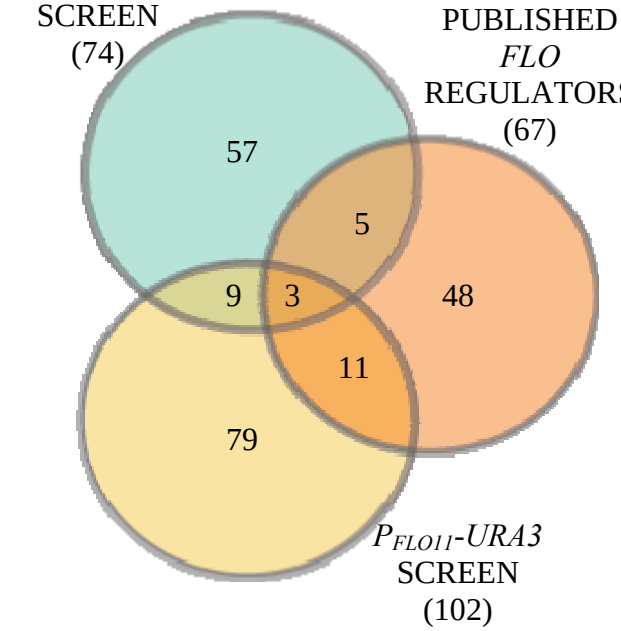

PUBLISHED REGULATORS OF *FLO* TRANSCRIPTION IDENTIFIED IN SCREENS

ELM1, *FLO8*, *HDA1*, *HDA2*, *HDA3*, *HSC82*, *IME2*, *IRA1*, *IRA2*, *MSN1*, *RIM13*, *SRB9*, *SRB10*, *SRB11*, *STE7*, *TEC1*, *TPK1*, *YDJ1*, and *ZUO1*

FIGURE 5 | **Components of the Rpd3L Histone Deacetylase Complex are required for transcriptional activation of both the *FLO10* and *FLO11* promoters.** *(A)* Tn3-insertion mutations in components of the Rpd3L complex result in decrease in expression from the *FLO11* promoter, visualized by serial dilutions of P_{FLO11}-*URA3* strains grown on selection media (-Ura and 5-FOA) and by FACS analysis of P_{FLO11}-*GFP* strains. The clean deletion mutant *cti6Δ* phenocopies the Tn3-insertion mutant, confirming a null phenotype in the Tn3 mutants. Deletion of the Rpd3S-specific subunit *EAF3* does not affect *FLO11* promoter activity, demonstrating that the Rpd3L, but not the Rpd3S, complex regulates *FLO11*. *(B)* P_{FLO10}-*URA3* and P_{FLO10}-*GFP* expressing strains demonstrate that Tn3-insertion mutations in *CTI6* and *ASH1* result in reduced expression from the *FLO10* promoter, as well, but this effect is not as pronounced as that observed at the *FLO11* promoter. The effect, if any, of mutating *RXT2* or *PHO23* is minor at the *FLO10* promoter.

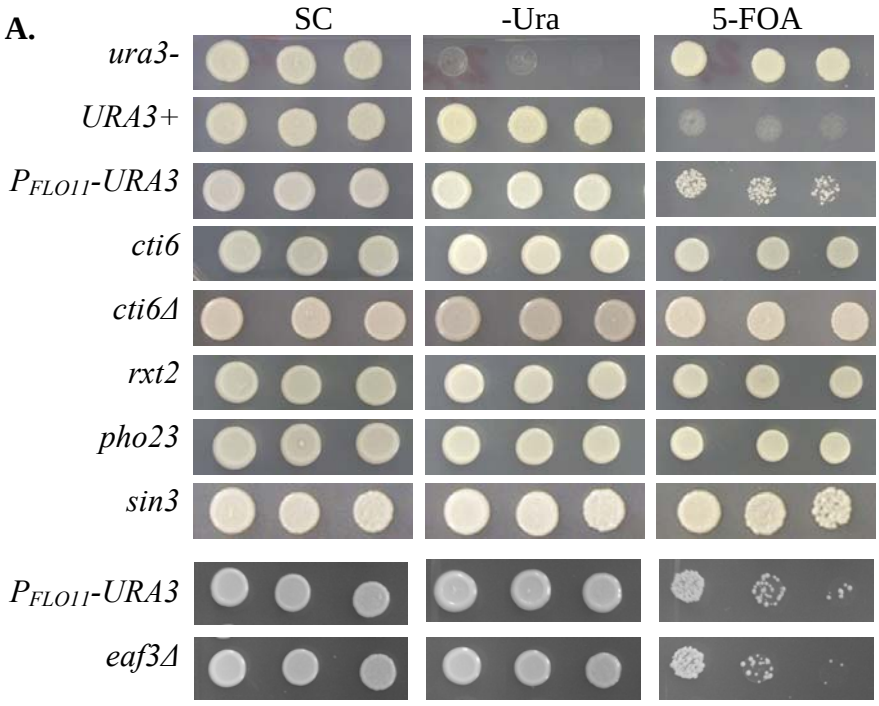

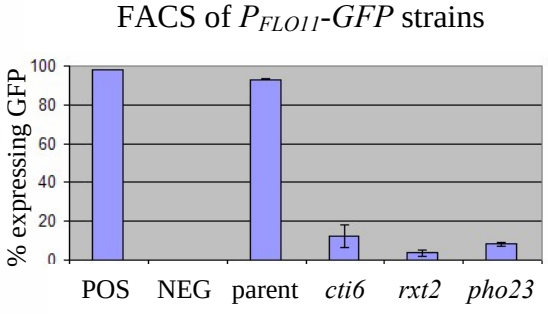

FIGURE 5 | **Components of the Rpd3L Histone Deacetylase Complex are required for transcriptional activation of both the *FLO10* and *FLO11* promoters, *continued*.**

B.

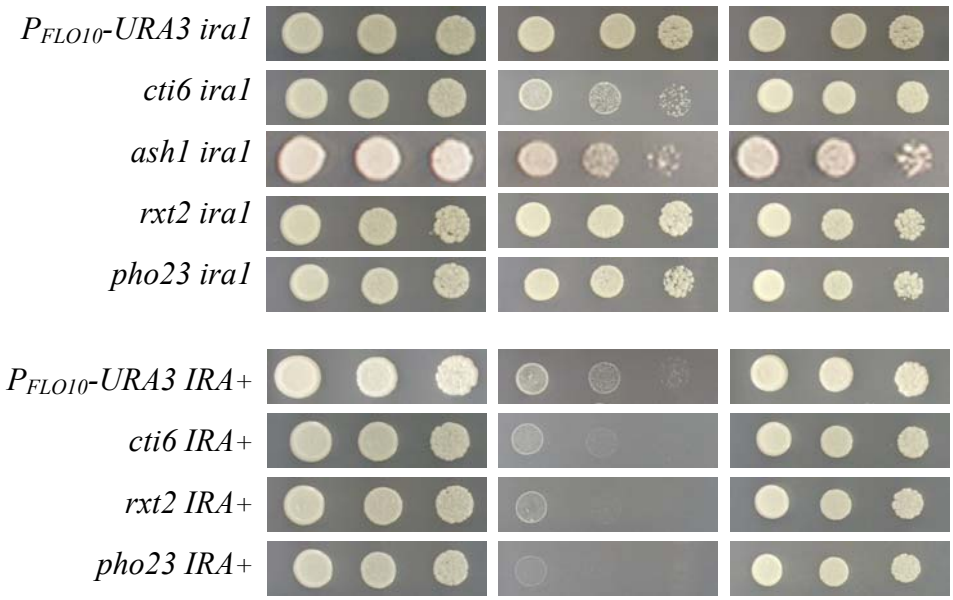

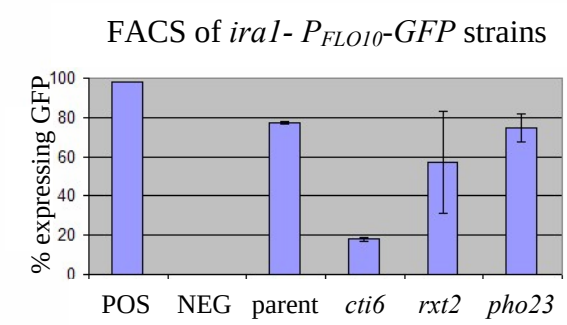

FIGURE 6 | **Reduced *FLO11* promoter activity in Rpd3L mutants results in loss of Flo11-dependent haploid adhesion and diploid pseudohyphal growth.** *(A)* Loss of Rpd3L function results in the inability of haploid yeast cells to adhere to YPD-agar in plate washing assays, performed after 4 days growth on YPD at 30 degrees C. *FLO11* is sufficient to rescue the defect, as seen when the mutant strains are transformed with a 2 micron plasmid carrying a P_{TEF}-*FLO11* construct. An *rpd3Δ* deletion mutant also exhibits loss of *FLO11*-dependent adhesion, demonstrating that the catalytic component of the Rpd3L histone deacetylase complex plays a role in activating *FLO11* promoter activity. *(B)* Mutation of Rpd3L subunits also completely abolishes *FLO11*-dependent diploid pseudohyphal growth under depleted nitrogen conditions. 6 days on SLAD media at 30 degrees C. *(C)* When mutant strains are transformed with a 2 micron plasmid carrying a P_{TEF}-*FLO11* construct, filamentation is recovered. 4 days on SLAD media at 30 degrees C

A.

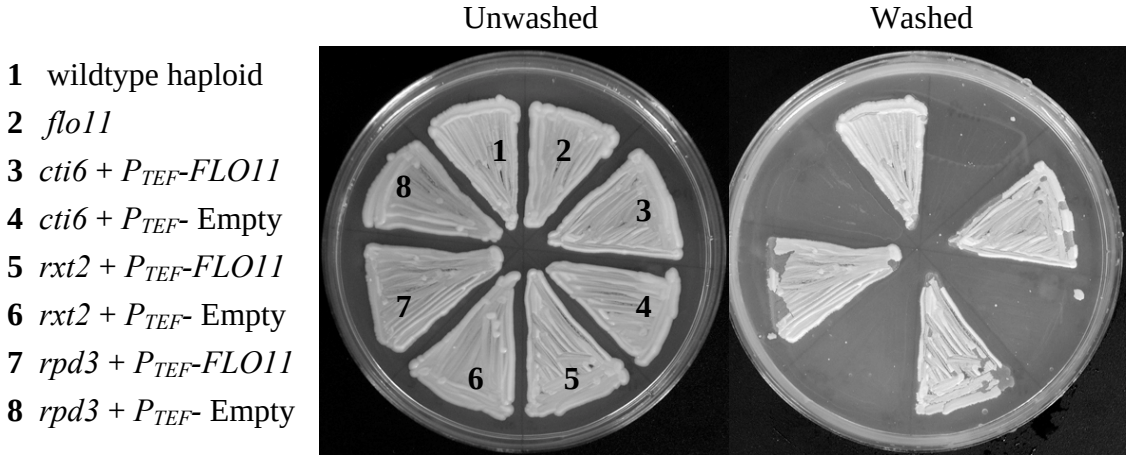

B.

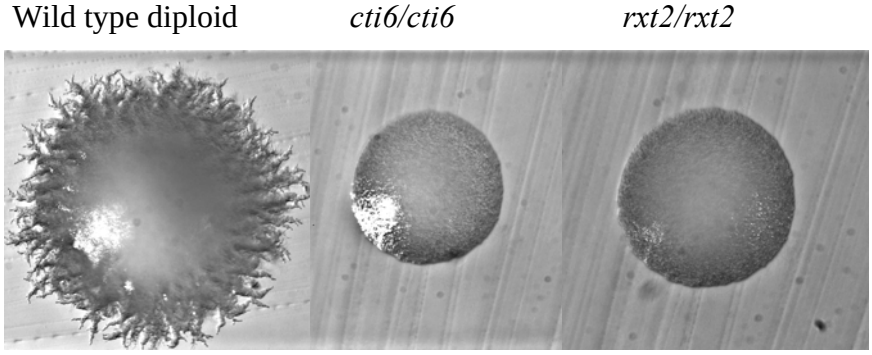

FIGURE 6 | **Reduced *FLO11* promoter activity in Rpd3L mutants results in loss of Flo11-dependent haploid adhesion and diploid pseudohyphal growth, *continued*.**

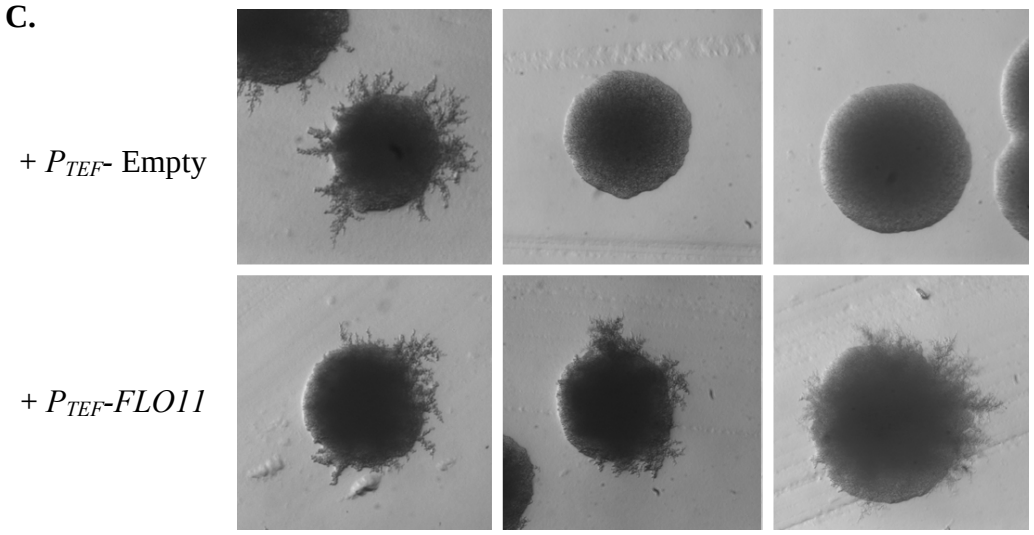

FIGURE 7 | **Mutations in components of the RSC, Swi/Snf, and SAGA complexes affect *FLO10* and *FLO11* promoter activity to different degrees.** *(A)* Tn3-insertion mutations in components of the RSC and Swi/Snf chromatin remodeling complexes have differential effects on the activity of the *FLO11* promoter, visualized by serial dilutions of P_{FLO11}-*URA3* expressing strains grown on selection media (-Ura and 5-FOA) and by FACS analysis of P_{FLO11}-*GFP* strains. The Swi/Snf subunit Swi1 is indispensable for *FLO11* expression. Promoter activity is still clearly detectable in the *rsc2* mutant, but is below wild type levels, suggesting some role for RSC in activation of the *FLO11* promoter. The SAGA histone acetyltransferase complex mutant *ada2* exhibits only a small decrease in *FLO11* promoter activity. *(B)* In contrast, activity of the *FLO10* promoter is heavily dependent on components of RSC, Swi/Snf, and the SAGA complex, visualized by serial dilutions of P_{FLO10}-*URA3* expressing strains grown on selection media (-Ura and 5-FOA) and by FACS analysis of P_{FLO10}-*GFP* strains.

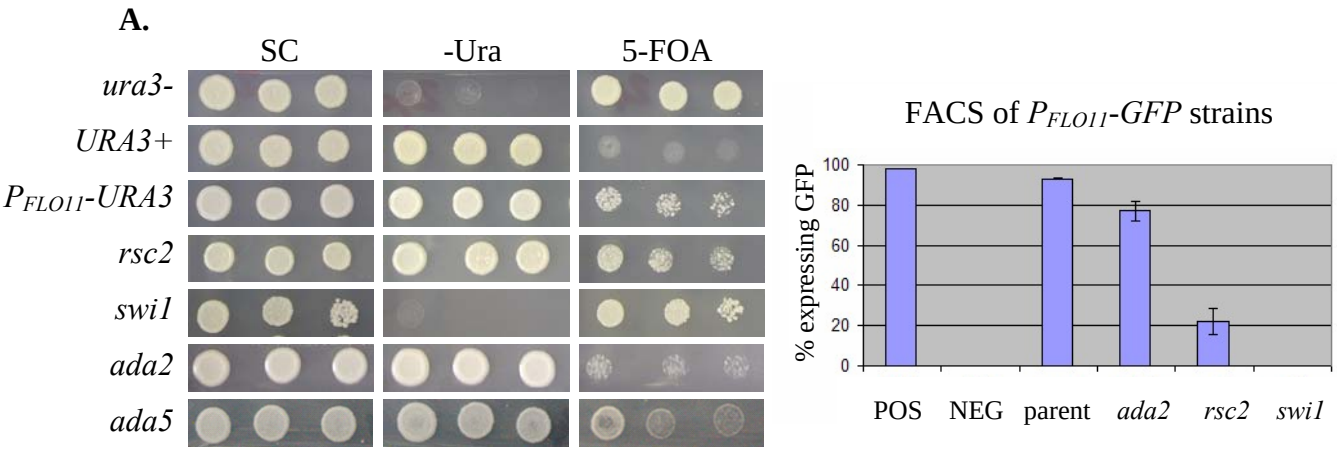

FIGURE 7 | **Mutations in components of the RSC, Swi/Snf, and SAGA complexes affect *FLO10* and *FLO11* promoter activity to different degrees, *continued*.**

B.

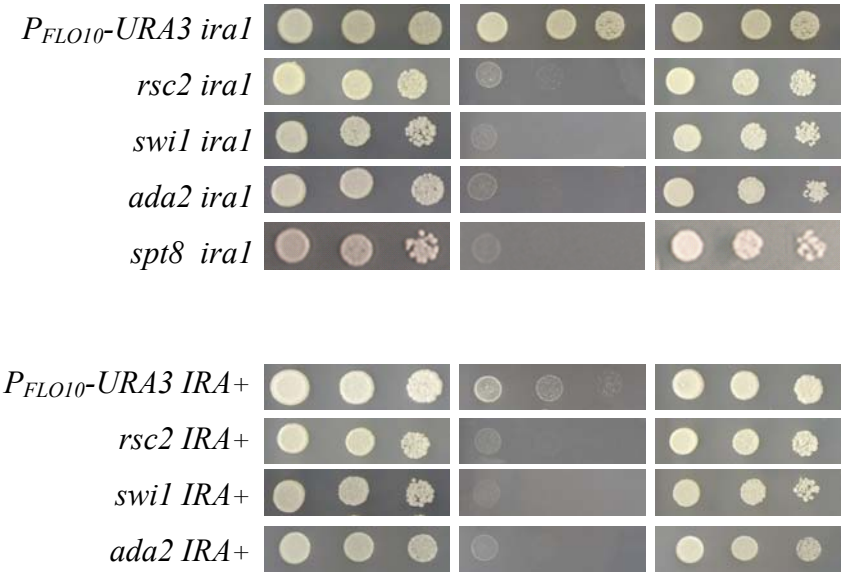

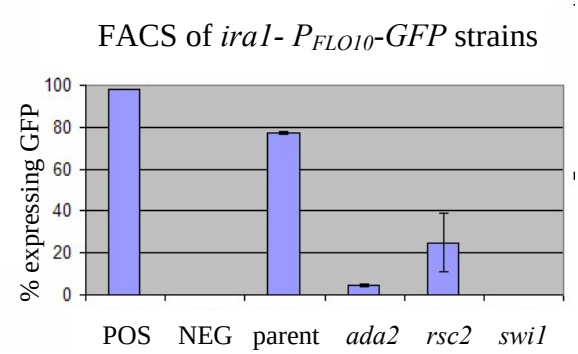

FIGURE 8 | **Effects of mutations in components of the RSC, Swi/Snf, and SAGA complexes on haploid adhesion and diploid pseudohyphal growth.** *(A)* Haploid adhesion to YPD-agar in the *rsc2*, *swi1*, and *ada2* mutants correlates well with levels of *FLO11* promoter activity detected using transcriptional reporter strains. Plate washing assays were performed after 4 days growth on YPD at 30 degrees C. *(B)* Diploid pseudohyphal growth under nitrogen starvation conditions is severely impaired in all three mutants, however, suggesting a possible diploid-specific or condition-specific role for SAGA in activating the *FLO11* promoter, or a *FLO11*-independent cause for these phenotypes. 6 days on SLAD media at 30 degrees C.

A.

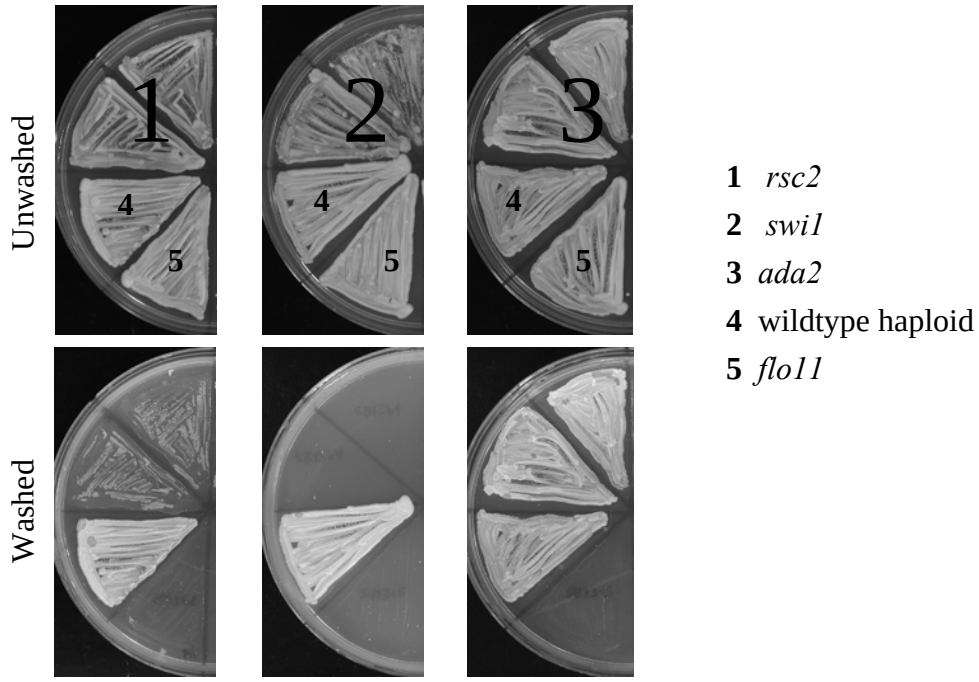

B.

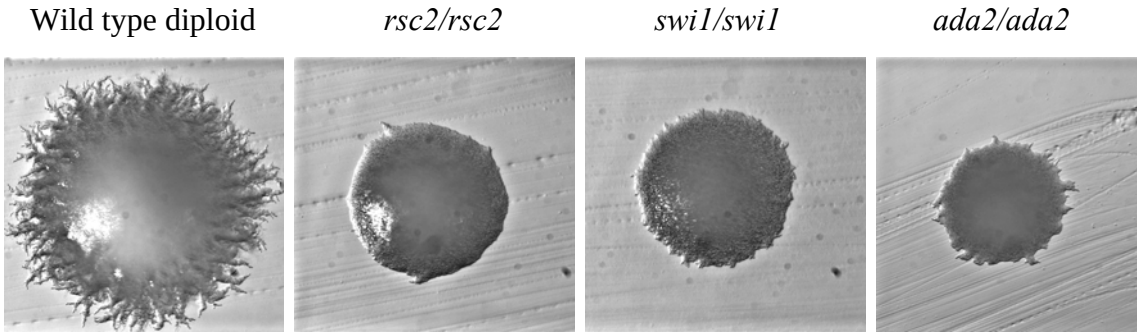

FIGURE 9 | **Mutations in components of the yeast Srb/Mediator abolish metastable silencing at the *FLO11* promoter and desilence the *FLO10* promoter in a wild type background.** *(A)* Serial dilutions of P_{FLO11}-*URA3* expressing strains on selection media (-Ura and 5-FOA) demonstrate that Tn3 mutations in components of the yeast Mediator middle module (*med1*, *med4*), tail module (*nut1*), and Srb corepressor complex (*srb8-11*) abolish metastable silencing at the *FLO11* promoter. The *med1Δ* mutant also exhibits this phenotype. *(B)* Serial dilutions of P_{FLO10}-*URA3* expressing strains on selection media (-Ura and 5-FOA) demonstrate that Srb/Mediator mutants have no effect on *FLO10* promoter activity in a genetic background in which Ras-cAMP signaling is enhanced by *ira1* mutation, suggesting a possible genetic interaction between the Ras-cAMP pathway and the Srb/Mediator complex. The *med1* and *srb11*, but not the *nut1*, mutants exhibit loss of the repression normally seen at the *FLO10* promoter in an *IRA+* background. This finding suggests a role for Srb/Mediator in silencing the *FLO10* promoter in wild type strains. (C) Comparison by fluorescence microscopy of populations of P_{FLO11}-*GFP* expressing cells in wild type and *med1* backgrounds also reveals loss of metastable silencing at the *FLO11* promoter. The increased cell-to-cell adherence seen in the *med1* population may be due to derepression of the intact *FLO10* gene in this strain.

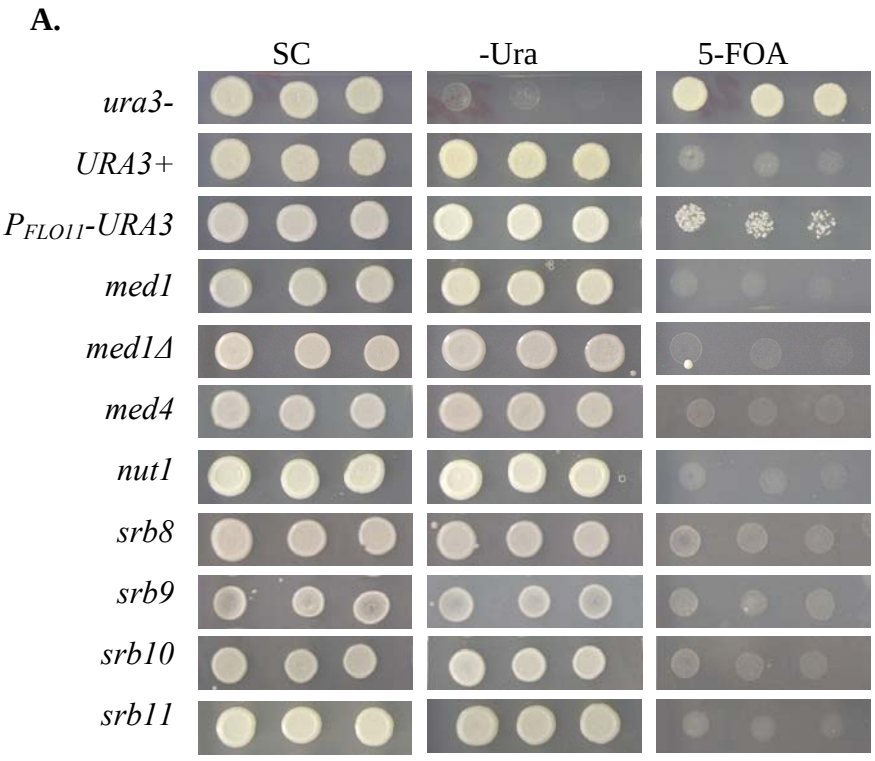

FIGURE 9 | **Mutations in components of the yeast Srb/Mediator abolish metastable silencing at the *FLO11* promoter and desilence the *FLO10* promoter in a wild type background, *continued*.**

B.

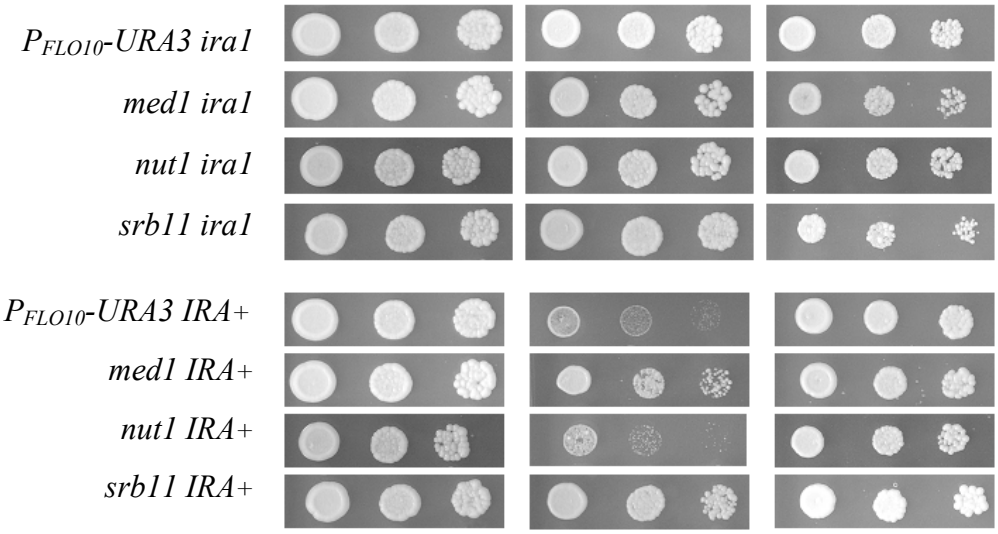

C.

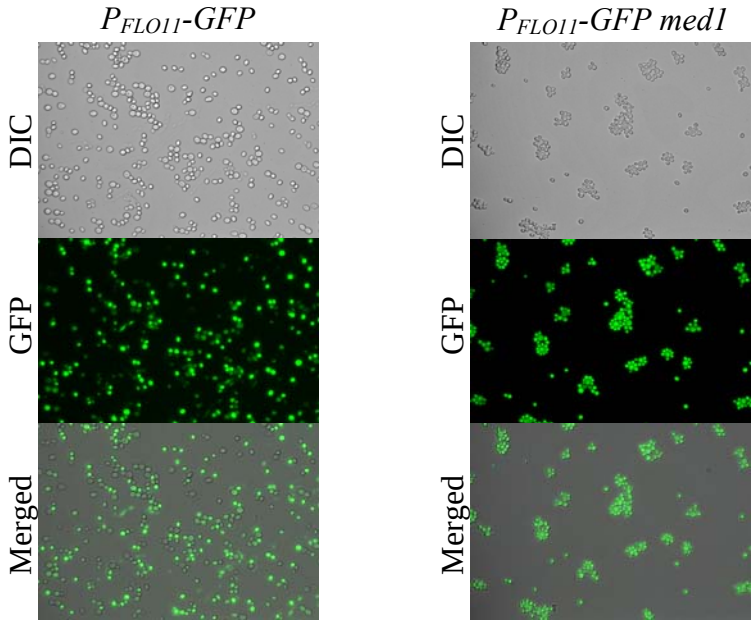

FIGURE 10 | **Enhanced *FLO11*-dependent colony morphology and adhesion phenotypes are observed in Srb/Mediator mutants.** *A)* Mutations in *med1*, *nut1*, and *srb11* in haploid strains reveal crinkly *ira* (Halme et al., 2004) and *sfl1*-like*FLO11*-dependent colony morphologies after 3 days growth on YPD plates. The addition of a *flo11* mutation abolishes these phenotypes. *(B)* This crinkly colony phenotype extends to *med1/med1* homozygous diploids after 6 days growth on YPD plates. *(C)* Haploid adhesion to YPD-agar depends on *FLO11* even in the *med1* mutant. The derepression of the *FLO10* promoter (demonstrated by serial dilutions of P_{FLO10}-*URA3* expressing strains in Figure 11) is not sufficient to promote adhesion to YPD-agar in the *med1 flo11* strain. Homozygous *med1/med1* diploids adhere to YPD-agar as well as a haploid strain adheres.

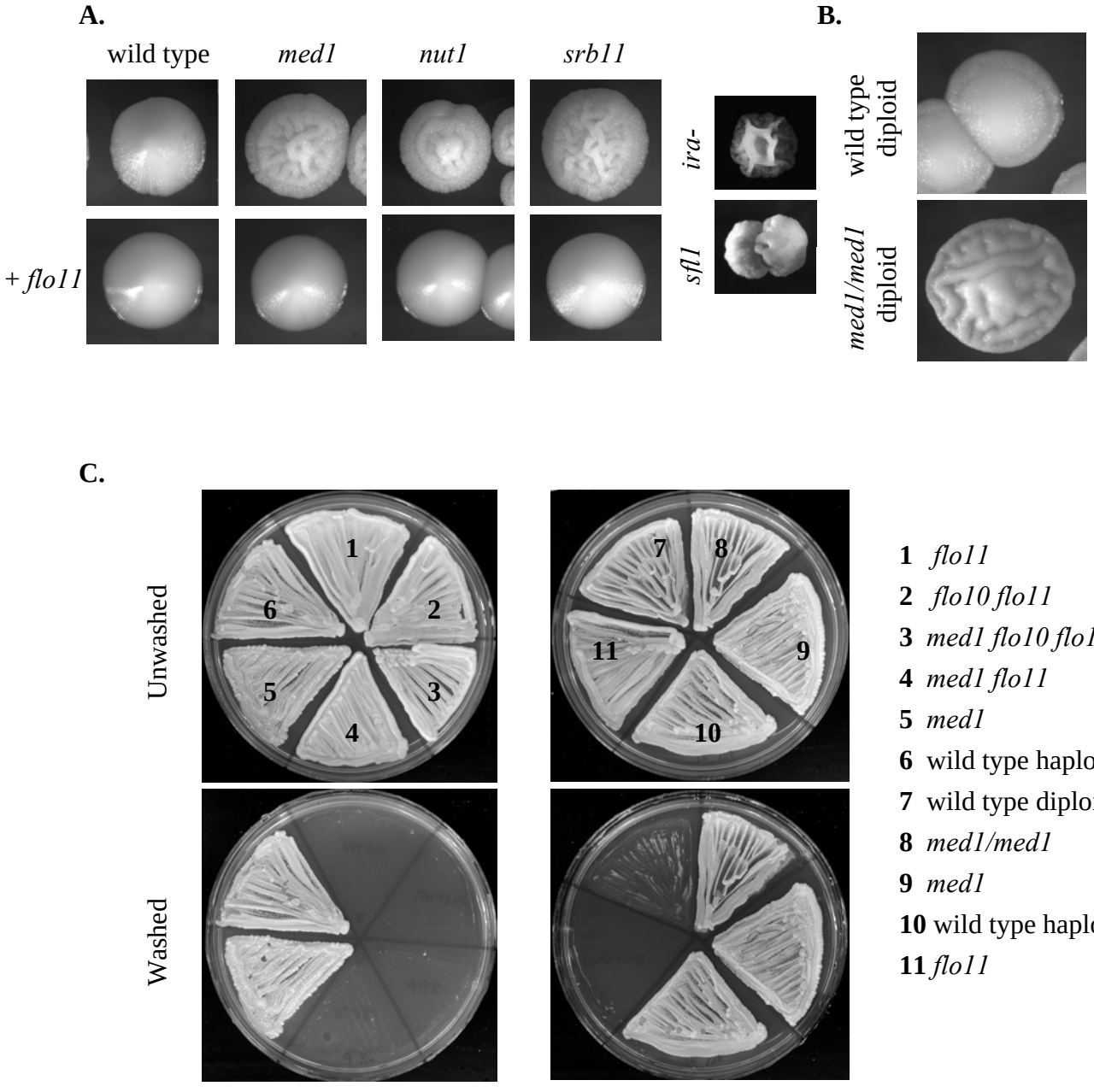

FIGURE 11 | **Mutations in components of the COMPASS Histone Methyltransferase Complex abolish metastable silencing at the *FLO11* promoter, but have no effect on *FLO10* promoter activity.** *(A)* Tn3-insertion mutations in components of the COMPASS complex result in loss of metastable silencing at *FLO11* promoter, visualized by serial dilutions of P_{FLO11}-*URA3* strains grown on selection media (-Ura and 5-FOA). The clean deletion mutant *set1Δ* phenocopies the Tn3-insertion mutant, confirming a null phenotype in the Tn3 mutants. Deletion of *SET2*, another yeast methyltransferase, has no effect on *FLO11* promoter activity, demonstrating a specific role for the COMPASS complex at the *FLO11* promoter. *(B)* COMPASS mutants show no change in activity from the *FLO10* promoter, visualized using P_{FLO10}-*URA3* expressing strains. The *set2Δ* mutant exhibits no change in *FLO10* promoter activity either.

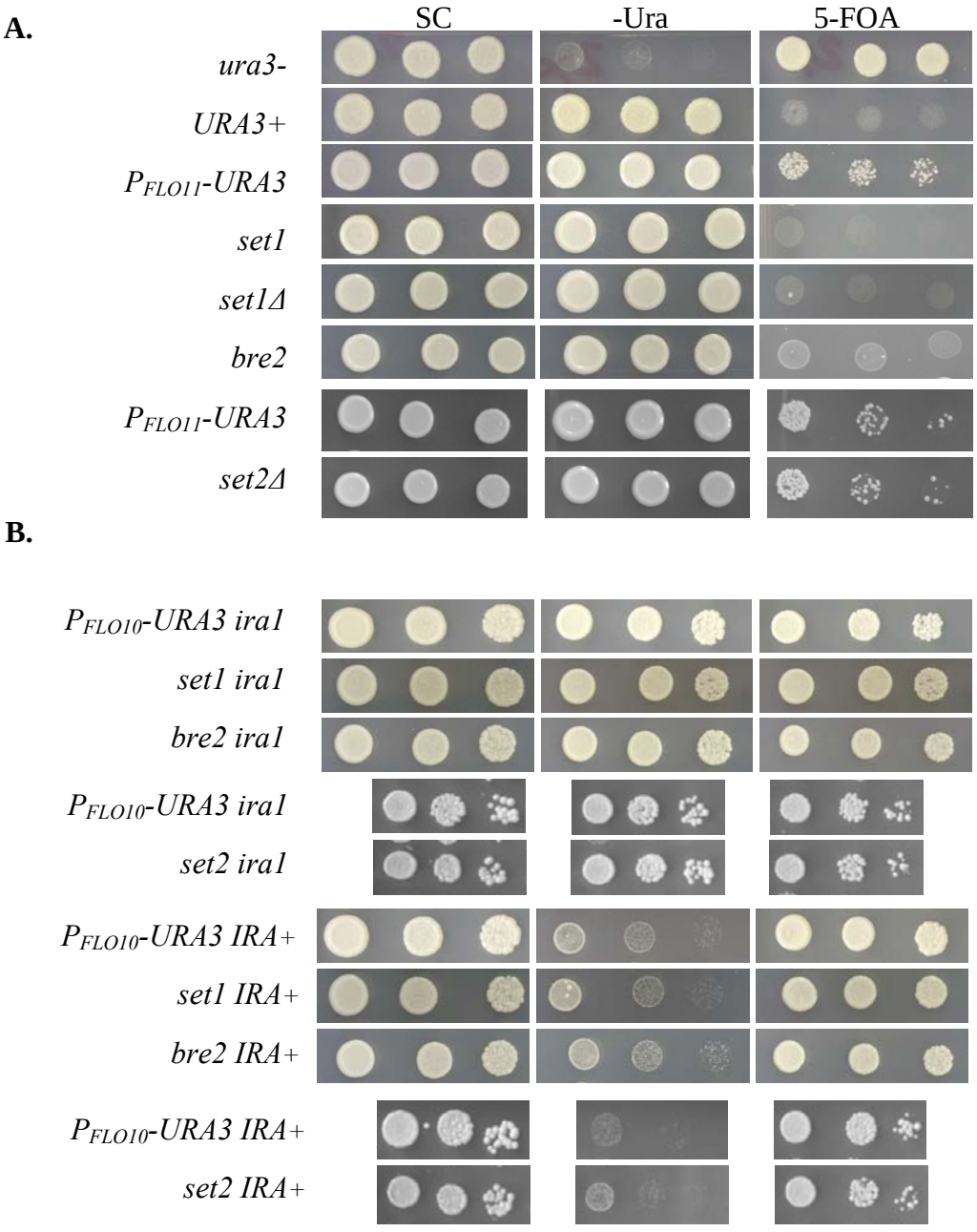

FIGURE 12 | **COMPASS mutants resemble the wild type strain with respect to Flo11-dependent haploid invasive growth and diploid pseudohyphal growth.** Indistinguishable from a wild type strain, the COMPASS mutants *(A)* adhere to YPD-agar after 4 day growth at 30 degrees C, followed by plate washing assay, and *(B)* undergo the transition to filamentous growth under nitrogen starvation conditions. 6 days growth on SLAD at 30 degrees C.

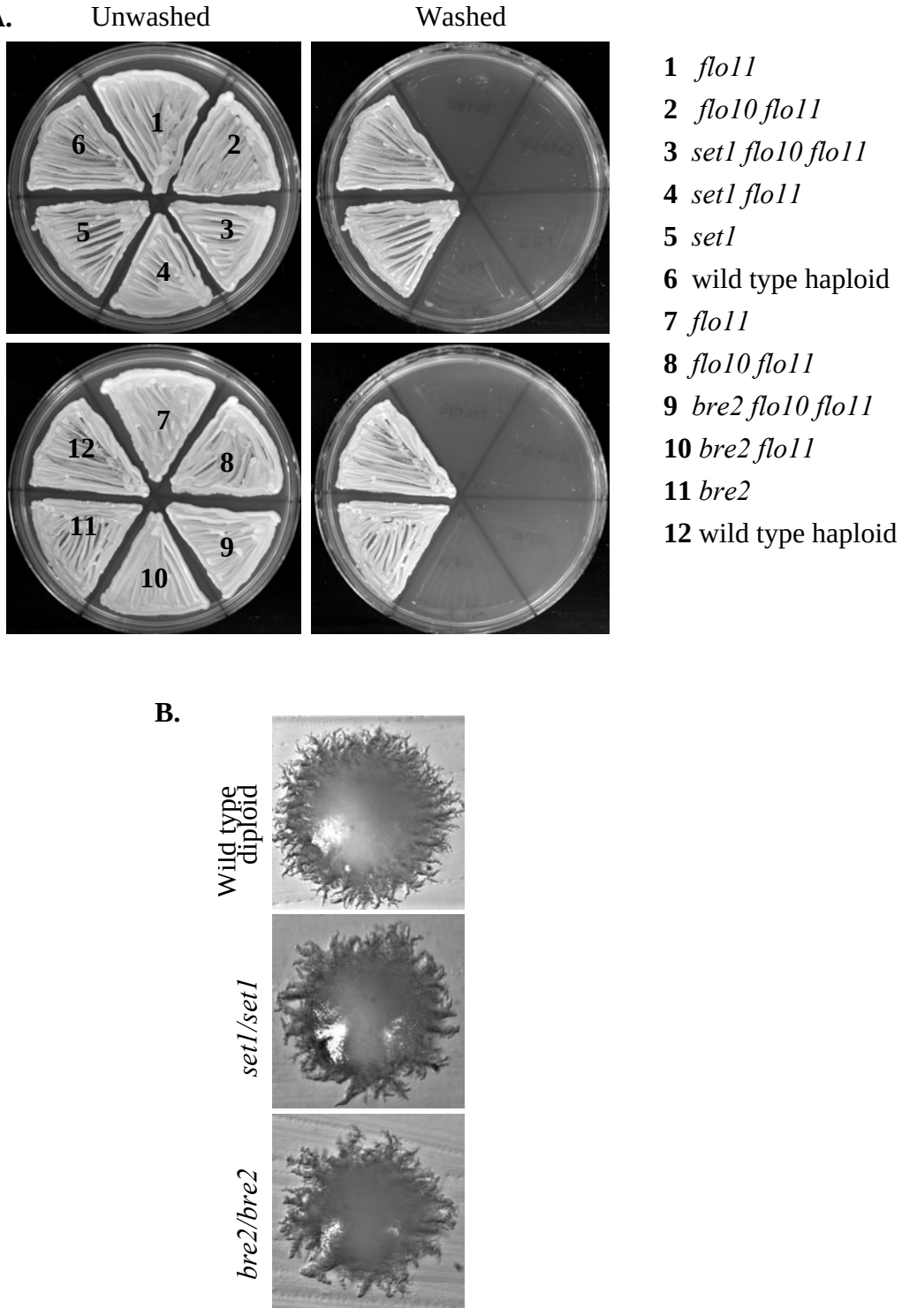

FIGURE 13 | **The loss of silencing at the *FLO11* promoter can be rescued with plasmids carrying *SET1* gene sequence.** Transforming a *set1Δ* strain with an expression plasmid carrying either the full-length *SET1* gene (nucleotides 1-1080) or a fragment of the *SET1* gene (nucleotides 829-1080), which maintains the mono- and di-, but not the trimethylation function of Set1 (Fingerman et al., 2005), rescues metastable silencing at the *FLO11* promoter.

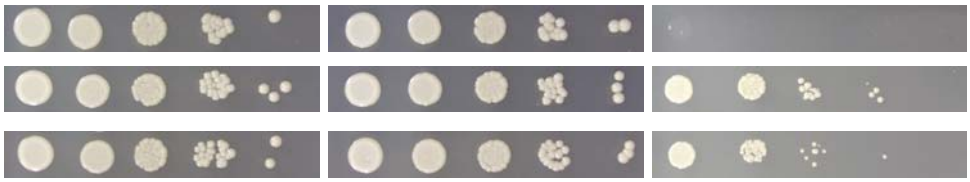

1 P_{FLO11}*-URA3 set1Δ + empty vector*

2 P_{FLO11}*-URA3 set1Δ + SET1(1-1080)*

3 P_{FLO11}*-URA3 set1Δ + SET1(829-1080)*

FIGURE 14 | **Double mutant analyses reveal epistasis of *med1* and *sfl1* phenotypes over *cti6, ste12,* and *flo8* phenotypes.** *(A)* Serial dilutions of P_{FLO11}-*URA3* expressing cells reveal that the *med1* and *sfl1* phenotypes are epistatic to the *cti6* and *ste12* phenotypes. The *med1* mutation activates the *FLO11* promoter in a larger population of cells than is normally seen in a *flo8* background. *(B)* The epistasis of the *med1* phenotype to the *cti6* phenotype is also apparent in the haploid colony morphologies of strains with an intact *FLO11* gene (after 3 days growth on YPD at 30 degrees C), and *(C)* in YPD-agar adhesion assays in these strains (after 4 days growth on YPD at 30 degrees C, followed by plate washing assay).

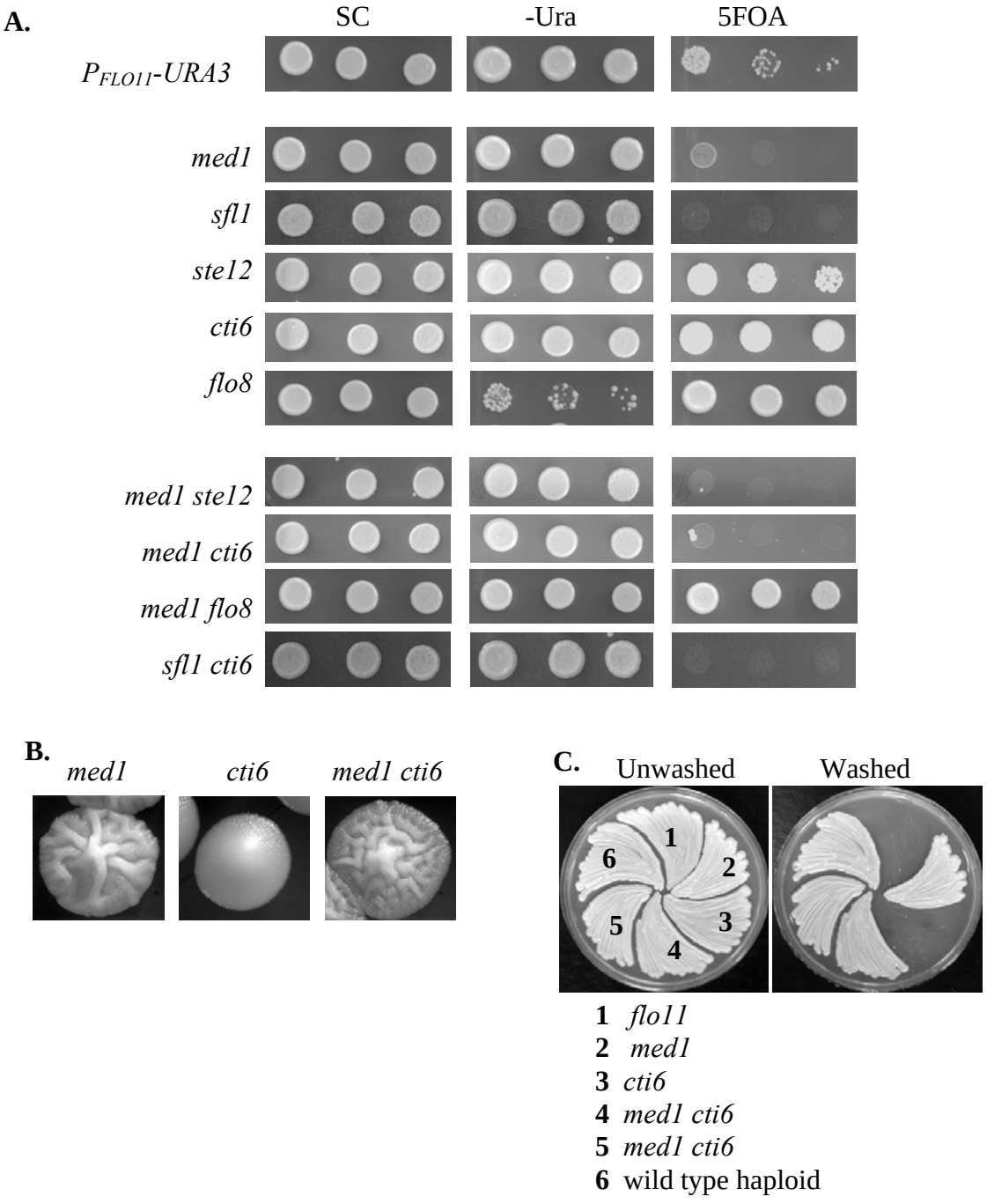

TABLE 1 | *Saccharomyces cerevisiae* strains used in this study.

Strain	Genotype		Source
10560-4A	*MATa*	*ura3-52 leu2::hisG trp1::hisG his3::hisG*	Fink lab collection
10560-6B	*MATx*	*ura3-52 leu2::hisG trp1::hisG his3::hisG*	Fink lab collection
AHY764	*MATa*	*ura3-52*	Halme et al., 2004
AHY783	*MATa*	*URA3*	Halme et al., 2004
SBY001	*MATx*	*ura3-52 leu2::hisG his3::hisG ira1::KanR flo11::HIS3 trp1::hisG flo10::pFLO10-GFP-TRP1*	Halme et al., 2004
SBY022	*MATa*	*ura3-52 leu2::hisG his3::hisG ira1::KanR flo11::HIS3 flo10::pFLO10-URA3*	Halme et al., 2004
SBY170	*MATx*	*ura3-52 leu2::hisG FLO11+ trp1::hisG sfl1::kanR IRA1+ his3::hisG*	This study
SBY206	*MATx*	*flo11::pFLO11::GFP::kanMX6 his3^ ura3^ leu2^*	This study
SBY251	*MATa*	*ura3-52 flo11::pFLO11::URA3 leu2::hisG trp1::hisG*	Halme et al., 2004
SBY305	*MATa*	*ura3-52 flo10::pFLO10::URA3 IRA1+ his3::hisG flo11::HIS3 leu2::hisG*	This study
SBY384	*MATa*	*ura3-52 flo11::pFLO11::URA3 leu2::hisG trp1::hisG ada2::Tn3::LEU2*	This study
SBY385	*MATa*	*ura3-52 leu2::hisG his3::hisG ira1::kanR flo11::HIS3 trp1::hisG flo10::pFLO10-URA3 ada2::Tn3::LEU2*	This study
SBY395	*MATa*	*ura3-52 leu2::hisG his3::hisG ira1::kanR flo11::HIS3 trp1::hisG flo10::pFLO10-URA3 ssn8::Tn3::LEU2*	This study
SBY406	*MATa*	*ura3-52 leu2::hisG his3::hisG ira1::kanR flo11::HIS3 trp1::hisG flo10::pFLO10-URA3 sin3::Tn3::LEU2*	This study
SBY409	*MATa*	*ura3-52 flo11::pFLO11::URA3 leu2::hisG trp1::hisG pho23::Tn3::LEU2*	This study
SBY411	*MATa*	*ura3-52 flo11::pFLO11::URA3 leu2::hisG trp1::hisG cti6::Tn3::LEU2*	This study
SBY413	*MATa*	*ura3-52 leu2::hisG his3::hisG ira1::kanR flo11::HIS3 trp1::hisG flo10::pFLO10-URA3 cti6::Tn3::LEU2*	This study
SBY415	*MATa*	*ura3-52 flo11::pFLO11::URA3 leu2::hisG trp1::hisG rxt2::Tn3::LEU2*	This study
SBY488	*MATa*	*ura3-52 leu2::hisG his3::hisG IRA1+ flo11::HIS3 flo10::pFLO10-URA3 med1::Tn3::LEU2*	This study
SBY491	*MATx*	*ura3-52 leu2::hisG his3::hisG ira1::kanR flo11::HIS3 flo10::pFLO10-URA3 med1::Tn3::LEU2*	This study
SBY492	*MATa*	*ura3-52 leu2::hisG his3::hisG IRA1+ flo11::HIS3 flo10::pFLO10-URA3 bre2::Tn3::LEU2*	This study
SBY495	*MATx*	*ura3-52 leu2::hisG his3::hisG ira1::kanR flo11::HIS3 flo10::pFLO10-URA3 bre2::Tn3::LEU2*	This study
SBY496	*MATa*	*ura3-52 leu2::hisG his3::hisG IRA1+ flo11::HIS3 flo10::pFLO10-URA3 swi1::Tn3::LEU2*	This study
SBY497	*MATa*	*ura3-52 leu2::hisG his3::hisG ira1::kanR flo11::HIS3 flo10::pFLO10-URA3 swi1::Tn3::LEU2*	This study
SBY508	*MATa*	*ura3-52 leu2::hisG his3::hisG IRA1+ flo11::HIS3 flo10::pFLO10-URA3 nut1::Tn3::LEU2*	This study
SBY509	*MATa*	*ura3-52 leu2::hisG his3::hisG ira1::kanR flo11::HIS3 flo10::pFLO10-URA3 nut1::Tn3::LEU2*	This study
SBY519	*MATa*	*ura3-52 leu2::hisG trp1::hisG flo11::pFLO11::URA3 set1::LEU2 pADH1::TRP1*	This study
SBY522	*MATa*	*ura3-52 leu2::hisG trp1::hisG flo11::pFLO11::URA3 set1::LEU2 pADH1::SET1 1-1080::TRP1*	This study
SBY527	*MATa*	*ura3-52 leu2::hisG trp1::hisG flo11::pFLO11::URA3 set1::LEU2 pADH1::SET1 829-1080::TRP1*	This study
SBY558	*MATx*	*ura3-52 trp1::hisG leu2::hisG his3::hisG ada2::Tn3::LEU2*	This study
SBY561	*MATa*	*ura3-52 flo11::pFLO11::URA3 leu2::hisG trp1::hisG swi1::Tn3::LEU2*	This study
SBY564	*MATx*	*ura3-52 trp1::hisG leu2::hisG his3::hisG swi1::Tn3::LEU2*	This study
SBY566	*MATa*	*ura3-52 flo10::pFLO10::URA3 IRA1+ his3::hisG flo11::HIS3 leu2::hisG rsc2::Tn3::LEU2*	This study
SBY569	*MATx*	*ura3-52 trp1::hisG leu2::hisG his3::hisG rsc2::Tn3::LEU2*	This study
SBY572	*MATa*	*ura3-52 flo11::pFLO11::URA3 leu2::hisG trp1::hisG bre2::Tn3::LEU2*	This study
SBY575	*MATx*	*ura3-52 trp1::hisG leu2::hisG his3::hisG bre2::Tn3::LEU2*	This study
SBY578	*MATa*	*ura3-52 flo11::pFLO11::URA3 leu2::hisG trp1::hisG med1::Tn3::LEU2*	This study
SBY581	*MATx*	*ura3-52 trp1::hisG leu2::hisG his3::hisG med1::Tn3::LEU2*	This study

TABLE 1 | *Saccharomyces cerevisiae* strains used in this study, Continued…

Strain	Genotype		Source
SBY588	*MATa*	*ura3-52 flo10::pFLO10::URA3 IRA1+ his3::hisG flo11::HIS3 leu2::hisG cti6::Tn3::LEU2*	This study
SBY590	*MATa*	*ura3-52 flo10::pFLO10::URA3 IRA1+ his3::hisG flo11::HIS3 leu2::hisG cti6::Tn3::LEU2*	This study
SBY591	*MATx*	*ura3-52 his3::hisG leu2::hisG trp1::hisG cti6::Tn3::LEU2*	This study
SBY594	*MATa*	*ura3-52 flo10::pFLO10::URA3 IRA1+ his3::hisG flo11::HIS3 leu2::hisG rxt2::Tn3::LEU2*	This study
SBY594	*MATa*	*ura3-52 flo10::pFLO10::URA3 IRA1+ his3::hisG flo11::HIS3 leu2::hisG rxt2::Tn3::LEU2*	This study
SBY597	*MATx*	*ura3-52 his3::hisG leu2::hisG trp1::hisG rxt2::Tn3::LEU2*	This study
SBY600	*MATa*	*ura3-52 flo10::pFLO10::URA3 IRA1+ his3::hisG flo11::HIS3 leu2::hisG pho23::Tn3::LEU2*	This study
SBY603	*MATx*	*ura3-52 his3::hisG leu2::hisG trp1::hisG pho23::Tn3::LEU2*	This study
SBY634	*MATa/x*	*+/ FLO11::HA ura3-52 / ura3-52 +/ trp1::hisG leu2::hisG / leu2::hisG his3::hisG / his3::hisG*	This study
SBY635	*MATa/x*	*+/ FLO11::HA ura3-52 / ura3-52 +/ trp1::hisG leu2::hisG / leu2::hisG his3::hisG / his3::hisG ada2::Tn3::LEU2/ada2::Tn3::LEU2*	This study
SBY637	*MATa/x*	*+/ FLO11::HA ura3-52 / ura3-52 +/ trp1::hisG leu2::hisG / leu2::hisG his3::hisG / his3::hisG rsc2::Tn3::LEU2/rsc2::Tn3::LEU2*	This study
SBY639	*MATa/x*	*+/ FLO11::HA ura3-52 / ura3-52 trp1::hisG/ trp1::hisG leu2::hisG / leu2::hisG his3::hisG / his3::hisG set1:LEU2 / set1::LEU2*	This study
SBY641	*MATa/x*	*+/ FLO11::HA ura3-52 / ura3-52 +/ trp1::hisG leu2::hisG / leu2::hisG his3::hisG / his3::hisG bre2:Tn3::LEU2 / bre2::Tn3::LEU2*	This study
SBY643	*MATa/x*	*+/ FLO11::HA ura3-52 / ura3-52 +/ trp1::hisG leu2::hisG / leu2::hisG his3::hisG / his3::hisG cti6:Tn3::LEU2 / cti6::Tn3::LEU2*	This study
SBY645	*MATa/x*	*+/ FLO11::HA ura3-52 / ura3-52 +/ trp1::hisG leu2::hisG / leu2::hisG his3::hisG / his3::hisG rxt2:Tn3::LEU2 / rxt2::Tn3::LEU2*	This study
SBY646	*MATa/x*	*+/ FLO11::HA ura3-52 / ura3-52 +/ trp1::hisG leu2::hisG / leu2::hisG his3::hisG / his3::hisG pho23:Tn3::LEU2 / pho23::Tn3::LEU2*	This study
SBY648	*MATa/x*	*+/ FLO11::HA ura3-52 / ura3-52 +/ trp1::hisG leu2::hisG / leu2::hisG his3::hisG / his3::hisG med1::Tn3::LEU2 / med1::Tn3::LEU2*	This study
SBY654	*MATa/x*	*+/ FLO11::HA ura3-52 / ura3-52 +/ trp1::hisG leu2::hisG / leu2::hisG his3::hisG / his3::hisG swi1::Tn3::LEU2 / swi1::Tn3::LEU2*	This study
SBY725	*MATa*	*ura3-52 leu2::hisG his3::hisG ira1::kanR flo11::HIS3 set1::LEU2 trp1::hisG flo10::PFLO10::URA3 + pADH1::TRP1*	This study
SBY729	*MATa*	*ura3-52 leu2::hisG his3::hisG ira1::kanR flo11::HIS3 set1::LEU2 trp1::hisG flo10::PFLO10::URA3 + pADH1::SET1 1-1080::TRP1*	This study
SBY734	*MATa*	*ura3-52 leu2::hisG his3::hisG ira1::kanR flo11::HIS3 set1::LEU2 trp1::hisG flo10::PFLO10::URA3+ pADH1::SET1 829-1080::TRP1*	This study
SBY741	*MATa*	*ura3-52 leu2::hisG his3::hisG IRA1+ flo11::HIS3 flo10::pFLO10-URA3 flo8::kanR med1::Tn3::LEU2*	This study
SBY778	*MATa*	*ura3-52 flo11::pFLO11::URA3 leu2::hisG trp1::hisG set2::kanR*	This study
SBY779	*MATa*	*ura3-52 flo11::pFLO11::URA3 leu2::hisG trp1::hisG set2::kanR*	This study
SBY782	*MATa*	*ura3-52 flo11::pFLO11::URA3 leu2::hisG trp1::hisG flo8::kanR*	This study
SBY786	*MATa*	*ura3-52 flo11::pFLO11::URA3 leu2::hisG trp1::hisG eaf3::kanR*	This study
SBY797	*MATa/x*	*+/ FLO11::HA ura3-52 / ura3-52 trp1::hisG/ trp1::hisG leu2::hisG / leu2::hisG his3::hisG / his3::hisG set1:LEU2 / set1::LEU2*	This study
SBY847	*MATa*	*rpd3::KanR can1-^::ste2pr-HIS3 ura3^ leu2^ his3^::hisG lyp1-^::ste3pr-LEU2*	Owen Ryan
SBY849	*MATx*	*set1::KanR*	This study
SBY850	*MATa*	*set1:KanR*	This study
SBY852	*MATa/x*	*set1::KanR / set1::KanR*	This study
SBY853	*MATa/x*	*+/ FLO11::HA ura3-52 / ura3-52 +/ trp1::hisG + / leu2::hisG his3::hisG / his3::hisG pTEF-URA3*	This study
SBY856	*MATa/x*	*+/ FLO11::HA ura3-52 / ura3-52 +/ trp1::hisG + / leu2::hisG his3::hisG / his3::hisG pTEF-FLO11-URA3*	This study
SBY859	*MATa/x*	*+/ FLO11::HA ura3-52 / ura3-52 +/ trp1::hisG leu2::hisG / leu2::hisG his3::hisG / his3::hisG cti6:Tn3::LEU2 / cti6::Tn3::LEU2 pTEF-URA3*	This study

TABLE 1 | ***Saccharomyces cerevisiae*** **strains used in this study, Continued…**

Strain	***Genotype***		***Source***
SBY862	*MATa/x*	*+/ FLO11::HA ura3-52 / ura3-52 +/ trp1::hisG leu2::hisG / leu2::hisG his3::hisG / his3::hisG cti6:Tn3::LEU2 / cti6::Tn3::LEU2 pTEF-FLO11-URA3*	This study
SBY871	*MATa/x*	*+/ FLO11::HA ura3-52 / ura3-52 +/ trp1::hisG leu2::hisG / leu2::hisG his3::hisG / his3::hisG rxt2:Tn3::LEU2 / rxt2::Tn3::LEU2 pTEF-URA3*	This study
SBY874	*MATa/x*	*+/ FLO11::HA ura3-52 / ura3-52 +/ trp1::hisG leu2::hisG / leu2::hisG his3::hisG / his3::hisG rxt2:Tn3::LEU2 / rxt2::Tn3::LEU2 pTEF-FLO11-URA3*	This study
SBY883	*MATx*	*rpd3::KanR lyp1-^::ste3pr-LEU2 his3^::hisG ura3^ leu2^ can1-^::ste2pr-HIS3 + pTEF-URA3*	This study
SBY886	*MATx*	*rpd3::KanR lyp1-^::ste3pr-LEU2 his3^::hisG ura3^ leu2^ can1-^::ste2pr-HIS3 pTEF-FLO11-URA3*	This study
SBY891	*MATx*	*ura3-52 his3::hisG leu2::hisG trp1::hisG rxt1::Tn3::LEU2 pTEF-FLO11-URA3*	This study
SBY892	*MATx*	*ura3-52 his3::hisG leu2::hisG trp1::hisG rxt1::Tn3::LEU2 pTEF-URA3*	This study
SBY898	*MATx*	*ura3-52 his3::hisG leu2::hisG trp1::hisG rxt2::Tn3::LEU2 pTEF-URA3*	This study
SBY901	*MATx*	*ura3-52 his3::hisG leu2::hisG trp1::hisG rxt2::Tn3::LEU2 pTEF-FLO11-URA3*	This study
SBY979	*MATa*	*ura3-52 leu2::hisG trp1::hisG his3::hisG med1::Tn3::LEU2 cti6::Tn3::LEU2 flo11::pFLO11::URA3*	This study
SBY985	*MATx*	*ura3-52 leu2::hisG trp1::hisG med1::Tn3::LEU2 cti6::Tn3::LEU2*	This study
SBY1024	*MATa*	*swi1::Tn3::LEU2 ura3-52 trp1::hisG leu2::hisG his3::hisG*	This study
SBY1065	*MATa*	*cti6::KanR ura3-52 flo11::pFLO11::URA3 leu2::hisG trp1::hisG*	This study
SBY1075	*MATa*	*med1::KanR ste12::KanR ura3-52 flo11::pFLO11::URA3 leu2::hisG trp1::hisG*	This study
SBY1083	*MATa*	*med1::KanR ura3-52 flo11::pFLO11::URA3 leu2::hisG trp1::hisG*	This study
SBY1087	*MATa*	*ste12::KanR ura3-52 flo11::pFLO11::URA3 leu2::hisG trp1::hisG*	This study
SBY1090	*MATa*	*sfl1::KanR ura3-52 flo11::pFLO11::URA3 leu2::hisG trp1::hisG*	This study

TABLE 2 | **Plasmids used in this study.**

Plasmid	***Insert***	***Reference***
pQF328.2	P_{TEF}-*FLO11*; *URA3*	Fink Laboratory Collection
p416TEF	P_{TEF}- (empty vector); *URA3*	Mumberg et al., 1995
pFA6a	*KanMX* deletion cassette	Longtine et al., 1998
pRS405	*LEU2* deletion cassette	Sikorski and Hieter, 1989
pRS416-*SET1(1-1080)*	Full length *SET1* ORF (1-1080); *TRP1*	Briggs et al., 2001
pRS416-*SET1 (829-1080)*	*SET1* fragment (829-1080); *TRP1*	Fingerman et al., 2005
pRS416	*TRP1*	Sikorski and Hieter, 1989

TABLE 3 | **Primers used in this study.**

Primer	Sequence (5' to 3')	*Description*
PSB069	TAACATTCCTTATTTGTTGAATCTTTATAAGAGGTCTCTGCGTTTAGAGAA GATTGTACTGAGAGTGCAC	*To generate set1::LEU2*
PSB070	AGCAACGATATGTTAAATCAGGAAGCTCCAAACAAATCAATGTATCATCG CTGTGCGGTATTTCACACCG	*To generate set1::LEU2*
PSB073	AGTCGTGCTGTCAAACCTTTCTCCTTTCCTGGTTGTTGTTTTACGTGATCAG ATTGTACTGAGAGTGCAC	*To generate set2::LEU2*
PSB074	CTTTGGGACAGAAAACGTGAAACAAGCCCCAAATATGCATGTCTGGTTAA CTGTGCGGTATTTCACACCG	*To generate set2::LEU2*
PSB110	ACAGCGAAGGCATAGAATCG	*To amplify ada2::Tn3*
PSB111	ACATCCAATTCTGGCTCTGG	*To amplify ada2::Tn3*
PSB112	AAAATAATTTTTCTCTAATCACCCTCCATTTTCGATAAAATATCAGCGTAG TCTGAAAATATATACATTAAGCAAAAAGAAGATTGTACTGAGAGTGCAC	*To generate ada2::LEU2*
PSB113	TAAAATCGAGACAAGGTCCCTTTATGACTTGGCCAATAATAACTAGTGAC AATTGTAGTTACTTTTCAATTTTTTTTTTGCTGTGCGGTATTTCACACCG	*To generate ada2::LEU2*
PSB122	GCGCATTATACAAGGACCTG	*To amplify rsc2::Tn3*
PSB123	CATCTGGTGTCTTCCATAGCC	*To amplify rsc2::Tn3*
PSB124	TAACAGTTCAATACGTGATCAAATATACAGCACGTCGCGCAGAACCAGAC GAAGCGGAGAATATTCTACA TTGACAGTGCAGATTGTACTGAGAGTGCAC	*To generate rsc2::LEU2*
PSB125	TTTGAAGTTTGACTCTGCTCGCGGAGGGTAATGCGCAATGGGAAGATATT ATGCTGCCATTGCTTTTACAATAAAGGTGACTGTGCGGTATTTCACACCG	*To generate rsc2::LEU2*
PSB134	CGAAGCCTCTGCTAATGGAG	*To amplify spt8::Tn3*
PSB135	CCACACAGGCATTCCTTCTC	*To amplify spt8::Tn3*
PSB146	GCAGCAAGTGTTATCGCAATC	*To amplify swi1::Tn3*
PSB147	GCGCTCTTCCGACTGTATTG	*To amplify swi1::Tn3*
PSB148	TTCTTTCTTTTCGTGTCTTATAATAATAATAATAATAATAATAATAAAAAT AGTAATAATAAAAATAGTA ATAAATAAAGAGATTGTACTGAGAGTGCAC	*To generate swi1::LEU2*
PSB149	ATTTTATATAGGTTTATAAAAAGAAAATAGTGCGCAAGGAAGAAATAAGC AGTAAAAGAATATTGTTTAAAAAAATCGCACTGTGCGGTATTTCACACCG	*To generate swi1::LEU2*
PSB152	CCTGCAATAGAGGTACCAGGTC	*To amplify ssn8::Tn3*
PSB153	TCCATTGTTCGTGGTACTTGTC	*To amplify ssn8::Tn3*
PSB154	ACTCATATTGTTCGAACAAAAAATGCCCTCTCAAACTTTAGTTGAAGAGC GATAAGGCATCTGAATCTCAAAAGTTAGACAGATTGTACTGAGAGTGCAC	*To generate ssn8::LEU2*
PSB155	AACATTTCCAAAACGGATCATCACCACCATAATGATTGAATTTACAGGCTT AACGGTTTTTAAATTTATTCTTCGCATGACTGTGCGGTATTTCACACCG	*To generate ssn8::LEU2*
PSB197	TCCAATTGTGAGTGGCAAAC	*To amplify pho23::Tn3*
PSB198	TTCTAACCGGGACGTCAATC	*To amplify pho23::Tn3*
PSB201	GTAAACCGCACAGCACAATC	*To amplify cti6::Tn3*
PSB202	TTGCTTCGCCAGTATCTGTG	*To amplify cti6::Tn3*
PSB205	TTCGAATGGAGAGGCATAGG	*To amplify rxt2::Tn3*
PSB206	CTCGACGTTGATGTCAGGTG	*To amplify rxt2::Tn3*
PSB209	TCTGCCACATCCAACAGAAG	*To amplify sin3::Tn3*
PSB210	GGATGCAGGCAGTACACTTG	*To amplify sin3::Tn3*
PSB217	TACCACAGATGGAAGCAACG	*To amplify bre2::Tn3*
PSB218	GCAGGACGCTATTTCTCCAG	*To amplify bre2::Tn3*
PSB229	TTGGGTCTCGAGTCCTTCAC	*To amplify med1::Tn3*

TABLE 3 | **Primers used in this study, Continued…**

Primer	Sequence (5' to 3')	*Description*
PSB230	CGAGTGTACGGTCCACAATG	*To amplify med1::Tn3*
PSB233	TTCCACACGGCTGTACTGAG	*To amplify nut1::Tn3*
PSB234	AGAACCAGGGACCCCATAAG	*To amplify nut1::Tn3*
PSB237	GCATAATTCACTCGCGTTGG	*To amplify set1::Tn3*
PSB238	AAACCCCAGTTGTGAATTGC	*To amplify set1::Tn3*
PSB332	TAGCATCTGTGAGGCCTCGTCACTGGATTTACCCTATTGAAGAACGTATAA GATTGTACTGAGAGTGCAC	*To generate eaf3::LEU2*
PSB333	TACGGAAGAACTAAATACTAGAAATAATCCCAAGCTAGAATATAAACGTC CTGTGCGGTATTTCACACCG	*To generate eaf3::LEU2*
PSB522	AATATTGTAATTCGACACTATTTGGTACATTCAGAGGGTCCTAAGACAGC ACAAATCAGTCGGATCCCCGGGTTAATTAA	*To generate sfl1::KanMx*
PSB523	AATAAACATACAGTGAGGTGCTTTGAACTTTTAGACAATTAGAGATTAAA AAGGCAAAGAGAATTCGAGCTCGTTTAAAC	*To generate sfl1::KanMx*
PSB528	AGAACTCCTAATCAAAAGCAAAGAAAACATAGAACAAAAGCCAACAAAA CTCTTTTGGAGCGGATCCCCGGGTTAATTAA	*To generate med1::KanMx*
PSB529	AAACCTAAACTCCATCGAGTGTACGGTCCACAATGTGTATTTGAGCCACT CCGTACCTCCGAATTCGAGCTCGTTTAAAC	*To generate med1::KanMx*
PSB532	TTTACTTTGCGTAACCTTACTAAAAGATAGCATAAACATATAGGAGTATA GAGAAGAGTACGGATCCCCGGGTTAATTAA	*To generate cti6::KanMx*
PSB533	TGTTTGTTCGCCTCATTACAGTTATACTTTGGTTGAGAATAATATTGCAGT GTTTTGCGTGAATTCGAGCTCGTTTAAAC	*To generate cti6::KanMx*
PSB536	AGAAAACACACTTTTATAGCGGAACCGCTTTCTTTATTTGAATTGTCTTGT TCACCAAGGCGGATCCCCGGGTTAATTAA	*To generate ste12::KanMx*
PSB537	TGTAGTTTTGGAGGTCATGTTAAGAAACTCATTGATATTTATATTACATAC TGTGACGCTGAATTCGAGCTCGTTTAAAC	*To generate ste12::KanMx*

TABLE 4 | **Mutants with reduced *FLO11* promoter activity identified in Tn3 insertion screen.** See Figure 2 for information regarding qualitative assessment of strength of phenotype. (#) indicates the number of unique Tn3 insertions identified at the indicated locus, if greater than one.

A. MILD PHENOTYPES:

GENE	(#)	BIOLOGICAL PROCESS
ECM17		Cell wall organization and biogenesis
IME2		Regulation of meiosis
LRG1		Cell wall biogenesis
RRN9		Transcription from RNA polymerase I promoter
SIN3	(2)	Histone deacetylation (Rpd3L complex)
UBP9		Protein deubiquitination
YGR071C		Unknown

B. MODERATE PHENOTYPES:

GENE	(#)	BIOLOGICAL FUNCTION
ASC1		Invasive growth, G-protein coupled receptor protein signaling
CTI6/RXT1		Histone deacetylation (Rpd3L complex)
DBR1	(2)	Pseudohyphal growth; RNA catabolic process
FAR7		Cell cycle
FMO1		Protein folding
GPG1		Invasive growth; Signal transduction
HMT1		Protein amino acid methylation; RNA export from nucleus
HRP1		mRNA processing
KIN4		Cell Cycle
MF(ALPHA)1		Mating
MKC7		Cell wall organization and biogenesis
MSN1		Invasive and pseudohyphal growth; Activation of transcription
OST6		Protein modification; Glycosylation
PHO23		Histone deacetylation (Rpd3L complex)
RXT2		Histone deacetylation (Rpd3L complex)
TEP1		Cell wall organization and biogenesis
TPK1		Invasive and pseudohyphal growth; Ras-cAMP signaling
YVC1		Vacuolar function

TABLE 5 | **Mutants with increased *FLO11* promoter activity identified in Tn3 insertion screen.** See Figure 2 for information regarding qualitative assessment of strength of phenotype. (#) indicates the number of unique Tn3 insertions identified at the indicated locus, if greater than one.

A. MILD PHENOTYPES:

GENE	(#)	BIOLOGICAL PROCESS
APL5		Protein sorting and transport
AVL9		Protein sorting and transport
MSH1		Mitochondrial function
PET111	(2)	Mitochondrial function
PET56		Mitochondrial function
TAT2		Membrane transport

B. MODERATE PHENOTYPES:

GENE	(#)	BIOLOGICAL FUNCTION
ADA5/SPT20		Histone acetylation (SAGA complex)
AIM8		Mitochondrial function
ATP25		Mitochondrial function
GRR1	(2)	Protein ubiquitination
IFM1		Mitochondrial function
IMG1		Mitochondrial function
MAM33		Mitochondrial function
MRM1		Mitochondrial function
PPH22		Signal transduction

C. STRONG PHENOTYPES:

GENE	(#)	BIOLOGICAL FUNCTION
AKR1		Protein sorting and transport
ATG18		Protein sorting and transport
ATP1	(3)	Mitochondrial function
BRE2	(7)	Histone methylation (COMPASS complex)
CDC5/MSD2		Cell Cycle; Cytokinesis
COX11	(2)	Mitochondrial function
COX15	(2)	Mitochondrial function
COX18		Mitochondrial function
COX4		Mitochondrial function
DNF3		Protein sorting and transport
FLC3		Membrane transport
GIS4		Signalling from the plasma membrane
GPB1	(4)	Invasive and pseudohyphal growth; Ras-cAMP signaling
HDA1	(4)	Histone deacetylation (Hda1 complex)

Table 5, continued. Mutants with increased *FLO11* promoter activity identified in Tn3 insertion screen.

C. STRONG PHENOTYPES, continued:

GENE	(#)	BIOLOGICAL FUNCTION
HDA2	(7)	Histone deacetylation (Hda1 complex)
HDA3	(11)	Histone deacetylation (Hda1 complex)
HSC82		Protein folding
IML1		Vacuolar function
IOC3		Chromatin remodeling (Isw1a complex)
IPK1	(2)	Inositol phosphate biosynthesis
IRA1	(4)	Invasive and pseudohyphal growth; Ras-cAMP signaling
IRC3		Mitochondrial function
IRA2	(3)	Invasive and pseudohyphal growth; Ras-cAMP signaling
MCK1	(4)	Cell Cycle
MED1	(5)	Transcription from RNA polymerase II promoter (Mediator complex)
MED4		Transcription from RNA polymerase II promoter (Mediator complex)
MET18		Transcription from RNA polymerase II promoter
MON2		Protein sorting and transport
NTO1	(4)	Histone acetylation (NuA3 complex)
NUT1/MED5		Transcription from RNA polymerase II promoter (Mediator complex)
PCP1	(2)	Mitochondrial function
CSR2		Cell wall organization and biogenesis
PDE1	(2)	Ras-cAMP signaling
PET100		Mitochondrial function
PET54		Mitochondrial function
PIL1		Endocytosis
PIN4		Cell Cycle
PAU7		Unknown; Regulated by anaerobiosis
RDN25-1	(2)	Translation
REG1	(2)	Regulation of transcription from RNA polymerase II promoter
RGT1		Regulation of transcription from RNA polymerase II promoter
RRF1		Mitochondrial function
RRI2		Protein deneddylation
RSE1		mRNA processing
SCH9		Pseudohyphal growth; Regulation of transcription from RNA polymerase
SET1	(4)	Histone methylation (COMPASS complex)
SLG1		Cell wall organization and biogenesis
SNT1		Histone deacetylation (Set3C complex)
SRB8/SSN5		Transcription from RNA polymerase II promoter (Mediator complex)
SRB9/SSN2		Transcription from RNA polymerase II promoter (Mediator complex)
SRB10/SSN3	(2)	Transcription from RNA polymerase II promoter (Mediator complex)

Table 5, continued. Mutants with increased *FLO11* promoter activity identified in Tn3 insertion screen.

C. STRONG PHENOTYPES, continued:

GENE		BIOLOGICAL FUNCTION
SRB11/SSN8	(4)	Transcription from RNA polymerase II promoter (Mediator complex)
SRY1		Amino acid catabolism
TRM10		tRNA methylation
TRX1		Protein sorting and transport
UBC8		Protein ubiquitination
VAC8		Protein sorting and transport
YDJ1		Protein folding
YGL242C		Unknown
YIL077C		Mitochondrial function
YLR030W		Unknown
ZUO1		Protein folding

TABLE 6 | **Mutants with reduced *FLO10* promoter activity identified in Tn3 insertion screen.** See Figure 2 for information regarding qualitative assessment of strength of phenotype. (#) indicates the number of unique Tn3 insertions identified at the indicated locus, if greater than one. *Indicates ambiguity due to sequence identity.

A. MILD PHENOTYPES:

GENE	(#)	BIOLOGICAL PROCESS
AFR1		Cellular morphogenesis
ASN1 or *ASN2**		Asparagine biosynthesis
AXL1	(2)	Cellular morphogenesis
CIN8		Chromosome segregation
ECM7		Cell wall organization and biogenesis
GCN2		Translation
MCH1		Plasma membrane transport
MRN1	(4)	Unknown; Putative RNA binding
ASH1		Regulation of Transcription from RNA polymerase II promoter
PRE9		Ubiquitin-dependent protein degradation
RDN25-1	(3)	Translation
RVS161		Cellular morphogenesis
SED4		Protein sorting and transport
TEP1		Cell wall organization and biogenesis
YOL036W		Unknown

B. MODERATE PHENOTYPES:

GENE	(#)	BIOLOGICAL FUNCTION
BUD3		Cellular morphogenesis
CRM1		Nuclear membrane transport
MOG1		Nuclear membrane transport
RPN9		Ubiquitin-dependent protein degradation
SHO1		Pseudohyphal growth; Ras-cAMP signaling
UBP6	(2)	Ubiquitin-dependent protein degradation
YDJ1		Protein sorting and transport
YGP1		Cell wall organization and biogenesis

C. STRONG PHENOTYPES:

GENE	(#)	BIOLOGICAL FUNCTION
ACS1		Histone acetylation
ADA2		Histone acetylation (SAGA complex)
ATH1		Cell wall organization and biogenesis
CSF1		Fermentation
ECM33		Cell wall organization and biogenesis
FLO8		Invasive and pseudohyphal growth; Ras-cAMP signaling

Table 6, continued. Mutants with reduced *FLO10* promoter activity identified in Tn3 insertion screen.

C. STRONG PHENOTYPES, continued:

GENE	(#)	BIOLOGICAL FUNCTION
GUP1		Plasma membrane transport
KTI11	(2)	Metal ion binding (Zinc)
MET17		Methionine biosynthesis
OPY2	(2)	Signalling from the plasma membrane
DLD3		Pseudohyphal growth
PPS1		Cell Cycle
SRY1		Amino acid catabolism
ZRC1		Metal ion transport (Zinc)
RIM13		Protein degradation
RIM21		Cell wall organization and biogenesis
RPL43A		Translation
RPS19A		Translation
RSC2	(3)	Chromatin remodeling (RSC complex)
SAS5		Histone acetylation (SAS complex)
SFI1		Cell cycle
SLX4		DNA replication
SPT8		Transcription from RNA polymerase II promoter (SAGA complex)
STE7	(2)	Invasive and pseudohyphal growth; Ras-cAMP signaling
SWI1		Chromatin remodeling (SWI/SNF complex)
UBP14		Ubiquitin-dependent protein degradation
YPR091C		Unknown

TABLE 7 | **Mutants with increased *FLO10* promoter activity identified in Tn3 insertion screen.** See Figure 2 for information regarding qualitative assessment of strength of phenotype. (#) indicates the number of unique Tn3 insertions identified at the indicated locus, if greater than one.

A. MILD PHENOTYPES:

GENE	(#)	BIOLOGICAL PROCESS
COA1		Mitochondrial function
ERG3		Ergosterol biosynthesis
MID1		Ion transport (Calcium)
SCH9		Pseudohyphal growth; Regulation of transcription from Pol II promoter

B. MODERATE PHENOTYPES:

GENE	(#)	BIOLOGICAL PROCESS
ACB1		Fatty acid transport
ELM1	(2)	Cellular morphogenesis
NAS2		Ubiquitin-dependent protein degradation
SSD1	(2)	Cell wall organization and biogenesis

C. STRONG PHENOTYPES:

GENE	(#)	BIOLOGICAL PROCESS
AKR1		Protein sorting and transport
CAK1	(2)	Cell cycle
CSR2		Cell wall organization and biogenesis
GRR1		Protein ubiquitination
IRA2	(3)	Invasive and pseudohyphal growth; Ras-cAMP signaling
MAM33		Mitochondrial function
OLE1		Mitochondrial function; Fatty acid synthesis
REG1		Regulation of transcription from RNA polymerase II promoter
RNH203		Ribonuclease activity (Ribonuclease H2 complex)
ROT2		Cell wall organization and biogenesis
SDC25		Ras-cAMP signaling
SEC1		Exocytosis
SRB11/SSN8		Transcription from RNA polymerase II promoter (Mediator complex)
TEC1		Invasive and pseudohyphal growth; Ras-cAMP signaling
VMA2		Vacuolar function
YOR296W		Unknown

References

Balciunas, D., Galman, C., Ronne, H., and Bjorklund, S. (1999). The Med1 subunit of the yeast mediator complex is involved in both transcriptional activation and repression. Proceedings of the National Academy of Sciences of the United States of America *96*, 376-381.

Battaglioli, E., Andres, M.E., Rose, D.W., Chenoweth, J.G., Rosenfeld, M.G., Anderson, M.E., and Mandel, G. (2002). REST repression of neuronal genes requires components of the hSWI.SNF complex. The Journal of Biological Chemistry *277*, 41038-41045.

Belandia, B., Orford, R.L., Hurst, H.C., and Parker, M.G. (2002). Targeting of SWI/SNF chromatin remodelling complexes to estrogen-responsive genes. The EMBO Journal *21*, 4094-4103.

Belotserkovskaya, R., Sterner, D.E., Deng, M., Sayre, M.H., Lieberman, P.M., and Berger, S.L. (2000). Inhibition of TATA-binding protein function by SAGA subunits Spt3 and Spt8 at Gcn4-activated promoters. Molecular and Cellular Biology *20*, 634-647.

Beve, J., Hu, G.Z., Myers, L.C., Balciunas, D., Werngren, O., Hultenby, K., Wibom, R., Ronne, H., and Gustafsson, C.M. (2005). The structural and functional role of Med5 in the yeast Mediator tail module. The Journal of Biological Chemistry *280*, 41366-41372.

Bjorklund, S., Buzaite, O., and Hallberg, M. (2001). The yeast mediator. Molecules and Cells *11*, 129-136.

Boeke, J.D., Trueheart, J., Natsoulis, G., and Fink, G.R. (1987). 5-Fluoroorotic acid as a selective agent in yeast molecular genetics. Methods in Enzymology *154*, 164-175.

Briggs, S.D., Bryk, M., Strahl, B.D., Cheung, W.L., Davie, J.K., Dent, S.Y., Winston, F., and Allis, C.D. (2001). Histone H3 lysine 4 methylation is mediated by Set1 and required for cell growth and rDNA silencing in Saccharomyces cerevisiae. Genes & Development *15*, 3286-3295.

Brownell, J.E., and Allis, C.D. (1996). Special HATs for special occasions: linking histone acetylation to chromatin assembly and gene activation. Current Opinion in Genetics & Development *6*, 176-184.

Cairns, B.R., Lorch, Y., Li, Y., Zhang, M., Lacomis, L., Erdjument-Bromage, H., Tempst, P., Du, J., Laurent, B., and Kornberg, R.D. (1996). RSC, an essential, abundant chromatin-remodeling complex. Cell *87*, 1249-1260.

Candau, R., and Berger, S.L. (1996). Structural and functional analysis of yeast putative adaptors. Evidence for an adaptor complex in vivo. The Journal of Biological Chemistry *271*, 5237-5245.

Candau, R., Zhou, J.X., Allis, C.D., and Berger, S.L. (1997). Histone acetyltransferase activity and interaction with ADA2 are critical for GCN5 function in vivo. The EMBO Journal *16*, 555-565.

Cao, Y., Cairns, B.R., Kornberg, R.D., and Laurent, B.C. (1997). Sfh1p, a component of a novel chromatin-remodeling complex, is required for cell cycle progression. Molecular and Cellular Biology *17*, 3323-3334.

Carrozza, M.J., Florens, L., Swanson, S.K., Shia, W.J., Anderson, S., Yates, J., Washburn, M.P., and Workman, J.L. (2005a). Stable incorporation of sequence specific repressors Ash1 and Ume6 into the Rpd3L complex. Biochimica et Biophysica Acta *1731*, 77-87; discussion 75-76.

Carrozza, M.J., Li, B., Florens, L., Suganuma, T., Swanson, S.K., Lee, K.K., Shia, W.J., Anderson, S., Yates, J., Washburn, M.P.*, et al.* (2005b). Histone H3 methylation by Set2 directs deacetylation of coding regions by Rpd3S to suppress spurious intragenic transcription. Cell *123*, 581-592.

Cheng, H., He, X., and Moore, C. (2004). The essential WD repeat protein Swd2 has dual functions in RNA polymerase II transcription termination and lysine 4 methylation of histone H3. Molecular and Cellular Biology *24*, 2932-2943.

Clarke, L., and Carbon, J. (1992). A colony bank containing synthetic Col El hybrid plasmids representative of the entire E. coli genome. 1976. Biotechnology *24*, 179-187.

Cullen, P.J., Sabbagh, W., Jr., Graham, E., Irick, M.M., van Olden, E.K., Neal, C., Delrow, J., Bardwell, L., and Sprague, G.F., Jr. (2004). A signaling mucin at the head of the Cdc42- and MAPK-dependent filamentous growth pathway in yeast. Genes & Development *18*, 1695-1708.

Damelin, M., Simon, I., Moy, T.I., Wilson, B., Komili, S., Tempst, P., Roth, F.P., Young, R.A., Cairns, B.R., and Silver, P.A. (2002). The genome-wide localization of Rsc9, a component of the RSC chromatin-remodeling complex, changes in response to stress. Molecular Cell *9*, 563-573.

De Nadal, E., Zapater, M., Alepuz, P.M., Sumoy, L., Mas, G., and Posas, F. (2004). The MAPK Hog1 recruits Rpd3 histone deacetylase to activate osmoresponsive genes. Nature *427*, 370-374.

Dehe, P.M., and Geli, V. (2006). The multiple faces of Set1. Biochemistry and cell Biology *84*, 536-548.

Du, J., Nasir, I., Benton, B.K., Kladde, M.P., and Laurent, B.C. (1998). Sth1p, a Saccharomyces cerevisiae Snf2p/Swi2p homolog, is an essential ATPase in RSC and differs from Snf/Swi in its interactions with histones and chromatin-associated proteins. Genetics *150*, 987-1005.

Dudley, A.M., Rougeulle, C., and Winston, F. (1999). The Spt components of SAGA facilitate TBP binding to a promoter at a post-activator-binding step in vivo. Genes & Development *13*, 2940-2945.

Fingerman, I.M., Wu, C.L., Wilson, B.D., and Briggs, S.D. (2005). Global loss of Set1-mediated H3 Lys4 trimethylation is associated with silencing defects in Saccharomyces cerevisiae. The Journal of Biological Chemistry *280*, 28761-28765.

Gancedo, J.M. (2001). Control of pseudohyphae formation in Saccharomyces cerevisiae. FEMS Microbiology Reviews *25*, 107-123.

Grant, P.A., Duggan, L., Côté, J., Roberts, S.M., Brownell, J.E., Candau, R., Ohba, R., Owen-Hughes, T., Allis, C.D., Winston, F., Berger, S.L., and Workman, J.L. (1997). Yeast Gcn5 functions in two multisubunit complexes to acetylate nucleosomal histones: characterization of an ADA complex and the SAGA (Spt/Ada) complex. Genes & Development *11*, 1640-1650.

Grunstein, M. (1997). Histone acetylation in chromatin structure and transcription. Nature *389*, 349-352.

Guenther, M.G., Levine, S.S., Boyer, L.A., Jaenisch, R., and Young, R.A. (2007). A chromatin landmark and transcription initiation at most promoters in human cells. Cell *130*, 77-88.

Guo, B., Styles, C.A., Feng, Q., and Fink, G.R. (2000). A Saccharomyces gene family involved in invasive growth, cell-cell adhesion, and mating. Proceedings of the National Academy of Sciences of the United States of America *97*, 12158-12163.

Guthrie, C., and Fink, G.R. (2001). Guide to Yeast Genetics and Molecular and Cell Biology. Methods of Enzymology *350* and *351*.

Halme, A., Bumgarner, S., Styles, C., and Fink, G.R. (2004). Genetic and epigenetic regulation of the FLO gene family generates cell-surface variation in yeast. Cell *116*, 405-415.

Hassan, A.H., Neely, K.E., and Workman, J.L. (2001). Histone acetyltransferase complexes stabilize swi/snf binding to promoter nucleosomes. Cell *104*, 817-827.

Hassan, A.H., Prochasson, P., Neely, K.E., Galasinski, S.C., Chandy, M., Carrozza, M.J., and Workman, J.L. (2002). Function and selectivity of bromodomains in anchoring chromatin-modifying complexes to promoter nucleosomes. Cell *111*, 369-379.

Hengartner, C.J., Myer, V.E., Liao, S.M., Wilson, C.J., Koh, S.S., and Young, R.A. (1998). Temporal regulation of RNA polymerase II by Srb10 and Kin28 cyclin-dependent kinases. Molecular Cell *2*, 43-53.

Hepworth, S.R., Friesen, H., and Segall, J. (1998). NDT80 and the meiotic recombination checkpoint regulate expression of middle sporulation-specific genes in Saccharomyces cerevisiae. Molecular and Cellular Biology *18*, 5750-5761.

Holstege, F.C., Jennings, E.G., Wyrick, J.J., Lee, T.I., Hengartner, C.J., Green, M.R., Golub, T.R., Lander, E.S., and Young, R.A. (1998). Dissecting the regulatory circuitry of a eukaryotic genome. Cell *95*, 717-728.

Horiuchi, J., Silverman, N., Pina, B., Marcus, G.A., and Guarente, L. (1997). ADA1, a novel component of the ADA/GCN5 complex, has broader effects than GCN5, ADA2, or ADA3. Molecular and Cellular Biology *17*, 3220-3228.

Ikeda, K., Steger, D.J., Eberharter, A., and Workman, J.L. (1999). Activation domain-specific and general transcription stimulation by native histone acetyltransferase complexes. Molecular and Cellular Biology *19*, 855-863.

Jackson, J.C., and Lopes, J.M. (1996). The yeast UME6 gene is required for both negative and positive transcriptional regulation of phospholipid biosynthetic gene expression. Nucleic Acids Research *24*, 1322-1329.

Kadosh, D., and Struhl, K. (1997). Repression by Ume6 involves recruitment of a complex containing Sin3 corepressor and Rpd3 histone deacetylase to target promoters. Cell *89*, 365-371.

Kadosh, D., and Struhl, K. (1998a). Histone deacetylase activity of Rpd3 is important for transcriptional repression in vivo. Genes & Development *12*, 797-805.

Kadosh, D., and Struhl, K. (1998b). Targeted recruitment of the Sin3-Rpd3 histone deacetylase complex generates a highly localized domain of repressed chromatin in vivo. Molecular and Cellular Biology *18*, 5121-5127.

Kelleher, R.J., 3rd, Flanagan, P.M., and Kornberg, R.D. (1990). A novel mediator between activator proteins and the RNA polymerase II transcription apparatus. Cell *61*, 1209-1215.

Kim, T.S., Lee, S.B., and Kang, H.S. (2004). Glucose repression of STA1 expression is mediated by the Nrg1 and Sfl1 repressors and the Srb8-11 complex. Molecular and Cellular Biology *24*, 7695-7706.

Krogan, N.J., Dover, J., Khorrami, S., Greenblatt, J.F., Schneider, J., Johnston, M., and Shilatifard, A. (2002). COMPASS, a histone H3 (Lysine 4) methyltransferase required for telomeric silencing of gene expression. The Journal of Biological Chemistry *277*, 10753-10755.

Krogan, N.J., Dover, J., Wood, A., Schneider, J., Heidt, J., Boateng, M.A., Dean, K., Ryan, O.W., Golshani, A., Johnston, M.*, et al.* (2003). The Paf1 complex is required for histone H3 methylation by COMPASS and Dot1p: linking transcriptional elongation to histone methylation. Molecular Cell *11*, 721-729.

Kumar, A., Vidan, S., and Snyder, M. (2002). Insertional mutagenesis: transposon-insertion libraries as mutagens in yeast. Methods in Enzymology *350*, 219-229.

Kuo, M.H., Brownell, J.E., Sobel, R.E., Ranalli, T.A., Cook, R.G., Edmondson, D.G., Roth, S.Y., and Allis, C.D. (1996). Transcription-linked acetylation by Gcn5p of histones H3 and H4 at specific lysines. Nature *383*, 269-272.

Laprade, L., Boyartchuk, V.L., Dietrich, W.F., and Winston, F. (2002). Spt3 plays opposite roles in filamentous growth in Saccharomyces cerevisiae and Candida albicans and is required for C. albicans virulence. Genetics *161*, 509-519.

Lee, T.I., and Young, R.A. (2000). Transcription of eukaryotic protein-coding genes. Annual Review of Genetics *34*, 77-137.

Li, B., Carey, M., and Workman, J.L. (2007a). The role of chromatin during transcription. Cell *128*, 707-719.

Li, B., Gogol, M., Carey, M., Pattenden, S.G., Seidel, C., and Workman, J.L. (2007b). Infrequently transcribed long genes depend on the Set2/Rpd3S pathway for accurate transcription. Genes & Development *21*, 1422-1430.

Li, Y., Bjorklund, S., Jiang, Y.W., Kim, Y.J., Lane, W.S., Stillman, D.J., and Kornberg, R.D. (1995). Yeast global transcriptional regulators Sin4 and Rgr1 are components of mediator complex/RNA polymerase II holoenzyme. Proceedings of the National Academy of Sciences of the United States of America *92*, 10864-10868.

Liu, H., Styles, C.A., and Fink, G.R. (1996). Saccharomyces cerevisiae S288C has a mutation in FLO8, a gene required for filamentous growth. Genetics *144*, 967-978.

Longtine, M. S., McKenzie, A., 3rd, Demarini, D. J., Shah, N. G., Wach, A., Brachat, A., Philippsen, P., and Pringle, J. R. (1998). Additional modules for versatile and economical PCR-based gene deletion and modification in Saccharomyces cerevisiae. Yeast *14*, 953-961.

Lorch, Y., Beve, J., Gustafsson, C.M., Myers, L.C., and Kornberg, R.D. (2000). Mediator-nucleosome interaction. Molecular Cell *6*, 197-201.

Lorch, Y., Zhang, M., and Kornberg, R.D. (1999). Histone octamer transfer by a chromatin-remodeling complex. Cell *96*, 389-392.

Marmorstein, R., and Berger, S.L. (2001). Structure and function of bromodomains in chromatin-regulating complexes. Gene *272*, 1-9.

Martens, J.A., and Winston, F. (2002). Evidence that Swi/Snf directly represses transcription in S. cerevisiae. Genes & Development *16*, 2231-2236.

Martens, J.A., and Winston, F. (2003). Recent advances in understanding chromatin remodeling by Swi/Snf complexes. Current Opinion in Genetics & Development *13*, 136-142.

McKenzie, E.A., Kent, N.A., Dowell, S.J., Moreno, F., Bird, L.E., and Mellor, J. (1993). The centromere and promoter factor, 1, CPF1, of Saccharomyces cerevisiae modulates gene activity through a family of factors including SPT21, RPD1 (SIN3), RPD3 and CCR4. Mol Gen Genet *240*, 374-386.

Mueller, J.E., Canze, M., and Bryk, M. (2006). The requirements for COMPASS and Paf1 in transcriptional silencing and methylation of histone H3 in Saccharomyces cerevisiae. Genetics *173*, 557-567.

Mumberg, D., Muller, R. & Funk, M. (1995). Yeast vectors for the controlled expression of heterologous proteins in different genetic backgrounds. Gene *156*, 119–122.

Myers, L.C., and Kornberg, R.D. (2000). Mediator of transcriptional regulation. Annual Review of Biochemistry *69*, 729-749.

Nagy, P.L., Griesenbeck, J., Kornberg, R.D., and Cleary, M.L. (2002). A trithorax-group complex purified from Saccharomyces cerevisiae is required for methylation of histone H3. Proceedings of the National Academy of Sciences of the United States of America *99*, 90-94.

Natarajan, K., Jackson, B.M., Rhee, E., and Hinnebusch, A.G. (1998). yTAFII61 has a general role in RNA polymerase II transcription and is required by Gcn4p to recruit the SAGA coactivator complex. Molecular Cell *2*, 683-692.

Nelson, C., Goto, S., Lund, K., Hung, W., and Sadowski, I. (2003). Srb10/Cdk8 regulates yeast filamentous growth by phosphorylating the transcription factor Ste12. Nature *421*, 187-190.

Ng, H.H., Robert, F., Young, R.A., and Struhl, K. (2002). Genome-wide location and regulated recruitment of the RSC nucleosome-remodeling complex. Genes & Development *16*, 806-819.

Ng, H.H., Robert, F., Young, R.A., and Struhl, K. (2003). Targeted recruitment of Set1 histone methylase by elongating Pol II provides a localized mark and memory of recent transcriptional activity. Molecular Cell *11*, 709-719.

Nislow, C., Ray, E., and Pillus, L. (1997). SET1, a yeast member of the trithorax family, functions in transcriptional silencing and diverse cellular processes. Molecular Biology of the Cell *8*, 2421-2436.

Palecek, S.P., Parikh, A.S., and Kron, S.J. (2000). Genetic analysis reveals that FLO11 upregulation and cell polarization independently regulate invasive growth in Saccharomyces cerevisiae. Genetics *156*, 1005-1023.

Palecek, S.P., Parikh, A.S., and Kron, S.J. (2002). Sensing, signalling and integrating physical processes during Saccharomyces cerevisiae invasive and filamentous growth. Microbiology *148*, 893-907.

Pan, X., and Heitman, J. (2002). Protein kinase A operates a molecular switch that governs yeast pseudohyphal differentiation. Molecular and Cellular Biology *22*, 3981-3993.

Pokholok, D.K., Harbison, C.T., Levine, S., Cole, M., Hannett, N.M., Lee, T.I., Bell, G.W., Walker, K., Rolfe, P.A., Herbolsheimer, E.*, et al.* (2005). Genome-wide map of nucleosome acetylation and methylation in yeast. Cell *122*, 517-527.

Ricci, A.R., Genereaux, J., and Brandl, C.J. (2002). Components of the SAGA histone acetyltransferase complex are required for repressed transcription of ARG1 in rich medium. Molecular and Cellular Biology *22*, 4033-4042.

Roberts, S.M., and Winston, F. (1997). Essential functional interactions of SAGA, a Saccharomyces cerevisiae complex of Spt, Ada, and Gcn5 proteins, with the Snf/Swi and Srb/mediator complexes. Genetics *147*, 451-465.

Roguev, A., Schaft, D., Shevchenko, A., Pijnappel, W.W., Wilm, M., Aasland, R., and Stewart, A.F. (2001). The Saccharomyces cerevisiae Set1 complex includes an Ash2 homologue and methylates histone 3 lysine 4. The EMBO Journal *20*, 7137-7148.

Rundlett, S.E., Carmen, A.A., Kobayashi, R., Bavykin, S., Turner, B.M., and Grunstein, M. (1996). HDA1 and RPD3 are members of distinct yeast histone deacetylase complexes that regulate silencing and transcription. Proceedings of the National Academy of Sciences of the United States of America *93*, 14503-14508.

Rundlett, S.E., Carmen, A.A., Suka, N., Turner, B.M., and Grunstein, M. (1998). Transcriptional repression by UME6 involves deacetylation of lysine 5 of histone H4 by RPD3. Nature *392*, 831-835.

Rupp, S., Summers, E., Lo, H.J., Madhani, H., and Fink, G. (1999). MAP kinase and cAMP filamentation signaling pathways converge on the unusually large promoter of the yeast FLO11 gene. The EMBO Journal *18*, 1257-1269.

Saleh, A., Lang, V., Cook, R., and Brandl, C.J. (1997). Identification of native complexes containing the yeast coactivator/repressor proteins NGG1/ADA3 and ADA2. The Journal of Biological Chemistry *272*, 5571-5578.

Santos-Rosa, H., Schneider, R., Bannister, A.J., Sherriff, J., Bernstein, B.E., Emre, N.C., Schreiber, S.L., Mellor, J., and Kouzarides, T. (2002). Active genes are tri-methylated at K4 of histone H3. Nature *419*, 407-411.

Schneider, J., Wood, A., Lee, J.S., Schuster, R., Dueker, J., Maguire, C., Swanson, S.K., Florens, L., Washburn, M.P., and Shilatifard, A. (2005). Molecular regulation of histone

H3 trimethylation by COMPASS and the regulation of gene expression. Molecular Cell *19*, 849-856.

Seringhaus, M., Kumar, A., Hartigan, J., Snyder, M., and Gerstein, M. (2006). Genomic analysis of insertion behavior and target specificity of mini-Tn7 and Tn3 transposons in Saccharomyces cerevisiae. Nucleic Acids Research *34*, e57.

Sertil, O., Vemula, A., Salmon, S.L., Morse, R.H., and Lowry, C.V. (2007). Direct role for the Rpd3 complex in transcriptional induction of the anaerobic DAN/TIR genes in yeast. Molecular and Cellular Biology *27*, 2037-2047.

Sharma, V.M., Tomar, R.S., Dempsey, A.E., and Reese, J.C. (2007). Histone deacetylases RPD3 and HOS2 regulate the transcriptional activation of DNA damage-inducible genes. Molecular and Cellular Biology *27*, 3199-3210.

Sikorski, R. S. and Hieter, P. (1989). A system of shuttle vectors and yeast host strains designed for efficient manipulation of DNA in Saccharomyces cerevisiae. Genetics *122*, 19-27.

Song, W., and Carlson, M. (1998). Srb/mediator proteins interact functionally and physically with transcriptional repressor Sfl1. The EMBO Journal *17*, 5757-5765.

Song, W., Treich, I., Qian, N., Kuchin, S., and Carlson, M. (1996). SSN genes that affect transcriptional repression in Saccharomyces cerevisiae encode SIN4, ROX3, and SRB proteins associated with RNA polymerase II. Molecular and Cellular Biology *16*, 115-120.

Sterner, D.E., and Berger, S.L. (2000). Acetylation of histones and transcription-related factors. Microbiol Mol Biol Rev *64*, 435-459.

Stillman, D.J., Dorland, S., and Yu, Y. (1994). Epistasis analysis of suppressor mutations that allow HO expression in the absence of the yeast SW15 transcriptional activator. Genetics *136*, 781-788.

Sudarsanam, P., Cao, Y., Wu, L., Laurent, B.C., and Winston, F. (1999). The nucleosome remodeling complex, Snf/Swi, is required for the maintenance of transcription in vivo and is partially redundant with the histone acetyltransferase, Gcn5. The EMBO Journal *18*, 3101-3106.

Tompa, R., and Madhani, H.D. (2007). Histone H3 lysine 36 methylation antagonizes silencing in Saccharomyces cerevisiae independently of the Rpd3S histone deacetylase complex. Genetics *175*, 585-593.

Utley, R.T., Ikeda, K., Grant, P.A., Cote, J., Steger, D.J., Eberharter, A., John, S., and Workman, J.L. (1998). Transcriptional activators direct histone acetyltransferase complexes to nucleosomes. Nature *394*, 498-502.

Verdin, E., Dequiedt, F., and Kasler, H.G. (2003). Class II histone deacetylases: versatile regulators. Trends Genet *19*, 286-293.

Vidal, M., and Gaber, R.F. (1991). RPD3 encodes a second factor required to achieve maximum positive and negative transcriptional states in Saccharomyces cerevisiae. Molecular and Cellular Biology *11*, 6317-6327.

Vidal, M., Strich, R., Esposito, R.E., and Gaber, R.F. (1991). RPD1 (SIN3/UME4) is required for maximal activation and repression of diverse yeast genes. Molecular and Cellular Biology *11*, 6306-6316.

Wallberg, A.E., Neely, K.E., Gustafsson, J.A., Workman, J.L., Wright, A.P., and Grant, P.A. (1999). Histone acetyltransferase complexes can mediate transcriptional activation by the major glucocorticoid receptor activation domain. Molecular and Cellular Biology *19*, 5952-5959.

Winston, F., and Allis, C.D. (1999). The bromodomain: a chromatin-targeting module? Nature Structural Biology *6*, 601-604.

Winzeler, E.A., Shoemaker, D.D., Astromoff, A., Liang, H., Anderson, K., Andre, B., Bangham, R., Benito, R., Boeke, J.D., Bussey, H.*, et al.* (1999). Functional characterization of the S. cerevisiae genome by gene deletion and parallel analysis. Science *285*, 901-906.

Xin, X., Lan, C., Lee, H.C., and Zhang, L. (2007). Regulation of the HAP1 gene involves positive actions of histone deacetylases. Biochemical and Biophysical Research Communications *362*, 120-125.

Yang, X.J., and Seto, E. (2008). The Rpd3/Hda1 family of lysine deacetylases: from bacteria and yeast to mice and men. Nature Reviews *9*, 206-218.

Yu, Y., Eriksson, P., and Stillman, D.J. (2000). Architectural transcription factors and the SAGA complex function in parallel pathways to activate transcription. Molecular and Cellular Biology *20*, 2350-2357.

Zhang, Z.K., Davies, K.P., Allen, J., Zhu, L., Pestell, R.G., Zagzag, D., and Kalpana, G.V. (2002). Cell cycle arrest and repression of cyclin D1 transcription by INI1/hSNF5. Molecular and Cellular Biology *22*, 5975-5988.

Chapter 4

The Generation of Cell-Surface Diversity in Yeast by Rpd3L- and Sfl1-Regulated Noncoding RNAs

Abstract | Histone deacetylases are generally considered repressors of transcription due to their ability to stimulate the condensation of chromatin structure by modifying histones. In the yeast *Saccharomyces cerevisiae,* however, the histone deacetylase complex Rpd3L, which is known to act as a repressor of transcription at some target promoters, plays an apparently direct role in activating transcription elsewhere in the genome. In this chapter, I argue that this seemingly paradoxical observation points to the existence of an additional mechanism of transcriptional regulation at work for some protein-encoding genes: the chromatin-regulated transcription of noncoding RNAs from within the promoters of these genes. We have found that net activation of *FLO11* transcription by Rpd3L results from Rpd3L-mediated repression of a noncoding RNA *ICR1* (Interfering Crick RNA) that initiates within and is transcribed in the Crick direction through most of the *FLO11* promoter region. In the absence of Rpd3L function, increased levels of *ICR1* transcript correlate with decreased *FLO11* expression, loss of TATA binding protein (TBP) binding, and decreased nucleosome ejection from the core promoter of *FLO11*. These findings suggest that transcription of *ICR1* interferes with binding of basal transcription machinery and chromatin remodelers that promote transcription initiation at the *FLO11* core promoter. A transcription terminator that disrupts *ICR1* results in recovery of *FLO11* expression in an Rpd3L$^-$ null mutant. The direct role of Rpd3L at the *FLO11* locus is repression of *ICR1*, which itself negatively regulates *FLO11* expression. Thus, the net effect of Rpd3L on *FLO11* expression is positive. We have also detected a second noncoding RNA, *PWR1* (Promoting Watson RNA), that initiates within the *FLO11* promoter and is transcribed in the Watson direction convergently and overlapping with the *ICR1* transcript. Transcription of *PWR1* is repressed by Sfll1, a transcriptional repressor of *FLO11*. When *SFL1* is deleted, elevated levels of *PWR1* transcript correlate with increased *FLO11* expression. I hypothesize that *PWR1* promotes *FLO11* expression by competing with *ICR1* for its

template region, thereby preventing *ICR1* transcription from proceeding along the *FLO11* promoter region. Our data suggest that the well established role of Sfl1 in repression of *FLO11* expression is an indirect effect of its role in regulating *PWR1* transcription. Our findings also point to a new model for the mechanism underlying transcriptional variegation of *FLO* genes. This model involves regulatory noncoding RNAs, bistable changes in local chromatin structure resulting from recruitment of histone deacetylases, and competitive binding to DNA by proteins that determine whether histone deacetylases are present or absent at local regions within the *FLO* promoters.

INTRODUCTION

In his principles for sound scientific reasoning, Sir Isaac Newton advised fellow scientists to propose no more causes of natural things than are both "true and sufficient" to explain their appearances (Newton, 1687). This rule of parsimony proves very useful in guiding the formation of scientific hypotheses. But the most parsimonious hypotheses regarding the relationship between chromatin structure and transcription have in recent years fallen short of explaining the entire set of observed phenomena. The canon that histone deacetylases repress transcription owing to their ability to catalyze the condensation of chromatin structure has been called into question by observations that these enzymes also appear to play a direct role in activating transcription at some loci. In particular, the yeast Rpd3L histone deacetylase complex, which has been soundly demonstrated to repress transcription at many target promoters, has recently been shown to play an apparently direct role in activating transcription at other target promoters (Carrozza et al., 2005; Kadosh and Struhl, 1997, 1998; Rundlett et al., 1998; Sertil et al., 2007; Sharma et al., 2007; Xin et al., 2007; De Nadal et al., 2004), thus raising an apparent paradox regarding the effect of histone deacetylase function on transcription. In

this chapter, I explore a resolution to this apparent paradox and propose that there is an additional "cause" at work that explains these apparently contradictory appearances regarding Rpd3L function.

Within clonal populations of *Saccharomyces cerevisiae* Sigma 1278b, some cells exhibit active transcription of *FLO11* whereas other cells in the same population are silenced at the *FLO11* promoter (Halme et al., 2004). A similar phenomenon is observed at the *FLO10* promoter (Halme et al., 2004) in this yeast. We have previously reported that this variegated silencing of *FLO* gene expression is directly dependent on the activity of histone deacetylases. Hda1 functions in the epigenetic silencing of both the *FLO11* and the *FLO10* promoters (Halme et al., 2004). Hst1 and Hst2 also function in the epigenetic silencing of the *FLO10* promoter (Halme et al., 2004). Deletion of any of these histone deacetylases results in a loss of silencing of the *FLO* promoter(s) under their control (Halme et al., 2004). Thus, Hda1, Hst1, and Hst2 each plays the expected role for a histone deacetylase in regulating gene expression: repression of transcription.

In a screen conducted to identify transcriptional regulators of the variegating *FLO* gene family in *S. cerevisiae*, I found that the Rpd3L histone deacetylase complex is a strong transcriptional activator, rather than a transcriptional repressor, of *FLO* gene expression. In the absence of Rpd3L function, a clonal population of Sigma 1278b yeast cells is pushed into a more silenced state at the *FLO11* and *FLO10* promoters. This reduction of *FLO11* promoter activity in Rpd3L$^-$ mutants has phenotypic effects, including total loss of the ability of diploids to initiate pseudohyphal growth under appropriate stress conditions and the loss of the ability of haploids to adhere to and invade inert surfaces (discussed in Chapter 3). Specific disruption of the alternative

Rpd3-containing histone deacetylase complex in yeast, Rpd3S (Carrozza et al., 2005a; Carrozza et al., 2005b), had no effect on expression of *FLO* genes, indicating a specific role for the Rpd3L complex in this process.

My finding that loss of Rpd3L function results in decreased *FLO* transcription is seemingly at odds with reports supporting a role for Rpd3L as a transcriptional repressor at many target promoters in the yeast genome. The catalytic component of the Rpd3L histone deacetylase complex, Rpd3 itself, was originally discovered as a transcriptional repressor of genes involved in a diverse set of biological processes including meiosis, cell-type specificity, potassium transport, phosphate metabolism, methionine biosynthesis, and phospholipids metabolism (Hepworth et al., 1998; Jackson and Lopes, 1996; Kadosh and Struhl, 1997; McKenzie et al., 1993; Stillman et al., 1994; Vidal and Gaber, 1991; Vidal et al., 1991).

Despite these many reports that Rpd3L functions as a transcriptional repressor, my finding that Rpd3L also has an important role in activating transcription adds the *FLO* genes to a growing list of stress-responsive genes that have been shown to be transcriptionally activated by this histone deacetylase complex. In recent years, the Rpd3L complex has been reported to play apparently direct roles in transcriptional activation at several target promoters within the yeast genome. The *DAN/TIR* genes induced during anaerobic growth (Sertil et al., 2007), the DNA damage-inducible gene *RNR3* (Sharma et al., 2007), the *HAP1* gene which encodes a transcription factor involved in oxygen and heme regulation (Xin et al., 2007), and osmoresponsive genes such as *HSP12* (De Nadal et al., 2004) are all transcriptionally activated by Rpd3 localizing to their promoters. Epitope-tagged Rpd3 or epitope-tagged Sin3 (a subunit

specific to the Rpd3L complex) have been shown to localize to the promoters of *RNR3* and *HSP12* by chromatin immunoprecipitation (ChIP), suggesting a *direct* role for Rpd3 in activating transcription of these genes (De Nadal et al., 2004; Sharma et al., 2007). Furthermore, Rpd3-mediated histone *de*acetylation accompanies transcriptional activation at *DAN4* (Sertil et al., 2007), *RNR3* (Sharma et al., 2007), and *HSP12* (De Nadal et al., 2004), suggesting a mechanism of transcriptional activation by Rpd3 that is in apparent conflict with the general rules of chromatin structure-mediated transcriptional regulation and the predictions of an elegant "histone code" hypothesis (Grunstein, 1997; Sertil et al., 2007; Sharma et al., 2007; De Nadal et al., 2004; Jenuwein and Allis, 2001; Taverna et al., 2007).

I argue that this apparent paradox in Rpd3L function reflects a fundamental mechanism in transcriptional regulation that has until very recently remained underappreciated, especially where the yeast *Saccharomyces cerevisiae* is concerned. This mechanism is the transcriptional regulation of protein-coding genes by noncoding RNAs located within their promoters, and I propose this mechanism as a "cause" to explain the apparent paradox regarding Rpd3L function.

S. cerevisiae, which lacks key components of the conserved machinery required for RNAi-mediated regulation of gene expression, was long thought to lack mechanisms of transcriptional regulation involving noncoding RNAs. Over the past few years, however, a flurry of publications has reported various examples of noncoding RNAs that regulate transcription in yeast (Camblong et al., 2007; Hongay et al., 2006; Martens et al., 2004; Martens et al., 2005; Uhler et al., 2007). The reported mechanisms do not require the RNAi machinery. Rather, noncoding RNAs are shown to regulate transcription in *cis*

by mechanisms that include (i) remodeling chromatin structure, (ii) competing for template sequence by running antisense into the transcript that they regulate, and (iii) occluding transcription factor binding sites within promoters by the act of transcription itself (Berretta et al., 2008; Camblong et al., 2007; Hongay et al., 2006; Martens et al., 2004; Martens et al., 2005).

The mechanism by which the yeast *SER3* gene is repressed during growth in rich media (Martens et al., 2004; Martens et al., 2005) is of particular interest with respect to the work I present in this chapter, because the regulatory mechanism observed at *SER3* seems most closely to resemble the regulatory mechanism that we observe at the *FLO11* locus. During growth in rich media, a noncoding RNA is transcribed from within the promoter sequence of *SER3*. This noncoding RNA, called *SRG1*, is required for repression of *SER3*. The *SRG1* transcript is transcribed by RNA polymerase II promoted by a canonical TATA box sequence located upstream in the *SER3* promoter. *SRG1* terminates just upstream of the *SER3* ORF. When *SRG1* is transcribed, binding of transcriptional activators, such as RNA polymerase II, is reduced at the *SER3* core promoter. Thus, this example of noncoding RNA-mediated repression seems to occur by a regulated transcription-interference mechanism in which transcription across the *SER3* promoter interferes with the binding of transcriptional activators to core promoter elements.

In this chapter, I show by chromatin immunoprecipitation that Rpd3L associates directly with the promoter of *FLO11*, suggesting that Rpd3L's role in activating *FLO11* expression is a direct effect of its localization to the *FLO11* locus. Furthermore, whole-genome expression assays comparing mRNA levels in wild type versus an Rpd3L$^-$

mutant did not reveal differential expression of known transcriptional regulators of *FLO11*, again supporting a direct role for Rpd3L in regulating *FLO11* expression.

I propose that Rpd3L's role as an activator of *FLO11* expression is an indirect effect of its chromatin-mediated transcriptional repression of a noncoding RNA transcribed from a region upstream of the *FLO11* ORF. We have identified a noncoding RNA transcript, *ICR1* (for Interfering Crick RNA), that initiates within and is transcribed through most of the length of the *FLO11* promoter region (Figure 1). When components of the Rpd3L histone deacetylase complex are deleted, we find that the resulting elevation in steady-state levels of the *ICR1* transcript correlates with loss of *FLO11* expression, loss of TATA binding protein (TBP) association at the core promoter of *FLO11*, and decreased nucleosome ejection from the core promoter of *FLO11*. These findings suggest that transcription of *ICR1* somehow interferes with the binding of basal transcription machinery and chromatin remodelers that promote transcription initiation at the core promoter of *FLO11*. Thus, *ICR1* inhibits expression of *FLO11*. A transcription terminator placed within *ICR1* results in the recovery of *FLO11*-dependent phenotypes in an Rpd3L$^-$ mutant, suggesting a causal role for the *ICR1* transcript in inhibiting *FLO11* expression. I conclude that, although the indirect effect of Rpd3L histone deacetylase activity is the activation of *FLO11* expression, its local direct effect on transcription of the regulatory noncoding RNA *ICR1* is repressive, thus resolving the apparent paradox regarding Rpd3L function.

The DNA-binding protein Sfl1 is a well documented repressor of *FLO* gene transcription. Sf11 has been shown to interact directly with the *FLO11* promoter, and the Sfl1 binding region has been narrowed to a 250-bp window located between -1400 and

-1150 relative to the *FLO11* ORF (Pan and Heitman, 2002 and Figure 1). Studies of the *FLO11*-like *STA1* promoter in the yeast *S. diastaticus* have confirmed Sfl1 binding in this region, which is contained within the UAS2 element of *FLO11* promoter (Kim et al., 2004a; Kim et al., 2004b). This is also the region of the *FLO11* promoter reported to be bound competitively by the transcriptional activator of *FLO11*, Flo8 (Pan and Heitman, 2002 and Figure 1). At the *STA1* promoter, however, Sfl1 reportedly competes with the transcriptional activators Ste12 and Tec1 for binding to the UAS2 element, and Flo8 reportedly binds to the UAS1 element located further upstream (-1760 to -2175 relative to the *FLO11* ORF) (Kim et al., 2004a; Kim et al., 2004b; Figure 1). We and others have previously reported that Sfl1 is important for the recruitment of histone deacetylases, such as Hda1, Hst1, and Hst2, to target promoters in yeast (Halme et al., 2004; Conlan and Tzamarias, 2001; Davie et al., 2003; Figure 1). Consequently, the transcriptional repression of *FLO* genes by Sfl1 proceeds, at least in part, by chromatin-mediated mechanism.

In this chapter, I report our discovery of a new component in the mechanism through which Sfl1 mediates transcriptional repression of *FLO11*. We have identified a second regulatory noncoding RNA transcript, *PWR1* (for Promoting Watson RNA), that also initiates within the *FLO11* promoter and is transcribed in the Watson direction convergently and overlapping with the *ICR1* transcript (Figure 1). Transcription of *PWR1* is repressed by the DNA-binding protein Sfl11. When *SFL1* is deleted, elevated steady-state levels of the *PWR1* transcript correlate with increased *FLO11* expression. I hypothesize that *PWR1* promotes *FLO11* expression by competing with *ICR1* for its template region and preventing *ICR1* transcription from proceeding along the length of

the *FLO11* promoter, thereby inhibiting the *ICR1*-mediated transcriptional repression of *FLO11* expression. The findings I report here suggest that the long-known role of Sfl1 in repression of *FLO11* expression may be an indirect effect of its repression of *PWR1* transcription.

I also report in this chapter that we have discovered a similar pair of convergent, overlapping noncoding transcripts initiating within the *FLO10* promoter. This finding suggests that transcriptional regulation by noncoding RNAs may be a mechanism that extends to other members of the variegating *FLO* gene family, and perhaps to other genes that exhibit net-positive transcriptional regulation by Rpd3L.

Our findings also point to a new model for the mechanism underlying transcriptional variegation of *FLO* genes that I will present at the end of this chapter. This model involves regulatory noncoding RNAs, bistable changes in local chromatin structure resulting from recruitment of histone deacetylases, and competitive binding to DNA by proteins, such as Sfl1 and Flo8, that may determine whether histone deacetylases are present or absent at local regions within *FLO* promoters.

Materials and Methods

Strains, media, microbiological techniques and growth conditions | Yeast strains utilized in these studies are listed in Table 1 of this chapter. All strains were derived from the Σ1278b genetic background (also known as MB1000 (Brandriss and Magasanik, 1979; Grenson et al., 1966) and MB758-5B (Siddiqui and Brandriss, 1988)). Standard yeast media, yeast transformations and genetic manipulations were performed as described in Guthrie and Fink (2001). For analysis of P_{FLO10}-*URA3* or P_{FLO11}-*URA3*,

strains were grown overnight in YPD liquid media, then diluted 1:50 in YPD liquid media and grown to OD_{600} 0.8-1.2 at 30 degrees C. Cell densities were adjusted to OD_{600} 1, then cultures were serially diluted (10-fold dilutions for P_{FLO10}-*URA3* stains and 2-fold or 5-fold dilutions for P_{FLO11}-*URA3* strains) and plated on synthetic complete (SC), SC-Ura, and SC+5-FOA (0.1%) agar plates. For visualization of P_{FLO10}-*GFP* or P_{FLO11}-*GFP* by fluorescent microscopy or FACS, cells were streaked onto YPD plates and harvested after one day of growth at 30 degrees C. Haploid adhesion assays were performed as described (Guo et al., 2000). For northern analysis, real time PCR analysis, chromatin immunoprecipitation, RACE, and microarray expression analysis, cells were grown overnight in YPD liquid media, diluted 1:50 into 50 ml liquid YPD media, grown to OD_{600} 0.8-1.2, and then harvested for use in the experiments.

Yeast strain construction | Yeast strains carrying gene deletions were constructed by PCR amplification of a P_{TEF} promoter-driven yeast *LEU2* or bacterial kanamycin-resistance gene (Longtine et al., 1998) with flanking sequences that would direct the deletion cassette to the appropriate locus via homologous recombination. All deletions remove the full ORF (ATG to Stop codon).

To generate the Rpd3-Myc strains, an 18-Myc epitope-tagged allele was generated through homologous integration of a *TRP1*-tagged 18-*MYC* epitope into the carboxy terminus coding region of the *RPD3* gene. The Rpd3-18-Myc protein is functional, as assessed by YPD-agar adhesion tests and in tests of *FLO11* promoter activity by serial dilutions onto SC–Ura and SC+5-FOA selection media of strains carrying both the epitope-tagged Rpd3 allele and the P_{FLO11}-*URA3* construct.

The *K. lactis URA3-terminator* construct was generated by PCR amplification of this reporter gene with its endogenous promoter and terminator from plasmid pUG72 template (Gueldener et al., 2002) with homologous flanking sequence to the target site 3041 basepairs upstream of the *FLO11* ORF, within the *FLO11* promoter region.

Plasmids used in this study are listed in Table 2. Table 3 provides a list of oligonucleotide primers used in this study.

Poly-A RNA Purification | Total RNA was obtained by standard acid phenol extraction from 10 ml aliquots of 50 ml YPD cultures grown to OD_{600} 0.8-1.2, then harvested. Poly-A RNA was purified from the total RNA using oligo-dT cellulose columns from MRC, Inc. The RNA was diluted into lithium chloride binding buffer to a final concentration of 1 mg/ml, incubated for 5 minutes at 70 degrees to remove secondary structure, and then loaded onto an oligo-dT column that had been pre-washed with binding buffer. Columns were washed and poly-A RNA was eluted and precipitated with lithium chloride and polyacryl carrier plus one volume of isopropanol. After centrifugation and washing with 70% ethanol, the RNA pellets were dried briefly and then resuspended in DEPC-treated water. RNA concentrations were determined by OD 260/280 spectrophotometry.

Northern Blot Analysis | For the northern blot shown in Figure 2, total RNA was DNase-treated to remove any residual genomic DNA and 10 ug of this DNase-treated RNA were loaded per sample. For all other northern blots, Poly-A RNA was purified from total RNA and 3ug of this Poly-A RNA were loaded per sample. RNA samples were run on formaldehyde-agarose denaturing gels at 100 volts for four to six hours. The

electrophoresed RNA was transferred to Hybond-N nylon membranes using 20X SSC buffer. After UV cross-linking, these membranes were hybridized with ^{32}P (exo-) Kleenow-labeled DNA probes (for the northern blot in Figure 1 and for all *SCR1* load controls) or ^{32}P-labeled strand-specific RNA probes generated using the Ambion T7 Maxiscript Kit (for all other northern hybridizations). Hybridizations were performed at 65 degrees C overnight in sodium phosphate buffer containing 7% SDS and 1% BSA. Membranes were washed three times at 65 degrees C for 20-30 minutes with 0.2X SSC, 0.1% SDS and exposed on a phosphoimager screen. Before hybridizing the membranes with *SCR1* load control probes, the original radioactive probe was twice stripped from the membranes by pouring boiling 0.1% SDS onto them and rocking them at room temperature in this solution for 30 minutes.

Microarray Design | Custom microarrays were designed and used in the ChIP-chip and whole genome expression assays. Sigma 1278b genomic probes were designed to be as unique as possible across the Sigma 1278b genome and to avoid repetitive or low complexity sequences. Potential probes were assigned a score that reflected how well the probe's predicted melting temperature (Tm) matched the target Tm, a measure of sequence complexity, and the ratio of the intensities expected by the intended match relative to unintended matches. Probes were then selected for inclusion on the array by balancing their score with the probe's distance to the previous probe, attempting to achieve the target average probe spacing of 25 basepairs. The resulting two array set was utilized for expression analysis. A one array design, used for Chip-chip analysis, was generated by dropping every other probe from the set, resulting in probes spaced

approximately 50 basepairs apart. For both designs, strand specificity is obtained by utilizing the reverse complement of every other probe on the array.

Chromatin Immunoprecipitations | Protocols describing all materials and methods have been previously described (Lee et al., 2006). Briefly, 50 ml cultures of cells were grown in YPD liquid to an OD_{600} of 0.8 - 1. Cells were chemically crosslinked for 30 minutes at room temperature by the addition of formaldehyde to a final concentration of 1%. Cells were washed with PBS, harvested, and flash frozen in liquid nitrogen.

Cells were resuspended, lysed in lysis buffers, and sonicated to solubilize and shear crosslinked DNA. An aliquot of whole cell extract (WCE) was reserved as a control for input. 500 ul of WCE from each sample were incubated overnight at 4 degrees C with Dynal Protein G magnetic beads that had been preincubated with antibodies against the Myc-epitope (Covance 9E-11 MMS-164P), the histone H4-pan (Upstate Millipore 05-858), or yeast TBP (Santa Cruz SC-33736). Beads and immunoprecipitated chromatin were washed according to protocol. The chromatin was eluted from the magnetic beads. The crosslinks were reversed for both the immunoprecipitated chromatin samples (IPs) and the control WCE samples. IPs and WCEs were purified by phenol-chloroform extraction and were ethanol precipitated.

Enriched chromatin IPs and WCEs were analyzed using either gene-specific or genome-wide approaches. For gene-specific ChiP, SYBR Green Real Time PCR (Applied Biosystems) reactions were performed on the IP and WCE (input) templates, using gene-specific primers that amplified specific regions of the *FLO11* promoter or other control regions in the yeast genome. For genome-wide ChIP, Cy-5 labeled

immunoprecipitated chromatin and Cy-3 labeled WCE samples were assayed using *S. cerevisiae* Sigma 1278b custom genomic tiling microarrays (Agilent, one-array set with 50 bp probe spacing). Cy-labeling of samples was achieved by treatment with T4 DNA polymerase to generate blunt ends, followed by ligation to annealed JW102/103 primers by overnight incubation with T4 DNA ligase. Ligation-mediated PCR was performed using either Cy-3 or Cy-5 dyes. The amount of incorporated dye was quantified and equal amounts were hybridized to arrays for 42-to-60 hours at 65 degrees C. Arrays were washed and scanned with an Agilent scanner. Array data was normalized using a three step process. First, cross talk normalization provided coefficients for Cy5->Cy3 and Cy3->Cy5 to generate corrected intensities for each channel. The resulting values were then median normalized. The final step of the normalization procedure assumes Cy3=Cy5 is a good fit for the data and transforms the data accordingly. The joint binding deconvolution (JBD) algorithm was utilized on the normalized data to identify binding events (Qi et. al., 2006).

Whole genome expression analysis | Poly-A RNA was treated with DNase I. Cy-3 or Cy-5 labeled cDNA was generated using Superscript II reverse transcriptase, which generates single-stranded DNAs complementary to the RNA templates. Cy-5 labeled and Cy-3 labeled cDNA was hybridized at 65 degrees C for ~16 hours to *S. cerevisiae* Sigma 1278b custom genomic tiling microarrays (Agilent, two-array set with 25 bp probe spacing). Arrays were then washed according to standard protocol and scanned with an Agilent scanner. The expression values were normalized using a three step process. First, cross talk normalization provided coefficients for Cy5->Cy3 and Cy3->Cy5 to generate corrected intensities for each channel. The resulting values were then median

normalized. The final step of the normalization procedure assumes Cy3=Cy5 is a good fit for the data and transforms the data accordingly. Differential expression between samples on the same array was determined by the difference in median intensity of the probes that cover a given transcript.

RNA Analysis by Real Time PCR | Total RNA was obtained by standard acid phenol extraction from 10 ml aliquots of 50 ml YPD cultures grown to OD_{600} 0.8-1.2, then harvested. The Qiagen QuantiTect Reverse Transcription Kit was used to remove any residual genomic DNA and to reverse transcribe the RNA templates to generate cDNAs. Aliquots of cDNA were used in Real Time PCR analyses with reagents from Applied Biosystems and the ABI 7500 real-time PCR system. Normalization was to *SCR1*, a gene transcribed by RNA polymerase III.

Rapid Amplification of cDNA Ends (RACE) | Mapping of 5′ and 3′ ends of Poly-A RNA was carried out using the GeneRacer Kit from Invitrogen. Total RNA was purified using standard acid phenol extraction from cultures harvested at OD_{600} 0.8-1.2. The RNA was then treated with calf intestinal phosphatase to remove 5′ phosphates from non-mRNAs and truncated mRNAs, and was then treated with tobacco acid pyrophosphatase to decap the full length mRNA. GeneRacer RNA Oligo was ligated to the RNA and RACE PCR was performed using either (1) the GeneRacer 5′ primer and a reverse primer specific to the target RNA to clone the 5′ end of the transcript or (2) the GeneRacer 3′ primer and a forward primer specific to the target RNA to clone the 3′ end of the transcript. This treatment was sufficient to obtain a clean band for the 3′ end of the *ICR1* noncoding transcript. However an additional round of PCR using

GenerRacer nested primers and a second target-specific primer nested internal to the first amplified region was required to obtain the 5′ end of *ICR1* and both the 5′ and 3′ ends of the *PWR1* noncoding transcript. The target-specific primer sequences used in these assays are included in Table 3. The RACE products were cloned into pCR 4-TOPO plasmids and were transformed into One Shot Top 10 chemically competent *E. coli* cells. Plasmid DNA was purified from individual clones and sequenced to obtain the 5′ and 3′ ends of the target RNAs.

TATA Box Search | We scanned the *FLO11* promoter sequence using the yeast TATA motif from Transfac v9.4 (Motif # 713) to identify putative TATA box locations (Matys et al., 2003). Each position of the sequence was scored on both the forward and reverse strands. We used a threshold of 60% of the maximum positive score (MacIsaac et al., 2006).

RESULTS

The Rpd3L complex has a net activating effect on *FLO* promoter activity | Mutants with defects in the Rpd3L complex have a net silencing effect on *FLO11*. In populations of Sigma 1278b cells, more cells within the population are silenced at the *FLO11* promoter when components of the Rpd3L histone deacetylase complex are disrupted compared to the number of silenced cells observed in variegating wild type populations. Mutation in RpdL subunits Rpd3, Cti6, Pho23, or Rxt2 result in significantly reduced transcription from the *FLO11* promoter, as visualized by promoter fusions to the reporter genes *GFP* or *URA3* at the endogenous *FLO11* locus (Chapter 3 of this thesis and Figure

2 of this chapter). Similar phenotypes are observed at the *FLO10* promoter (Chapter 3 of this thesis). Deletion of *eaf3*, a subunit specific to the alternative Rpd3-containing histone deacetylase complex Rpd3S had no effect on *FLO11* expression in variegating populations of cells, indicating a specific role for the Rpd3L complex in this process (Chapter 3 and Figure 2D). For the remainder of this chapter, the *cti6* mutant, which is specific to the Rpd3L complex, is used to examine the role of Rpd3L in regulating *FLO* gene expression. In contrast to the effects of Rpd3L disruption, deletion of the gene-specific DNA binding protein Sfl1 or the histone deacetylase Hda1 disrupts the epigenetic silencing of *FLO11* such that all cells within the population exhibit a transcriptionally active *FLO11* promoter (Halme, et al., 2004 and Figure 2E). Taken together, these results demonstrate a net activating effect on transcription from the *FLO11* promoter by the Rpd3L histone deacetylase complex, in contrast to the net repressive effect on transcription from the *FLO11* promoter by Sfl1 and Hda1.

The effects on transcription observed with the *URA3* and *GFP* reporter constructs driven by the *FLO11* promoter are reinforced by direct measurements of *FLO11* mRNA levels (Figure 3). Northern blot analysis using a ^{32}P labeled DNA probe specific to a region near the 3' end of the *FLO11* ORF (bp +3502 to 4093) shows that, relative to wild type levels, *FLO11* RNA is more than five-fold reduced in the *cti6* mutant but, as expected, is upregulated in the *sfl1* mutant.

Changes in *FLO11* mRNA levels result in morphological and developmental phenotypes in the *cti6* and *sfl1* mutants. The *cti6* mutant has lost the *FLO11*-dependent abilities to adhere to and invade inert surfaces and to undergo the developmental switch to pseudohyphal growth under conditions of nitrogen starvation (Chapter 3 of this thesis).

The *sfl1* mutation, on the other hand, results in enhanced *FLO11*-dependent phenotypes, owing to the desilencing of the *FLO11* promoter. Colonies of *sfl1* cells have a wrinkled morphology, an enhanced adhesion to inert surfaces, and a hyperfilamentous phenoytype under appropriate inducing conditions (Chapter 3 of this thesis; Pan and Heitman, 2002).

Rpd3 localizes to the *FLO11* promoter | To determine whether the role of Rpd3L in regulating *FLO11* promoter activity is due to a direct or indirect effect of its histone deacetylase function, we used both gene-specific and whole-genome microarray-based chromatin immunoprecipitation (ChIP) assays to determine whether the catalytic component of the Rpd3L complex, Rpd3 itself, localizes to the *FLO11* promoter. An 18-Myc epitope-tagged allele was generated through homologous integration of a *TRP1*-tagged 18-*MYC* epitope into the carboxy terminus coding region of the *RPD3* gene. The Rpd3-18-Myc protein is functional as assessed by YPD-agar adhesion tests and in tests of *FLO11* promoter activity by serial dilutions onto –Ura and 5-FOA selection media of strains carrying both the epitope-tagged Rpd3 allele and the P_{FLO11}-*URA3* construct (Supplemental Figure 1). Immunoprecipitation of Rpd3-associated chromatin was performed using anti-Myc antibodies on whole cell extracts (WCEs) obtained from strains carrying either the Myc-tagged or the untagged allele (negative control).

In the gene-specific ChIP assays, immunoprecipitated chromatin and WCEs (input) were analyzed by real-time PCR using primers specific to the *FLO11* promoter. We observed enrichment of *FLO11* promoter chromatin in the immunoprecipitated samples (Figure 4A and 4B). Enrichment of Rpd3-Myc at the *FLO11* promoter was even greater than that detected at the *INO1* promoter, where enrichment of Rpd3 has been previously shown (Robert et al., 2004; Figure 4A and 4B). Rpd3-Myc is enriched at the

FLO11 promoter more than four-fold over the unbound genes, *APL2* and *ARG2*, identified in whole genome Rpd3 binding studies (Figure 4A). Whole-genome microarray-based chromatin immunoprecipitation (ChIP-chip) results corroborate the gene-specific ChIP results, identifying a region of Rpd3-localization to the *FLO11* promoter located at approximately -1250 and another located at approximately -2850 relative to the beginning of the *FLO11* ORF (Figure 4C).

Rpd3L does not indirectly regulate *FLO11* transcription through known regulators | Because Rpd3L is a histone deacetylase complex, we expect it to behave as a transcriptional repressor owing to its catalytic ability to condense chromatin structure by removing acetyl marks on nucleosomal histones (Kadosh and Struhl, 1998). Our Rpd3 localization data, however, suggests a direct role for Rpd3L in activating *FLO11* transcription. As a further test to check whether loss of *FLO11* expression in the *cti6* mutant could be an indirect result of Rpd3L-mediated repression of a transcriptional activator of *FLO11* transcription, we conducted whole genome poly-A RNA expression analysis using Sigma 1278b genomic high-density tiled microarrays.

The first set of arrays compares expression in wild type cells to expression in the *cti6* mutant cells. We compared the list of differentially expressed genes from the array data to a list of 75 published (confirmed or putative) regulators of *FLO* gene transcription compiled from the literature ((Cullen et al., 2004; Gancedo, 2001; Halme et al., 2004; Kim et al., 2004a; Kim et al., 2004b; Palecek et al., 2002; Pan and Heitman, 2002; Rupp et al., 1999) and Supplemental Table 1). Only one gene from the list of published regulators appears in the group of differentially expressed genes from this set of arrays: *MSB2* just makes the cutoff for being significantly downregulated in *cti6* relative to wild

type (Figure 5A and Table 4). *MSB2* encodes a cell-surface signaling mucin reported to promote the filamentation MAP kinase pathway (Cullen et al., 2004). In the second set of arrays, we compared expression in the *cti6* mutant to expression in the *sfl1* mutant. Since *FLO11* expression is variegated within a wild type population of cells and the arrays offer a glimpse only at the average expression profile across the entire population, the measurement of transcription in this mixed population is not maximally informative. However, comparing a mutant (*cti6*) that is shifted into a more silent promoter state to a mutant that is more desilenced at *FLO11* (*sfl1*) could reveal differences. None of the 75 published *FLO11* regulators was differentially expressed in these array data (Figure 5B and Table 4). The *MSB2* result was not reproduced in these data (Figure 5B and Table 4). *SFL1* itself appears as an artifact of experimental design on the list of differentially expressed genes in the *cti6* versus *sfl1* mutant comparison because it is deleted in the *sfl1* strain and is therefore not expressed (Figure 5B and Table 4).

Interestingly, the most downregulated gene in *cti6* compared to wild type is *FLO11* itself, confirming that the Rpd3L histone deacetylase complex plays a very important role in activating *FLO11* expression (Figure 5A and Table 4). In the *cti6* versus *sfl1* mutant comparison, the most differentially expressed gene is *FLO10*, followed by *FLO11* (Figure 5B and Table 4). Both genes are downregulated in the *cti6* mutant compared to the *sfl1* mutant. The enrichment of *FLO* genes ("mannose binding") among the differentially expressed genes in the *cti6* versus *sfl1* mutant comparison is significant (p = 1.27e-05) according to GO enrichment analysis (Table 5).

The Rpd3L$^-$ mutant *cti6* has elevated levels of noncoding transcription in the *FLO11* promoter region | We speculated that *FLO11* expression could be regulated by an

Rpd3L-repressed noncoding transcript, similar to *SRG1*-regulation of *SER3* expression in yeast (Martens et al., 2004; Martens et al., 2005). To test this hypothesis, we isolated RNA from WT, *cti6*, and *sfl1* strains, reverse transcribed the samples to generate cDNA from each genotype, and assayed for transcripts originating from within the *FLO11* promoter by quantitative real time PCR. We initially used two pairs of real time primers specific the *FLO11* promoter sequence. One pair of primers was designed to detect transcription at a region located -600 from the beginning of the *FLO11* ORF. The other pair of primers was designed to detect transcription at a region located -1300 from the beginning of the *FLO11* ORF. Both sets of primers detected transcription deriving from *FLO11* promoter sequence. The highest steady-state levels of noncoding transcription from within the *FLO11* promoter region were detected in the *cti6* mutant, which is also the most silenced in terms of *FLO11* expression of the three genotypes tested (Figure 6). In the *sfl1* mutant, the level of detected noncoding transcription from within the *FLO11* promoter region was less than half of the amount detected in the *cti6* mutant (Figure 6). In the wild type strain, which exhibits variegated expression of *FLO11* within populations of cells, an intermediate level of these noncoding transcripts deriving from *FLO11* promoter sequence was detected (Figure 6). Rather than an intermediate steady-state level of noncoding transcription in every wild type cell, we suspect that this intermediate level of transcription represents the average level deriving from the *FLO11* promoter region in a variegating population in which transcriptionally silenced cells have higher levels of noncoding transcription from within the *FLO11* promoter region and transcriptionally active cells have little or no noncoding transcription from within the *FLO11* promoter region. Because both sets of primers detected similar transcription

profiles (Figure 6), we conjectured that both sets of primers were detecting a single long transcript that spanned the regions assayed by both primer sets.

To obtain a higher density view of noncoding transcription occurring within the *FLO11* promoter region, we utilized real time primer pairs designed to amplify 100-mer regions tiled every 30 base pairs from +120 inside the *FLO11* ORF to -2280 upstream of the *FLO11* ORF within the *FLO11* promoter region. Because these primers were not optimized, only those that amplified a genomic DNA template with efficiency 1.5 times that of the *SCR1* control primers on the same template were used in the final data analysis. This experiment was repeated several times using independent isolates of RNA from biological replicates of wild type, *cti6*, *sfl1*, and a strain in which the *FLO11* promoter has been deleted (p_{flo11}) to ensure specificity of the signal. Figure 7 shows two representative sets of results. In each experiment conducted, the data indicate that noncoding transcription from the *FLO11* promoter template in the *cti6* mutant is always elevated relative to levels in the *sfl1* mutant. The wild type strain generally exhibits intermediate levels of noncoding transcription from within the *FLO11* promoter region relative to *cti6* and *sfl1*, but also shows more variability, likely owing to variegation of *FLO11* in wild type populations of cells. The *cti6* and *sfl1* mutants, however, show a clear inverse correlation between the amount of noncoding transcription occurring within the *FLO11* promoter and the amount of expression of the *FLO11* ORF itself.

Strand-specific northern blot analyses reveal the ~3.2-kb Crick-strand noncoding RNA *ICR1* transcribed from within the *FLO11* promoter sequence | We performed northern blot analysis using poly-A selected RNA from wild type, *cti6*, *sfl1*, and p_{flo11} cells (Figure 8). For probing, we used ^{32}P-labeled strand-specific RNA probes that

hybridize to three different regions of the *FLO11* promoter sequence. Probes 1, 2, and 3 hybridize to regions located -284 to -819, -1653 to -2255, and -2631 to -3226 relative to the beginning of the *FLO11* ORF, respectively. The results obtained using Crick strand-specific probes are shown in Figure 8. All three probes detect a specific transcript of approximately 3.2 kb that is most highly expressed in the *cti6* mutant and is hardly expressed at all in the *sfl1* mutant. These results indicate that a single ~3.2 kb noncoding transcript *ICR1* (Interfering Crick transcript) is indeed being transcribed in the Crick direction along nearly the entire length of the ~3.6 kb *FLO11* promoter. The steady-state levels of this *ICR1* transcript are inversely correlated with expression of the *FLO11* coding sequence in *cti6*, *sfl1*, and wild-type strains. The results obtained using Watson-strand specific probes will be discussed later in this chapter (Figure 14).

To test whether the *ICR1* transcript runs significantly into the *FLO11* coding sequence, we performed northern blot analysis using poly-A selected RNA from wild type, *cti6*, *sfl1*, and p_{flo11} cells and probed using a Crick strand-specific ^{32}P-labeled RNA probe that hybridizes to the region +93 to +568 of the *FLO11* ORF sequence. This probe detected the ~4.1 kb *FLO11* transcript itself in wild type, and *sfl1*, but it detected nothing at all in the *cti6* lane (data not shown). This result indicates that either the *ICR1* transcript doesn't run into the *FLO11* ORF as far as +93 or that there is an insufficient length of complementary sequence between the ends of the transcript and the probe to allow for efficient hybridization and detection.

5' and 3' RACE indicates that *ICR1* transcription initiates ~3.4 kb upstream of the *FLO11* ORF and is transcribed along much of the length of the *FLO11* promoter | We used rapid amplification of cDNA ends (RACE) to map the 3′ and 5′ ends of the

ICR1 transcript in wild type, *cti6*, *sfl1*, and p_{flo11} cells. The 3′ ends of *ICR1* identified by RACE in wild type, *cti6*, and *sfl1* cells are represented as blue lollipops in Figure 9 and are summarized by their location in Table 6. No 3′ends were obtained from the p_{flo11} negative control cells. In the other genotypes, a strong stop is detected at -209, which is located approximately 120 basepairs upstream of the putative *FLO11* TATA box present at -92. Interestingly, only the *cti6* strain, in which *FLO11* is transcriptionally silenced, and in the wild type strain, in which *FLO11* expression variegates, do we detect some 3′ends that extend up to and even running as far as 24 bases *into* the *FLO11* coding sequence.

The 5′ ends of *ICR1* that we identified are represented by blue arrows in Figure 9. Of the cloned 5′ ends that mapped to the *FLO11* promoter sequence, the *cti6* mutant exhibits the highest number (50%) of cloned 5′*ICR1* sequences that map to a region of the *FLO11* promoter (+3421 to +3197) that is sufficiently far away from the identified 3′ ends to produce the ~3.2 kb band observed in the northern blots (Figure 9 and Table 7). We also identified 5′*ICR1* ends in this region for wild type and *sfl1*, but these occurred at much lower frequency than in *cti6*. No 5′ends were obtained from the p_{flo11} negative control cells (Figure 9 and Table 7). Some additional 5′ends were detected at various locations (indicated by the blue tick marks on the diagrams in Figure 9) along the *FLO11* promoter sequence, but none of these additional 5′ends corresponds in size to any abundant transcripts observed by northern analysis, suggesting that these may be artifacts of the sensitivity of the RACE assay or the products of incomplete RACE amplification. Rather than a single strong 5′start site for ICR1, we identified transcripts initiating over a range of ~200 basepairs, a finding that is apparently not unusual for noncoding RNAs.

Loss of TATA binding protein association and decreased nucleosome ejection from the core promoter of *FLO11* are observed when *ICR1* transcript levels are elevated | We examined yeast TATA binding protein (TBP) localization to the *FLO11* promoter by performing ChIP-chip analyses using anti-TBP antibody on whole cell extracts derived from wild type, *cti6*, and *sfl1* cells (Figure 10). TBP localization to the *FLO11* core promoter is abolished in the *cti6* mutants in which steady-state *ICR1* transcript levels are elevated, a finding reminiscent of the mechanism of promoter occlusion proposed for *SRG1*-regulation of *SER3* (Martens et al., 2004; Martens et al., 2005). Conversely, TBP localization to the *FLO11* core promoter in the *sfl1* mutant appears to be elevated well above wild type levels.

Chromatin remodeling at the *FLO11* core promoter in wild type, *cti6*, and *sfl1* cells was assayed by performing ChIP-chip analyses using an anti-H4 antibody on whole cell extracts derived from these three genotypes. Nucleosome eviction fails to occur at the *FLO11* core promoter in the *cti6* mutant (Figure 11). This result suggests that chromatin remodelers, such as Swi/Snf and RSC (discussed in Chapter 3 of this thesis), may not have access to the *FLO11* core promoter in the *cti6* mutant in which *ICR1* transcription is elevated. Conversely, nucleosome eviction at the *FLO11* core promoter is elevated over wild type in the *sfl1* mutant in which *ICR1* transcription is low.

Taken together, the observations described above suggest that *ICR1* inhibits *FLO11* expression by interfering with the ability of basal transcription machinery and chromatin remodeling complexes to access the core promoter of *FLO11* in a manner similar to that observed at the *SER3* locus (Martens et al., 2004; Martens et al., 2005).

Termination of *ICR1* in the Rpd3L$^-$ mutant *cti6* results in the recovery of *FLO11*-dependent haploid adhesion | To test the model that *ICR1* has a causal effect in repressing *FLO11* expression by the act of its being transcribed through the *FLO11* promoter, we performed an experiment to determine whether termination of *ICR1* transcription could recover *FLO11* expression, as assayed by the recovery of *FLO11*-dependent haploid adhesion.

Computational approaches using yeast genome conservation analysis and motif discovery tools (Matys et al., 2003; MacIsaac and Fraenkel, 2006) revealed canonical TATA box sequences only in the core promoters of *FLO11* and *MRS1* (the next upstream gene); therefore, there are no obvious candidate TATA sequences to mutate in order to disrupt *ICR1* transcription. Our inability to identify a canonical TATA box for *ICR1* suggests that noncoding transcription across the *FLO11* promoter proceeds by a non-canonical TATA element or by TATA-less initiation, a phenomenon that has been described in eukaryotes from yeast to human (Singer, et al., 1990; Smale, 1996; Weis and Reinberg, 1997; Joazeiro et al., 1994).

In lieu of this approach, we constructed wild type, *cti6*, and *sfl1* strains in which *ICR1* is disrupted by a eukaryotic transcriptional terminator. We inserted a 1.4-kb construct containing the *K. lactis URA3* gene under its own promoter and with its transcriptional terminator intact in the Crick direction at -3041 within the *FLO11* promoter region. This insertion places the construct downstream of the *ICR1* transcription initiation region.

Wild type, *cti6*, and *sfl1* strains, with and without this *URA3*-terminator construct, were patched onto YPD-agar plates and grown for four days at 30 degrees C before being

subjected to the standard plate washing assay for yeast haploid adhesion (Guo et al., 2000). The phenotypes resulting from insertion of the *URA3*-terminator construct in *ICR1* supports the model in which this noncoding RNA regulates *FLO11* expression. As previously observed, the *cti6* mutant without the *URA3*-terminator construct fails to adhere to the YPD-agar, but the *cti6* strain carrying the *URA3*-terminator construct, by contrast, shows a rescue of the non-adherent *cti6* phenotype (Figure 12). Most of the *cti6* cells carrying the *URA3*-terminator construct adhered to the YPD-agar.

A second noncoding transcript, *PWR1*, is repressed by Sfl1 and is transcribed in the Watson direction covergently and overlapping with *ICR1* | To characterize further the transcription occurring within the *FLO11* promoter, we performed expression analysis using *S. cerevisiae* Sigma 1278b genomic high-density tiling microarrays with Crick and Watson strand specificity. For these arrays, Superscript reverse transcriptase is used to generate Cy-labeled single strands of cDNA complementary to the isolated collection of RNA templates. A comparison of the transcriptional profiles in *sfl1* cells versus *cti6* cells revealed the presence, not only of the *ICR1* transcript, but also of a second noncoding transcript *PWR1* (for Promoting Watson RNA) that initiates approximately 2.3 kilobases away from the beginning of the *FLO11* ORF and is transcribed in the Watson direction convergently with the *ICR1* transcript (Figure 13). In these data, transcription of *PWR1* is observed in the *sfl1* mutant, but not at all in the *cti6* mutant.

Strand-specific northern blot analyses confirm the existence of a ~1.2-kb Watson-strand noncoding RNA *PWR1* transcribed from within the *FLO11* promoter sequence | We performed northern blot analysis using poly-A selected RNA from wild

type, *cti6*, *sfl1*, and p_{flo11} cells. For probing, we used ^{32}P-labeled strand-specific RNA probes that hybridize to three different regions of the *FLO11* promoter sequence. Probes 1, 2, and 3 hybridize to regions located -284 to -819, -1653 to -2255, and -2631 to -3226 relative to the beginning of the *FLO11* ORF, respectively. The results obtained using Watson strand-specific probes are shown in Figure 14. Probes 2 and 3 detect a specific transcript of approximately 1.2 kb that is most highly expressed in the *sfl1* mutant and is not expressed in the *cti6* mutant. An intermediate level of this transcript is observed in the variegating wild type cells. The steady-state levels of this *PWR1* transcript are positively correlated with expression of the *FLO11* coding sequence in *cti6*, *sfl1*, and wild-type strains.

Transcription of *PWR1* appears to be repressed by the DNA-binding protein Sfl11. In the *sfl1* mutant, elevated steady-state levels of the *PWR1* transcript correlate with increased *FLO11* expression. This observation suggests that the long-known role of Sfl1 in repression of *FLO11* expression may be an indirect effect of its repression of *PWR1* transcription.

5' and 3' RACE indicates that the *PWR1* transcript initiates ~2.3 kb upstream of the *FLO11* ORF and terminates near the transcription initiation site of *ICR1* | We used rapid amplification of cDNA ends (RACE) to map the 3′ and 5′ ends of the *PWR1* transcript in wild type and *sfl1* cells. Because *PWR1* is not expressed in *cti6* cells, we did not perform the RACE assay on this genotype.

The 3′ ends of *PWR1* identified by RACE in wild type and *sfl1* cells are represented as red lollipops in Figure 15 and are summarized by their location in Table 8. The termination sites cluster between -3155 and -3409 relative to the beginning of the

FLO11 ORF. Thus, the termination site for *PWR1* is in the same region of the *FLO11* promoter as the initiation site for ICR1.

The 5′ ends of the *PWR1* transcript are represented as red arrows in Figure 15 and summarized by their location in Table 9. Rather than a single strong 5′ start site for *PWR1*, we identified transcripts initiating over a short range of ~150 basepairs, clustered around -2300 relative to the beginning of the *FLO11* ORF. This places the start site of *PWR1* just upstream of the UAS1 region, located between -1760 and -2175.

The *PWR1* transcript interferes with expression of a convergent and overlapping Crick-strand reporter construct | I hypothesize that *PWR1* promotes *FLO11* expression by competing with *ICR1* for its template region and preventing *ICR1* transcription from proceeding along the length of the *FLO11* promoter, thereby inhibiting the *ICR1*-mediated transcriptional repression of *FLO11* expression.

This model is supported by our observation that transcription of *PWR1* can interfere with expression of the *K. lactis URA3* reporter construct integrated at position -3041 in the *FLO11* promoter (Figure 16). The *URA3* reporter is transcribed in the Crick direction convergently and overlapping with *PWR1* in an *ICR1*-like manner.

Using the size of colonies growing on SC-Ura media as an indicator of *URA3* reporter expression, our results demonstrate that the *URA3* gene is expressed most highly in *cti6* cells, in which no *PWR1* transcript is detected (Figure 16A and Figure 14). In the *sfl1* mutant background in which *PWR1* transcript levels are elevated, *URA3* reporter expression is very low, resulting in only microcolonies growing on the SC-Ura media (Figure 16A and Figure 14). Wild type cells, which exhibit an intermediate level of

PWR1 expression, also exhibit a level of *URA3* reporter expression that is intermediate between *cti6* and *sfl1* (Figure 16A and Figure 14).

Serial dilutions of these strains onto SC+5-FOA and SC–Ura also confirm these findings (Figure 16B). More cells in the *cti6* background are actively expressing the *URA3* reporter construct, therefore more cells of this genotype are able to grow on SC–Ura and fewer on SC+5-FOA. Conversely, more cells in the *sfl1* background are silenced for *URA3* reporter expression as a result of elevated *PWR1* transcription, therefore more of these cells are able to grow on SC+5-FOA and fewer on SC–Ura. The *URA3* construct effectively variegates in the wild type cells.

A similar pair of a convergent and overlapping noncoding RNAs are transcribed within the *FLO10* promoter region | Expression analyses using *S. cerevisiae* Sigma 1278b genomic high-density tiling microarrays with Crick and Watson strand specificity, also reveal the presence of a similar pair of convergent, overlapping noncoding transcripts initiating within the *FLO10* promoter region (Figure 17). A comparison of the transcriptional profiles in *sfl1* cells versus *cti6* cells demonstrates that *FLO10* expression is upregulated in the *sfl1* mutant, and that this upregulation is correlated with the transcription of a noncoding transcript that is (i) derepressed in the *sfl1* mutant (ii) transcribed divergently from the protein-coding *FLO10* gene (which is transcribed in the Watson direction), and (iii) transcribed convergently and overlapping with a second noncoding transcript that is detected in both the *sfl1* and *cti6* mutants. These observations suggest that transcriptional regulation by noncoding RNAs may be a mechanism that extends to other members of the variegating *FLO* gene family.

A new model to inform the mechanism underlying variegated transcription of *FLO* genes | Our findings provide new insight into a model for the mechanism underlying transcriptional variegation of *FLO* genes. This model involves regulatory noncoding RNAs, bistable changes in local chromatin structure resulting from recruitment of histone deacetylases, and competitive binding to DNA by proteins, such as Sfl1 and Flo8, that may determine whether histone deacetylases are present or absent at local regions within *FLO* promoters. The model is summarized in Figure 18 and is discussed below.

DISCUSSION

In this chapter, I have presented results that form the basis for an explanation of how a histone deacetylase, i.e., a canonical repressor of transcription, can play a direct role in activating expression of the *FLO11* gene. We have shown that the Rpd3L histone deacetylase complex represses the transcription of the noncoding *ICR1* transcript that is transcribed across the *FLO11* promoter in the Crick direction. When components of the Rpd3L histone deacetylase complex are deleted, we find that steady-state levels of the *ICR1* transcript are elevated and *FLO11* is not expressed. A transcription terminator placed within *ICR1* results in recovery of *FLO11*-dependent phenotypes in the Rpd3L$^-$ mutant, suggesting a causal role for the *ICR1* transcript in preventing *FLO11* expression. Thus, although the indirect effect of Rpd3L histone deacetylase activity is the activation of *FLO11* expression, its local direct effect on transcription of the regulatory noncoding RNA *ICR1* is repressive, thus resolving the apparent paradox regarding Rpd3L function.

Our discovery that transcription of *ICR1* initiates ~-3400 basepairs from the beginning of the *FLO11* ORF expands the regulatory region of the *FLO11* promoter

beyond that identified in previous studies (Rupp et al., 1999). The region of the *FLO11* promoter dissected by Rupp et al. did not extend sufficiently far upstream of the *FLO11* ORF to identify the *ICR1* transcription initiation region (Rupp et al., 1999).

I have also reported that the well documented transcriptional regulator of *FLO* genes Sfl1 represses the transcription of a second regulatory noncoding RNA *PWR1* that also initiates within the *FLO11* promoter region and is transcribed in the Watson direction convergently and overlapping with the *ICR1* transcript. This observation suggests that Sfl1-mediated repression of *FLO11* expression involves its regulation of a noncoding RNA. The fact that Sfl1 is important for the recruitment of the Hda1 histone deacetylase to target promoters and that Hda1 is also required for epigenetic silencing of *FLO11* suggests that Hda1 may also play a role in repressing *PWR1* transcription, but more experiments are required to test this hypothesis.

Transcription of *PWR1* has a positive effect on *FLO11* expression. I believe that, by competing with the *ICR1* transcript for its DNA template region, *PWR1* prevents the *ICR1* noncoding transcript from proceeding through the *FLO11* promoter and thereby prevents *ICR1*-mediated repression of *FLO11* expression. The fact that the *PWR1* transcript is capable of interfering with the expression of a *URA3* reporter gene inserted in its path supports this hypothesis. The transcription start site of *PWR1* is located just upstream of the UAS1 region of the *FLO11* promoter. This observation suggests the following hypotheses: (i) *PWR1* may have evolved to prevent *ICR1* from proceeding into the UAS1 region and (ii) proteins that bind to the UAS1 region, such as Flo8, may be directly involved in regulating transcription of *PWR1*.

Based on the findings reported in this chapter, I propose a new model that helps to explain the transcriptional variegation observed at *FLO11* (Figure 18). Although the model is based on the transcriptional analysis of chromatin binding mutants, the identification of the opposing noncoding transcripts provides a window into events occurring in wild type populations of cells. The promoter of *FLO11* is under dynamic targeting by DNA-binding proteins and chromatin modifying complexes. Competitive binding of proteins, such as Sfl1 and Flo8, may determine whether histone deacetylases are present or absent at local regions within the *FLO11* promoter and could result in bistable switching of local chromatin structure. If Rpd3L binds to the *FLO11* promoter, preventing *ICR1* transcription, then *FLO11* will be transcribed. Similarly, if Flo8 and or Ste12/Tec1 bind and thereby prevent Sfl1 from associating with the promoter, *PWR1* is transcribed; *PWR1* transcription then interferes with *ICR1* transcription, thereby allowing *FLO11* to be transcribed. However, if Sfl1 binds to the promoter and recruits Hda1, *PWR1* transcription is repressed, *ICR1* is transcribed, and *FLO11* transcription is repressed.

The new model proposes that transcriptional activity from the core promoter of *FLO11* is ultimately regulated by the opposing actions of the two noncoding RNAs, *ICR1* and *PWR1*. The transcription of *ICR1* somehow results in the core promoter of *FLO11* becoming inaccessible to chromatin remodelers, such as Swi/Snf, and the basal transcription machinery, including TBP. Transcription of *PWR1* likely interferes in *cis* with *ICR1* transcription by competing for its DNA template region, and thereby promotes *FLO11* core promoter activity. Experiments to test whether *PWR1* and *ICR1* have any *trans*-acting effects on *FLO11* expression are underway.

Competitive binding of transcription factors that generate different outputs to the same regulatory site in DNA has been shown to form the basis of a simple exclusive toggle switch between two transcriptional states (Warren and Rein ten Wolde, 2004). At the *FLO11* locus, competitive binding of *trans*-acting protein factors that cause a switch between two chromatin states, one permissive of noncoding transcription and the other repressive of noncoding transcription, could be the basis of exactly such a simple toggle switch between an active or inactive core promoter state. The percentage of active versus inactive *FLO11* core promoters within a population of wild-type variegating yeast cells may reflect the likelihood of binding for each of the two *trans*-acting proteins competing for the same binding region at each *FLO11* promoter within the population.

If competitive binding of proteins is sufficient to bring about a toggle between alternative chromatin states, which in turn change the transcription profiles of *cis*-acting regulatory noncoding RNAs, then we have moved a step forward in understanding the mechanisms that might underlie transcriptional variegation of *FLO* genes. But, the mechanism of transcriptional memory observed in chains of filamentous cells, all of which express *FLO11* (Halme et al., 2004), remains a mystery at this point in our research. Our model requires components that could facilitate a feedback loop that would lead to a persistence of one local chromatin state or the other. As yet, the components necessary for such a feedback loop have not been identified.

Although we have identified histone deacetylases that act at the *FLO11* promoter, the manner in which local chromatin states are "reset" to allow continuing interconversion between repressive and permissive structure at the *FLO11* promoter also remains a mystery. A progression through the cell cycle and new histone deposition may

be required. Further experiments are required to test this hypothesis. Further characterization of the molecular roles of the *trans*-acting factors that function at various sites within the expansive *FLO11* promoter may also shed light on this question.

Our findings at *FLO11* reveal a mechanism of transcriptional control that is likely soon to be accepted as a common regulatory strategy in yeast. A number of other recent publications also report cases of regulation of gene expression by noncoding transcripts in *S. cerevisiae*. The genes *IME4*, *SER3*, *PHO5*, and *PHO84* have all been found to be transcriptionally regulated by noncoding RNAs (Camblong et al., 2008; Hongay et al., 2006; Martens et al., 2004; Martens et al., 2005; Uhler et al., 2007). Furthermore, genome-wide analysis has lead to the discovery of 667 transcripts occurring in intergenic regions, as well as antisense transcripts detected at 367 confirmed genes in yeast (Miura et al., 2006). The very recent deep sequencing of the yeast transcriptional landscape has revealed the presence of potential regulatory secondary transcripts within 6% of yeast promoter regions and has also shown that 11.8% of yeast transcripts have overlapping 3′ ends that could allow genes to influence the transcription of their neighbors (Nagalakshmi et al., 2008). Thus, the regulatory mechanisms described for the *FLO11* locus in this thesis, along with other recent reports of such phenomena, are likely a harbinger of new view of transcriptional control.

FIGURES AND TABLES

FIGURE 1 | A summary of the regulators of *FLO11* transcription discussed in this chapter. Net activators of *FLO11* expression are shown in light blue. Net repressors of *FLO11* expression are shown in red. Both Sfl1 and Flo8, the downstream effectors of PKA signaling, have been shown to bind competitively to the same region of the *FLO11* promoter located between -1150 to -1400 relative to the beginning of the *FLO11* ORF (Pan and Heitman, 2002; Rupp et al., 1999; Gancedo, 2001; Palecek et al., 2002). Sfl1 has also been shown to recruit the Hda1 histone deacetylase to promoters, suggesting the participation of Sfl1 in chromatin-mediated repression of *FLO11* expression (Halme et al., 2004; Conlan and Tzamarias, 2001; Wu et al., 2001). Studies of the *FLO11*-like *STA1* promoter in the yeast *S. diastaticus* have identified two UAS regions that are likely functional in the *FLO11* promoter, as well (Kim et al., 2004a; Kim et al., 2004b); UAS1 spans the region -1760 to -2175 and UAS2 spans the region -1000 to -1498 relative to the beginning of the *FLO11* ORF. In the *STA1* promoter studies, Sfl1 was shown to compete with the Ste12-Tec1 activator complex, the downstream effector of the filamentation MAPK pathway, for binding of the UAS2 region (Kim et al., 2004b; Rupp et al., 1999; Gancedo, 2001; Palecek et al., 2002). The Ste12-Tec1 complex then recruits the Swi-Snf chromatin remodeling complex (Kim et al., 2004a; Kim et al., 2004b). The Swi-Snf complex and Flo8, in turn, facilitate recruitment of the basal transcription machinery to the core promoter (Kim et al., 2004a; Kim et al., 2004b). We have found that components of the Rpd3L histone deacetylase complex, including Rpd3, Cti6, Rxt2, and Pho23, behave as net activators of *FLO11* expression. In this study, we report the discovery of two noncoding RNAs that also regulate *FLO11* expression. Rpd3L represses the *ICR1* noncoding transcript which, itself, represses *FLO11* expression, perhaps by interfering with the access of Swi-Snf, other chromatin remodelers, and the basal transcription machinery to the core promoter of *FLO11*. Sfl1, perhaps through its recruitment of the Hda1 histone deacetylase, represses the *PWR1* noncoding transcript which, itself, promotes *FLO11* expression.

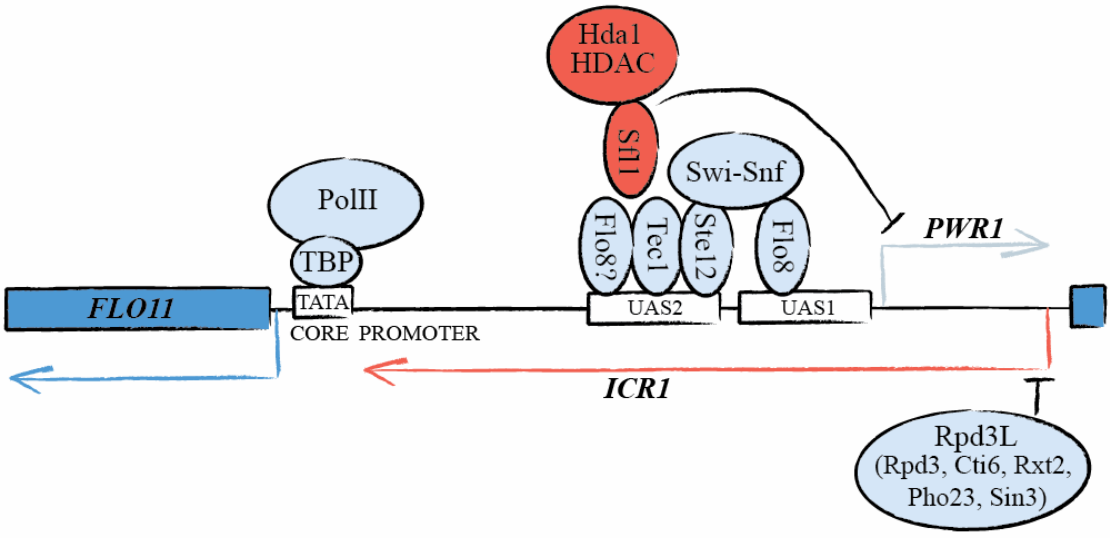

TABLE 1 | *Saccharomyces cerevisiae* strains used in this study.

Strain	***Genotype***		***Source***
10560-4A	*MATa*	*ura3-52 leu2::hisG trp1::hisG his3::hisG*	Fink lab collection
10560-6B	*MATx*	*ura3-52 leu2::hisG trp1::hisG his3::hisG*	Fink lab collection
SBY170	*MATx*	*sfl1::kanR ura3-52 leu2::hisG trp1::hisG his3::hisG*	This study
SBY251	*MATa*	*flo11::pFLO11::URA3 ura3-52 leu2::hisG trp1::hisG*	Halme et al., 2004
SBY408	*MATa*	*pho23::Tn3::LEU2 ura3-52 flo11::pFLO11::URA3 leu2::hisG trp1::hisG*	This study
SBY411	*MATa*	*cti6::Tn3::LEU2 ura3-52 flo11::pFLO11::URA3 leu2::hisG trp1::hisG*	This study
SBY415	*MATa*	*rxt2::Tn3::LEU2 ura3-52 flo11::pFLO11::URA3 leu2::hisG trp1::hisG*	This study
SBY591	*MATx*	*cti6::Tn3::LEU2 ura3-52 his3::hisG leu2::hisG trp1::hisG cti6::Tn3::LEU2*	This study
SBY786	*MATa*	*eaf3::Tn3::LEU2 ura3-52 flo11::pFLO11::URA3 leu2::hisG trp1::hisG*	This study
SBY847	*MATa*	*rpd3::KanR can1-^::ste2pr-HIS3 ura3^ leu2^ his3^::hisG lyp1-^::ste3pr-LEU2*	Owen Ryan
SBY910	*MATx*	*Rpd3-18myc-TRP1 ura3-52 trp1::hisG leu2::hisG*	This study
SBY931	*MATa*	*Rpd3-18myc-TRP1 flo11::pFLO11::URA3 ura3-52 trp1::hisG leu2::hisG*	This study
SBY934	*MATx*	*Rpd3-18myc-TRP1 flo11::pFLO11::URA3 ura3-52 trp1::hisG leu2::hisG*	This study
SBY946	*MATa*	*Rpd3-18myc-TRP1 ura3-52 trp1::hisG leu2::hisG*	This study
SBY1062	*MATa*	*pflo11::KanMx ura3-52 trp1::hisG leu2::hisG NUP49-GFP-HIS3MX6*	Chia Wu
SBY1065	*MATa*	*cti6::KanR flo11::pFLO11::URA3 ura3-52 leu2::hisG trp1::hisG*	This study
SBY1091	*MATx*	*pFLO11::I::K.l.URA3-term ura3-52 his3::hisG leu2::hisG*	This study
SBY1097	*MATx*	*cti6::Tn3::LEU2 pFLO11::I::K.l.URA3-term ura3-52 his3::hisG leu2::hisG*	This study
SBY1103	*MATx*	*sfl1::KanR pFLO11::I::K.l.URA3-term ura3-52 his3::hisG leu2::hisG*	This study
AHY959	*MATa*	*hda1::kanr flo11::pFLO11::URA3 ura3Δ0*	Halme et al., 2004
AHY960	*MATa*	*sfl1::kanr flo11::pFLO11::URA3 ura3Δ0*	Halme et al., 2004

TABLE 2 | Plasmids used in this study.

Plasmid	**Insert**	**Reference**
pQF382.2	P_{TEF}-*FLO11*; *URA3*	Fink Laboratory Collection
p416TEF	P_{TEF}-(empty vector); *URA3*	Mumberg et al., 1995
pUG72	*K. lactis URA3* under its own promoter and terminator sequence	Gueldener et al., 2002
Y1p365-FLO11::lacZ	Sigma 1278b P_{FLO11}-*lacZ-LEU2*	Fink Laboratory Collection

TABLE 3 | Oligos used in this study.

Primer	Sequence (5' to 3')	*Description*
CW352	CTGCCGCGAAAGTTTAATTTG	*Real time primer for PFLO11 Opt-1 For*
CW353	CCTAGTGATCTTTTCCTGACTCCAA	*Real time primer for PFLO11 Opt-1 Rev*
CW354	CGTACTGGGACATCGCATACC	*Real time primer for PFLO11 Opt-2 For*
CW355	TTGTGCCCGTATTGTTGCA	*Real time primer for PFLO11 Opt-2 Rev*
PSB322	AGCTAGTGGCCGCTTCGAT	*pINO1 real time primer*
PSB323	TTCCGGCTTTTTCAAGTCAAG	*pINO1 real time primer*
PSB366	CTGCAATGATTATGTGGTATGATCAG	*PFLO11 real time primer: -2800 For*
PSB367	CGGTCCCATTGAGCCAAA	*PFLO11 real time primer: -2800 Rev*
PSB368	TGCACTCGTTTTCCATGTTCTT	*PFLO11 real time primer: -2400 For*

TABLE 3 | **Oligos used in this study: Continued …**

Primer	Sequence (5' to 3')	*Description*
PSB369	GGCCCTGAGATGCTCAACTG	*PFLO11 real time primer: -2400 Rev*
PSB370	AAGCTGTGCGGGAAAACG	*PFLO11 real time primer: -1800 For*
PSB371	TTCATGTGGTGGAAATACCGATT	*PFLO11 real time primer: -1800 Rev*
PSB372	CGCCGGCAGGCAAAT	*PFLO11 real time primer: -1400 For*
PSB373	GAGAAACTGAAAGGCAAAAAAGAAA	*PFLO11 real time primer: -1400 Rev*
PSB374	TGCAACAATACGGGCACAA	*PFLO11 real time primer: -700 For*
PSB375	TCACACCACCGATAGGCAATAG	*PFLO11 real time primer: -700 Rev*
PSB376	CGGATAACTCATAGACTTACCAGTACAAG	*PFLO11 real time primer: -300 For*
PSB377	GATGAATAGGGTGCTTTTTATACGTTT	*PFLO11 real timeprimer: -300 Rev*
PSB450	CGGGTTATTTCGAACTCATGTTT	*ARK1 real time primer*
PSB451	GGCTTAGAATTCGGACCCTATTG	*ARK1 real time primer*
PSB460	TGCATGGCAATCAGAACGAT	*APL2 real time primer*
PSB461	GGCGGAGTGGTGTTTCAATG	*APL2 real time primer*
PSB464	GCGCATGAACTCAAGTATGATCA	*ARG2 real time primer*
PSB465	CGTTTTGTAGCGGTTGTATTCAGA	*ARG2 real time primer*
PSB495	GCTGCCGGTGAAACTACATC	*To generate 3' FLO11 probe*
PSB496	TGGAAGAGCGAGTAGCAACC	*To generate 3' FLO11 probe*
PSB501	GGACATCGCATGCCTTGGGATTCCGTAA	*3' RACE ICR1-specific primer*
PSB503	CGGGCACAACTCATTCTGCGCTAT	*3' RACE Nested ICR1-specific primer*
PSB516	CCTATACTCTTAAACAGATCAGTCATTCAT	*To generate Crick Riboprobe 1*
PSB517	TCCTCAGATAAGACAAGTCTAACAGTTAAT	*To generate Watson Riboprobe 1*
PSB518	ccaagcttctaatacgactcactatagggagCCTATACTCTTAAACAGATCAGTCATTCAT	*To generate Watson Riboprobe 1*
PSB519	ccaagcttctaatacgactcactatagggagTCCTCAGATAAGACAAGTCTAACAGTTAAT	*To generate Crick Riboprobe 1*
PSB557	TGTTAGGGTCCGTTTTCCCGCACAGCTT	*5' RACE ICR1-specific primer*
PSB558	AATGTCCCGTCTGCGTCAGCAGCTCAGA	*5' RACE Nested ICR1-specific primer*
PSB561	CGCTGGCCCTGAGATGCTCAACTGTAAG	*5' RACE ICR1-specific primer*
PSB562	CAGTTTGACCAGTGCTACTTGGCGCTGT	*5' RACE Nested ICR1-specific primer*
PSB565	TCCGAAGGAACTAGCTGTAATTCTA	*To generate 5' FLO11 ORF probe (Crick)*
PSB566	ccaagcttctaatacgactcactatagggagGTTTGAGAGTAGCCTTGATTGTCAT	*To generate 5' FLO11 ORF probe (Crick)*
PSB571	CTAATGTATCCCTCATTTCATACCG	*To generate Crick Riboprobe 2*
PSB572	ccaagcttctaatacgactcactatagggagGAGTCTAAGTTGACAAGGCTACGAA	*To generate Crick Riboprobe 2*
PSB577	CTATCTCCACATACCAATCACTCG	*To generate Crick Riboprobe 3*
PSB578	ccaagcttctaatacgactcactatagggagCCCTGAGATGCTCAACTGTAAGTA	*To generate Crick Riboprobe 3*
PSB579	CTTAGCGTGGGTGCTTCTGCTCAGTCTTCGTTTCCTATCTCCACATACCAATCAC TCGTTggtctagagatcccaatacaacaga	*To generate K. lactis URA3-term construct*
PSB580	TATTCAGATTTAGTTGGCGGTACGACTCCTTACAGCAGTAAATTATTCGAATTAG TAACAgggttctcgagagctcgttt	*To generate K. lactis URA3-term construct*
PSB637	ccaagcttctaatacgactcactatagggagCTAATGTATCCCTCATTTCATACCG	*To generate Watson Riboprobe 2*
PSB638	GAGTCTAAGTTGACAAGGCTACGAA	*To generate Watson Riboprobe 2*

TABLE 3 | **Oligos used in this study: Continued …**

Primer	Sequence (5' to 3')	*Description*
PSB643	ccaagcttctaatacgactcactatagggagCTATCTCCACATACCAATCACTCG	*To generate Watson Riboprobe 3*
PSB644	CCCTGAGATGCTCAACTGTAAGTA	*To generate Watson Riboprobe 3*
PSB649	GAACAGCGCCAAGTAGCAACTGGTCAA	*5' RACE Nested PWR1-specific primer*
PSB649	GAACAGCGCCAAGTAGCAACTGGTCAA	*5' RACE Nested PWR1-specific primer*
PSB650	CCCTCTTCCTCTCACTGCACTTCAA	*5' RACE PWR1-specific primer*
PSB651	GCGGTACGACTCCTTACAGCAGT	*3' RACE PWR1-specific primer*
PSB652	ACTGAGCAGAAGCACCCACGCTAA	*3' RACE Nested PWR1-specific primer*
P1D11-P2D11	ATCGGTATTTCCACCACATGAA/TGGAACTGAGTCTAAGTTGACA	*HiDensity PFLO11 real time pair @ -1620*
P1E1-P2E1	AAAATTCATTCGTAGCCTTGTC/AACATAGAACAAATCTCGCCCG	*HiDensity PFLO11 real time pair @ -1560*
P1E3-P2E3	TATGAATAAAAGGATCCACGGG/CTGGCGTAGGCACACAATCCGG	*HiDensity PFLO11 real time pair @ -1500*
P1E5-P2E5	CACAAAACTTTAGGAATACCGG/TTCCTATTGGAGCCAGGAAAAG	*HiDensity PFLO11 real time pair @ -1440*
P1E7-P2E7	GCTGTAATTCCTCGTGATCTTT/GAAAGGCAAAAAAGAAAAGCCT	*HiDensity PFLO11 real time pair @ -1380*
P1E8-P2E8	CCAATAGGAACGCCGGCAGGCA/TGCTTATGTAATGCCACATTCC	*HiDensity PFLO11 real time pair @ -1350*
P1F2-P2F2	AATGTCGCCCAAAGAGTTTCGG/AGCCTAATTTTGCAGTGATCGC	*HiDensity PFLO11 real time pair @ -1170*
P1F7-P2F7	GGGCTAAGAATGGACTTCCCTT/CACCTTCTAAACGCTCGGACTG	*HiDensity PFLO11 real time pair @ -1020*
P1G10-P2G10	CATTGTCCAACCCTAAAAGTGC/CAATCGTACCCTAATAGTTGCT	*HiDensity PFLO11 real time pair @ -840*
P1G1-P2G1	GCACAAACTTTTTTATTTCTGC/CGGAATCCCAAGGCATGCGATG	*HiDensity PFLO11 real time pair @ -750*
P1G4-P2G4	TGGGATTCCGTAATTAGGTGCA/AATTGTTAATCACACCACCGAT	*HiDensity PFLO11 real time pair @ -720*
P1G5-P2G5	GGCACAACTCATTCTGCGCTAT/TTGAAAATCCATTCCAAGCTCT	*HiDensity PFLO11 real time pair @ -690*
P1G6-P2G6	ACAGAACTTCTATTGCCTATCG/AAACAAACGAATACCTCCAAAT	*HiDensity PFLO11 real time pair @ -570*
P1H2-P2H2	CAATCGTACCCTAATAGTTGCT/GAAGTATATTGCGATGATGCCT	*HiDensity PFLO11 real time pair @ -450*
P1H7-P2H7	CTTGTCTTATCTGAGGAATGTC/AGCGCAGTAACCTACATGCTTG	*HiDensity PFLO11 real time pair @ -300*
P3A2-P3D2	CACCCTATTCATCAGTATACTC/GTCTTTGCATAGTGTGCGTATA	*HiDensity PFLO11 real time pair @ -90*
P3A4-P3D4	GTAGGCCTCAAAAATCCATATA/TTGGAAAACCCAAAGCTGAGTA	*HiDensity PFLO11 real time pair @ -30*
P3A5-P3D5	ATGCAAAGACCATTTCCATTCG/CTTCGGAGGATCCTCTAGGAAC	*HiDensity PFLO11 real time pair @ +1*
P3A6-P3D6	GTCCTTTCGCTTCTATTTTACT/AGCCATTAACGATAGAATTACA	*HiDensity PFLO11 real time pair @ +30*

FIGURE 2 | **The Rpd3L histone deacetylase complex has a net activating effect on *FLO11* expression, whereas Sfl1 and the Hda1 histone deacetylase have net repressing effects**. *(A)* *FLO11* promoter activity was monitored using two different reporter genes, *GFP* or *URA3*, driven at the endogenous *FLO11* locus. *(B)* In wild type Sigma 1278b cells, transcription from the *FLO11* promoter variegates as a result of reversible epigenetic silencing in a subset of cells, as seen by fluorescence microscopy of a clonal population of P_{FLO11}-*GFP* cells. *(C)* FACS analysis of cells carrying the *GFP* construct shows a decrease in the percentage of cells with an active *FLO11* promoter when components of the Rpd3L complex, including *cti6*, *rxt2*, and *pho23*, are mutated. The positive control was a P_{URA3}-*GFP* strain. The negative control was a strain carrying no *GFP* gene. *(D)* Serial dilutions of strains expressing the P_{FLO11}-*URA3* construct onto SC–Ura and SC+5FOA selection media show that mutation of components of Rpd3L results in more cells having a silent *FLO11* promoter, and are therefore able to grow on SC+5-FOA compared to wild type. *(E)* Mutation of *sfl1* or *hda1* results in loss of epigenetic silencing at the *FLO11* promoter (Halme et al., 2004), thus no cells of these genotypes are able to grow on SC+5-FOA.

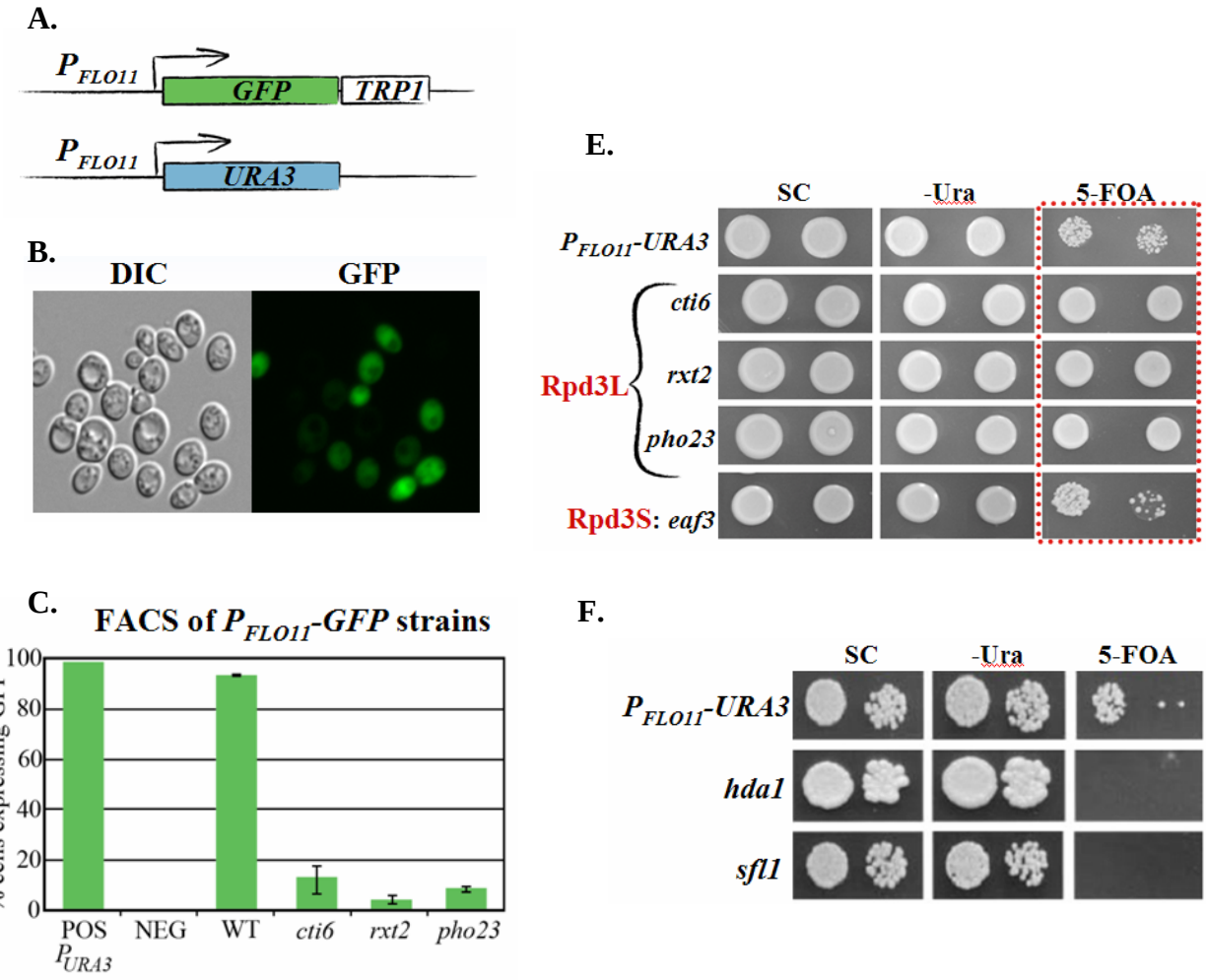

FIGURE 3 | **Northern blot analysis confirms that *FLO11* mRNA levels are reduced in an Rpd3L$^-$ (*cti6*) mutant and elevated in an *sfl1* mutant.** *(A)* Total RNA was DNase-treated to remove any residual genomic DNA and 10 ug of this DNase-treated RNA were loaded per sample. Northern blot analysis using a ^{32}P-labeled DNA probe specific to a region near the 3′ end of the *FLO11* ORF (bp +3502 to 4093) shows that, relative to wild type levels, *FLO11* RNA is more than five-fold reduced in the *cti6* mutant and, as expected, is upregulated in the *sfl1* mutant. *(B* Signal was quanitified and normalized to the SCR1 load control using ImageQuant software. *(C)* A map of the probe location.

A.

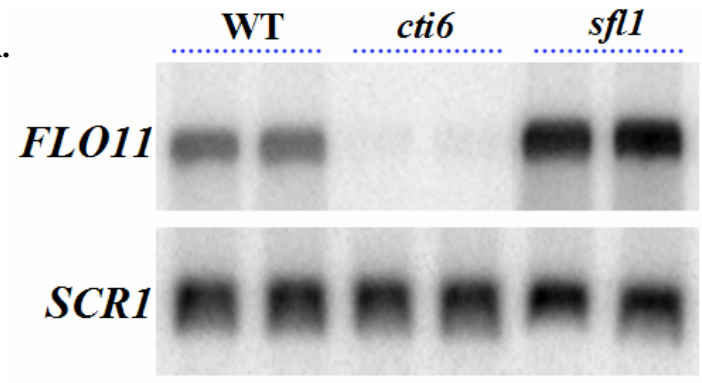

B.

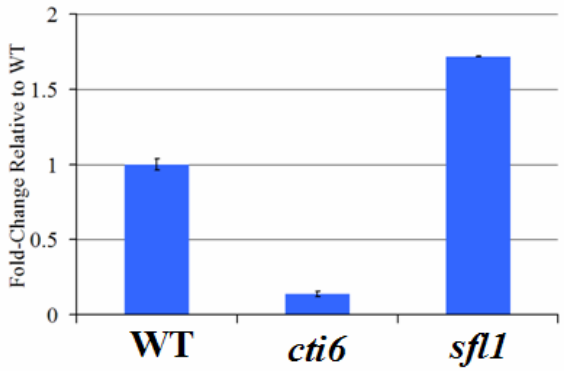

C.

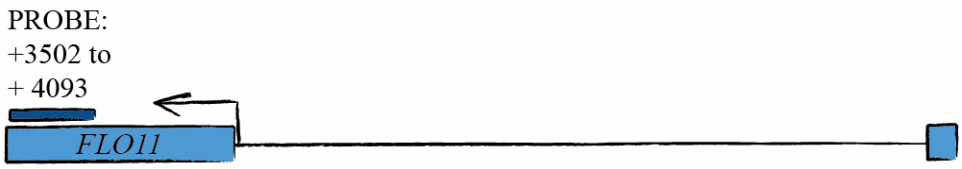

FIGURE 4 | **Rpd3L localizes to the *FLO11* promoter.** *(A)* Gene-specific ChIP was performed using a functional 18-Myc epitope-tagged allele of Rpd3. WCEs were precipitated using an antibody against the Myc-epitope. Real time PCR was performed on the immunoprecipitated chromatin and WCE input using primers specific to the *FLO11* promoter region and control primers specific to the *INO1* promoter, previously shown to be bound by Rpd3 (Robert et al., 2004), and the unbound genes, *APL2* and *ARG2*, identified in whole genome Rpd3 binding studies. The data were normalized relative to another unbound region (*ARK1*). For the *FLO11* promoter region, the results using a primer pair that amplifies a region located -1400 relative to the *FLO11* ORF are shown below. Enrichment of Rpd3-Myc at the *FLO11* promoter was greater than that at the *INO1* promoter. *(B)* Immunoprecipitations were also performed on untagged strains to ensure specificity of the signal. *(C)* Whole genome ChIP-chip was performed using *S. cerevisiae* Sigma 1278b custom genomic tiling microarrays. These assays identified a region of Rpd3-localization spanning approximately -900 to -1400, and another located at approximately -2850 relative to the beginning of the *FLO11* ORF.

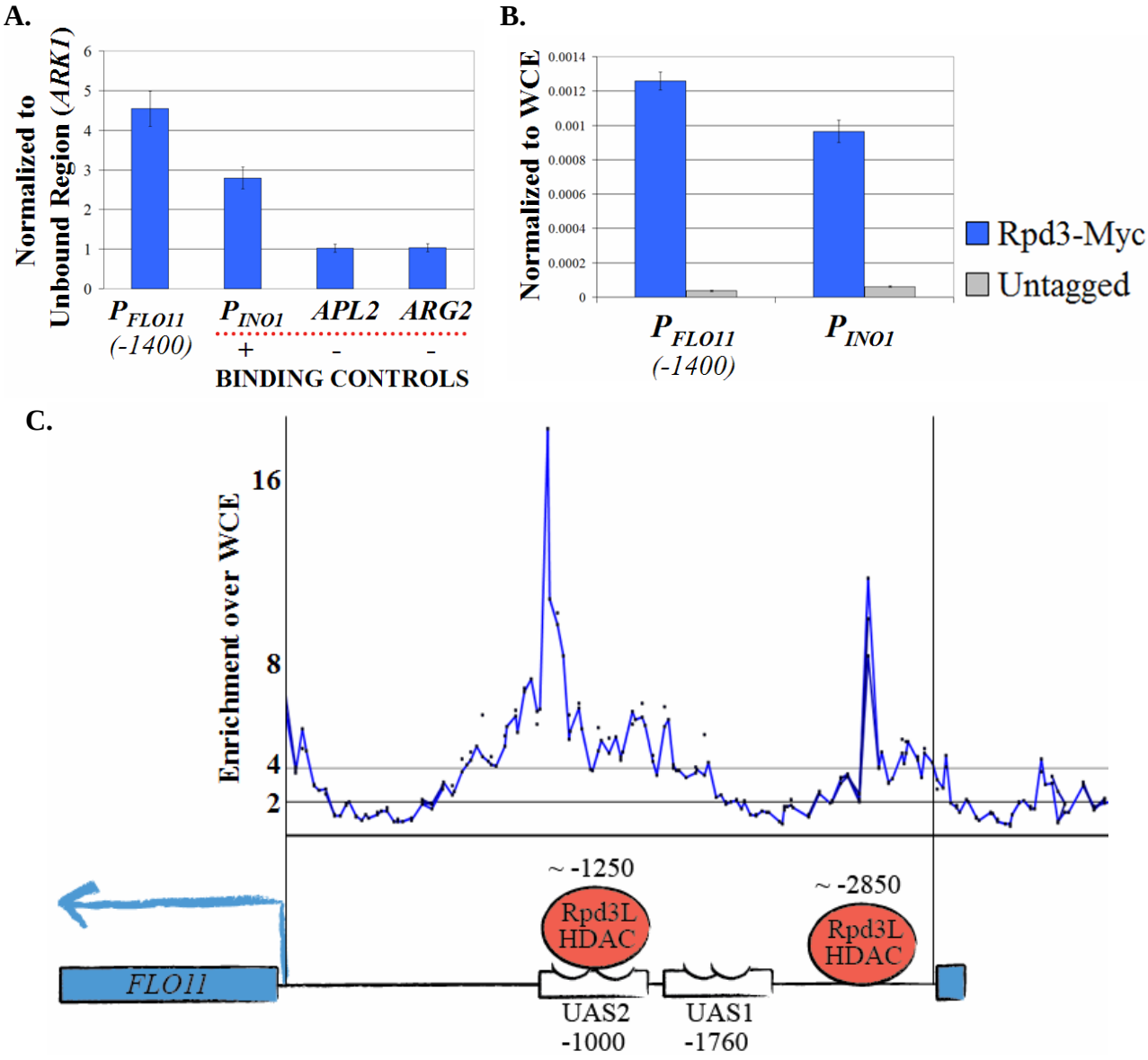

FIGURE 5 | **Rpd3L does not indirectly regulate *FLO11* expression through known regulators.** *(A)* Whole genome poly-A RNA expression analyses using Sigma 1278b genomic high-density tiled microarrays as a further test to check whether loss of *FLO11* expression in the *cti6* mutant could be an indirect result of Rpd3L-mediated repression of a transcriptional activator of *FLO11* transcription. The first set of arrays compared expression in wild type versus *cti6*. We compared the list of differentially expressed genes from the array data to a list of 75 published (confirmed or putative) regulators of *FLO* gene transcription compiled from the literature ((Cullen et al., 2004; Gancedo, 2001; Halme et al., 2004; Kim et al., 2004a; Kim et al., 2004b; Palecek et al., 2002; Pan and Heitman, 2002; Rupp et al., 1999) and Supplemental Table 1). Only one gene from the list of published regulators appears in the group of differentially expressed genes from this set of arrays: *MSB2* just makes the cutoff for being significantly differentially expressed at a lower level in *cti6* relative to wild type. *(B)* The second set of arrays compared expression in *cti6* versus the *sfl1*. None of the 75 published *FLO11* regulators was differentially expressed in these data. The *MSB2* result was not confirmed. *SFL1* itself appears as an artifact of experimental design because it is deleted in the *sfl1* strain and is therefore not expressed.

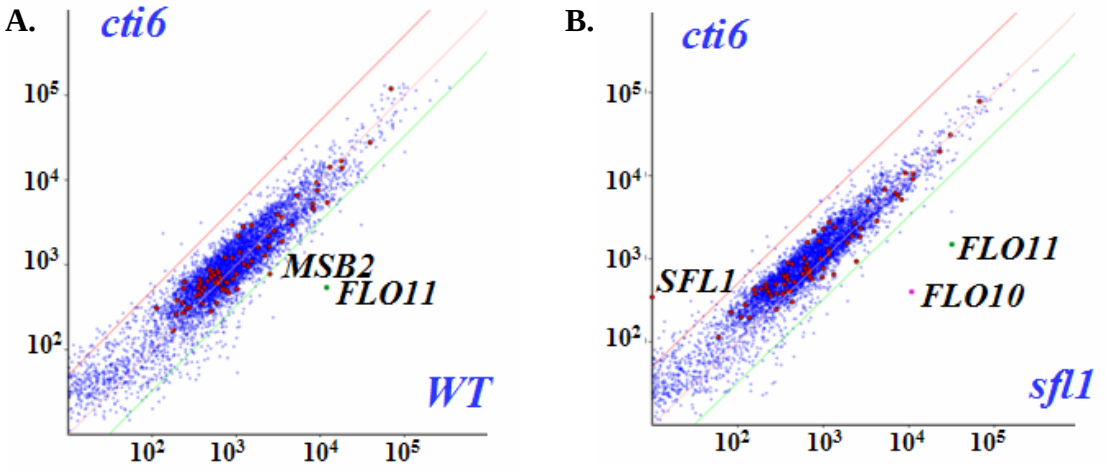

TABLE 4 | **Differential Expression of *FLO* genes and published regulators.**

WT vs. *cti6* :

Rank	Score	Gene
5698	-1.158	*MSB2*
5784	-3.108	*FLO11*

ranking = 1 (most upregulated in *cti6*) to 5784 (most downregulated in cti6)

***sfl1* vs. *cti6* :**

Rank	Score	Gene
1	3.656	*SFL1 (b/c deleted* in *sfl1* strain)
5775	-3.116	*FLO11*
5776	-3.301	*FLO10*

ranking = 1 (most upregulated in *cti6*) to 5776 (most downregulated in cti6)

score = difference in median log intensity between the Cy5 and Cy3 channels at locus
cutoff scores for differential expression = 1.62 (upregulated) & -1.12 (downregulated)

TABLE 5 | **GO enrichments for all differentially expressed genes (genome-wide).**

WT vs. *cti6* :	***sfl1* vs. *cti6* :**
Upregulated in *cti6* relative to WT:	Upregulated in *cti6* relative to *sfl1* :
Biological Process unknown (61/74 genes)	No enrichment
Downregulated in *cti6* relative to WT:	Downregulated in *cti6* relative to *sfl1* :
Transmembrane transporter (*p* =0.005)	Mannose binding (*p* =1.27e-05) (*FLO10* , *11*)

FIGURE 6 | **Quantitative Real Time PCR detects differential levels of transcription from within the *FLO11* promoter region in *cti6* and *sfl1* mutants.** Quantitative real time PCR (with 2-fold dilutions) was performed using two pairs of real time primers specific to the *FLO11* promoter region, and normalized to levels of *SCR1* (an RNA PolIII -transcribed housekeeping RNA). Both sets of primers detected transcription products deriving from *FLO11* promoter sequence. These transcription products were elevated in the *cti6* mutant, which has the most silent *FLO11* promoter of the strains tested. In the *sfl1* mutant, the level of detected transcription was less than half the amount detected in the *cti6* mutant. In the variegating wild type strain, an intermediate level of transcription was detected. Both sets of primers detected similar transcription profiles, suggesting the detection of a single long transcript species rather than two separate transcripts.

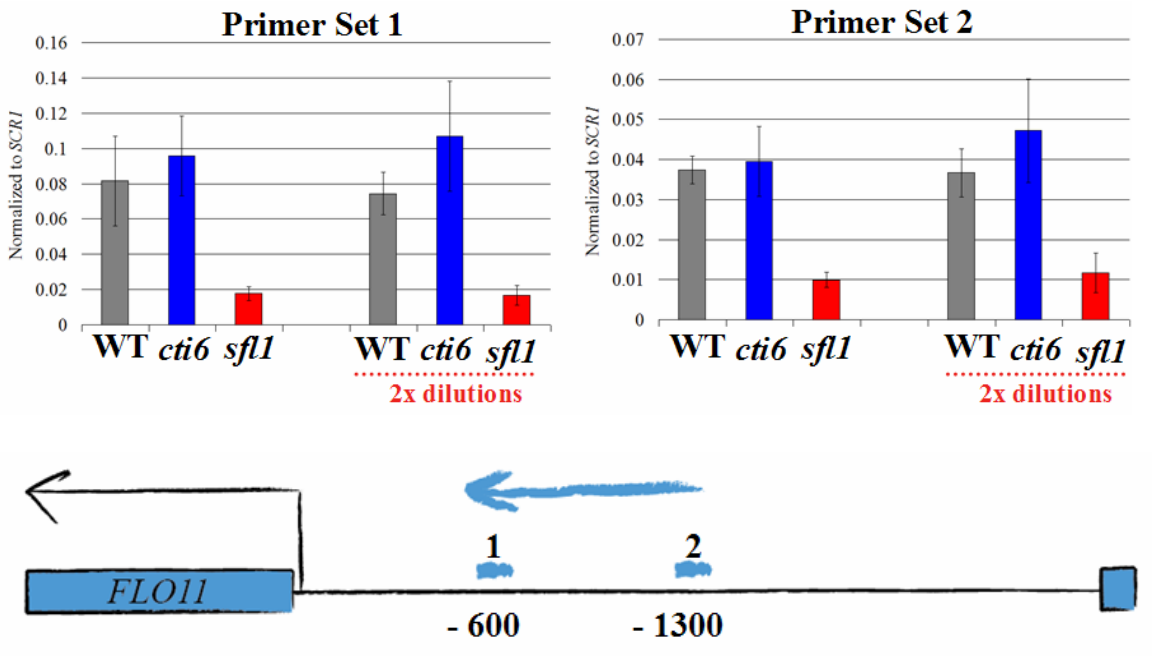

FIGURE 7 | **Real time PCR using primer pairs tiled along the *FLO11* locus reveals an inverse correlation in the *cti6* and *sfl1* mutants between the amount of transcription occurring within the *FLO11* promoter and the amount of expression of the *FLO11* ORF itself.** We used real time PCR to examine transcription in biological replicates of wild type, *cti6*, *sfl1*, and a strain in which the *FLO11* promoter has been deleted (p_{flo11}) over a region extending from +120 inside the *FLO11* ORF to -2280 of the *FLO11* promoter. Data was normalized to levels of *SCR1* (an RNA PolIII-transcribed housekeeping RNA). Two representative sets of results are presented below. In each experiment performed, transcription deriving from the *FLO11* promoter sequence was elevated in the *cti6* mutant relative to levels in the *sfl1* mutant. Conversely, expression of the *FLO11* ORF itself is vastly downregulated in the *cti6* mutant relative to the *sfl1* mutant.

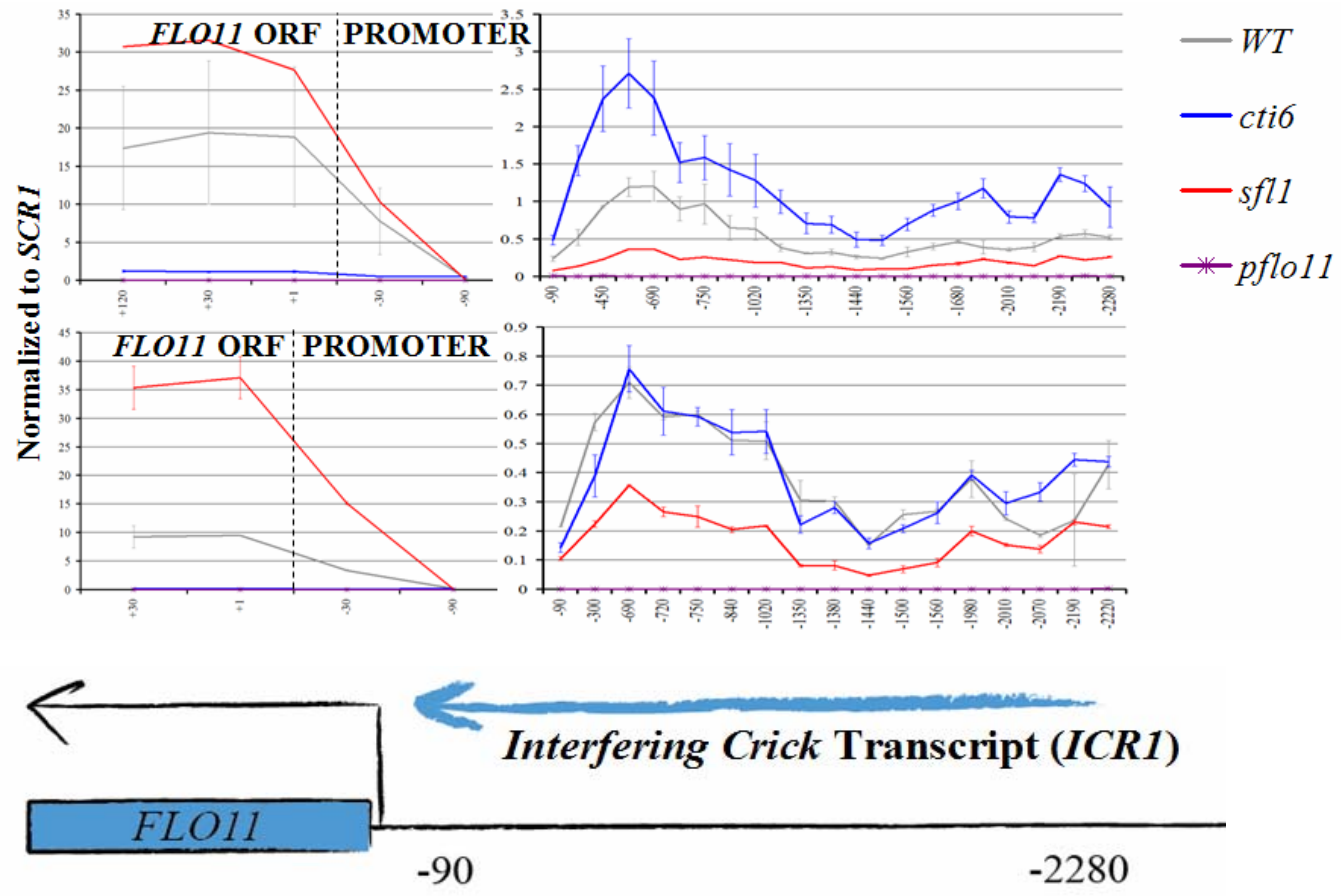

FIGURE 8 | **Strand-specific northern blot analyses reveal a ~3.2-kb Crick-strand noncoding RNA *ICR1* transcribed from within the *FLO11* promoter sequence.** Northern blot analysis was performed using poly-A selected RNA from wild type, *cti6*, *sfl1*, and *pflo11*. For probing, we used ^{32}P-labeled strand-specific RNA probes that hybridize to three different regions of the *FLO11* promoter sequence, as indicated in the diagram below. Probes 1, 2, and 3 hybridize to regions located -284 to -819, -1653 to -2255, and -2631 to -3226 relative to the beginning of the *FLO11* ORF, respectively. The results obtained using Crick strand-transcript specific probes are shown below. All three probes detect a specific transcript of approximately 3.2 kb that is most highly expressed in the *cti6* mutant and is expressed only at very low levels in the *sfl1* mutant. Signal was quantified and normalized to the *SCR1* loading control using ImageQuant software; histograms above each blot indicate the amount of transcript detected relative to the *SCR1* load control. These results indicate that a single ~3.2 kb noncoding transcript *ICR1* (Interfering Crick transcript) is indeed being transcribed in the Crick direction along nearly the entire length of the ~3.6 kb *FLO11* promoter. The steady-state levels of this *ICR1* transcript are inversely correlated with expression of the *FLO11* coding sequence in *cti6*, *sfl1*, and wild-type strains.

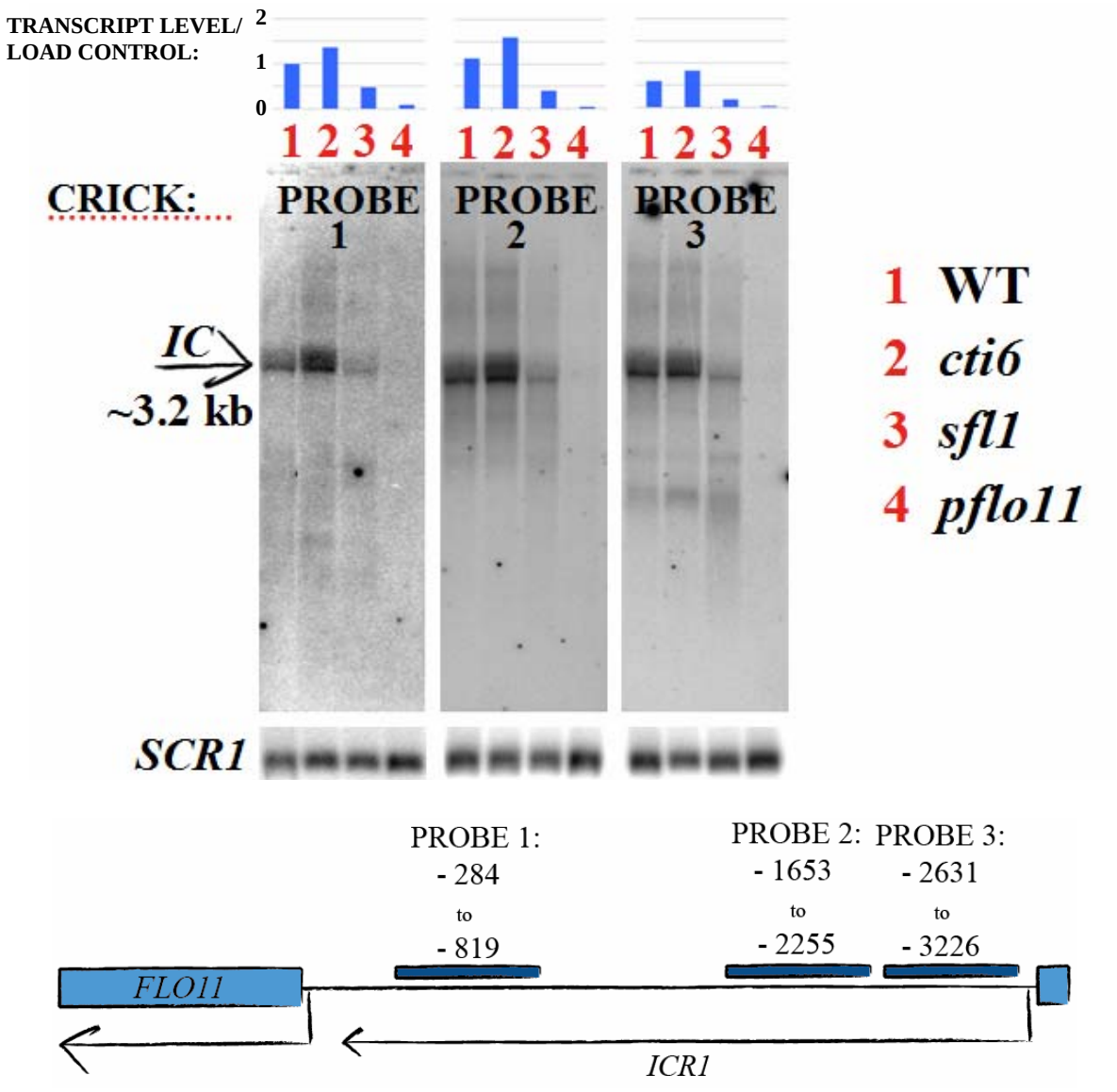

FIGURE 9 | **The *ICR1* transcript initiates at ~ - 3400 and terminates near or within the *FLO11* ORF.** Rapid amplification of cDNA ends (RACE) was used to map the 3′ and 5′ ends of the *ICR1* transcript in wild type, *cti6*, *sfl1*, and p_{flo11} cells. The 3′ ends of *ICR1* identified by RACE in wild type, *cti6*, and *sfl1* cells are represented as blue lollipops. In wild type, *cti6*, and *sfl1*, a strong stop was detected at -209, which is located approximately 120 basepairs upstream of the putative *FLO11* TATA box present at -92. Some 3′ends that extend up to or run into the *FLO11* coding sequence were detected in *cti6* and in wild type. No 3′ends were obtained from the p_{flo11} negative control cells. The detected 5′ ends of *ICR1* are represented by blue arrows. Of the cloned 5′ ends that mapped to the *FLO11* promoter sequence, the *cti6* mutant exhibits the highest number (50%) of cloned 5′*ICR1* sequences in a region of the *FLO11* promoter (-3421 to -3197) that is sufficiently far away from the identified 3′ ends to produce the ~3.2 kb band observed in the northern blots. We also identified 5′*ICR1* ends in this region for wild type and *sfl1*, but these occurred at much lower frequency than in *cti6*. No 5′ends were obtained from the p_{flo11} negative control cells. Some additional 5′ends were detected at various locations (indicated by the blue tick marks) along the *FLO11* promoter sequence, but none of these additional 5′ends corresponds in size to any abundant transcripts observed by northern analysis. Rather than a single strong 5′start site for *ICR1*, we identified transcripts initiating over a range of ~200 basepairs. Black arrows indicate the binding locations of target-specific oligos used; oligo sequences are included in Table 3.

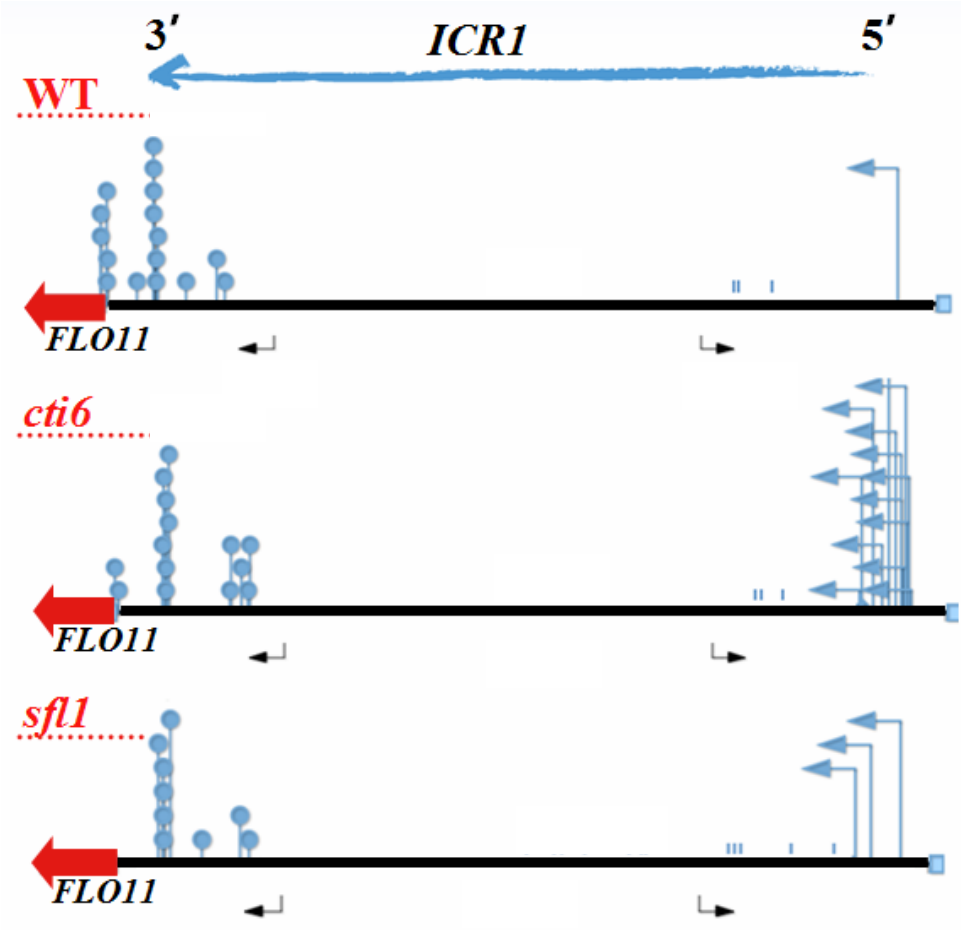

TABLE 6 | **Summary of 3' ends of the *ICR1* transcript detected by RACE.** A strong stop was detected at -209 (highlighted in royal blue). Only in *cti6* and in wild type do we observe *ICR1* transcripts that extend to within a few base pairs of, and sometimes into, the *FLO11* ORF sequence (highlighted in light blue).

cti6	WT	*sfl1*	*pflo11*
+ 10	+ 24	- 189	none
- 6	+ 24	- 209	
- 195	- 2	- 209	
- 200	- 2	- 209	
- 209	- 4	- 209	
- 209	- 132	- 238	
- 209	- 209	- 366	
- 221	- 209	- 521	
- 222	- 209	- 557	
- 486	- 209		
- 490	- 214		
- 535	- 215		
- 563	- 222		
- 572	- 343		
	- 475		
	- 510		

TABLE 7 | **Summary of 5' ends of the *ICR1* transcript detected by RACE.** Rather than a single strong 5′ start site for *ICR1*, we identified transcripts initiating over a range of ~200 basepairs. 50% of cloned 5′ ends from *cti6* map to a region of the *FLO11* promoter (+3421 to +3197) that is sufficiently far away from the identified 3′ ends to produce the ~3.2 kb band observed in the northern blots.

WT	*cti6*	*sfl1*	*pflo11*
- 3407	- 3421	- 3445	none
	- 3411	- 3315	
	- 3398	- 3244	
	- 3397		
	- 3385		
	- 3375		
	- 3375		
	- 3351		
	- 3321		
	- 3294		
	- 3256		
	- 3204		
	- 3197		
11.1%	50.0%	17.6%	0.0%

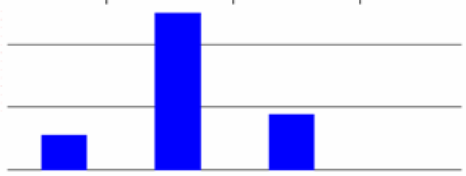

FIGURE 10 | **Elevated *ICR1* levels correlates with loss of TBP binding to the *FLO11* core promoter in the *cti6* mutant.** Examination of yeast TATA binding protein (TBP) localization to the *FLO11* promoter was performed by ChIP-chip analyses using anti-TBP antibody on whole cell extracts derived from wild type, *cti6*, and *sfl1* cells. TBP localization to the *FLO11* core promoter is abolished in the *cti6* mutants, in which steady-state *ICR1* transcript levels are elevated, a finding reminiscent of the mechanism of promoter occlusion proposed for *SRG1*-regulation of *SER3* (Martens et al., 2004; Martens et al., 2005). TBP localization to the *FLO11* core promoter in the *sfl1* mutant appears to be increased above wild type levels of localization.

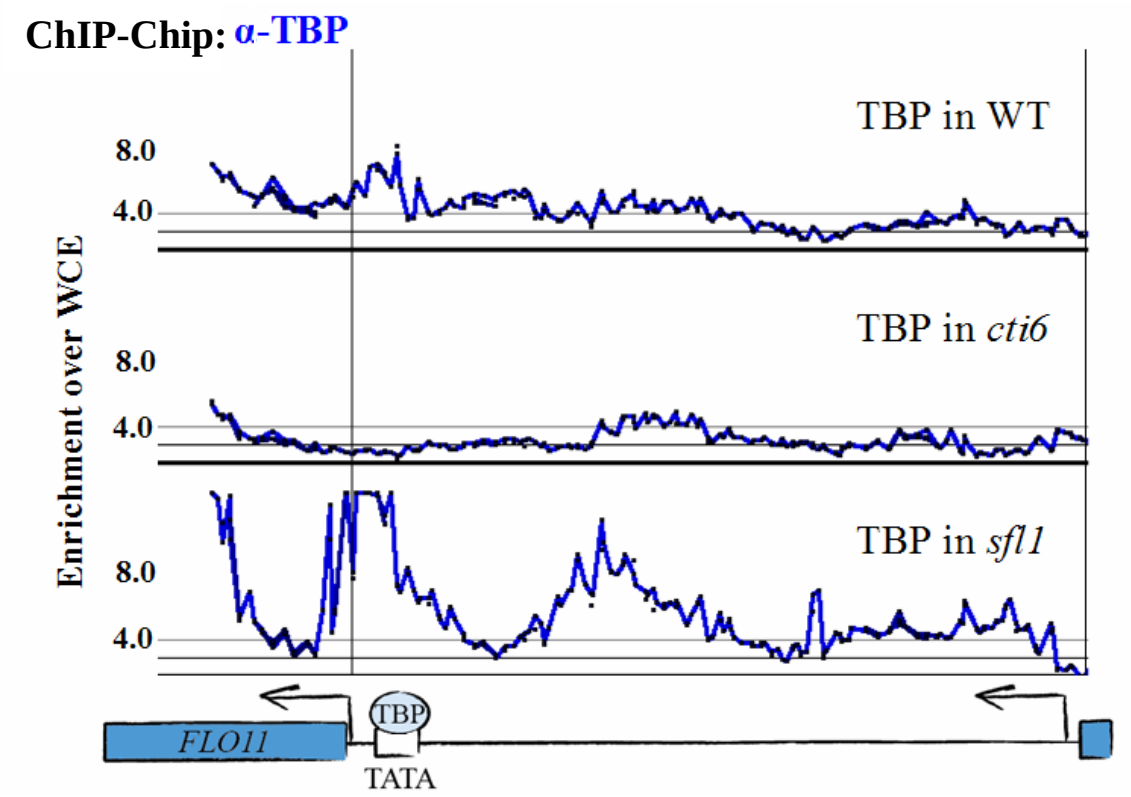

FIGURE 11 | **Elevated *ICR1* levels correlate with decreased nucleosome ejection from the *FLO11* core promoter in the *cti6* mutant.** *(A)* Gene-specific ChIP using anti-H3 and anti-H4 antibodies on wild type cells provides a baseline for nucleosome positioning along the *FLO11* promoter. *(B)* ChIP-chip analyses using an anti-H4 antibody on whole cell extracts derived from wild type, *cti6*, and *sfl1* cells reveals that nucleosome eviction fails to occur at the *FLO11* core promoter in the *cti6* mutant. Conversely, nucleosome eviction at the *FLO11* core promoter is elevated over wild type in the *sfl1* mutant, in which *ICR1* transcription is low.

A.

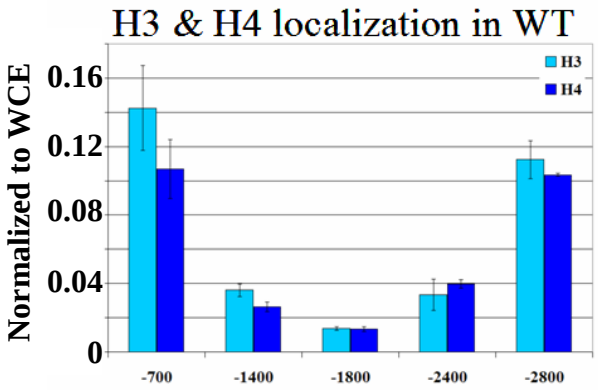

B.

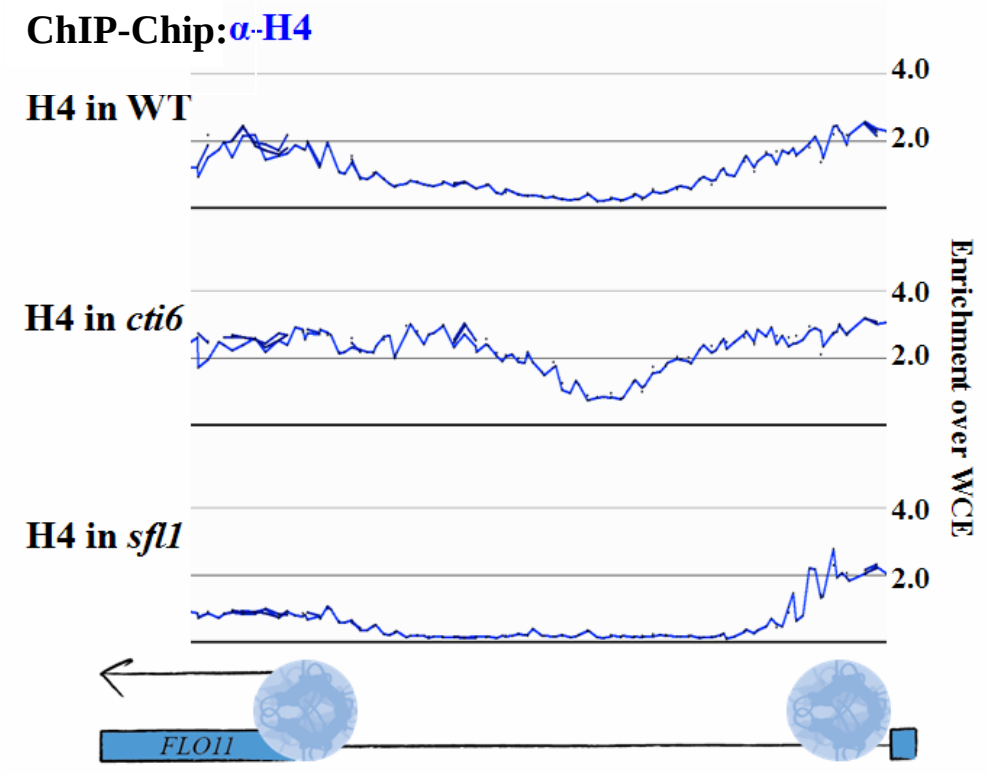

FIGURE 12 | **Termination of *ICR1* in the Rpd3L- mutant *cti6* results in the recovery of *FLO11*-dependent haploid adhesion.** To test the model that *ICR1* has a causal effect in repressing *FLO11* expression by the act of its being transcribed through the *FLO11* promoter, we performed an experiment to determine whether termination of *ICR1* transcription could recover *FLO11* expression, as assayed by the recovery of *FLO11*-dependent haploid adhesion. *(A)* We inserted a 1.4-kb construct containing the *K. lactis URA3* gene under its own promoter and with its transcriptional terminator intact in the Crick direction at -3041 within the *FLO11* promoter region. This insertion places the construct downstream of the *ICR1* transcription initiation region. *(B)* Wild type, *cti6*, and *sfl1* strains, with and without the *URA3*-terminator construct, were patched onto YPD-agar plates and allowed to grow for four days at 30 degrees C before being subjected to the standard plate washing assay for yeast haploid adhesion (Guo et al., 2000). As previously observed, the *cti6* mutant without the *URA3*-terminator construct fails to adhere to the YPD-agar, but the *cti6* strain carrying the *URA3*-terminator construct shows a rescue of the non-adherent *cti6* phenotype.

A.

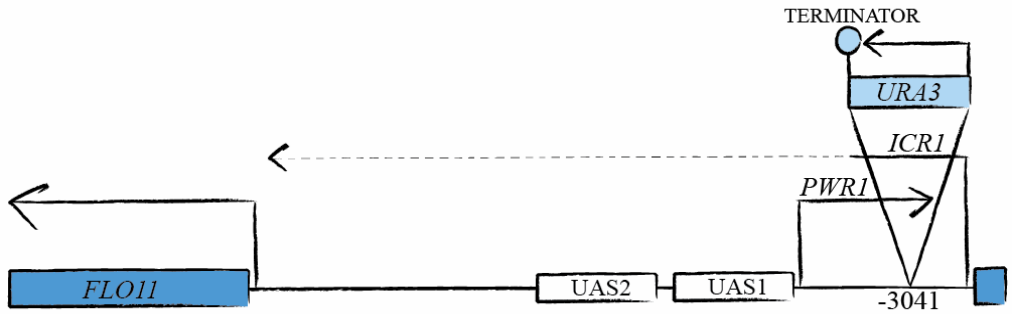

B.

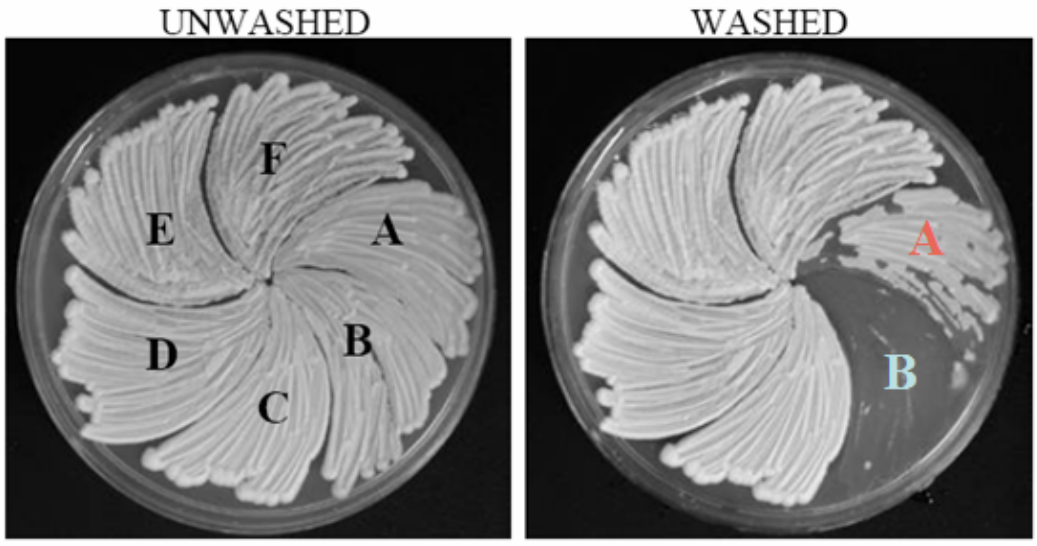

A	***cti6* + P_{FLO11}-*Terminator***
B	***cti6***
C	***WT* + P_{FLO11}-*Terminator***
D	***WT***
E	***sfl1* + P_{FLO11}-*Terminator***
F	***sfl1***

FIGURE 13 | **A second noncoding transcript, *PWR1*, is repressed by Sfl1 and is transcribed in the Watson direction covergently and overlapping with *ICR1*.** To characterize further the transcription occurring within the *FLO11* promoter, we performed expression analysis using *S. cerevisiae* Sigma 1278b genomic high-density tiling microarrays with Crick and Watson strand specificity. Crick strand transcription is indicated by a minus (-) sign and Watson strand transcription is indicated by a plus (+) sign. A comparison of the transcriptional profiles in *sfl1* cells (Cy-5 labeled strand-specific cDNA reverse-transcribed from Poly-A RNA, shown in red) versus *cti6* cells (Cy-3 labeled strand-specific cDNA reverse-transcribed from Poly-A RNA, shown in green) revealed the presence, not only of the *ICR1* transcript, but also of a second noncoding transcript *PWR1* (for Promoting Watson RNA) that initiates approximately 2.3 kilobases away from the beginning of the *FLO11* ORF and is transcribed in the Watson direction convergently and overlapping with the *ICR1* transcript. In these data, transcription of *PWR1* is observed in the *sfl1* mutant, but not at all in the *cti6* mutant.

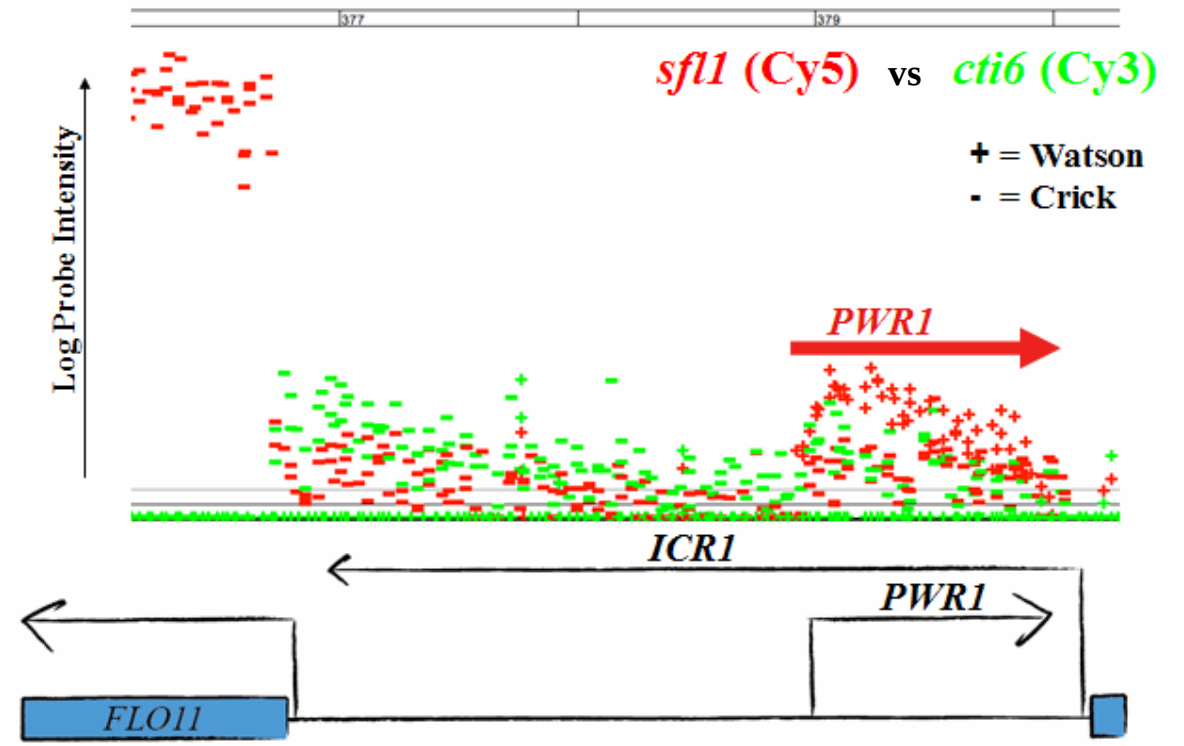

FIGURE 14 | **Strand-specific northern blot analyses confirm the existence of a ~1.2-kb Watson-strand noncoding RNA *PWR1* transcribed from within the *FLO11* promoter sequence.** Northern blot analysis was performed using poly-A selected RNA from wild type, *cti6*, *sfl1*, and *pflo11*. For probing, we used ^{32}P-labeled strand-specific RNA probes that hybridize to three different regions of the *FLO11* promoter sequence, as indicated in the diagram below. Probes 1, 2, and 3 hybridize to regions located -284 to -819, -1653 to -2255, and -2631 to -3226 relative to the beginning of the *FLO11* ORF, respectively. The results obtained using Watson strand-transcript specific probes are shown below. Signal was quantified and normalized to the *SCR1* loading control using ImageQuant software; histograms above each blot indicate the amount of transcript detected relative to the *SCR1* load control. Probes 2 and 3 detect a specific transcript of approximately 1.2 kb that is most highly expressed in the *sfl1* mutant and is not expressed in the *cti6* mutant. An intermediate level of this transcript is observed in the variegating wild type cells. The steady-state levels of this *PWR1* transcript are positively correlated with expression of the *FLO11* coding sequence in *cti6*, *sfl1*, and wild-type strains. Transcription of *PWR1* appears to be repressed by the DNA-binding protein Sfl11. In the *sfl1* mutant, elevated steady-state levels of the *PWR1* transcript correlate with increased *FLO11* expression.

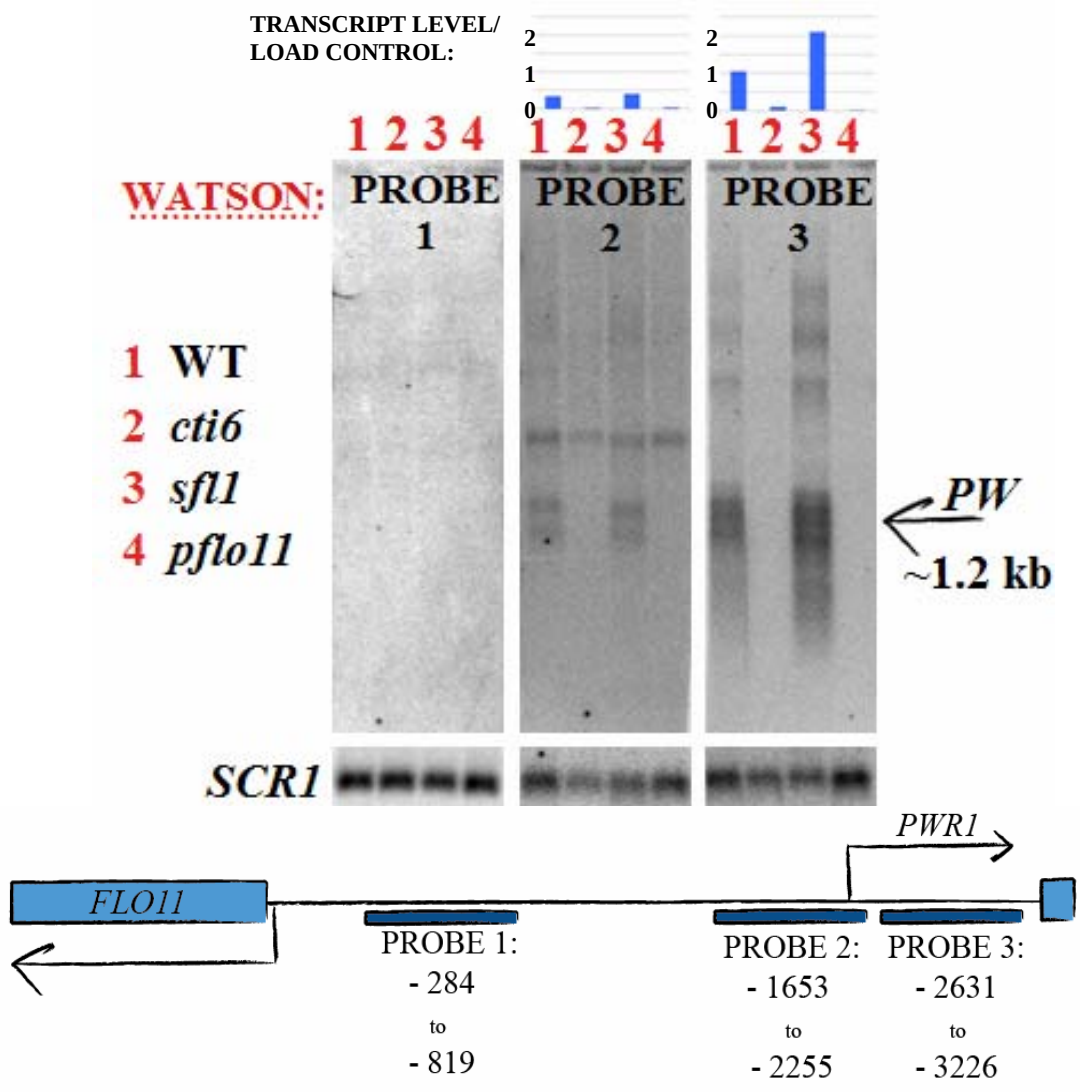

FIGURE 15 | **5' and 3' RACE indicates that the *PWR1* transcript initiates ~2.3 kb upstream of the *FLO11* ORF and terminates near the transcription initiation site of *ICR1*.** RACE was used to map the 3′ and 5′ ends of the *PWR1* transcript in wild type and *sfl1* cells. The identified 3' ends of *PWR1* are represented as red lollipops. The termination sites cluster between -3155 and -3409 relative to the beginning of the *FLO11* ORF, indicating that *PWR1* terminates near the transcription start site of *ICR1*. The 5′ ends of the *PWR1* transcript are represented as red arrows. Rather than a single strong 5′start site for *PWR1*, we identified transcripts initiating over a short range of ~150 basepairs, clustered around -2300 relative to the beginning of the *FLO11* ORF. Black arrows indicate the binding locations of target-specific oligos used; oligo sequences are included in Table 3.

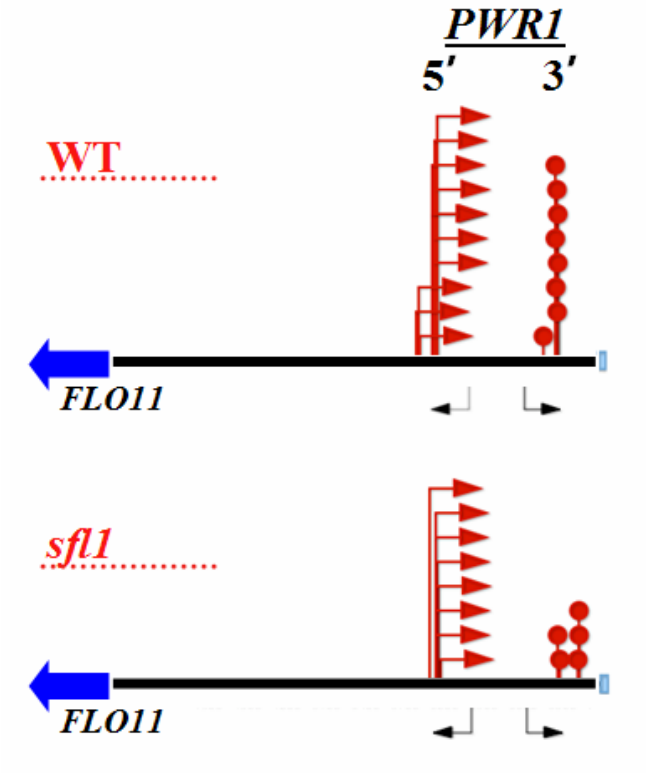

TABLE 8 | **Summary of 3' ends of the *PWR1* transcript detected by RACE.** The termination sites of PWR1 cluster between -3155 and -3409 relative to the beginning of the *FLO11* ORF, indicating that *PWR1* terminates near the transcription start site of *ICR1*.

WT	*sfl1*
- 3155	- 3246
- 3155	- 3263
- 3246	- 3399
- 3250	- 3408
- 3258	- 3409
- 3260	
- 3264	
- 3264	

TABLE 9 | **Summary of 5' ends of the *PWR1* transcript detected by RACE.** The transcription start sites of PWR1 cluster around -2300 relative to the beginning of the *FLO11* ORF. This places the start site of *PWR1* just upstream of the UAS1 region.

WT	*sfl1*
- 2190	- 2270
- 2206	- 2315
- 2213	- 2315
- 2306	- 2324
- 2306	- 2328
- 2306	- 2334
- 2324	- 2339
- 2324	
- 2324	
- 2324	
- 2342	
- 2350	

FIGURE 16 | **The *PWR1* transcript interferes with expression of a convergent and overlapping Crick-strand reporter construct.** Transcription of *PWR1* interferes with expression of the *K. lactis URA3* reporter construct integrated at position -3041 in the *FLO11* promoter. The *URA3* reporter is transcribed in the Crick direction convergently and overlapping with *PWR1* in an *ICR1*-like manner. *(A)* The size of colonies growing on SC-Ura media, used an indicator of *URA3* expression, demonstrates that the *URA3* gene is expressed most highly in the *cti6* mutant, in which no *PWR1* transcript is detected. In the *sfl1* mutant background, in which *PWR1* transcript levels are elevated, *URA3* reporter expression is very low, resulting in only microcolonies growing on the SC-Ura media. Wild type cells, which exhibit an intermediate level of *PWR1* expression, also exhibit a level of *URA3* reporter expression that is intermediate between *cti6* and *sfl1*. *(B)* Serial dilutions of these strains onto SC+5-FOA and SC–Ura also confirm these findings. More cells in the *cti6* background are actively expressing the *URA3* reporter construct, therefore more cells of this genotype are able to grow on SC–Ura and fewer on SC+5-FOA. Conversely, more cells in the *sfl1* background are silenced for *URA3* reporter expression, therefore more of these cells are able to grow on SC+5-FOA and fewer on SC–Ura.

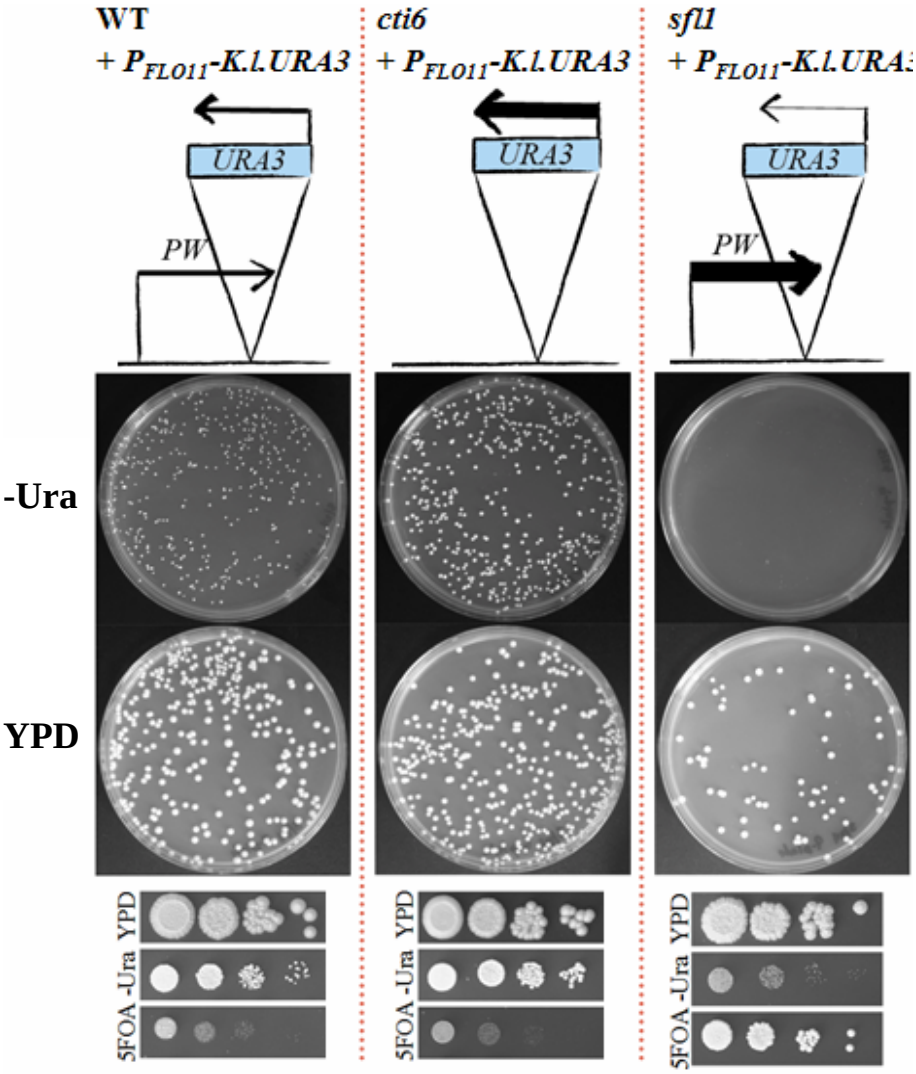

FIGURE 17 | **A similar pair of a convergent and overlapping noncoding RNAs are transcribed within the *FLO10* promoter region.** We performed expression analysis using *S. cerevisiae* Sigma 1278b genomic high-density tiling microarrays with Crick and Watson strand specificity. Crick strand transcription is indicated by a minus (-) sign and Watson strand transcription is indicated by a plus (+) sign. A comparison of the transcriptional profiles in *sfl1* cells (Cy-5 labeled strand-specific cDNA reverse-transcribed from Poly-A RNA, shown in red) versus *cti6* cells (Cy-3 labeled strand-specific cDNA reverse-transcribed from Poly-A RNA, shown in green) reveal the presence of a similar pair of convergent, overlapping noncoding transcripts initiating within the *FLO10* promoter region. *FLO10* expression is upregulated in the *sfl1* mutant and this upregulation is correlated with the transcription of a noncoding Crick-strand RNA that is (i) derepressed in the *sfl1* mutant (ii) transcribed divergently from the protein-coding *FLO10* gene (which is transcribed in the Watson direction), and (iii) transcribed convergently and overlapping with a second noncoding Watson-strand transcript that is detected in both the *sfl1* and *cti6* mutants.

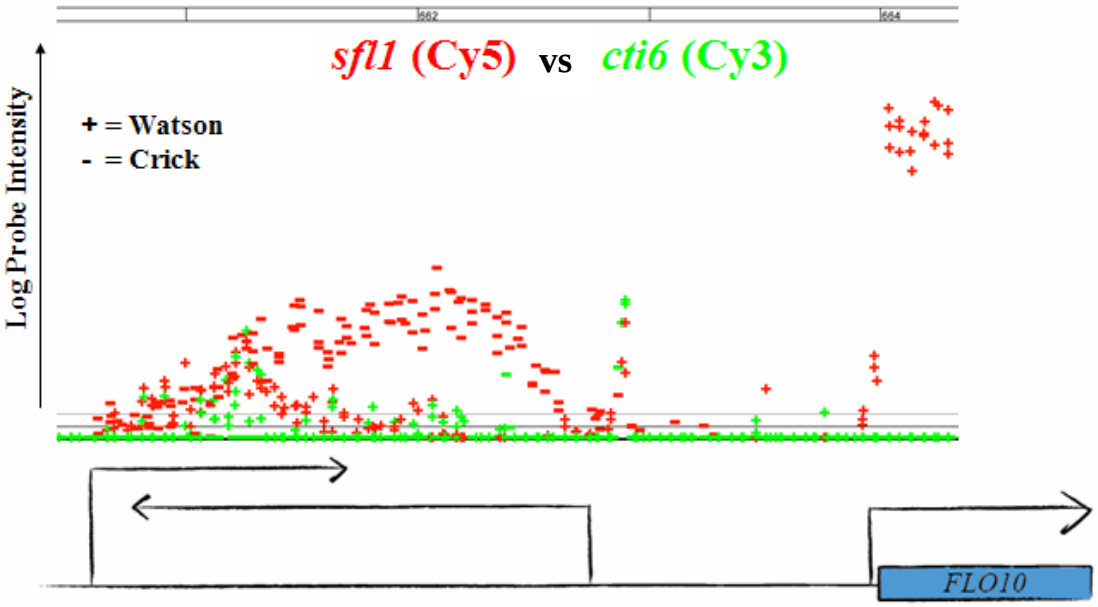

FIGURE 18 | **A new model to inform the mechanism underlying variegated transcription of *FLO* genes.** Components shown in light blue have net positive effects on *FLO11* transcription. Components shown in red have net negative effects on *FLO11* transcription. Components represented as ovals are confirmed *trans*-acting protein factors involved in the regulation of *FLO11* transcription. Question marks (?) indicate unknown components.

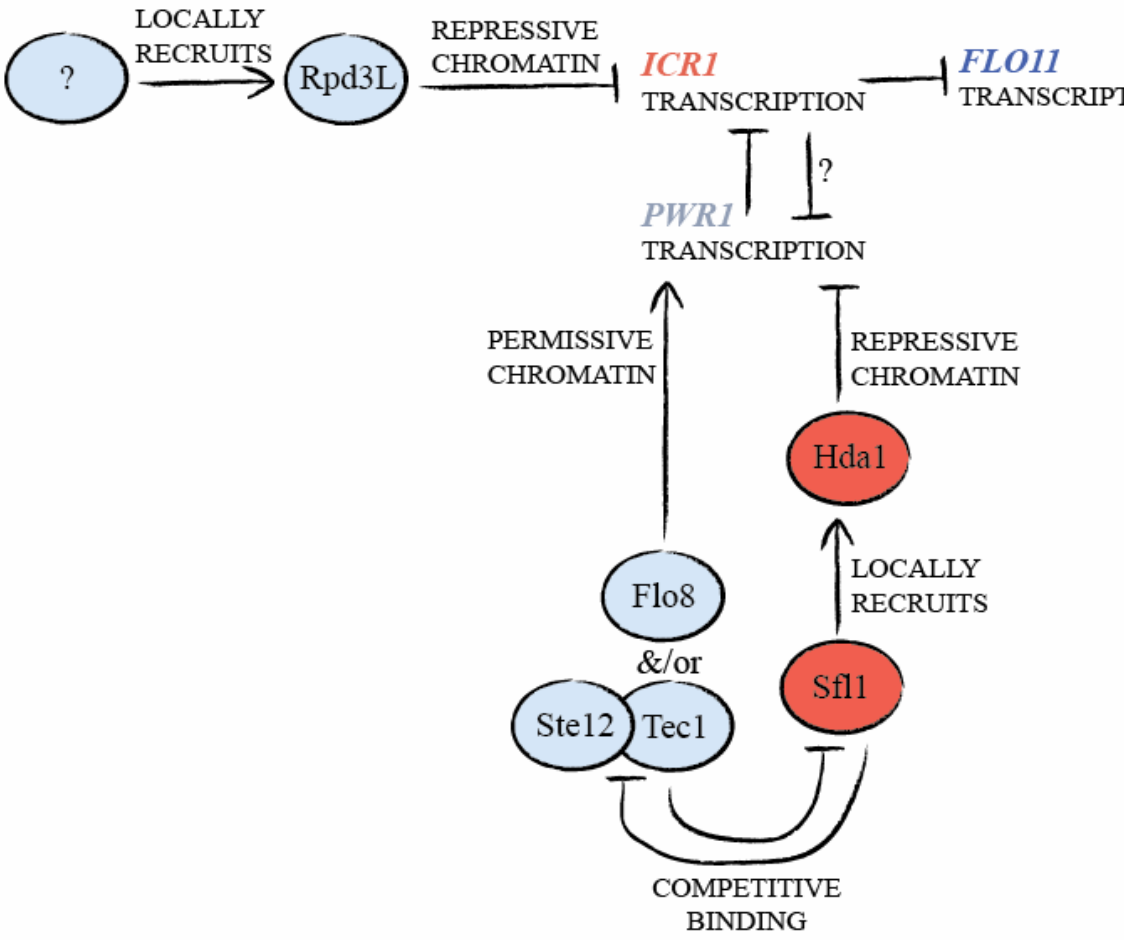

SUPPLEMENTAL TABLE 1 | The list of 75 published (confirmed or putative) regulators of FLO11 transcription used in differential expression analysis summarized in Figure 5 of this chapter.

ADH1	*GND1*	*RAS2*
ARO7	*GPA2*	*RGA1*
AXL1	*GPR1*	*RIM1*
BCY1	*GTR1*	*RIM13*
BEM2	*HDA1*	*RIM8*
BMH1	*HDA2*	*RIM9*
BMH2	*HDA3*	*SFL1*
BPL1	*HSC82*	*SKN7*
BUD10	*HSL1*	*SRB10*
BUD3	*HSL7*	*SRB11*
BUD4	*HSM2*	*SRB9*
CDC24	*IME2*	*SSN6*
CDC42	*IRA1*	*STE11*
CDC53	*IRA2*	*STE12*
CSE2	*KSS1*	*STE20*
CYR1	*MED1*	*STE50*
DIA1	*MEP2*	*STE7*
DIA2	*MGA1*	*TAF25*
DIA3	*MSB2*	*TEC1*
DIA4	*MSN1*	*TPK1*
DIG1	*MSN5*	*TPK2*
DIG2	*MSS11*	*TPK3*
ELM1	*OPI1*	*TUP1*
FLO8	*PGI1*	*YDJ1*
GCR1	*PLC1*	*ZUO1*

Note: DIA3 was removed from the final analysis b/c of outliers,
but was not expressed above background.

SUPPLEMENTAL FIGURE 1 | **The Rpd3-Myc epitope-tagged allele maintains wild type Rpd3 function.** *(A)* Haploid-adhesion tests were performed to ensure that the Myc-tag did not compromise Rpd3 function. Wild-type (10560-6B), *rpd3* (SBY847), and strains carrying the Rpd3-Myc allele (SBY910 *MATx* and SBY946 *MATa*) were patched onto YPD-agar plates and allowed to grow for four days at 30 degrees C before being subjected to the standard plate washing assay for yeast haploid adhesion (Guo et al., 2000). The Rpd3-Myc strains adhered to the agar as well as wld-type, indicating that the epitope tag has not compromised Rpd3 function. *(B)* Serial dilutions onto SC, SC-Ura, and SC+5FOA of strains carrying the reporter P_{FLO11}-*URA3* construct as well as the Rpd3-Myc allele (SBY931 *MATa* and SBY934 *MATx*) also indicate that this epitope-tagged allele is functional. The Rpd3-Myc strains variegate in their expression from the *FLO11* promoter indistinguishably from the strain carrying unmodified Rpd3 (SBY251), as determined by their ability to grow on the selective media.

A.

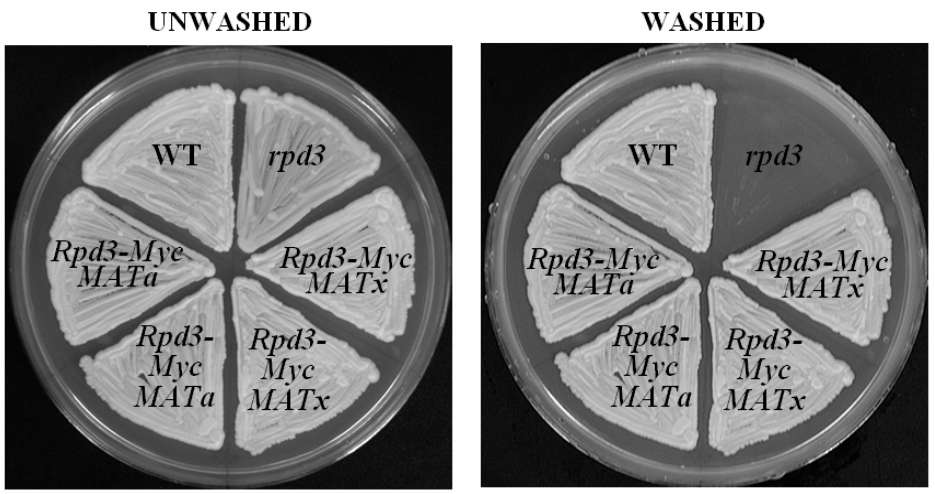

B.

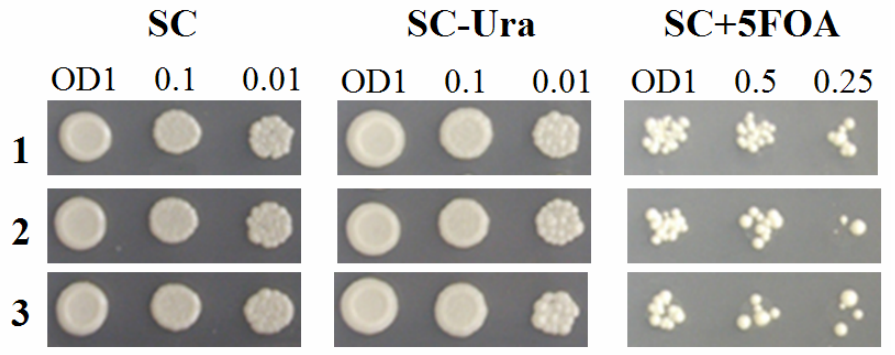

1 P_{FLO11}-*URA3*
2 P_{FLO11}-*URA3 Rpd3-Myc MATa*
3 P_{FLO11}-*URA3 Rpd3-Myc MATx*

References

Andrau, J.C., van de Pasch, L., Lijnzaad, P., Bijma, T., Koerkamp, M.G., van de Peppel, J., Werner, M., and Holstege, F.C. (2006). Genome-wide location of the coactivator mediator: Binding without activation and transient Cdk8 interaction on DNA. Molecular Cell *22*, 179-192.

Berretta, J., Pinskaya, M., and Morillon, A. (2008). A cryptic unstable transcript mediates transcriptional trans-silencing of the Ty1 retrotransposon in S. cerevisiae. Genes & Development *22*, 615-626.

Camblong, J., Iglesias, N., Fickentscher, C., Dieppois, G., and Stutz, F. (2007). Antisense RNA stabilization induces transcriptional gene silencing via histone deacetylation in S. cerevisiae. Cell *131*, 706-717

Carrozza, M.J., Florens, L., Swanson, S.K., Shia, W.J., Anderson, S., Yates, J., Washburn, M.P., and Workman, J.L. (2005a). Stable incorporation of sequence specific repressors Ash1 and Ume6 into the Rpd3L complex. Biochimica et Biophysica Acta *1731*, 77-87; discussion 75-76.

Carrozza, M.J., Li, B., Florens, L., Suganuma, T., Swanson, S.K., Lee, K.K., Shia, W.J., Anderson, S., Yates, J., Washburn, M.P., *et al.* (2005b). Histone H3 methylation by Set2 directs deacetylation of coding regions by Rpd3S to suppress spurious intragenic transcription. Cell *123*, 581-592.

Conlan, R.S., and Tzamarias D. (2001). Sfl1 functions via the co-repressor Ssn6-Tup1 and cAMP-dependent protein kinase Tpk2. Journal of Molecular Biology *309*, 1007-1015.

Cullen, P.J., Sabbagh, W., Jr., Graham, E., Irick, M.M., van Olden, E.K., Neal, C., Delrow, J., Bardwell, L., and Sprague, G.F., Jr. (2004). A signaling mucin at the head of the Cdc42- and MAPK-dependent filamentous growth pathway in yeast. Genes & Development *18*, 1695-1708.

Davie, J.K., Edmondson, D.G., Coco, C.B., and Dent, S.Y. (2003). Tup1-Ssn6 interacts with multiple class I histone deacetylases *in vivo*. Journal of Biological Chemistry *278*, 50158-50162.

De Nadal, E., Zapater, M., Alepuz, P.M., Sumoy, L., Mas, G., and Posas, F. (2004). The MAPK Hog1 recruits Rpd3 histone deacetylase to activate osmoresponsive genes. Nature *427*, 370-374.

Gancedo, J.M. (2001). Control of pseudohyphae formation in Saccharomyces cerevisiae. FEMS Microbiology Reviews *25*, 107-123.

Grunstein, M. (1997). Histone acetylation in chromatin structure and transcription. Nature *389*, 349-352.

Gueldener,U., Heinisch,J., Koehler,G.J., Voss,D. and Hegemann,J.H. (2002) A second set of loxP marker cassettes for Cre-mediated multiple gene knockouts in budding yeast. Nucleic Acids Research *30*, e23.

Guo, B., Styles, C.A., Feng, Q., and Fink, G.R. (2000). A Saccharomyces gene family involved in invasive growth, cell-cell adhesion, and mating. Proceedings of the National Academy of Sciences of the United States of America *97*, 12158-12163.

Guthrie, C., and Fink, G.R. (2001). Guide to Yeast Genetics and Molecular and Cell Biology. Methods of Enzymology *350* and *351*.

Halme, A., Bumgarner, S., Styles, C., and Fink, G.R. (2004). Genetic and epigenetic regulation of the FLO gene family generates cell-surface variation in yeast. Cell *116*, 405-415.

Hengartner, C.J., Myer, V.E., Liao, S.M., Wilson, C.J., Koh, S.S., and Young, R.A. (1998). Temporal regulation of RNA polymerase II by Srb10 and Kin28 cyclin-dependent kinases. Molecular Cell *2*, 43-53.

Hepworth, S.R., Friesen, H., and Segall, J. (1998). NDT80 and the meiotic recombination checkpoint regulate expression of middle sporulation-specific genes in Saccharomyces cerevisiae. Molecular and Cellular Biology *18*, 5750-5761.

Hongay, C.F., Grisafi, P.L., Galitski, T., and Fink, G.R. (2006). Antisense transcription controls cell fate in Saccharomyces cerevisiae. Cell *127*, 735-745.

Jackson, J.C., and Lopes, J.M. (1996). The yeast UME6 gene is required for both negative and positive transcriptional regulation of phospholipid biosynthetic gene expression. Nucleic Acids Research *24*, 1322-1329.

Joazeiro, C.A., Kassavetis, G.A., and Geiduschek, E.P. (1994). Identical components of yeast transcription factor IIIB are required and sufficient for transcription of TATA box-containing and TATA-less genes. Molecular and Cellular Biology *14*, 2798-2808.

Kadosh, D., and Struhl, K. (1997). Repression by Ume6 involves recruitment of a complex containing Sin3 corepressor and Rpd3 histone deacetylase to target promoters. Cell *89*, 365-371.

Kadosh, D., and Struhl, K. (1998). Targeted recruitment of the Sin3-Rpd3 histone deacetylase complex generates a highly localized domain of repressed chromatin in vivo. Molecular and Cellular Biology *18*, 5121-5127.

Kim, T.S., Kim, H.Y., Yoon, J.H., and Kang, H.S. (2004a). Recruitment of the Swi/Snf complex by Ste12-Tec1 promotes Flo8-Mss11-mediated activation of STA1 expression. Molecular and Cellular Biology *24*, 9542-9556.

Kim, T.S., Lee, S.B., and Kang, H.S. (2004b). Glucose repression of STA1 expression is mediated by the Nrg1 and Sfl1 repressors and the Srb8-11 complex. Molecular and Cellular Biology *24,* 7695-7706.

Lee, T.I., and Young, R.A. (2000). Transcription of eukaryotic protein-coding genes. Annual Review of Genetics *34*, 77-137.

Lee, T.I., Johnstone, S.E., and Young, R.A. (2006). Chromatin immunoprecipitation and microarray-based analysis of protein location. Nature Protocols *1*, 729-748.

MacIsaac, K.D., and Fraenkel, E. (2006). Practical strategies for discovering regulatory DNA sequence motifs. PLoS Computational Biology *2,* e36.

Martens, J.A., Laprade, L., and Winston, F. (2004). Intergenic transcription is required to repress the Saccharomyces cerevisiae SER3 gene. Nature *429,* 571-574.

Martens, J.A., Wu, P.Y., and Winston, F. (2005). Regulation of an intergenic transcript controls adjacent gene transcription in Saccharomyces cerevisiae. Genes & Development *19,* 2695-2704.

Matys, V., Fricke, E., Geffers, R., Gobling, E., Haubrock, M., Hehl, R., Hornischer, K., Karas, D., Kel, A.E., Kel-Margoulis, O.V., Kloos, D.U., Land, S., Lewicki-Potapov, B., Michael, H., Munch, R., Reuter, I., Rotert, S., Saxel, H., Scheer, M., Thiele, S., Wingender, E. (2003). TRANSFAC: transcriptional regulation, from patterns to profiles. Nucleic Acids Research *31,* 374-378.

McKenzie, E.A., Kent, N.A., Dowell, S.J., Moreno, F., Bird, L.E., and Mellor, J. (1993). The centromere and promoter factor, 1, CPF1, of Saccharomyces cerevisiae modulates gene activity through a family of factors including SPT21, RPD1 (SIN3), RPD3 and CCR4. Mol Gen Genet *240,* 374-386.

Miura, F., Kawaguchi, N., Sese, J., Toyoda, A., Hattori, M., Morishita, S., and Ito, T. (2006). A large-scale full-length cDNA analysis to explore the budding yeast transcriptome. Proceedings of the National Academy of Sciences of the United States of America *103*, 17846-17851.

Mumberg, D., Muller, R. & Funk, M. (1995) Yeast vectors for the controlled expression of heterologous proteins in different genetic backgrounds. Gene *156*, 119–122.

Nagalakshmi, U., Wang, Z., Waern, K., Shou, C., Raha, D., Gerstein, M., and Snyder, M. (2008). The Transcriptional Landscape of the Yeast Genome Defined by RNA Sequencing. Science *320,* 1344-1349.

Nelson, C., Goto, S., Lund, K., Hung, W., and Sadowski, I. (2003). Srb10/Cdk8 regulates yeast filamentous growth by phosphorylating the transcription factor Ste12. Nature *421*, 187-190.

Newton, I. (1687). Philosophiae Naturalis Principia Mathematica.

Palecek, S.P., Parikh, A.S., and Kron, S.J. (2000). Genetic analysis reveals that FLO11 upregulation and cell polarization independently regulate invasive growth in Saccharomyces cerevisiae. Genetics *156*, 1005-1023.

Palecek, S.P., Parikh, A.S., and Kron, S.J. (2002). Sensing, signalling and integrating physical processes during Saccharomyces cerevisiae invasive and filamentous growth. Microbiology *148*, 893-907.

Pan, X., and Heitman, J. (2002). Protein kinase A operates a molecular switch that governs yeast pseudohyphal differentiation. Molecular and Cellular Biology *22*, 3981-3993.

Qi, Y., Rolfe, A., MacIsaac, K.D., Gerber, G.K., Pokholok, D., Zeitlinger, J., Danford, T., Dowell, R.D., Fraenkel, E., Jaakkola, T.S., Young, R.A., and Gifford, D.K. (2006) High-resolution computational models of genome binding events. Nature Biotechnology *24*, 963-970.

Robert, F., Pokholok, D.K., Hannett, N.M., Rinaldi, N.J., Chandy, M., Rolfe, A., Workman, J.L., Gifford, D.K., and Young, R.A. (2004). Global position and recruitment of HATs and HDACs in the yeast genome. Molecular Cell *16*, 199-209.

Rupp, S., Summers, E., Lo, H.J., Madhani, H., and Fink, G. (1999). MAP kinase and cAMP filamentation signaling pathways converge on the unusually large promoter of the yeast FLO11 gene. The EMBO Journal *18*, 1257-1269.

Sertil, O., Vemula, A., Salmon, S.L., Morse, R.H., and Lowry, C.V. (2007). Direct role for the Rpd3 complex in transcriptional induction of the anaerobic DAN/TIR genes in yeast. Molecular and Cellular Biology *27*, 2037-2047.

Sharma, V.M., Tomar, R.S., Dempsey, A.E., and Reese, J.C. (2007). Histone deacetylases RPD3 and HOS2 regulate the transcriptional activation of DNA damage-inducible genes. Molecular and Cellular Biology *27*, 3199-3210.

Singer, V.L., Wobbe, C.R., and Struhl, K. (1990). A wide variety of DNA sequences can functionally replace a yeast TATA element for transcriptional activation. Genes & Development *4*, 636-645.

Smale, S.T., Transcription initiation from TATA-less promoters within eukaryotic protein-coding genes. Biochimica et Biophysica Acta *1351*,73–88.

Stillman, D.J., Dorland, S., and Yu, Y. (1994). Epistasis analysis of suppressor mutations that allow HO expression in the absence of the yeast SW15 transcriptional activator. Genetics *136*, 781-788.

Uhler, J.P., Hertel, C., and Svejstrup, J.Q. (2007). A role for noncoding transcription in activation of the yeast PHO5 gene. Proceedings of the National Academy of Sciences of the United States of America *104*, 8011-8016.

Vidal, M., and Gaber, R.F. (1991). RPD3 encodes a second factor required to achieve maximum positive and negative transcriptional states in Saccharomyces cerevisiae. Molecular and Cellular Biology *11*, 6317-6327.

Vidal, M., Strich, R., Esposito, R.E., and Gaber, R.F. (1991). RPD1 (SIN3/UME4) is required for maximal activation and repression of diverse yeast genes. Molecular and Cellular Biology *11*, 6306-6316.

Warren, P.B., and Rein ten Wolde, P. (2004). Enhancement of the stability of genetic switches by overlapping upstream regulatory domains. Physical Review Letters *92*, 128101.

Weis, L., and Weinberg, D. (1997). Accurate positioning of RNA polymerase II on a natural TATA-less promoter is independent of TATA-binding-protein-associated factors and initiator-binding proteins. Molecular and Cellular Biology *17*, 2973-2984.

Xin, X., Lan, C., Lee, H.C., and Zhang, L. (2007). Regulation of the HAP1 gene involves positive actions of histone deacetylases. Biochemical and Biophysical Research Communications *362*, 120-125.

Chapter 5

Summary, Discussion, and Future Directions

Summary and Discussion

The *FLO11* promoter is one of the largest promoters in yeast, a characteristic that sets apart the promoters of all members of the yeast *FLO* (Flocculin) gene family. These promoters receive a complex combination of signals from upstream signaling pathways and the DNA binding factors and chromatin remodelers that associate with them. The net effect of the regulatory stimulus on *FLO11* promoters within a population of yeast cells is variegated silencing that results in phenotypic variation within the clonal population of yeast cells (Halme et al., 2004). A similar silencing phenomenon is observed at the *FLO10* promoter. Variegated transcription of *FLO10* and *FLO11* results in yeast cells that, at the population level, exhibit variability in their behavior regarding flocculation (cell-to-cell adhesion), adhesion to and invasion of inert surfaces and, in diploids, the formation of long filaments called pseudohyphae (Halme et al., 2004).

In Chapter Two, I presented our characterization of the variegated transcription that is observed from the promoters of the *FLO* gene family in *S. cerevisiae* and our finding that, as is the case in other examples of variegated expression observed across biological kingdoms, chromatin structure at *FLO* promoters is a critical component in the mechanism underlying the observed variegation (Halme et al., 2004). We identified several *trans*-acting regulators of the epigenetic silencing observed at *FLO10* and *FLO11* that function in the modification of nucleosomal histones, important in determining chromatin structure (Halme et al., 2004). We found that the histone deacetylase Hda1,

along with the DNA binding protein Sfl1, functions in the silencing observed at *FLO11*. Hdal also plays a role in silencing *FLO10,* but the histone deacetylases Hst1 and Hst2, which are homologs of Sir2, have a more important role in the silencing at this locus and are recruited to the *FLO10* promoter by a Sfl1-dependent mechanism (Halme et al., 2004).

In Chapter Three, I presented the results of two genome-wide screens that I conducted to identify additional effectors of the variegated transcription at *FLO* promoters. The screens identified chromatin remodelers and other transcriptional regulators not previously known to affect *FLO* gene transcription. Among candidates identified in the screens were components of the Rpd3L histone deacetylase complex, the Srb/Mediator complex, the COMPASS histone methyltransferase complex, and other chromatin remodeling factors such as Rsc2, Ada2, and Swi1. Many of these mutants behaved as would be expected, according to contemporary knowledge of the effects of chromatin modification and remodeling on transcription. Others presented phenotypes that were unanticipated given their particular function in chromatin modification. One complex stood out as being particularly curious: the Rpd3L histone deacetylase complex. Because histone deacetylation is known to mediate transcriptional repression (Grunstein, 1997), the observation that Rpd3L behaves as a net transcriptional activator of *FLO* promoters seemed initially paradoxical.

In Chapter Four, I presented findings that resolve the apparent paradox of Rpd3L's net activating effect on *FLO* gene transcription. At the *FLO11* locus in yeast, the Rpd3L histone deacetylase complex represses a regulatory noncoding RNA *ICR1* (Interfering Crick RNA) that initiates more than 3 kilobases away from the *FLO11* ORF,

is transcribed in the Crick direction across the *FLO11* promoter, and prevents *FLO11* expression by somehow interfering with the binding of transcriptional activators and chromatin remodeling at the core promoter. The net effect of Rpd3L action is positive on *FLO11* expression, but its local effect on the transcription of *ICR1* is negative, thus resolving the paradox regarding Rpd3L's role in regulating transcription via chromatin modification. A transcription terminator that disrupts *ICR1* has the predicted effect of rescuing *FLO11*-dependent phenotypes, supporting our hypothesis that *ICR1* has a causal role in preventing *FLO11* expression. Sfl11, likely accompanied by the histone deacetylase Hda1, acts to repress the transcription of a second regulatory noncoding RNA *PWR1* (Promoting Watson RNA) that initiates approximately 2 kilobases from the *FLO11* ORF and is transcribed in the Watson direction convergently and overlapping with the *ICR1* transcript. When *SFL1* is deleted, elevated levels of *PWR1* transcript correlate with increased *FLO11* expression. I hypothesize that *PWR1* promotes *FLO11* expression by competing with *ICR1* for its template region, thereby preventing *ICR1* transcription from proceeding along the *FLO11* promoter region. The fact that the *PWR1* transcript is capable of interfering with the expression of a *URA3* reporter gene inserted in its path supports this hypothesis.

We have detected an apparently similar pair of noncoding transcripts initiating in regions of the *FLO10* promoter, suggesting that regulation by *cis*-acting noncoding RNAs may be a mechanism that extends to other members of the *FLO* gene family, and perhaps to other genes that exhibit net-positive transcriptional regulation by Rpd3L (Sertil et al., 2007; Sharma et al., 2007; Xin et al., 2007; De Nadal et al., 2004).

In summary, I have examined the chromatin modifying proteins that localize to the *FLO10* and *FLO11* promoters and that act in *trans* to affect their transcription and epigenetic silencing. I describe the results of genome-wide screens to identify additional *trans*-acting chromatin modifying factors that play a role in transcriptional regulation of the *FLO* promoters. Some of the candidates identified in the screens, the components of the Rpd3L histone deacetylase complex in particular, had effects on *FLO11* transcription that initially seemed paradoxical because their net effect on *FLO11* transcription was the opposite of that anticipated given the known functions of these complexes. Careful analysis of these mutants, their phenotypes, the transcription of *FLO11*, and most importantly, the noncoding transcripts that we have detected in the promoter region of *FLO11*, have revealed the basis for this paradox.

Our findings point to a new model for the mechanism underlying transcriptional variegation of *FLO* genes. This model incorporates the findings reported in Chapter Four and involves dynamic and competitive binding to promoter DNA by proteins that may determine alternate chromatin structures via recruitment of histone deacetylases. These alternate chromatin structures regulate transcription of *cis*-acting regulatory noncoding RNAs, which in turn regulate *FLO* gene expression. Competitive binding of transcription factors that generate different outputs to the same regulatory site in DNA has been shown to form the basis of a simple exclusive toggle switch between two transcriptional states (Warren and Rein ten Wolde, 2004). At the *FLO11* locus, competitive binding of *trans*-acting protein factors that cause a switch between two chromatin states, one permissive of noncoding transcription and the other repressive of noncoding transcription, could be the basis of exactly such a simple toggle switch between an active or inactive core promoter

state. The percentage of active versus inactive *FLO11* core promoters within a population of wild-type variegating yeast cells may reflect the likelihood of binding for each of the two *trans*-acting proteins competing for the same binding region at each *FLO11* promoter within the population.

Our discovery that Rpd3L- and Sfl1-regulated noncoding RNAs play a role in regulating *FLO11* expression is likely a harbinger of a new view of transcriptional control. In addition to our findings at the *FLO11* locus, there has been a recent flurry of reports of cases of regulation of gene expression by noncoding transcripts in *S. cerevisiae* (Camblong et al., 2007; Hongay et al., 2006; Martens et al., 2004; Martens et al., 2005; Uhler et al., 2007). The existence of many more, as yet uncharacterized, noncoding RNAs in the yeast transcriptome suggests that noncoding transcripts play a more important role in transcriptional regulation in yeast than has been previously appreciated (Miura et al., 2006; Nagalakshmi et al., 2008; David et al., 2006; Davis and Ares, 2006; Samanta et al, 2006; Steinmetz et al., 2006). Thus, the regulatory mechanisms that we describe here at the *FLO11* locus, along with other recent reports of such phenomena, are likely to be just the tip of an iceberg of regulation by noncoding RNAs in yeast.

Future Directions

Future experiments that follow from these studies can be divided into three categories:

1. Experiments to test further our model for noncoding RNA regulation at the *FLO11* promoter.
2. Experiments to test whether this model extends to the regulation of other members of the *FLO* gene family.
3. Genome wide experiments to examine whether our model is informative regarding the mechanisms by which other genes, especially those that exhibit net-positive regulation by Rpd3L, are transcriptionally regulated.

There are a number of experiments that should be conducted to test further our model for noncoding RNA regulation of *FLO11* expression. First, Northern blot analysis should be conducted to test, at the molecular level, that termination of the *ICR1* transcript has occurred in the Rpd3L$^-$ (*cti6*) mutant that carries the transcriptional terminator construct which rescues the *FLO11*-dependent haploid adhesion phenotype in this strain (Figures 12 of Chapter 4).

The *K. lactis URA3-terminator* construct used in our study is fairly large (1.4 kb). It is possible that this construct rescues haploid adhesion in the *cti6* mutant, not by terminating *ICR1*, but by interfering with some necessary tertiary structure of the *FLO11* promoter or by disrupting an undiscovered binding site for a repressor that lies very far upstream (> 3kb) of the *FLO11* ORF. We will address this concern in at least two experiments. In the first experiment, we will replace the 1.4 kb *URA3-terminator*

construct with the *HIS3* terminator sequence, which is fewer than 300 base pairs in length. This shorter DNA fragment should be less disruptive to any *FLO11* promoter tertiary structure that might be required for its regulation. In the second experiment, we will replace the *URA3-terminator* construct with the *HIS3* ORF sequence without its terminator. If *ICR1* transcription is truly important for *FLO11* regulation, then the insertion of the *HIS3* ORF sequence, which is predicted to be transcribed as part of the *ICR1* transcript without disrupting its procession through the *FLO11* promoter sequence, will not rescue the *cti6* haploid adhesion phenotype. This result would also confirm that the insertion site is not disrupting the binding of a *trans*-acting repressor. The *HIS3* ORF is approximately 600 base pairs long and has been used analogously in other studies as a control for transcriptional termination experiments (Martens et al., 2004). The effects of all of these constructs will also be examined at the molecular level by Northern blotting.

It would be very informative to examine the transcriptional profile of the three transcripts that we have detected at the *FLO11* locus (*ICR1*, *PWR1*, and *FLO11* itself) on a cell-by-cell basis to determine whether our prediction is correct that the *FLO11* transcript will be present in cells that also have *PWR1* transcript but not in cells that have *ICR1* transcript. To this end, a new technology called StarFISH might prove useful. This technology utilizes a large number of fluorescently labeled DNA probes that are complementary to a target RNA molecule. The probes are used to hybridize and fluorescently label target RNAs still contained within fixed cells. It is possible to utilize sets of probes for multiple RNA molecules. The number of RNAs that can be examined in any given cell is limited only by the number of distinct fluorophores available for labeling. The coexpression of two or more RNAs can readily be examined on a cell-by-

cell basis using fluorescence microscopy and FACS. This technology will enable us to examine the transcriptional profiles of the three transcripts that we have detected at the *FLO11* locus on a cell-by-cell basis in a wild type strain in which *FLO11* expression variegates. The fact that steady state *ICR1* transcript levels are low (according to our northern blot, microarray, and real time PCR analyses) might present difficulties for this approach, but the additional fact that this transcript is ~3.2 kb in length suggests that we might be able to overcome low RNA transcript levels by using a larger number of complementary fluorescently labeled probes for this transcript.

Examination of *ICR1* and *PWR1* transcript levels in additional mutants that affect *FLO11* expression should also prove useful in furthering our understanding of regulatory control at the *FLO11* promoter. For example, we suspect that the histone deacetylase Hda1 represses *PWR1* transcription via its recruitment to the *FLO11* promoter by Sfl1, but this has yet to be tested by northern analysis of transcripts derived from the *hda1* mutant strain.

It will be interesting to determine whether regulation by noncoding RNAs extends to other members of the *FLO* gene family. Our strand-specific genome-wide microarray expression data strongly suggest that a pair noncoding transcripts analogous to those that act at *FLO11* may be regulating *FLO10* expression, as well. Careful examination of *FLO10* regulation using the same experimental methods that we have employed to examine *FLO11* regulation will provide further insight.

Finally, it will be very interesting to take a genome-wide approach in determining the extent to which noncoding RNAs, such as those that we observe at the *FLO11* promoter, regulate protein-coding gene expression across the yeast genome, with special

attention to genes already known to be under net-positive regulation by Rpd3L. We will use genome-wide strand-specific microarrays to examine transcription in promoter regions, comparing wild type transcript levels to transcript levels in the Rpd3L$^-$ (*cti6*) mutant. We will search for noncoding transcripts that, when elevated, correlate with a concomitant decrease in expression from the associated protein-coding gene. We will also search for the presence of transcripts running convergently in a manner that might indicate competition in *cis* in these array data. A potential caveat to this approach is that the steady state levels of the noncoding transcripts that we are interested in may place them very near the noise boundary in the array data. We are hopeful that, by training our analysis algorithms on other noncoding regulatory RNAs, such as those detected at the *FLO11* promoter and at other genes including *SER3* and *IME4*, we may be able to overcome this hurdle in genome-wide detection. These experiments will be very useful in determining the extent to which the mechanism that we have discovered at *FLO11*, which resolves the paradox of RpdL-dependent activation at this promoter, applies to other genes across the yeast genome.

References

Camblong, J., Iglesias, N., Fickentscher, C., Dieppois, G., and Stutz, F. (2007). Antisense RNA stabilization induces transcriptional gene silencing via histone deacetylation in S. cerevisiae. Cell *131*, 706-717

David, L., Huber, W., Granovskala, M., Toedling J., Palm, C.J., Bofkin, L. Jones, T., Davis, R.W., and Steinmetz, L.M. (2006). A high-resolution map of transcription in the yeast genome. Proceedings of the National Academy of Sciences of the United States of America *103*, 5320-5325.

Davis, C.A., and Ares, M. (2006). Accumulation of unstable promoter-associated transcripts upon loss of the nuclear exosome subunit Rrp6p in Saccharomyces cerevisiae. Proceedings of the National Academy of Sciences of the United States of America *103*, 3262-3267.

De Nadal, E., Zapater, M., Alepuz, P.M., Sumoy, L., Mas, G., and Posas, F. (2004). The MAPK Hog1 recruits Rpd3 histone deacetylase to activate osmoresponsive genes. Nature *427*, 370-374.

Grunstein, M. (1997a). Histone acetylation in chromatin structure and transcription. Nature *389*, 349-352.

Halme, A., Bumgarner, S., Styles, C., and Fink, G.R. (2004). Genetic and epigenetic regulation of the FLO gene family generates cell-surface variation in yeast. Cell *116*, 405-415.

Hongay, C.F., Grisafi, P.L., Galitski, T., and Fink, G.R. (2006). Antisense transcription controls cell fate in Saccharomyces cerevisiae. Cell *127*, 735-745.

Martens, J.A., Laprade, L., and Winston, F. (2004). Intergenic transcription is required to repress the Saccharomyces cerevisiae SER3 gene. Nature *429*, 571-574.

Martens, J.A., Wu, P.Y., and Winston, F. (2005). Regulation of an intergenic transcript controls adjacent gene transcription in Saccharomyces cerevisiae. Genes & Development *19*, 2695-2704.

Miura, F., Kawaguchi, N., Sese, J., Toyoda, A., Hattori, M., Morishita, S., and Ito, T. (2006). A large-scale full-length cDNA analysis to explore the budding yeast transcriptome. Proceedings of the National Academy of Sciences of the United States of America *103*, 17846-17851.

Nagalakshmi, U., Wang, Z., Waern, K., Shou, C., Raha, D., Gerstein, M., and Snyder, M. (2008). The Transcriptional Landscape of the Yeast Genome Defined by RNA Sequencing. Science *320*, 1344-1349.

Samanta, M.P., Tongprasit, W., Sethi, H., Chin, C.S., and Stoic, V. (2006). Proceedings of the National Academy of Sciences of the United States of America *103*, 4192-4197.

Sertil, O., Vemula, A., Salmon, S.L., Morse, R.H., and Lowry, C.V. (2007). Direct role for the Rpd3 complex in transcriptional induction of the anaerobic DAN/TIR genes in yeast. Molecular and Cellular Biology *27*, 2037-2047.

Sharma, V.M., Tomar, R.S., Dempsey, A.E., and Reese, J.C. (2007). Histone deacetylases RPD3 and HOS2 regulate the transcriptional activation of DNA damage-inducible genes. Molecular and Cellular Biology *27*, 3199-3210.

Steinmetz, E.J., Warren, C.L., Kuehner, J.N., Panbehi, B., Ansari., A.Z., and Brow, D.A. (2006). Genome-wide distribution of yeast RNA polymerase II and its control by Sen1 helicase. Molecular Cell *24*, 735-746.

Uhler, J.P., Hertel, C., and Svejstrup, J.Q. (2007). A role for noncoding transcription in activation of the yeast PHO5 gene. Proceedings of the National Academy of Sciences of the United States of America *104*, 8011-8016.

Warren, P.B., and Rein ten Wolde, P. (2004). Enhancement of the stability of genetic switches by overlapping upstream regulatory domains. Physical Review Letters *92*, 128101.

Xin, X., Lan, C., Lee, H.C., and Zhang, L. (2007). Regulation of the HAP1 gene involves positive actions of histone deacetylases. Biochemical and Biophysical Research communications *362*, 120-125.